



Removal of Polycyclic Aromatic
Hydrocarbons and other Contaminants
from Hydrocarbon Fluids

Timothy James David McCabe

A thesis submitted for the
Degree of Doctor of Philosophy

Department of Pure and Applied Chemistry

2019

This thesis is the result of the author's original research. It has been composed by the author and has not been previously submitted for examination which has led to the award of a degree.

The copyright of this thesis belongs to the author under the terms of the United Kingdom Copyright Acts as qualified by University of Strathclyde Regulation 3.50. Due acknowledgement must always be made of the use of any material contained in, or derived from, this thesis.

Signed:

Date:

Abstract

Polycyclic aromatic hydrocarbons (PAHs), compounds that are produced during the combustion of fuels, is one example of contaminants found in automotive lubricants. PAHs can aggregate and form solid deposits. The deposits can be dispersed by the inclusion of oil-soluble additives into the lubricant. However, these additives can have negative effects on the lubricant performance. Unfortunately, current technologies do not remove contaminants; rather, they serve to minimise any damage caused by them. It is proposed that supplementing current technologies with suitable solid-phase, polymeric additives may be of benefit. It is hypothesised that contaminants can be removed from hydrocarbon fluids using polymer-supported chemistries in the solid-phase.

Precipitation polymerisation (PP) and non-aqueous dispersion (NAD) polymerisation were investigated to synthesise a library of aromatic-based, crosslinked polymer particles. Hypercrosslinking chemistry was also utilised to impart high specific surface areas into some materials. To test the applicability of removing PAHs from a hydrocarbon fluid, each polymer was contacted with a solution of PAHs in heptane.

These investigations proved fruitful, showing that upwards of 90% of certain PAHs could be removed from a heptane solution using crosslinked polymers.

The synthesis of polymer resins by suspension polymerisation was investigated, with an aim of producing polymer particles that were of an appropriate size for containment within an engine lubricant system. A library of resins was successfully designed, synthesised and characterised. Gel-type, macroreticular and hypercrosslinked materials were synthesised to give a breadth of specific surface areas bearing varied functionality.

Finally, contamination removal from an engine lubricant *in situ*, using some of the synthesised materials, was undertaken. It was concluded that using solid phase-polymers as contaminant removal devices was effective.

Some of the work presented in this thesis forms the basis for the patent application W02017178593A2 (Removal of aromatic compounds from a hydrocarbon fluid).

Abbreviations

4-VP – 4-Vinylpyridiene

ABDV – 2,2'-Azobis(2,4-dimethylvaleronitrile)

AIBN – 2,2'-Azobisisobutyronitrile

BET – Brunauer–Emmett–Teller

BJH - Barrett-Joyner-Halenda

CV – coefficient of variation

\bar{d} - average diameter

DVB – Divinylbenzene

EGDMA – Ethylene glycol dimethacrylate

FT-IR – Fourier Transform Infra-red

HXL – Hypercrosslinked

mbar – millibar

NAD – Non-aqueous dispersion

PAH – Polycyclic Aromatic Hydrocarbon

PP – Precipitation polymerisation

ppm – parts per million

psi – pounds per square inch

PVP – polyvinylpyrrolidone

SEM – Scanning Electron Microscopy

VBC – Vinylbenzyl chloride

Acknowledgments

The list of people who deserve my thanks is far too long to include everyone. If you are not named, please be rest assured you have my thanks and I am deeply grateful for everything!

To my supervisor at Strathclyde, Peter Cormack, thank you! The guidance and help you have given me throughout my research are greatly appreciated.

I am indebted to my industrial supervisors John Redshaw and Kevin West, and to all the other people from Castrol for your direction, as well as constructive feedback and openness to assisting me whenever asked.

I would like to thank both the EPSRC and Castrol for providing the financial support to undertake this work.

To all the members of the Cormack Group, past and present, who I have encountered on this journey, thank you! For the banter, the lab weekends away and help you all provided. For the intrigue in my research, the feedback on reports and presentations, I am truly grateful.

I feel a special thank you is owed to Stephen, Derek, Richard, Lucy, Alasdair, James, Jason, Colleen and all the other members of the chosen family. For your unending love and support, your sage wisdom and advice, and for all the times you have taken a genuine interest in my work, I thank you. You have all provided a love and friendship which I treasure.

A huge debt of gratitude is owed to my family. You have always supported me in everything I do and without you none of this would have been possible. You have shown love, care and support and I am eternally grateful.

To Father Doyle and the Poor Clare Sisters: your continued guidance, encouragement and prayers have fortified me on this journey. For this, I will be forever grateful.

Finally, and most importantly, Cairney. I love you! You have supported me throughout my PhD and beyond, and for this I am so thankful. I look forward to what the future holds!

Contents

Abbreviations	iii
Acknowledgments	iv
1. Introduction	1
1.1. Chain-Growth Polymerisation.....	4
1.2 Free Radical Polymerisation.....	7
1.3 Molecular weights of polymer chains	10
1.4 Crosslinked polymers	13
1.5 Gel-type and macroreticular polymer particles	14
1.6 Polymer microspheres and their synthesis	16
1.6.1 Suspension Polymerisation	17
1.6.1.1 The continuous phase	18
1.6.1.2 Suspension Stabiliser.....	18
1.6.1.3 Particle size and bead morphology.....	19
1.7 Precipitation Polymerisation	20
1.8 Dispersion Polymerisation	23
1.9 Hypercrosslinking	23
1.10 Crosslinked Polymer Particles and Their Applications.....	29
1.11 Solid-Phase Peptide Synthesis	29
1.12 Chromatography.....	31
1.13 Ion-Exchange and Sorption	32
1.14 Sorption of Polycyclic Aromatic Hydrocarbons (PAHs).....	37
1.15 Engine Lubricants	38
1.16 Soot Formation and its Growth from Polycyclic Aromatic Hydrocarbons (PAHs).....	38
1.16.1 Pyrolysis.....	39
1.16.2 Nucleation	39
1.16.3 Surface Growth.....	40
1.16.4 Coalescence and Agglomeration.....	40
1.17 Ways in which PAH and soot formation is suppressed or avoided	41
1.17.1 In-engine technologies.....	42
1.17.2 After-treatments to reduce soot and PM emissions.....	43
1.18 Engine Oil Dispersants.....	45

1.18.1	Properties of a Dispersant.....	45
1.18.2	Dispersant structure.....	46
1.18.3	The Hydrocarbon Tail.....	47
1.18.4	The Connecting Group and Polar Moieties	48
1.19	Polyisobutylene Succinimides	51
1.20	Succinic Esters.....	52
1.21	Mannich Dispersants.....	53
1.22	ExBox: A PAH scavenger.....	54
1.23	<i>In Situ</i> Soot and PAH Sorption	55
1.24	Hypothesis and project aims.....	57
2.0	Experimental.....	59
2.1	General	59
2.2	Equipment	60
2.3	Synthesis of 1 st generation materials <i>via</i> precipitation polymerisation and NAD polymerisation and the hypercrosslinking of materials thereof	62
2.3.1	General Procedures.....	62
2.3.2	Preparation of Polymer Particles.....	64
2.3.3	PAH Sorption Experiments using 1 st generation materials.....	73
2.4	Synthesis of 2 nd generation materials <i>via</i> suspension polymerisation and the hypercrosslinking of materials thereof.....	74
2.4.1	General Procedures.....	74
2.4.2	Preparation of Polymer Particles.....	75
2.4.3	PAH sorption experiments.....	81
2.5	Experimental for engine tests.....	82
2.5.1	Equipment	82
3.0	Results and Discussion.....	85
3.1	Synthesis of polymer microspheres by precipitation and non-aqueous dispersion polymerisation.....	85
3.1.1	Synthesis of Poly(DVB-80).....	85
3.1.2	Synthesis of Poly(DVB- <i>co</i> -4-vinylpyridine).....	87
3.1.3	Synthesis of Poly(DVB-80- <i>co</i> -VBC).....	93
3.1.4	Synthesis of hypercrosslinked (HXL) poly(VBC- <i>co</i> -DVB-80).....	96
3.2	Non-Aqueous dispersion (NAD) polymerisation	100
3.2.1	Synthesis of Poly(Styrene- <i>co</i> -ethylene glycol dimethacrylate (EGMDA)).....	101
3.2.2	Synthesis of poly(styrene- <i>co</i> -VBC- <i>co</i> -EGDMA).....	103

3.2.3	Synthesis of hypercrosslinked (HXL) poly(styrene-co-VBC-co-EGDMA).....	105
3.2.3	Synthesis of HXL poly(styrene-co-VBC-co-EGDMA) <i>via</i> a two-stage hypercrosslinking process	109
3.2.5	Synthesis of poly(styrene-co-4-VP-co-EGDMA).....	111
3.2.4	Synthesis of poly(VBC-co-4-VP-co-EGDMA) <i>via</i> NAD polymerisation	114
3.2.5	Hypercroslinking of poly(VBC-co-4-VP-co-EGDMA).....	116
3.2.6	Hypercroslinking of poly(VBC-co-4-VP-co-EGDMA) <i>via</i> a two-stage hypercrosslinking process	120
3.3	Application of Polymers in Sorption and Capture of PAHs	121
3.3.1	Smaller-scale sorption study.....	121
3.3.2	PAH Sorption using Non-Porous Polymers.....	123
3.3.3	PAH Sorption Using Porous Polymers.....	126
3.3.4	PAH sorption Using Ultra-High Specific Surface Area-Hypercrosslinked Polymers.....	128
3.4	Large-scale sorption study	130
3.4.1	Larger-scale PAH capture using non-porous polymers	131
3.4.2	Larger-scale sorption using macroreticular polymers.....	134
3.4.3	Larger-scale sorption of PAHs using hypercrosslinked polymers	137
3.5	Conclusion	140
3.6	Synthesis of polymers <i>via</i> suspension polymerisation	142
3.6.1	Synthesis of poly(VBC-co-DVB-80) <i>via</i> suspension polymerisation.....	142
3.6.2	Synthesis of hypercrosslinked (HXL) poly(VBC-co-DVB-80)	147
3.6.2	Synthesis of poly(DVB-80-co-4VP) <i>via</i> suspension polymerisation	150
3.6.3	Synthesis of poly(styrene-co-VBC-co-EGDMA) <i>via</i> suspension polymerisation	154
3.6.4	Synthesis of HXL poly(styrene-co-VBC-co-EGDMA)	157
3.6.5	Synthesis of poly(VBC-co-4-VP-co-EGDMA) <i>via</i> suspension polymerisation	161
3.6.6	Synthesis of HXL poly(VBC-co-4-VP-co-EGDMA) <i>via</i> a two-stage hypercrosslinking process	164
3.7	Larger-scale sorption studies	169
3.7.1	PAH sorption using gel-type polymers synthesised by suspension polymerisation	170
3.7.2	PAH removal using porous polymers synthesised by suspension polymerisation	171
3.8	Conclusions.....	174

3.9	Use of polymeric materials as soot and contaminant sorbents within a diesel engine	175
3.9.1	Initial engine test using a non-fired, research engine	176
3.9.2	Engine-based sorption study using poly(DVB-80-co-4-VP) as sorption media	180
3.9.3	Engine-based sorption study using poly(styrene-co-VBC-co-EGDMA) as sorption media	187
3.9.4	Engine-based sorption study using HXL poly(styrene-co-VBC-co-EGDMA) as sorption media	191
3.9.5	Engine-based sorption study using poly(VBC-co-4-VP-co-EGDMA) as sorption media	196
3.9.6	Engine-based sorption study using HXL poly(VBC-co-4-VP-co-EGDMA) as sorption media	199
3.10	Conclusions	204
3.11	Fired engine tests	206
3.11.2	Fired, engine-based sorption study using poly(DVB-80-co-4-VP) as sorption media	206
3.11.2	Fired, engine-based sorption study using poly(styrene-co-VBC-co-EGDMA) as sorption media	216
4.0	Conclusions	221
5.0	Future work	225
6.0	References	227

1. Introduction

Polymers are ubiquitous and affect our daily lives in a profound way. They range from the relatively mundane (polyethylene plastics used in food packaging and polyamide fibres used in the textile industry) through to more advanced and exotic applications (extremely high strength polyaramids, such as Kevlar[®], used in the ballistics and motorsport industry).¹ The vast array of polymers employed in the lubricant industry² – some of which will be explored later – are also very much part of this story.

Deriving from two ancient Greek words – *polús* meaning ‘many’ or ‘much’ and *méros* meaning ‘part’ – polymers are large molecules comprising of many simpler repeating units.

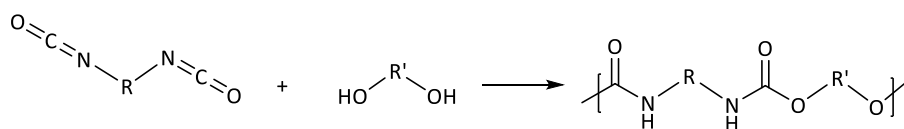
To understand polymers fully, one can begin by looking at polymer synthesis. There are numerous possible synthetic routes as well as many polymerisation techniques that can be used to transform monomer into polymers.

In 1929 W.H Carothers proposed that polymers which had been prepared *via* a stepwise reaction of monomers be distinguished from those which are formed *via* chain reactions.³ Thus, the classical subdivision of polymers came to be:

Condensation polymers – Formed by reactions that involve the elimination of a small molecule, usually water, at each step.

Addition polymers – Formed in a reaction where no such loss of a small molecule takes place.

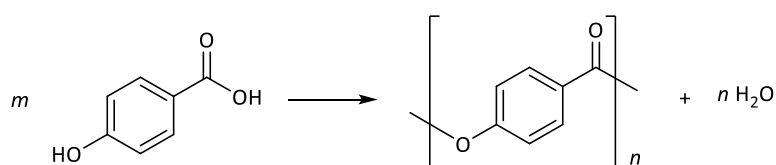
While at the time these definitions worked, it did not take long before notable exceptions began to appear, and a more reliable description was required. In 1953 P.J Flory argued that the term ‘condensation’ be replaced by ‘step-growth’.⁴ It is far more logical to speak of step-growth polymerisation rather than condensation polymerisation as there are polymers which grow in a step-wise fashion without the elimination of a small molecule. Polyurethanes are one such example, being synthesised typically from a diisocyanate and diaol (**Scheme 1**).



Scheme 1 – Step-growth synthesis of polyurethane

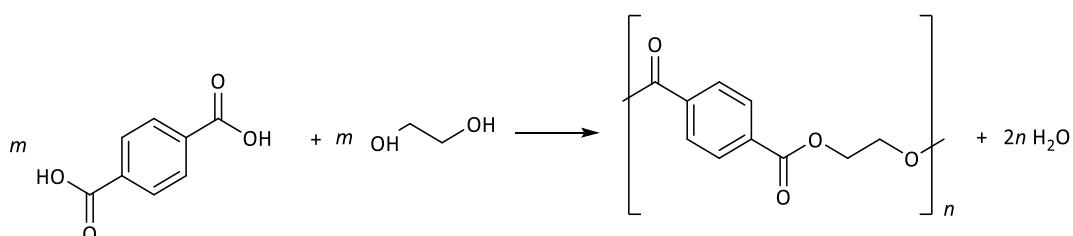
For two mutually reactive functional groups, there are two distinct ways in which linear step-growth polymers can be synthesised:

1 - Both functional groups can be in the same molecule, for example the synthesis of a polyester from a hydroxyacid molecule (**Scheme 2**).⁴



Scheme 2: Synthesis of a polyester from an AB monomer

2 – Polyesters can also be produced using two bi-functional monomers, a dibasic acid and a diol (**Scheme 3**).⁵



Scheme 3: Synthesis of a polyester using bi-functional monomers

In both cases the esterification can occur anywhere throughout the monomer matrix where two monomer molecules are orientated correctly and possess the correct collision energy. After the ester forms (with loss of water), the reactive end of the growing polymer can continue to react *via* either the hydroxyl or carboxylic acid group. The overall

effect is that the reaction consumes monomer rapidly but there is no corresponding large increase in molecular weight. This phenomenon is exemplified schematically below for 12 monomer units containing functional groups A and B (**Figure 1**).

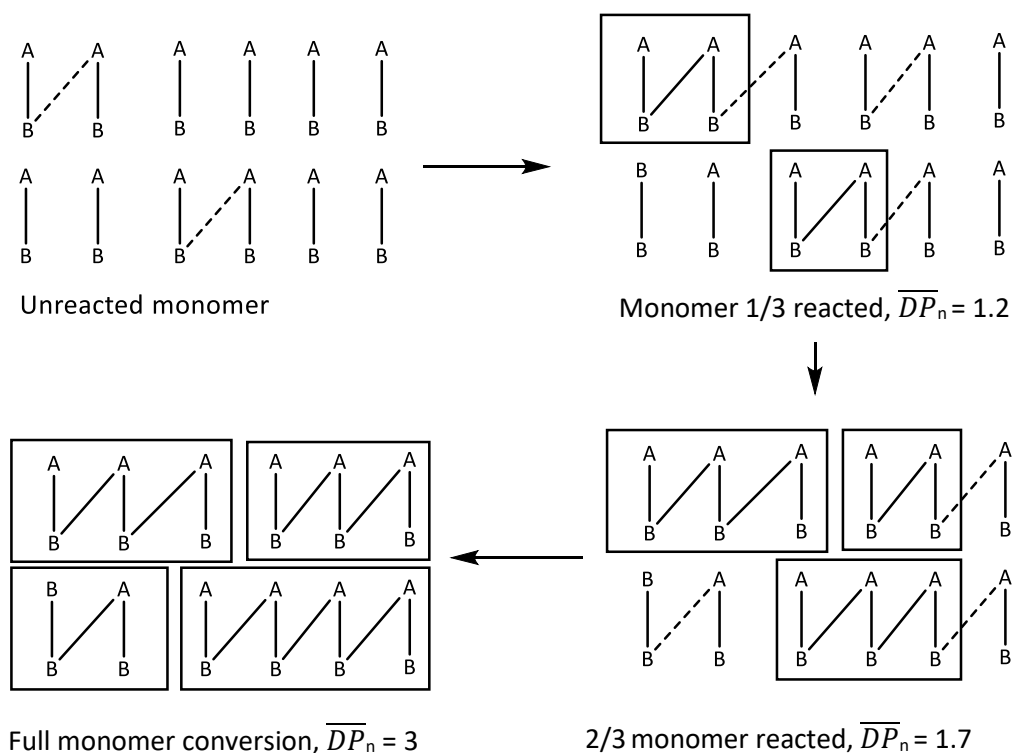


Figure 1 - Schematic representation of a step-growth polymerisation

When one third of the monomer has been converted to polymer (polymer is represented by boxes, and the dashed lines represent species which are reacting) it can be seen that the number average degree of polymerisation, \overline{DP}_n (the number of molecules present initially divided by the number of molecules that remain), is low. In fact, even at 100% monomer conversion the number average degree of polymerisation is still very low. The rate of polymerisation will decrease as the functional groups are consumed in the polymerisation. In turn, this means that even at high levels of monomer conversion the molecular weight of the polymer will increase rather slowly.

In 1935 Carothers developed a simplistic set of equations which related the number average degree of polymerisation, \overline{DP} , to the extent of monomer conversion, p .⁶

With these equations, Carothers was able to establish one of the fundamental facets of step-growth polymerisation, namely that exceptionally high conversion of monomer is required if usable high molecular weight polymers are to be produced. For example, the aliphatic polyamide Nylon-6,6, (**Figure 2**), can be used to make fibres. However, if high strength fibres are to be produced then the molecular weight of the polymer has to be in the range of 12,000 to 13,000 g mol⁻¹ which corresponds to a \overline{DP}_n of 106 to 116.⁷ For a polymerisation that has reached 99% completion, $\overline{DP}_n = 100$, showing that to get high quality polymer, the polymerisation must proceed beyond 99% monomer conversion. This demands that efficient polymerisation protocols are used as well as very high purity monomers and reagents.

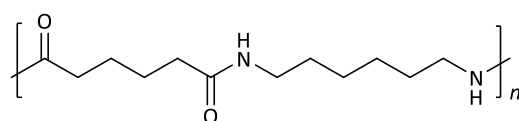


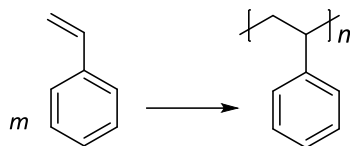
Figure 2: Nylon-6,6

As has been shown, in step-growth polymerisation polymer chains are built in a step-wise fashion through the union of monomers to form dimers, trimers and higher species throughout the monomer matrix. There is, however, another way in which polymer can be formed, and this is through chain-growth polymerisation.

1.1. Chain-Growth Polymerisation

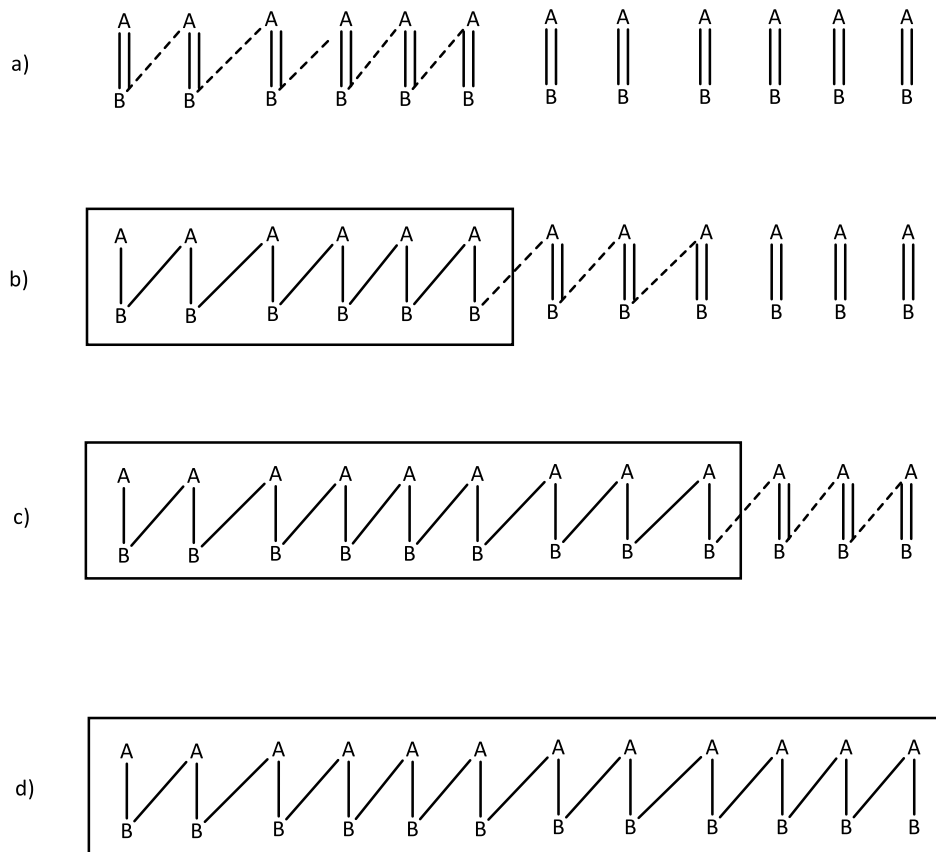
Chain-growth polymerisation is the process by which monomer is converted to polymer by the successive linkage of monomer molecules to the end of a propagating chain. The process begins with the formation of a reactive species (often a free radical or charged moiety) in a process called initiation. This active species is continuously regenerated during each monomer addition. Next, is the propagation step; the end groups of the propagating chain react with a monomer unit and transfer the reactive species onto the next monomer unit. Rounding off the polymerisation is the termination step. This step stops the formation of the reactive species on the growing polymer chain, effectively bringing the polymerisation to an end. Typically, the polymer which is formed has a

similar structure as the parent monomer that formed it, and there is also usually no loss of a small molecule (**Scheme 4**). However, when polymerising vinyl monomers such as styrene, a loss of unsaturation can occur. The same is true of dienes.



Scheme 4: Chain-growth polymerisation of styrene

Chain-growth polymerisation has one vital difference when compared to step-growth polymerisation; in step-growth polymerisation molecular weight increases slowly while monomer is consumed swiftly. In chain-growth polymerisation, however, high molecular weight polymer chains are attained even at low monomer conversion (**Figure 3**). The main differences between step growth and chain-growth polymerisation are highlighted in **Table 1**.



(a) Unreacted monomer; (b) 50% monomer reacted, $\overline{DP}_n = 1.7$; (c) 75% monomer reacted, $\overline{DP}_n = 3$; (d) 100% monomer reacted, $\overline{DP}_n = 12$ (boxes represent polymer and dashed lines represent species which are reacting)

Figure 3: Schematic representation of chain-growth polymerisation

Step-growth polymerisation	Chain-growth polymerisation
Reaction will proceed without the use of catalysts or initiators.	Initiator (or catalyst) is generally required to start reaction.
Polymer chains and monomers with appropriate end groups will act as the reacting species.	Only reactive species, such as radicals or ions, can propagate the reaction by addition of monomer to the growing polymer chain.
Polymer is formed late in the process. Oligomeric material is created first.	Polymer is formed very early in the reaction process.
The average molecular weight of the polymer increases with reaction time. Longer reaction times generally give higher molecular weight polymer.	The average molecular weight of the final polymer remains, with exceptions, largely unchanged by extending the reaction time.

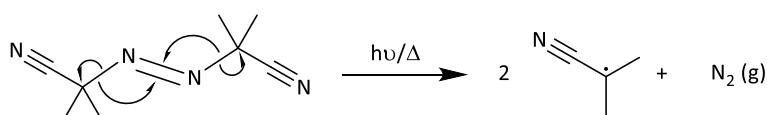
Table 1- Common differences between step-growth and chain-growth polymerisation

1.2 Free Radical Polymerisation

Free radical polymerisation is a type of chain-growth polymerisation that is of academic and industrial importance. Free radical polymerisation also encompasses all materials that were synthesised as part of the body of research presented in this thesis. Long polymer chains can be obtained readily from monomers that contain a vinyl functional group. Industrially, vinyl polymers are the most important of all polymer types, with polyethylene, poly(vinyl chloride), polypropylene and polystyrene all being produced in this way on a several million tonnes scale annually.^{8,9} This method is exploited widely in industry for a number of reasons: the vinyl monomer types that can be used in free radical polymerisation are many and varied; it is both safe and relatively easy to carry out, even on a multi-tonne scale; due to the very nature in which the polymerisation proceeds, high yielding reactions are typical; the reaction is generally tolerant of impurities that are present within the system; it is cost-effective.

A free radical polymerisation, as is the case most other types of chain-growth polymerisation, can be broken down into three distinct steps: 1 – initiation, where the reactive centre is created, and this is normally achieved by using a radical initiator; 2 – propagation, this stage of the polymerisation is where the macromolecular chain grows *via* a kinetic chain mechanism. This stage sees the repeated addition of monomer onto a propagating polymer chain; and 3 – termination, where the growth of the kinetic chain is stopped. This is achieved in one of two ways, either the active centre present at the end of the chain is terminated or it is transferred to a new polymer chain.

The initiation process is instigated using a radical initiator, with azo compounds and peroxides being the most common. This can be achieved either thermally or photolytically. The decomposition of 2,2'-azobis(isobutyronitrile) (AIBN) is shown in **Scheme 5**. Homolytic scission of two C-N single bonds results in two 2-cyanoisopropyl radical species and a mole of nitrogen gas:



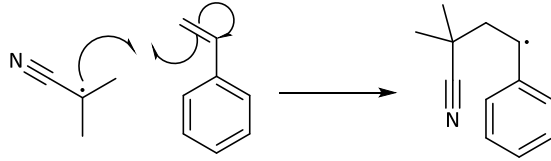
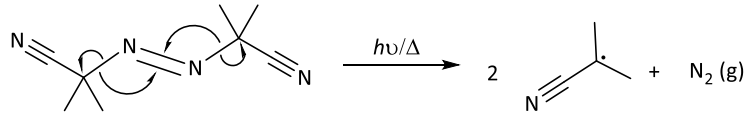
Scheme 5: Decomposition of AIBN

The 2-cyanoisopropyl radical is then available to react with a monomer. In the polymerisation of styrene (or indeed of any vinyl monomer), an electron pair is held between the two carbons in a σ bond. The other is held in a weaker π bond. The radical uses an electron from the π bond to form a stable σ bond with one of the two vinyl carbon atoms. The other π electron moves to the other vinyl carbon atom, thus producing another carbon-centred radical that can react with another monomer unit.

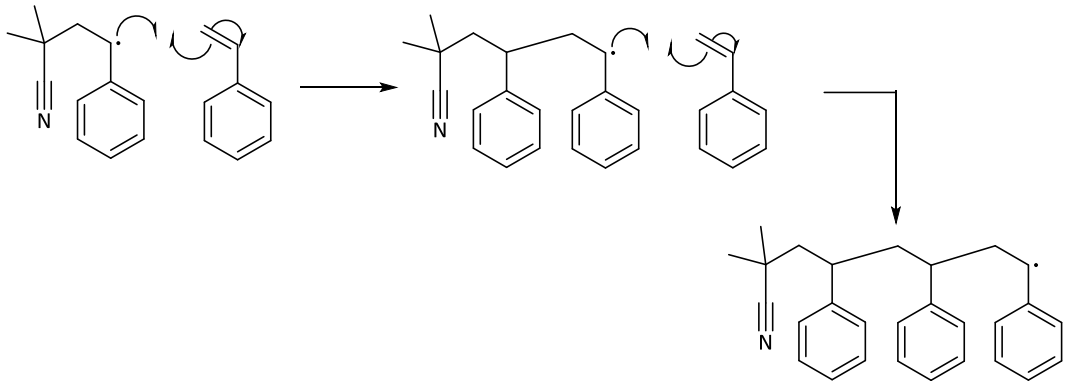
The polymerisation process is rounded off with termination. This is a process that can happen in a number of different ways, depending on which monomer is being used, or more specifically on the structure of the chain-end radical.^{5,7} Combination can occur, where two polymer radicals simply join together to form one long chain. Polystyryl radicals interact almost exclusively in this manner. Another form of termination is radical disproportionation; a radical from one chain abstracts a hydrogen atom from the end of another polymer radical. This produces a polymer with a terminal unsaturated group and

another polymer chain that has a saturated terminal group; poly(methyl methacrylate) radicals are more prone to this type of termination. An active chain-end can react with an initiator radical, rendering the chain inactive. Some impurities which are present in the system can end the polymerisation prematurely or greatly retard its progress. One such example is oxygen, where the growing chain-end will react with molecular oxygen, O_2 , thus producing a polymer chain with an oxygen centred radical on the end, a radical that is far less reactive than a carbon-centred one. The polymerisation of styrene to form polystyrene, with each step (initiation, propagation and termination) highlighted is, shown in **Scheme 6**.

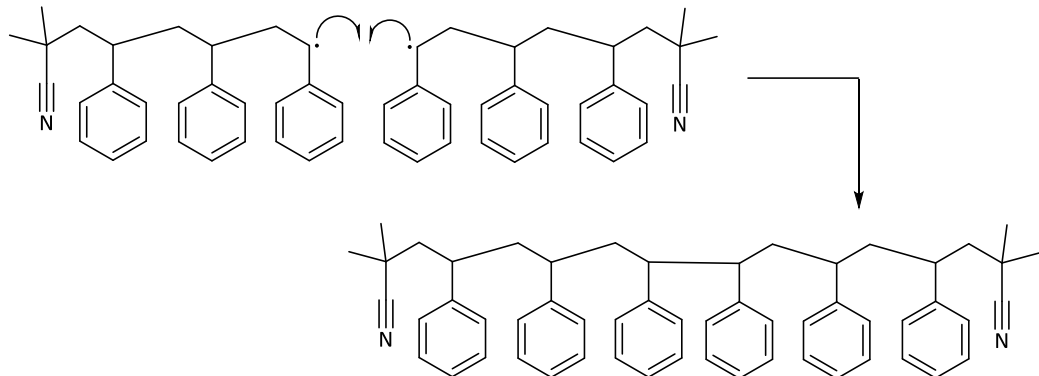
Initiation



Propagation



Chain Termination (by combination)



Scheme 6: Polymerisation of styrene

1.3 Molecular weights of polymer chains

What has been discussed thus far are linear synthetic polymers. These polymers are quite different to their small molecule counterparts, especially when it comes to describing the

molecular weight of a polymer. This is because rather than containing molecules which are all the same molecular weight, typically a given polymer sample contains a distribution of chains of differing length. In the chain termination step of a chain-growth polymerisation, the lengths of the two combining chains are likely to be dissimilar. This therefore results in chains of differing length and thus different molecular weights. The same is true of step-growth polymerisation; upon oligomers of different molecular weight reacting together, polymer chains of different molecular weight are produced. This then raises the question: When describing a polymer, which molecular weight should be quoted? The highest, lowest, or perhaps a range of masses? What is often done is that the spread of molecular weights is obtained, and a distribution graph of molecular weights can be produced from this data.⁷

Carrying this out, however, can be rather monotonous and time consuming. One would have to obtain all the data for all the different molecular weights that may be present in a polymer sample and arrange them according to how much of the polymer each of those molecular weights is made up of. However, with the aid of size exclusion chromatography (where analytes are separated based on hydrodynamic volume) this can be carried out as a matter of routine.

In terms of investigating the molecular weight ranges present in a polymer, what is often quoted is an average value. The most straight-forward method counts the number of molecules of a particular molecular weight and then sums them all together, before dividing this by the total number of molecules in the sample, *i.e.*, the arithmetic mean value. For example, if a polymer sample contained 100 molecules having a molecular weight of 400,000 g mol⁻¹ and 100 having a molecular weight of 600,000 g mol⁻¹, intuitively the average molecular weight would be 500,000 g mol⁻¹. This average is known as the *number average molecular weight*, and has the symbol \overline{M}_n

Mathematically, the number average molecular weight is calculated using the following formula:

$$\overline{M}_n = \frac{\sum N_i \cdot M_i}{\sum N_i}$$

Equation 1 - Equation used to calculate the number average molecular weight (M_n) of a polymer, where N_i is the number of molecules (polymer chains) which have a molecular weight of M_i

A method such as that described above which counts the number of molecules is known as a 'colligative method'. Colligative methods which can be used to measure \overline{M}_n for a polymer include: lowering of vapour pressure or freezing point, as well as the elevation of osmotic pressure or boiling point.¹⁰ However, it should be noted that in a polymer sample the actual number of molecules will be smaller when compared to a small-molecule sample. This, in turn, means that the observed effect in the lowering of freezing point or rising of osmotic pressure, *etc.*, will be much smaller and therefore harder to measure.¹¹

The other most commonly quoted average of a polymer sample is the mass (or weight) average molecular weight, \overline{M}_w . Just as the number average molecular weight took the average based on the number of molecules (polymer chains), the weight average molecular weight calculates the average based on the weight of the polymer chains using the following formula:

$$\overline{M}_w = \frac{\sum W_i \cdot M_i}{\sum W_i}$$

Equation 2 - Equation used to calculate the weight average molecular weight of a polymer, where W_i is the mass of polymer chains (molecules) which have a molecular weight M_i

The weight average molecular weight is a weighted average and accounts for the fact that larger molecules have more mass than smaller ones. This equation can also be written in terms of the numbers of molecules being counted rather than the mass of those molecules, where W_i is equal to N_i (the number of polymer chains) multiplied by M_i (molecular mass of polymer chains), as follows:

$$\overline{M}_w = \frac{\sum W_i \cdot M_i}{\sum W_i} = \frac{\sum N_i \cdot M_i^2}{\sum n_i \cdot M_i}$$

Equation 3 - Expressing \overline{M}_w in terms of number of molecules

The ratio of $\overline{M}_w / \overline{M}_n$ is called the *polydispersity index*, which is used to measure the dispersity of a system. The closer this ratio is to 1, the closer all the polymer chains in the sample are to one molecular weight. This can be a desirable trait in a polymer as the experimenter can have greater control over the physical and mechanical properties of the polymer.¹¹

This brief section describing molecular weights has been used to highlight the fact that polymers are quite different to their small molecule counterparts, and that when characterising molecular weight it is not as simple as quoting just one value as would happen with a small molecule. Numerous polymer textbooks contain a detailed explanation and analysis of polymer molecular weight distribution and how it is calculated.^{4,5,7,11}

1.4 Crosslinked polymers

Thus far, the polymers discussed have been linear. If, however, one of the monomers to be polymerised has two or more reactive moieties then these linear polymers can be chemically linked together to form crosslinked polymer chains. Such materials consist of an infinite network of interconnected linear polymers, making it effectively one single molecule. This means that the polymer effectively has an infinite molecular weight and there will no longer be a distribution of molecular weights as all the chains are joined together. One example of a crosslinker is divinylbenzene (DVB); **Figure 4** exemplifies the incorporation of DVB (highlighted in red) into two polystyrene polymer chains.

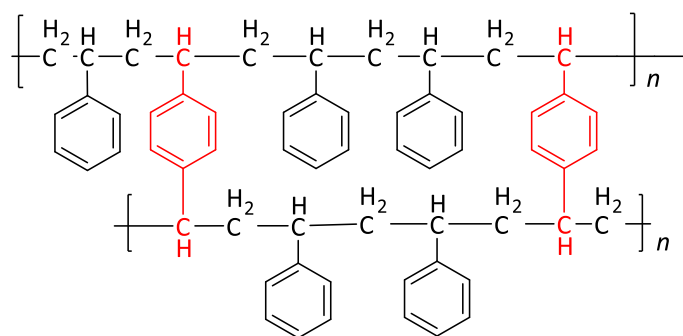


Figure 4: Covalently crosslinked polystyrene

Some other famous examples of crosslinked polymers include: Bakelite¹² (phenol-formaldehyde polymer) and vulcanised rubber (natural rubber treated with sulfur and heat to crosslink linear chains together).¹³ Only a small number of crosslinks are required to produce a material that is useful. However, higher degrees of crosslinking convey mechanical strength to the polymer as well as thermal stability. Crosslinking will also render the material insoluble. Nevertheless, in the presence of a solvent crosslinked polymers will tend to swell as the solvent is taken up by the polymer.¹⁴ The extent to which the polymer will swell is dependent on the affinity of the solvent for the polymer in question and indeed on the degree of crosslinking. This swellable nature of the polymer makes them very attractive for use as functional materials.

1.5 Gel-type and macroreticular polymer particles

The amount of crosslinker and types of solvents that are included in the polymer synthesis will have a bearing on the morphology of the resulting polymer particles. When the amount of crosslinker is low (<20% of the monomer feed)¹⁴ the resulting polymer will be an amorphous, infinite network of polymer chains which interpenetrate one another. The material will also be devoid of any fine structure in the dry state. All the polymer chains will be in contact with one another and the material will therefore have a very low specific surface area. These materials are known as *gel-type polymers*. When contacted

with an appropriate solvent (a solvent with a solubility parameter similar to that of the polymer), gel type polymers will swell and expose porosity within the polymer that can be accessed and utilised for a number of different purposes (some of these will be reviewed later). Unlike linear polymers, crosslinked polymer chains are attached to all the other chains creating an infinite network. This means that the polymer will swell up to a limit but will not dissolve. The amount of crosslinker that is used to create gel type polymers is very important. If too little is used (<1%) the resulting polymer will be weak when swollen and therefore easily damaged. If, however, too much crosslinker is used the material will not swell enough in an appropriate solvent; all the polymer chains will be bound together too tightly to allow penetration of the polymer network by solvent. These highly crosslinked materials would be of little use as the interior network would be inaccessible. This swelling phenomenon is only accomplished when an appropriate solvent is used. Gel-type polymers will not swell in solvents which have a solubility parameter which is significantly different to the polymer. Also, swollen, gel-type polymer beads tend to be soft and compressible which does not make them suited to certain applications.¹⁴

Macroreticular polymers can address some of these issues. The morphology of a macroreticular material is quite different to that of the gel-type materials discussed previously. The porosity in the macroreticular polymers is known to arise from micro-phase separation during the course of free radical polymerisation in the presence of a co-solvent, usually described as a porogen.¹⁵ If a thermodynamically good solvent for the polymer is used, this will help to solvate and swell the growing polymer chains. This allows the micro-phase separation of the polymer to occur at a relatively later stage in the polymerisation process. This causes some of the porogen to remain trapped in the growing polymer network's primary particles. As these primary particles collide and aggregate together, they form the final polymeric material. Upon drying, the trapped porogen is removed, leaving behind voids which are all interconnected, creating a permanently porous architecture. This means that, unlike gel-type polymers, macroreticular polymers have a permanent and well-defined pore structure, even in the dry-state, with typical specific surface areas ranging from ~50 to ~1000 m²/g.¹⁴

Non-solvents for the polymer can also be used as porogens, One good example being the use of *n*-heptane in the synthesis of poly(styrene-*co*-divinylbenzene).¹⁶ This non-solvent for the polymer leads to early phase separation of the growing microgels within the monomer droplets. Generally, albeit with some exceptions,¹⁷ this leads to materials that have much lower specific surface areas but higher overall pore volume when compared to the same material prepared with a thermodynamically good solvent as the porogen.¹⁸

Linear polymers and short oligomers have also been utilised as porogens. Polymethacrylates, polystyrene and poly(dimethylsiloxane) (PDMS), amongst others, have all been shown to be effective porogens for the formation of macroreticular materials.^{19–22} The mechanism by which porosity is imparted when using polymers and oligomers as porogens is similar to that observed when a non-solvent is used as a porogen.²³ Due to this mechanism, these materials will typically display low overall specific surface areas but higher pore volumes.²⁴ Interestingly, Macintyre and Sherrington reported²¹ that a bi-modal size distribution of pores was attainable in the polymerisation of DVB, whilst retaining modest specific surface area. A thermodynamically good solvent for DVB (toluene) was used along with PDMS as the porogen system. The toluene produced much smaller pores while the PDMS was able to produce much larger pores.

Unlike gel-type polymers, permanently porous materials do not require swelling for access to the porous interior of the particles. Therefore, as long as the polymer particles are suitably wetted with an appropriate solvent, the interior structure of a macroreticular polymer can be accessed by almost any solvent.

1.6 Polymer microspheres and their synthesis

Polymer microspheres are, as the name suggests, polymers that when synthesised take the form of very small beads or particles. The exact dimensions of the particles are dictated by the synthesis method that is used to make them. For clarity, some of the methods by which crosslinked polymer particles can be synthesised will now be briefly reviewed. Suspension, precipitation and dispersion polymerisation are all considered to be conventional polymerisation techniques, and are used routinely in academia and in

industry.²⁴ They also form the three main synthetic routes that were employed in the preparation of the materials presented in this work.

1.6.1 Suspension Polymerisation

Suspension polymerisation is an important process that is used to produce many industrially significant polymers, including, *inter alia*: polystyrene, poly(vinyl chloride) (PVC), poly(vinyl acetate), polyacrylates and numerous ion-exchange resins.^{14,25–28}

Producing polymer using a heterogeneous suspension of monomer droplets in a polymerisation medium, the latter often called the *continuous phase*, can trace its roots to the work of Hofman and Delbrück in the early 1900s.^{29,30,31} In most suspension polymerisations, polymer is formed *via* a chain-growth mechanism, as has been discussed previously. The process begins with the addition of an initiator to the monomer (including crosslinker) – the initiator should be soluble in the monomer. A porogen may also be included in the monomer phase if the desired polymer is to be macroreticular. This solution (or *monomer phase*) is then added to the polymerisation medium in which it is insoluble. The monomer phase is suspended as stable droplets in the continuous phase by stirring the mixture. The stability of the droplets is aided by the addition of suspension stabilisers. The polymerisation is then initiated, usually by heating. The monomer droplets are then converted directly into polymer microbeads of approximately the same dimensions as the monomer droplets. In suspension polymerisations, each monomer droplet can be viewed as an individual, small bulk or solution reactor. It is therefore presumed that the polymerisation kinetics are similar to the corresponding bulk polymerisation or, in cases where a porogen is included, solution polymerisation. This presumption is based upon seminal work investigating the polymerisation chemistry and reaction kinetics that occurs within the monomer droplets.²⁵ It has been noted²⁶ that polymer precipitation within the droplets may produce chemistry that is not observed in bulk polymerisation. Also, another complication that may cause the kinetics and mechanism to deviate from those observed in the bulk is radical desorption. If the monomer droplets are small enough, radical species (produced from the initiator) may desorb into the continuous phase. It has been

suggested that, in these cases, the reaction mechanism will become similar to that observed in microemulsion polymerisations.³²

1.6.1.1 The continuous phase

In most suspension polymerisations, the continuous phase is water. Due to most polymerisations being exothermic, the water allows for efficient heat transfer away from the polymerisation. These polymerisations are termed oil-in-water (O/W). If water soluble monomers are to be used to produce polymer, the suspension polymerisation can be carried out in the opposite way, *i.e.*, a water-in-oil (W/O) suspension. An aqueous solution which contains the monomer and initiator is suspended in a continuous phase that is usually a paraffin or silicon oil.²⁵ Some examples of polymers produced by this method include polyacrylates, as well as co-polymerisations of acrylamide and bisacrylamide to produce acrylamide polymer supports.^{25,33}

1.6.1.2 Suspension Stabiliser

A suspension stabiliser is included in the continuous phase to help avoid coalescence and agglomeration of the polymer particles as they form. The stabilisers are initially dispersed in the continuous phase where they quickly move to the surfaces of the monomer droplets. However, stability may not be achieved immediately as the stabiliser molecules rearrange on the surface of the monomer droplets.³⁴ One way in which stabilisers work is to lower the interfacial tension of the monomer droplets and therefore lower the amount of energy that is needed for the droplet to form.. Work by Borwanker *et al.* has shown that by increasing the amount of stabiliser the elastic properties of the forming beads can be improved and therefore improve the overall stability of the monomer droplets.³⁵ The stabilisers act to produce a protective film at the interface of the monomer droplets. This can help to stop polymer beads from coalescing and agglomerating together. Common stabilisers that are used in O/W suspensions are natural and synthetic water soluble polymers, including: polyvinylpyrrolidone (PVP), poly(vinyl alcohol), poly(vinyl acetate), as well as numerous natural gums and

cellulose.^{25,26} Some insoluble inorganic salts, including calcium phosphate, have also been used as stabilisers in suspension polymerisation. When inorganic molecules are used as suspension stabilisers, some surfactants may be necessary to aid stabilisation.^{36,37}

1.6.1.3 Particle size and bead morphology

Polymer particles produced by suspension polymerisation are usually in the size range of about 1 μm to 1 mm, with the particles that are produced usually being polydisperse. However, there are numerous factors that can affect the size of the monomer droplets and therefore the size of the resultant polymer beads, as well as the size distribution of these beads. The size of monomer droplet can be altered by changing the stirrer speed, the stirrer shape, the shape and dimensions of the reaction vessel as well as the volume ratio of monomer to continuous phase.²⁵ It has been shown that the concentration and chemical nature of the stabiliser used can have an effect on the polymer bead size.^{38,39} It has also been reported that the morphology (including porosity) and polymer particle size distribution can also be affected by the type of stabiliser that is used.⁴⁰⁻⁴² The effects that all of the above have on the particle size can be seen in the relationship shown in **Equation 4**.

$$\bar{d} \cong \frac{K, \sigma, \phi}{L, N, P}$$

Equation 4: Relationship between describing how suspension polymerisation parameters can affect average particle diameter, where \bar{d} is the average polymer particle diameter; K represents the reactor design, stirrer type, any self-stabilisation that may occur etc.; σ is the interfacial tension of the monomer droplets; ϕ is the volume fraction of the monomer droplets; L is the diameter of the stirrer; N is the stirrer speed and P is the density of the monomer droplets

Reports have also shown that the conditions within the reactor can have a large effect on the size and size distribution of the monomer droplets and therefore the resultant polymer beads. Due to the agitation of suspension polymerisations, excessive friction (viscous shear) or turbulence within the reactor can also cause monomer droplets to

break apart (see reference²⁶ for more details on viscous shear and turbulent flow in suspension polymerisation).

It can therefore be seen that producing high quality materials *via* suspension polymerisation is governed by numerous factors and can be incredibly difficult to do reliably and reproducibly. It is for this reason that suspension polymerisation is often described as an art form rather than an exact science.^{25,43} In certain applications,⁴⁴ it is of the utmost importance to have particles that are all monodisperse, *i.e.*, particles that are all the same size. While this can be seen as quite an obvious drawback to suspension polymerisation, suspension polymerisation is used routinely in industry nevertheless due to the low costs, versatility and the possibilities for upscaling. If particles of a specific size range are required, then the resultant polymer particles are simply sieved to obtain the size range of interest.

1.7 Precipitation Polymerisation

Precipitation polymerisation was first reported by Stöver and co-workers⁴⁵ in 1993 as an improvement on a method reported previously by Bamford *et al.*⁴⁶ Precipitation polymerisation begins with initiator and monomer (including crosslinker) dissolved in a solution of a near- Θ solvent and, if desired, a porogen (the continuous phase), to create a homogenous solution.

A Θ solvent for a given polymer, is one that can negate the effects of excluded volume expansion. In a dilute solution, the conformation of a polymer chain is dependent upon interactions between different sections of the polymer chain, as well as between the polymer chain and solvent molecules. Different sections of the polymer chain cannot physically occupy the same space at the same time. This excluded volume causes the polymer to expand, in attempts to minimise polymer-polymer interactions. In a thermodynamically good solvent, the polymer chain will extend to maximise polymer-solvent interactions. In a thermodynamically bad solvent, polymer-polymer interactions dominate, and the polymer coil will contract to maximise these interactions. A Θ solvent is just thermodynamically poor enough to cancel out the excluded volume effect, but not

so poor as to cause polymer-polymer interactions to dominate and cause contraction of the polymer chains.

Precipitation polymerisation is often still considered a heterogeneous technique, like suspension polymerisation, as polymer nuclei begin precipitating from the reaction mixture at a very early stage of the polymerisation. However, precipitation polymerisation is a nucleation and growth process, whereas the monomer droplets in suspension polymerisation are converted directly to polymer. Both oligomers and polymer nuclei are formed as the synthesis begins. The nuclei begin to precipitate out of solution while the oligomers remain soluble in the continuous phase. The nuclei grow *via* the addition of fresh monomer and oligomers that are still dissolved in solution. If a porogen is included in the polymerisation, as in suspension polymerisation the phase separation of the particles happens slightly later (in the case of thermodynamically good solvents) and some of the co-solvent is trapped within the growing polymer particles and, upon drying, a permanent porous structure is left, giving a macroreticular morphology.

The lack of stabilisers in precipitation polymerisation has led to some discourse within the academic community as to how stable particles are formed *via* this method. In 1991 Downey and co-workers proposed⁴⁷ that the surfaces of the polymer particles were composed of a partially crosslinked gel layer, which is swollen by the solvent, and is able to stabilise the particles as they form. The short-lived gel layer will desolvate and collapse in a decomposition that is both driven and curtailed by crosslinking. In 1999, Shim *et al.* proposed⁴⁸ that the particles produced were very much dependant on the level of crosslinker that is used. It was suggested that by increasing the levels of crosslinker, a greater degree of hardness is imparted into the polymer beads. This hardness helps to prevent discrete particles from fusing with one another.

Most polymers produced by precipitation polymerisation have some common features: for example, highly monodisperse particles are not uncommon, and with tailoring of reaction conditions the experimenter can expect beads in the 0.1 – 10 μm size range. Precipitation polymerisation is normally carried out using high levels of crosslinker, with instances of crosslinker being the only monomer present being reported commonly in the literature.^{49,50} The process of precipitation polymerisation is performed under highly dilute monomer concentrations (<5 % w/v monomer in relation to the total solvent

volume) in order to avoid coagulation of the polymer particles.⁴⁹ The problem with this method is that a lot of solvent is needed to produce a small mass of polymer, for example if one wanted to synthesise 2 kg of polymer upwards of 40 litres of solvent would be required, which is not very attractive to the industrial polymer chemist. However, repeated usage of solvent with monodisperse particles still being attainable has been reported in the literature.⁴⁹ This high dilution of monomer tends to result in precipitation polymerisations being rather sluggish when compared to suspension polymerisation. The overall yields in precipitation are often modest when compared to suspension polymerisation. However, precipitation polymerisation can be used routinely to produce near mono-disperse polymer particles.⁴³⁻⁴⁵ Having micron sized particles that are monodisperse make materials that are prepared *via* precipitation polymerisation very attractive for use in numerous applications. One particular example is chromatography - monodisperse particles can aid mass transfer of analyte on the column. It has also been found that column performance, in liquid chromatography, can be improved by reductions in the particle size distribution of particles used in the column.⁵⁴

Precipitation polymerisation is an attractive synthetic strategy as material can be produced quickly, efficiently and easily. This simplicity is highlighted by the fact that it does not require any additives or stabilisers and that low micron sized monodisperse or near monodisperse particles can be produced as a matter of routine.

As well as chromatography, precipitation polymerisation has been used to produce materials with interesting or unusual morphologies, such as Stöver's 'onion-type' microspheres⁵⁵; polymer supports for use in oxidative organic flow chemistry⁵⁶, the synthesis of molecularly imprinted polymers (MIPs)⁵⁷, as well as precursors to hypercrosslinked polymers^{52,58-61}.

1.8 Dispersion Polymerisation

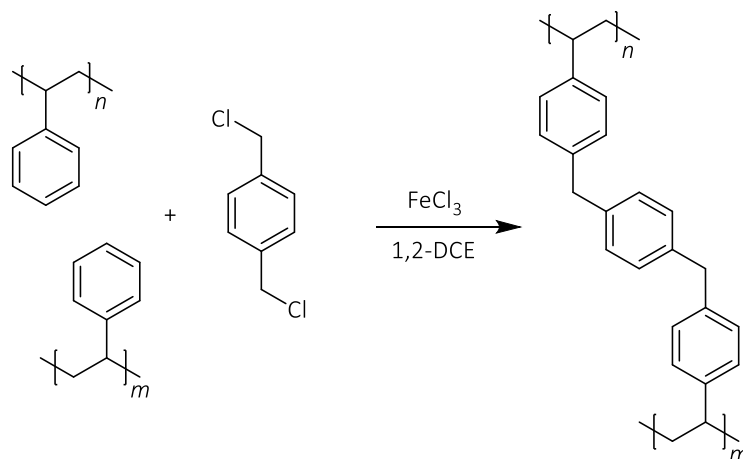
Dispersion polymerisation, like precipitation polymerisation, begins as a homogeneous solution. This method is usually used to produce linear or lightly crosslinked materials and polymers that are non-porous in the dry state.

Monomer, initiator, and a polymeric stabiliser (such as polyvinylpyrrolidone) are dissolved in solvent, usually an alcohol, for example ethanol or methanol. Upon heating, oligomers begin to form, all of which are still soluble in the reaction medium. As the oligomers grow, they begin to precipitate from solution, thus forming the nuclei of the polymer particles. These nuclei are stabilised by the polymeric species added at the beginning of the reaction. Again, polymer is formed from the nuclei's capture of monomer/oligomer from the solution. If crosslinker is to be added to the reaction it should preferably only be done so after the nucleation stage of the reaction, corresponding to $\sim 1\%$ monomer conversion. Winnik *et al.* have investigated and explained why the addition of crosslinker and certain co-monomers must be delayed.^{62,63} It was thought that the crosslinker and co-monomers were interfering with the highly sensitive nucleation phase of the reaction. If these reagents were added after the nucleation phase had occurred, it was found that they were incorporated into the final polymer without disturbing the size or the size distribution of the polymer particles. Extensive work in this area has also been carried out within the Cormack research group here at Strathclyde.⁶⁴ This body of work also highlighted the very sensitive nature of the nucleation phase, with very small changes to the reaction parameters having drastic effects on the resultant particles. Initial monomer concentration, solvent composition, the type of stirrer and even the material the stirrer is made of were all shown to influence particle size and particle size distribution.

1.9 Hypercrosslinking

In the early 1970s, Davankov *et al.* patented⁶⁵ a method for the formation of extensive crosslinking between the aromatic rings of linear polystyrenes. This was achieved

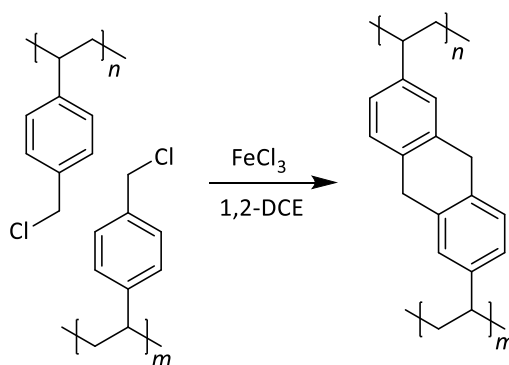
through a Friedel–Crafts reaction using an external electrophile as a crosslinking agent, in the presence of an appropriate Lewis acid. Originally, this process was carried out using external crosslinkers such as, chloromethyl ether (CME)^{66,67} and carbon tetrachloride.^{68,69} However, due to both reagents being acutely toxic and carbon tetrachloride being an ozone-depleting agent, their use in this regard has all but ceased. Molecules such as monochlorodimethyl ether⁷⁰ and 1,4-*bis*(chloromethyl),^{71,72} as shown in **Scheme 7**, are therefore more commonly used as external crosslinkers.



Scheme 7: Hypercrosslinking of polystyrene using the external electrophile 1,4-*bis*(chloromethyl)benzene

Davankov's hypercrosslinking was remarkable in that the polymer products produced can have specific surface areas greater than $1000 \text{ m}^2/\text{g}$.¹⁵

For polymers containing an appropriate comonomer, such as 4-(chloromethyl)styrene (vinylbenzyl chloride), hypercrosslinking is also possible. The polymer particles are simply swollen in a thermodynamically good solvent, such as dichloroethane, and heated in the presence of a Lewis acid, such as iron trichloride (**Scheme 8**).



Scheme 8: Hypercrosslinking of poly(vinylbenzyl chloride)

This intramolecular hypercrosslinking reaction has been shown to be highly efficient. Ahn *et al.*⁷³ reported that a gel-type resin prepared by suspension polymerisation could be almost exhaustively hypercrosslinked after only 15 minutes. This was evident by a drastic decrease in Cl content, falling from nearly 20% to less than 2%. This marked drop in chlorine content was also accompanied by a considerable increase in the dry state specific surface area of the sample, rising from almost no surface area whatsoever, in the dry state, to more than 1000 m²/g. The first materials to be hypercrosslinked were derived from linear polymer precursors. However, more recently, hypercrosslinked materials that were produced from lightly crosslinked polymer particles have also been synthesised. Non-porous, gel-type particles produced by either precipitation, suspension or dispersion polymerisation can be hypercrosslinked,^{51,52,74,75} with the non-aqueous dispersion (NAD) polymers tending to produce the most uniform and monodisperse hypercrosslinked polymer particles. Dispersion polymerisation routes tend to yield hypercrosslinked particles that are irregular in size and show a tendency to agglomerate. This is of importance due to the end applications of such materials, such as chromatography and solid-phase extraction, where the uniformity of particles is of importance. As previously discussed, beaded polymers rather than irregularly shaped particles (such as those obtained when hypercrosslinking linear polymers) are usually better in these applications. Abdullah⁶⁴ reported a novel method to produce monodisperse hypercrosslinked polymers where the precursor particles had been produced by dispersion polymerisation. This method involved partially hypercrosslinking the particles in a non-swelling solvent, such as heptane, in a bid to stabilise the particles.

This was followed by exhaustive hypercrosslinking in a swelling solvent. The need for this stabilisation step was proposed to be due to the precursor particles containing some soluble polymer. Upon swelling in solvent this soluble portion would be released and free to react with the polymer particles as they were hypercrosslinking, thus producing particles with rough and uneven surfaces.

Hypercrosslinked polymers can also be synthesised through the self-condensation of certain molecules. This works in much the same way as the internal or external electrophiles described above. However, in the self-condensation examples Friedel-Crafts chemistry is used to create methylene bridges between small molecules until a network is produced, rather than joining two polymer chains together. Davankov and co-workers showed that a microporous polymer could be produced from the self-condensation of 1,4-*bis*(chloromethyl)benzene.⁷⁶ However, the resultant microporous polymer had only a modest specific surface area. More recently, this body of work was investigated more thoroughly by Cooper *et al.*^{72,77} They found that by using the larger 4,4'-*bis*(chloromethyl)biphenyl, much higher specific surface areas could be achieved, with values upwards of 1800 m²/g being reported. Porosity and specific surface area could be enhanced or suppressed by tailoring of the reaction conditions. Continuing the theme of producing porous polymers directly from small molecules rather than the post-polymerisation chemical modification of polymers by utilizing 1,4-*bis*(chloromethyl)benzene and carbazole and reacting them *via* Friedel-Crafts alkylation, Buhnia *et al.* were able to produce a highly microporous hypercrosslinked polymer.⁷⁸ This material exhibited a BET specific surface area of nearly 1000 m²/g. Upon sulfonation, this material was shown to be a highly efficient solid acid catalyst that was used to produce biodiesels from fatty acids and esters.

Hypercrosslinking chemistry has also been shown to be a successful strategy in the production of somewhat more exotic hybrid materials. Benzyl chloride-terminated cubic siloxane cages can, through self-condensation, give an organic-inorganic hybrid material exhibiting an ultra-high specific surface area of 2500 m²/g.⁷⁹ With a pore volume of 3.3 cm³/g, this material was of particular interest. Such high pore volumes are unheard of in porous siloxane-based materials.⁵⁹ Carboranes have also been exploited in a similar fashion. By grafting two benzyl chloride moieties onto the carborane and then self-

polymerising this material, Yuan and co-workers produced a material that had a specific surface area of 864 m²/g.⁸⁰ While this may seem like a rather modest surface area when compared to some other hypercrosslinked materials, this material was of particular note because it possesses a highly electron deficient architecture. This electron-deficiency was shown to enhance hydrogen-polymer interactions and therefore this material exhibited very high H₂ adsorption.

Research towards the synthesis of high surface area materials using more facile chemistry, that utilises milder reaction conditions and less expensive starting materials, has been exhibited. In 2011, a new synthetic approach was proposed by Tan *et al.*⁸¹ Using straight-forward Friedel-Crafts chemistry, they were able to use formaldehyde dimethyl acetal (FDA) to link together simple small molecules, such as benzene and biphenol to produce hypercrosslinked materials. The term 'knitting' was used to describe this process. By varying the ratio of FDA to benzene, specific surface areas of up to 1300 m²/g could be achieved. Researchers have applied this 'knitting' strategy to larger planar aromatic molecules, such as triphenyl benzene as well as 3D building blocks such as tetraphenyl methane and triptycene.⁸²⁻⁸⁵ This later molecule, with an optimal FDA to monomer ratio, could exhibit a specific surface area as high as 1314 m²/g. Tetraphenyl methane containing knitted, hypercrosslinked polymers have shown promise as methane and carbon dioxide adsorptives.⁸² Linear polystyrenes have also been crosslinked to produce hypercrosslinked materials using FDA as a crosslinker, with surface areas of 974 m²/g being achieved.⁸⁶ Using FDA as an external crosslinker, hypercrosslinked polymers from a gel-type precursor have also been produced. Maya *et al.* demonstrated this using a poly(styrene-co-DVB) gel-type resin.⁸⁷ It can be seen, therefore, that this 'knitting' approach is versatile and applicable to a wide range of starting materials. Also, by using FDA as a crosslinking agent, the use of chlorinated crosslinkers and co-monomers such as 1,4-*bis*(chloromethyl) benzene or vinylbenzyl chloride can be avoided. This is of benefit due to the vast cost differential, with FDA being significantly cheaper. Also, removing chlorinated species has obvious environmental as well as health and safety benefits.

Computational chemistry has become an invaluable tool for synthetic chemists, and this is starting to see some use in the polymer chemistry sphere, specifically in the area of

hypercrosslinked materials. Using computer programs, such as *Polymatic*,⁸⁸ chemists are attempting to use molecular simulations to gain insight into both polymerisation and hypercrosslinking processes.⁸⁹ Colina and co-workers have simulated the hypercrosslinking of a linear poly(styrene-*co*-VBC) utilising the VBC moiety as an internal crosslinker.⁹⁰ In varying the VBC content of the simulated polymers, they were able to demonstrate similar trends in surface area as had been observed experimentally, *i.e.* higher levels of VBC will produce a material that displays a higher specific surface area. Further to this work, they have also simulated the hypercrosslinking process in a poly(styrene-*co*-VBC-*co*-DVB). In this work, Colina *et al.* were able to show that by varying the DVB content in the precursor polymer, the pore size of the final hypercrosslinked polymer could be tuned.⁹¹ This work was also shown to match previous experimental work by Li and co-workers.⁶⁰ Utilising computational chemistry in this manner, in conjunction with a synthetic approach, has aided experimentalists to gain much better insight into hypercrosslinking at the molecular level and reveal details about the process of pore formation that could not be obtained with experimentation alone. Also, by using computational chemistry to guide the synthesis, a potentially more effective and efficient approach can be taken to investigating these fascinating, high surface area materials.

One rather interesting feature of note for all hypercrosslinked materials is their ability to uptake not only thermodynamically compatible solvents, but also thermodynamically unfavourable or 'bad' solvents. This has been reported by different groups,^{53,73,92} and means that the polymers that can act, as Cormack and co-workers described in 2008, as 'amphipathic polymer sponges'. This unusual behaviour is thought to be caused by the swelling of the polymer particles during the hypercrosslinking process. After hypercrosslinking the solvent is removed, and this results in a partial collapse of the polymer network, leaving behind a now dry hypercrosslinked polymer that contains a great deal of strain. When the polymer is contacted with a solvent, either hydrophobic or indeed hydrophilic, the polymer is able to swell to some extent, relieving some of the stress. This solvent uptake, even of solvents that are thermodynamically unfavourable, is preferred over the strain experienced when the polymer is dry.

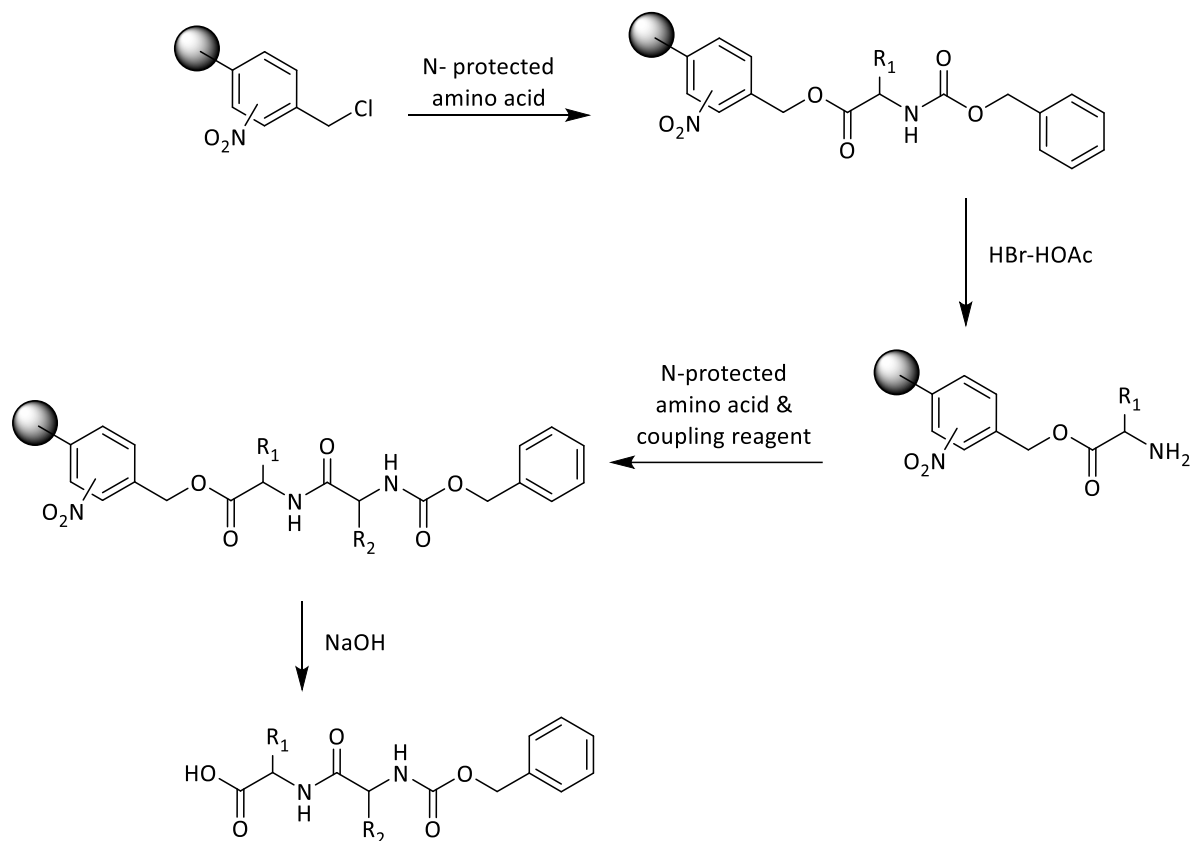
1.10 Crosslinked Polymer Particles and Their Applications

Attaching or installing a functional group into a polymer can be achieved in a number of different ways. The main motivation for doing this is that it allows the polymers to be tailored for a specific application. As well as synthesising copolymers of functionalised monomers, it is also possible to functionalise polymers post-polymerisation. Modifications or chemical reactions can be carried out on pendent functional groups, to impart a particular functional moiety, or to alter the physical properties of the polymer in some way, *e.g.*, though hypercrosslinking.

Polystyrene is the polymer most often used as a bearer of functionality. Polystyrene has high compatibility with many organic solvents, is relatively inexpensive and can undergo electrophilic aromatic substitution reactions giving a wide access to many different possible functionalities. Chloromethylstyrene is routinely used as a monomer instead of or in combination with styrene, and this installs a functional handle through which one can attach functional groups to the polymer. This can be achieved rather simply through either electrophilic or nucleophilic substitution reactions. Functionalised porous polymers have found applications in a wide variety of fields.

1.11 Solid-Phase Peptide Synthesis

In 1963 Robert Bruce Merrifield reported⁹³ a new method of peptide synthesis which involved the stepwise addition of protected amino acids to a growing peptide chain which was covalently attached to a solid-phase (polymer resin) *via* the C-terminus. Due to the growing peptide being in the solid state at all times, he used the term solid-phase peptide synthesis (SPPS) to describe this process. Robert Bruce Merrifield won the Nobel Prize in chemistry in 1984 for this work. A generalised reaction scheme for this method is shown in **Scheme 9**.



Scheme 9 – Solid-Phase Peptide Synthesis (SPPS)

A chloromethylated polymer support was used to provide an attachment point for the first amino acid in the peptide chain. The need for nitration of this polymer was reported to be because the HBr/acetic acid used in the cleavage of the peptide protecting group also caused cleavage of the ester linkage holding the peptide chain to the polymer. This method of peptide synthesis had many advantages over the usual (solution-phase) peptide synthesis methods of the time. By immobilising the peptide on a polymer, it is in a form that can be easily washed and filtered to free it from any contaminants or by-products after each of the steps in the reaction. It was also advantageous in that it shortened the amount of time taken to synthesise the peptides, and the methodology lends itself well to automation.

In the intervening 50 or so years since Merrifield's seminal work, there have been great leaps in SPPS, with more recent work⁹⁴ showing that coupling of amino acids onto resins which have amine functionality can be completed in less than an hour at ambient

temperatures. This is due in no small part to the extensive development of coupling reagents and catalysts over the years. These have been required as more molecules are discovered that can have very highly functionalised amino acids that cannot be synthesised as easily using more traditional synthesis methods.⁹⁵

Gel-type polymers are the polymer type most commonly encountered in SPPS. Due to their low levels of crosslinking, they are able to swell in an appropriate solvent. In his ground-breaking work, Merrifield discussed the swelling of the polymer and the importance of solvent choice in this regard. He noted that a swellable polymer was required to allow the penetration of reagents into the polymer network. Merrifield also observed that for the solvent to be effective it needed to possess not only an ability to swell the polymer but also have a high dielectric constant. This works well for a solvent that can swell the polymer, but what would happen if a non-solvent was required to complete the transformation? It is here that permanently porous polymers can be more appropriate. Sinigoi *et al.* have reported^{96,97} the use of Synbeads - rigid, macroporous methacrylate polymers - in solid-phase peptide synthesis. These novel materials showed not only ease of handling and high chemical stability, but also higher degrees of productivity when compared to gel-type swellable polymers. It was also noted that space restrictions can cause problems when the desired target molecule is quite large (such as a peptide). Macroporous polymers can be useful as they can provide room to accommodate the growing peptide chain. Generally speaking, small polymer particles can cause filters to clog during washing steps, and it is for this reason that much larger particles are preferred for this particular application, 100 – 500 μm being typical. Particle shape and indeed monodispersity are not normally a critical characteristic with solid-phase synthesis, therefore suspension polymerisation⁹⁸ is considered to be an appropriate method for the synthesis of particles to be used in solid-phase synthesis.

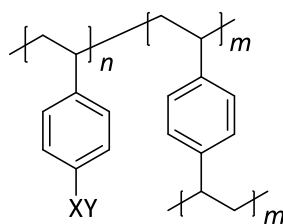
1.12 Chromatography

Beneš *et al.* discussed,¹⁸ at length, the manufacture and use of methacrylate-containing polymers in different types of chromatography. They opined that small (generally between 2 and 5 μm) beads that are monodisperse are required to obtain results that

are reproducible from a packed chromatography column. Whilst silica packed columns are the norm in HPLC, porous polymers have found use in certain types of size-exclusion chromatography (SEC). SEC separation of polymers is based on the premise that smaller polymer chains will spend a longer time within the pores of the packed beads in the column as compared to larger chain polymers. In 2005, Davankov eloquently demonstrated the use of microporous hypercrosslinked polystyrene as a medium for the selective separation of pairs of electrolytes.⁵⁸ It was found that the selectivity in separation was based upon the larger ion in each pair. It was also noted that, as the concentration of the solutions was increased the selectivity of the separation also improved. The electrolyte solution was the mobile phase, and as it became more concentrated more small ions were excluded into the smaller pores of the polymer column that the larger ions were not able to access.

1.13 Ion-Exchange and Sorption

Ion-exchange resins were one of the first porous polymers to yield a viable commercial product.⁹⁹ Many ion-exchange resins are based on crosslinked poly(styrene-co-DVB) which has been imparted with chemical functionality which displays ionic character (**Figure 5**). This allows the combination of a hydrophobic network with a high specific surface area, typically between 500 and 800 m²/g. The incorporation of ion-exchange functionality results in a material which will have a mixed-mode retention mechanism. That is, organic molecules have the ability to interact with the hydrophobic backbone of the polymer through hydrophobic effects, whilst any analytes with ionic functionality can interact with the ionic functionalities that have been installed into the polymer, provided that their functionalities are complementary.



Where X and Y are: SO_3^- and H^+ , CO_2^-
and Na^+ or NH_3^+ and HO^- etc.

Figure 5 - Typical structure of an ion-exchange resin

One example of particular note is the sulfonated cation-exchange resin first synthesised in the early 1950s by Pepper.²⁷ Poly(styrene-co-divinylbenzene) was prepared *via* suspension polymerisation and the resultant material was subsequently treated with excess concentrated sulfuric acid in the presence of a silver sulfate catalyst. This particular material has received much attention due to its ability to exchange ions such as calcium and magnesium, which has been of great use in softening water (**Figure 6**) where the sulfonate's counter-ion is exchanged for the cations present in hard water. The uncrosslinked variant, *i.e.*, poly(styrene sulfonate), has also found use in the medical field for more than 50 years, where it has been used to scavenge potassium ions in patients suffering from hyperkalaemia.¹⁰⁰ A patent filed in 1951 by the Monsanto Chemical Company makes claim to a method of producing non-crosslinked, water soluble, poly(styrene sulfonate).¹⁰¹ Polystyrene was sulfonated in a chlorinated solvent utilising a combination of sulphur trioxide and 1-chloro-2-(2-chloroethoxy)ethane as a sulfonating agent. The inventors explained that this method was developed as attempts to apply methods that had been used to produce crosslinked sulfonated polystyrenes in the manufacture of uncrosslinked variants had been unsuccessful. Sulfonating agents such as sulfuric acid, such as was described by Pepper,²⁷ sulfur trioxide or chlorosulfonic acid were all found to be unusable as the resultant polystyrene sulfonate could not be readily removed from the sulfonating reagent. Since then there have been disclosures of proprietary methods for producing poly(styrene sulfonate), using both sulfuric acid¹⁰² and chlorosulfonic acid.¹⁰³

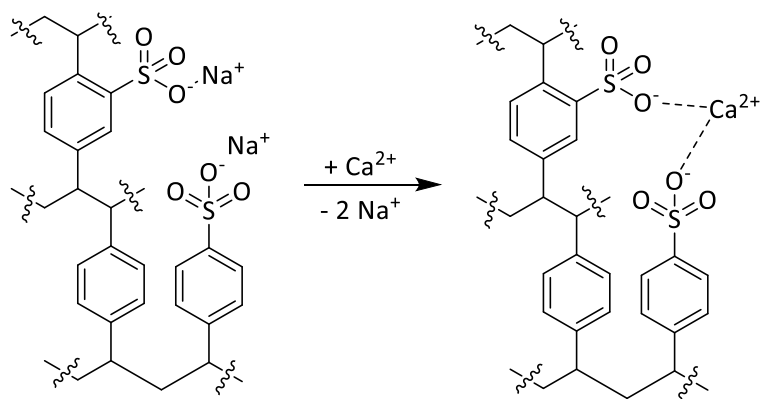
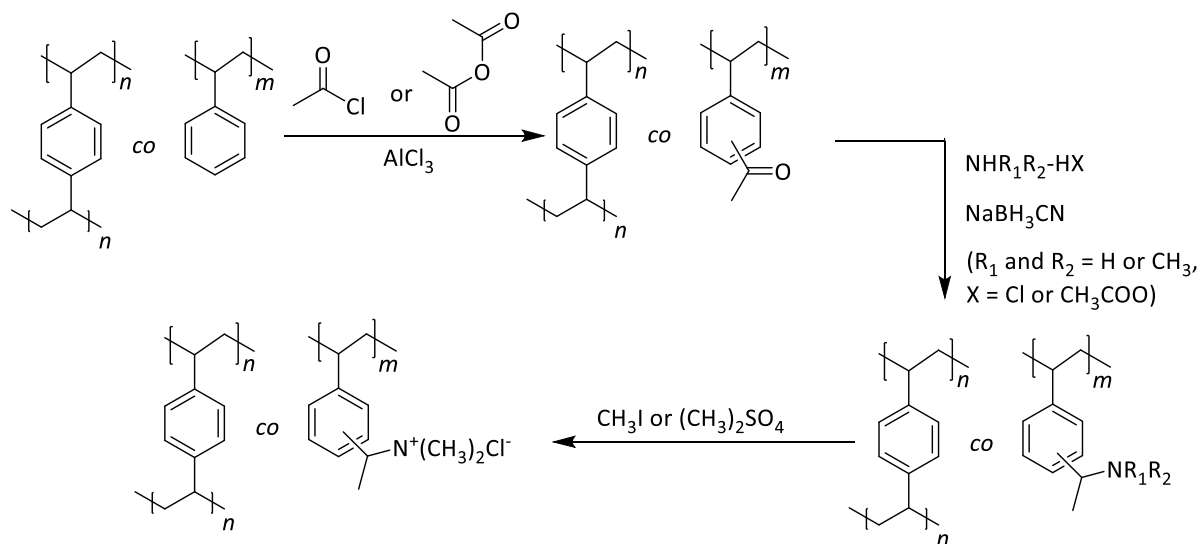


Figure 6: Water-softening cation exchange

The example presented in **Figure 6** is of a cation-exchanger, but the opposite is also possible where instead of a cationic functionality the polymer has been functionalised with moieties that exhibit anion-exchanging abilities. In 1999, Xu and co-workers presented a novel method for the preparation of anion exchangers accessed *via* the reductive amination of acetylated crosslinked polystyrene (**Scheme 10**).¹⁰⁴



Scheme 10- Preparation of polystyrene-based anion exchanger

The convention at that time for the preparation of anion-exchange resins was to react the unfunctionalised polystyrene with a chloromethylating agent, such as chlorodimethylether or *bis*-chlorodimethylether, both of which are known to be highly carcinogenic, followed by treatment with an amine to install anion-exchange functionality. By introducing acetyl groups instead, using either acetyl chloride or acetic anhydride, in the presence of a Friedel-Crafts catalyst, Xu *et al.* were able to avoid the use of rather toxic chloromethylating agents. This acetylated intermediate was then reacted further with an amine in the presence of a reducing agent, and the product could then be further reacted with methyl iodide to furnish the anion-exchange moiety. Xu reported that secondary amines prepared *via* this method were as good as their commercially available counterparts, and that quaternised exchange resins also showed high levels of exchange capacity.

Ion-exchange resins based upon hypercrosslinked polymers have also received much attention with regards to sorption and ion-exchange chemistry; one such application where they have been utilised widely is in solid-phase extraction (SPE).

SPE is a method of removing and enriching, for the purposes of chemical analysis, a solute from solution. Sorbent particles are packed into a cartridge which will adsorb (most often hydrophobic) solutes. The solutes can then be rinsed (eluted) from the sorbent, ready to be analysed. As one can envisage, the interaction time between the sorbent and the analyte is very short, therefore a very high demand is placed on the sorbent material. It is for this reason that hypercrosslinked polymers, with their high specific surface areas, have found extensive applications in this area.

Fontanals and co-workers presented⁵² a successful modification of hypercrosslinked polymers. After hypercrosslinking in the usual manner, as previously discussed, it was found that not all of the chloromethyl moieties had undergone hypercrosslinking. This allowed the now hypercrosslinked polymers to be subjected to post-polymerisation chemical modification reactions which exploited pendent (unreacted) chloromethyl groups. The sorbents were reacted with both piperazine and 1,2-diaminoethane to deliver materials that exhibited anion-exchanging capabilities. It was reported that the performance of these materials in the solid-phase extraction of analytes from real water samples was superior to that of commercially available sorbents. This was opined to be

due to the commercial examples having lower specific surface areas and therefore having poorer analyte retention.

Following on from this work, in 2010 the sorbents that had been produced were evaluated in on-line solid-phase extraction. This allowed for a degree of automated determination to be involved in the process.⁷⁵ Large volumes of water (purified, river water and effluent sewage water were all investigated) were introduced to the sorbent materials and it was reported that astonishingly high levels of acidic contaminants of interest could be recovered; recoveries were reported to be 100% in some cases.

Work by Cormack *et al.* has also highlighted the ability to produce hypercrosslinked polymers that exhibit cationic-exchange abilities.^{51,74} Carboxylic moieties present in methacrylic acid used as a comonomer resulted in polymers with weak-cation exchange character. It was also reported that by reacting hypercrosslinked polymers with either acetyl sulfonate or lauroyl sulphate a sulfonated material yielding strong cation-exchange character could be produced.⁵¹

Similar sorbents, albeit non-hypercrosslinked, have been commercialised by different companies for use in-solid phase extraction. Phenomenex's Strata-X brand¹⁰⁵ and the Oasis¹⁰⁶ range of products from Waters, are two such examples. Strata, a poly(styrene-co-divinylbenzene) copolymer modified with pyrrolidone moieties, has been functionalised with sulfonic acids and quaternary ammonium groups to produce materials exhibiting strong ion-exchange character. Carboxylic acid groups and piperazine functionality have also been used, imparting weak ion-exchange character. Waters, in a similar vein, have produced ion-exchange materials that are made from a specific ratio of hydrophobic divinylbenzene and hydrophilic *N*-vinyl pyrrolidone which is a neutral polar moiety giving enhanced retention of polar analytes. The different functionalities allow for different analytes to be adsorbed by the polymer depending on the application in mind and the molecules to be analysed. Hydrogen bonding, hydrophobic interactions, dipole-dipole interactions and π - π stacking interactions can all be exploited using polymers of this type. The companies highlighted above are just two commercial examples, with polymeric sorbents for use in SPE being commercialised by more than 50 companies.¹⁰⁷

1.14 Sorption of Polycyclic Aromatic Hydrocarbons (PAHs)

Polymeric materials such as those discussed above for use in SPE were used in the extraction of pharmaceuticals from both standard solutions and real water samples. Porous polymer particles and other macromolecular materials can also be used to sorb other analytes of interest. A group of analytes that are pertinent to the present study are polycyclic aromatic hydrocarbons (PAHs) (**Figure 7**).

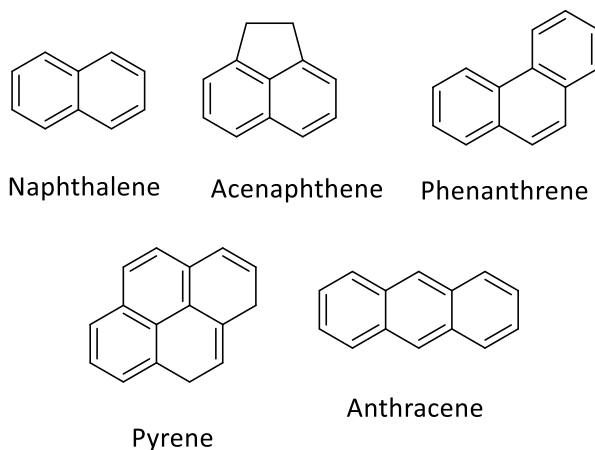


Figure 7 - Structure of various PAHs

Hypercrosslinked polymers have been used in this regard, in the removal of PAHs from aquatic sources.¹⁰⁸ This work investigated the kinetics of PAH removal using hypercrosslinked poly(styrene-*co*-DVB) instead of the usually employed activated carbon. It has been shown that hypercrosslinked poly(styrene-*co*-DVB) can be more easily regenerated than the more commonly used activated carbon.¹⁰⁹

Reports of porous poly(4-vinylpyridine-*co*-divinylbenzene) being used as sorption media for PAHs have also been made in the literature.¹¹⁰

Not only are PAHs of interest from an environmental point of view, they are also of interest to engine lubricant manufacturers; when present in lubricants PAHs have the potential to cause a great deal of harm to the internal components of engines.

1.15 Engine Lubricants

Soot is particulate in nature and is formed as a result of the incomplete combustion of fuel and any engine oil that has made its way to the combustion chamber, usually by passing by the piston ring, as described by Patterson and Henein in the early 1970s.¹¹¹ Soot is formed through a nucleation and growth process (analogous to the nucleation and growth process observed in precipitation polymerisation) of polycyclic aromatic hydrocarbons (PAHs).

1.16 Soot Formation and its Growth from Polycyclic Aromatic Hydrocarbons (PAHs)

PAHs are organic molecules which are composed of multiple fused rings. The properties and aromaticity of PAHs has long intrigued chemists.¹¹² In recent years there has been a resurgence in the interest of PAHs from different fields within academia and industry. There has been interest too from the medical field as PAHs have the potential to do catastrophic damage to the human body, with more than 10 PAHs being proven to be either carcinogenic, mutagenic or teratogenic,¹¹³ and numerous others being classed as probably cancer causing.¹¹⁴ There has also been a revived interest from the automotive industry, where PAHs have the potential to cause a great deal of damage to car engines.

PAHs are the precursors to soot – the particulate matter that results from the incomplete combustion of hydrocarbon fuels. One way in which soot is manifest is as the black smoke seen coming from the exhausts of many automobiles, especially those that have diesel engines. Of particular interest to the research presented herein is the presence of PAHs and soot within the lubricating oil of diesel engines. As they grow, soot particles will aggregate together. This is of major concern as it can cause oil thickening, and this is a very typical problem observed in heavy-duty diesel engines. If left untreated, ruinous engine failure can occur.^{115,116}

In recent years there has been a great deal of investigation into understanding PAHs and soot (and particulate matter) formation.^{117–120} Due to the high energy environment in

which soot is formed, there are still significant details of its formation that are not wholly understood.¹²¹ However, there is considerable agreement within the academic community on some of the general features of soot formation from PAHs. Five commonly identified processes are pyrolysis, nucleation, surface growth and agglomeration/coalescence.

1.16.1 Pyrolysis

Pyrolysis is the process by which organic compounds change their molecular structure at high temperature without significant oxidation. Tree and Svensson noted¹¹⁹ that the same species are produced in almost all cases: acetylenes, unsaturated hydrocarbons and PAHs. Smith also stated¹¹⁷ that if there is oxygen present in sufficient quantities these precursors can become oxidised *via* radical species.

1.16.2 Nucleation

The nucleation process sees the inception of the particulate soot system. That is, heavy PAH molecules begin to form the emerging soot particles. These soot particles generally have molecular masses of approximately 2000 amu and are usually about 1.5 nm in size.¹²¹ Through studies carried out by Glassman and co-workers,¹²² it was found that the smaller first and second ring structures are formed slowly, while the processes of growth to larger PAHs is much quicker. Therefore, the slow formation of the smaller aromatic rings controls the soot formation rate, which therefore determines the overall amount of soot formed. It has been suggested that soot is formed initially by two propynyl radicals, which form the first ring. This then adds alkyl groups and eventually forms a PAH structure. This PAH structure will eventually become big enough to form a particle nucleus, which will provide sites for surface growth.¹¹⁸

1.16.3 Surface Growth

Surface growth is the process by which mass is added to the nucleated soot particle. Tree and Svensson, in a review article published in 2007,¹¹⁹ noted that there are no clear distinctions between when nucleation ends and when surface growth begins. It was reported that the consensus is that both processes occur simultaneously. Throughout the surface growth process the surface of the soot nuclei are hot and accept gas-phase hydrocarbons. This leads to an increase in soot mass, but the actual number of soot particles does not increase. Bartok and Sarofim, whilst studying the surface growth process, recounted that the residence time of the surface growth process had a large bearing on the total soot mass/volume fraction because it is during this time that the soot gains the majority of its mass.¹²³ They also noted that smaller soot nuclei have more reactive radical sites than larger particles, therefore smaller particles have higher surface growth rates.

1.16.4 Coalescence and Agglomeration

Coalescence and agglomeration are routes by which soot particles combine together. Coalescence (sometimes referred to as coagulation) occurs when particles collide and coalesce. During coalescence, two particles which are spherical in shape combine to produce one larger spherical particle.¹¹⁷ This process decreases the number of particles but holds the combined mass constant.

The agglomeration route is slightly different. This process sees individual, discrete soot particles join together to form large chains of individual soot particles, which are reported to maintain their shape.¹¹⁹ In some cases it has been shown that the primary soot particles clump together, but they usually form chain-like structures.

1.17 Ways in which PAH and soot formation is suppressed or avoided

Diesel engines are amongst the most common type of combustion engines.¹²⁴ Generally exhibiting higher fuel efficiencies compared to gasoline engines, diesel engines also produce higher torque at lower engine speeds which makes them very useful in heavy duty and commercial vehicles.^{125,126} However, with technological and engineering advances, diesel engines have found use in smaller cars. Alongside the usual combustion products of CO₂ and water, diesel engines also produce, *inter alia*, CO, unburnt hydrocarbons (HC), oxides of nitrogen (NO_x) as well as particulate matter (PM). PM encompasses soot (and PAHs) as well as HC that are adhered to the soot surface.¹²⁴⁻¹²⁸ Legislation is in place to govern these emissions, with the European Union and others putting ever lower limits on the acceptable exhaust emissions of these pollutants. The most recent European emission standard for passenger cars and light duty vehicles (Tier Euro 6/VI), released in 2014 and updated in 2016, set the permissible limit of PM for new vehicles at 0.005 g/km.^{129,130} This is a reduction of over 96% since the introduction of the emission standards in 1992 (Euro Tier 1/I). It should be noted that heavy duty diesel vehicles are held to different but equally strict emission standards. These staged, increasingly stringent, emission limits were introduced with the aim of reducing diesel emissions, not only due to the long-term health effects of diesel emissions (especially PM and NO_x) but also due to damage that greenhouse gases and soot emissions have on the environment. These negative effects of diesel engines have also come to the attention of the wider public, not only through the current geopolitical arena - in relation to global warming - but also through accusations of the use of 'defeat devices' by engine manufacturers in attempts to circumvent emission tests.¹³¹ Reducing emissions is also in the best interest of engine and lubricant manufacturers as certain emissions such as soot and PM can create many problems within the lubricant system as well as inside the engine. With these stringent standards in place, engine and lubricant manufacturers have had to continuously implement technological and mechanical advances into their products to be able to meet the legal requirements while also ensuring that the engines run as efficiently and as economically as possible.

Generally, combating the problem of PAHs and soot fall into two categories:

1. Measures that tackle soot formation within the engine (these technologies usually aim to stop PAHs and soot from forming).
2. Measures that tackle soot, PAHs and PM external to the engine (these technologies are put in place to limit the damage that soot can do to the engine and the environment after it has formed, by removing it from the system).

1.17.1 In-engine technologies

Over the past quarter of a century or so, engine technology has been developed and advanced due to both legislative and environmental demands to address the problem of soot, PAHs, particulate and other emissions.¹²⁸ In the past, engine control was a mechanically controlled process, whereas more recently control of engine parameters has been achieved with the use of an engine control unit (ECU). This allows for much more precise control over areas such as fuel injection and injection pressures. Precise fuel injection parameters have been shown to greatly influence particulate emissions in diesel engines.¹³² In conjunction with these electronic developments, direct injection technology has been utilised: whereby the diesel fuel is injected directly into the combustion chamber rather than into a pre-combustion chamber as was carried out in the past. Direct injection allows for lower fuel consumption as well as higher fuel injection pressures. The result of this is smaller fuel droplets, and this in turn results in a reduction of particulate (soot) emissions.¹²⁸ Post injection (a smaller injection of fuel after the main injection) has also been successfully utilised to reduce soot and PAH formation within the engine. Enhanced mixing of the fuel air mixture has been proposed as the reason for post injection achieving reduced soot formation.¹³²

Another area of engine technology that has been explored is exhaust gas recirculation (EGR).¹³³ This technology has long been known to reduce NO_x emissions. EGR works by introducing waste exhaust gas back into the combustion chamber. This gas mixture when mixed with air in the next combustion cycle acts to absorb some of the heat of combustion, thereby lowering the peak combustion temperature.¹³⁴ This process reduces oxygen in the combustion chamber thus NO_x emissions are lowered. However, due to the lower oxygen concentrations, EGR generally increases soot formation. In

attempts to address the high levels of particulate emissions observed in EGR, engine manufacturers have used 'high pressure EGR'.¹³⁵ By removing exhaust gas from the exhaust (upstream of the turbocharger) and readmitting it downstream of the charge air cooler, the exhaust gas is at a higher temperature and pressure. This allows for the combustion air ratio to be increased, which has been shown to aid soot oxidation and lower soot emissions.¹²⁸

Utilising exhaust gas in other ways to aid reduction in soot and PAH emissions has also been demonstrated. Most modern diesel engines are turbocharged. In this scenario, a portion of the exhaust gas is used to drive a compressor. Before entering the combustion chamber, fresh air is run through this compressor. This means that a higher air mass per working cycle of the engine is supplied, allowing the engine output to be increased. While, intuitively, this might suggest an increase in emissions, it allows for the engine to be downsized, *i.e.*, a smaller turbocharged engine (producing less soot and other emissions) will have the same power output as a larger non-turbocharged engine.

Refinements of engine design have been used to gain more control over the air/fuel mixture (charge), which has been shown to reduce emissions, especially soot and particulate matter. Redesign of the cylinder to enhance air flow around the cylinder, the arrangement and geometry of inlet ports, and the geometry of the piston itself have all been shown to help in this regard.¹²⁸

1.17.2 After-treatments to reduce soot and PM emissions

No matter how hard technologists may try, some soot and particulate matter will form as a result of combustion. While the technologies described above attempt to subdue or retard the formation of PAHs, soot and eventually PM, if they do form, remedial technologies have been developed to try and reduce the damage these species can do within the engine and to avoid them being released to the atmosphere.

Diesel particulate filters (DPF) have been mandatory on diesel powered vehicles in the EU since the Euro 5 emission standards have been in place.¹²⁹ DPF are located in the exhaust system and act to remove particulate matter from exhaust gas before it is

released to the atmosphere. To aid capture of PM and soot, DPF generally have very large surface areas (honeycomb structures are used to achieve this) and are made of very durable ceramic materials such as silicon carbide and cordierite (an aluminium silicate).¹³⁶ However, if soot and PM build-up in DPF is not regularly removed, high back pressures within the exhaust system can occur, which can result in higher fuel consumption. While this is seen as a major drawback of DPF, they are nonetheless highly efficient, with nearly 100% removal of soot being readily attainable.¹³⁶ It should be noted that DPF technology only serves to remove soot from the exhaust stream, thereby stopping it from being released to the atmosphere. It will not stop soot and contamination from making its way into the lubricant system, where it may do a great deal of damage.¹²⁶

Before making its way to the exhaust system, PAHs, soot and PM can also be found in the lubricant system of the engine. Small amounts of PAHs and soot formed in the combustion chamber can be transported to the lubricant system *via* the piston ring. Once in the lubricant, soot has the potential to cause large amounts of damage. If it is not in solution with the oil and it is abrasive and will scratch surfaces and create excess wear on metal parts. It can also cause the oil to thicken, which can block vital pathways within the lubricant system. A blocked lubricant system leads to the engine being starved of oil which will result in a great deal of damage to the engine. Lubricant manufacturers have addressed this problem in a number of ways. One very simple solution to the problem is to filter the soot and PM out of the oil. This is achieved by using an oil filter. Oil filters are fairly primitive, mostly being a concertinaed cellulosic paper that acts to physically filter out the soot, PM and other contaminants from the lubricant. Generally speaking, these filters will only sequester soot for so long, since upon build-up of soot on the filter the pressure required to transport the lubricant through the filter will become too high. When this happens, a relief valve will open, and the lubricant will be free to bypass the filter. This occurs to avoid the engine being devoid of oil. The obvious drawback to this is dirty oil is then allowed to flow around the engine where soot and other contaminants may cause damage.

Another line of defence against the problems associated with PAHs, soot and PM is the lubricant itself. Lubricant manufacturers have developed additives that can be

introduced into the base oil, to avoid the negative consequences of soot and other harmful species. One such additive which can be used is a dispersant. There are a number of reports that describe dispersants in great detail,^{137,138,139} but for clarity a brief overview of their purpose, features and most common structures will be given here.

1.18 Engine Oil Dispersants

Engine lubricants are comprised of a base fluid - most commonly, this is a petroleum-derived (mineral) oil – and additives. Lubricating oils have a number of functions; not only is the lubricant oil present to prevent machinery parts from rubbing together, but it also helps cooling and in the prevention of corrosion. It also has the task of keeping engine components clean by suspending insoluble contaminants,¹⁴⁰ such as soot. Additives are present in the oil to enhance properties, such as viscosity or indeed to impart a new property that it would not possess otherwise, such as the ability to disperse insoluble contaminants.¹³⁷

Soot and other fuel and lubricant degradation products have a very low solubility in oil and therefore will have a tendency to fall out of solution in oil. The size of soot particles has a great influence on whether or not the soot will remain in solution, with smaller soot particles having a propensity to remain in solution.¹³⁷ The larger soot particles are formed as a result of agglomeration and dispersants interfere with this agglomeration process by associating with discrete soot particles. This results in these soot particles being unable to interact and agglomerate with other soot particles, therefore they remain small and in the solution phase. Rizvi and others have suggested that both steric and electronic factors are responsible for stopping soot particles that have interacted with a dispersant molecule from agglomerating.¹³⁹

1.18.1 Properties of a Dispersant

The main function of a dispersant is to disperse soot to stop it from causing damage to the engine. To perform efficiently and effectively, dispersants need to have some key

features: thermal stability, resistance to oxidation and the ability to work adequately at both low and high temperatures.¹³⁷ If the thermal stability is poor, at elevated temperatures the dispersant will break down and may be unable to perform at all. If a dispersant is poorly resistant to oxidation it can actually lend itself to the production of soot and other species that are harmful to the engine. Unsaturated olefins, highly branched aliphatics and aromatic species are all present in diesel fuel and are highly susceptible to degradation during the combustion process to form highly reactive peroxides, hydroperoxides and free radicals.¹⁴¹ These combustion products bypass the piston rings and can end up in the lubricating oil where they are able to attack the aliphatic hydrocarbon oil and, if it does not have oxidative resistance, the dispersants that are present. Cochrac, Rizvi and Ingold all reported that the harmful peroxide and hydroperoxide species, when in the lubricant oil, can break down thermally or oxidatively to form aldehydes, ketones and carboxylic acids.^{142,143}

A lubricant possessing a dispersant that is able to work at low temperatures is also of benefit. When an engine is first started it remains cold for some time and this can make it difficult for a lubricant to be circulated around the engine properly.

1.18.2 Dispersant structure

Dispersants possess a typical surfactant structure, and as such have a long hydrocarbon group, a functional tip and a connecting group to link the two together (**Figure 8**).

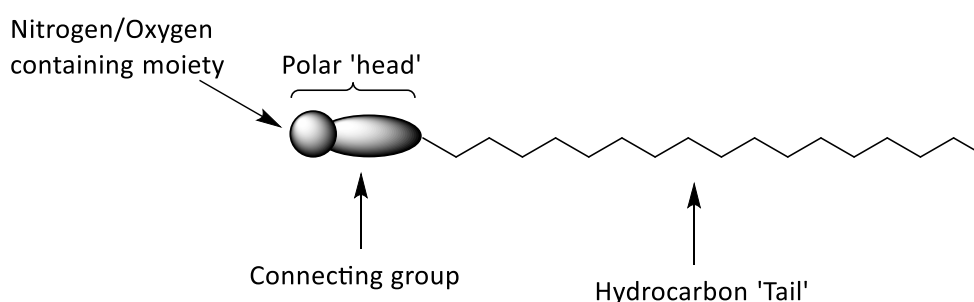
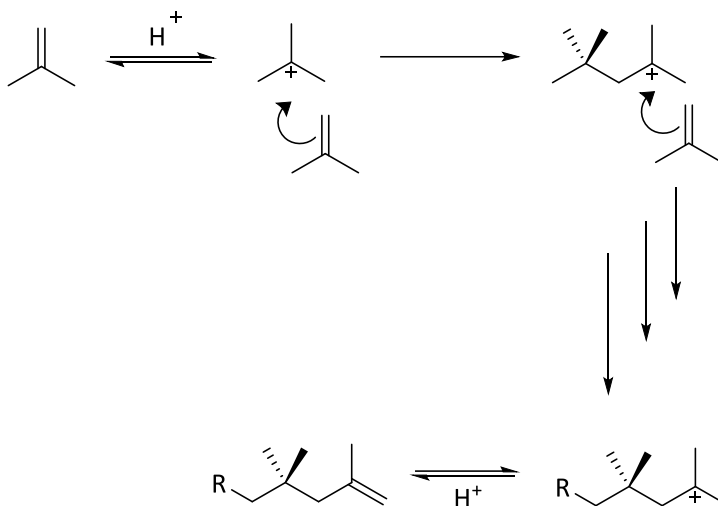


Figure 8: Typical dispersant molecule

1.18.3 The Hydrocarbon Tail

The most commonly encountered hydrocarbon tail is polyisobutylene (PIB). An acid-catalysed polymerisation of isobutylene is typical in the manufacture of polyisobutylene (Scheme 11).



Scheme 11: Acid-catalysed polymerisation of isobutylene

Scheme 11 shows the formation of a polyisobutylene with a terminal olefin. In practice, numerous isomers are formed, with vinylidene, tri-substituted and tetra-substituted olefins are all formed, depending on the catalyst used.¹³⁷ The reactivity of these olefins towards the connecting groups can vary. More highly substituted olefins have lower reactivity owing to steric effects. Also, when the number of isobutyl groups is increased, *i.e.*, the polymer's molecular weight is increased, this will also lead to a decrease in reactivity. Polyisobutylene is extensively branched, which gives it very good oil solubility, and it is for this reason that it is used extensively in this area. Oil solubility can be compromised if the alkyl chain is too short, so low molecular weight polymer chains are undesirable. To overcome this, lubricant manufacturers can use distillation to remove lower molecular weight polymer.¹³⁷

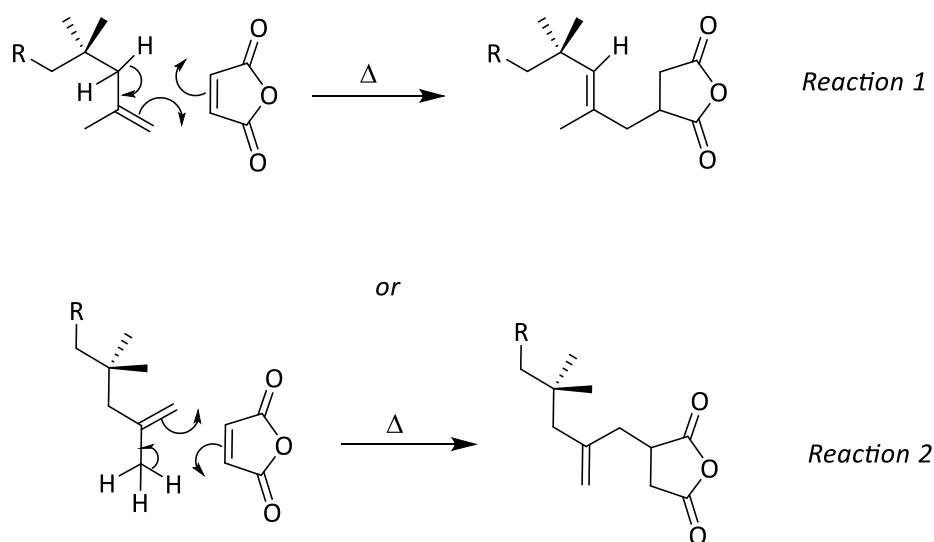
A new class of dispersants has been reported in the patent literature by technologists at Exxon. Dispersants that are produced from an ethylene- α olefin copolymer have been patented.^{144,145} These dispersants are claimed to have enhanced viscosities at both high

and low temperatures,^{137,146} *i.e.*, the viscosity does not change much with variation in temperature.

1.18.4 The Connecting Group and Polar Moieties

The connecting group is required due to the fact that attaching the polar group directly to the hydrocarbon tail can be rather difficult. The most common connecting groups which are employed in industry are succinic anhydride and phenol, although phosphonate connecting groups can also be used.¹³⁸

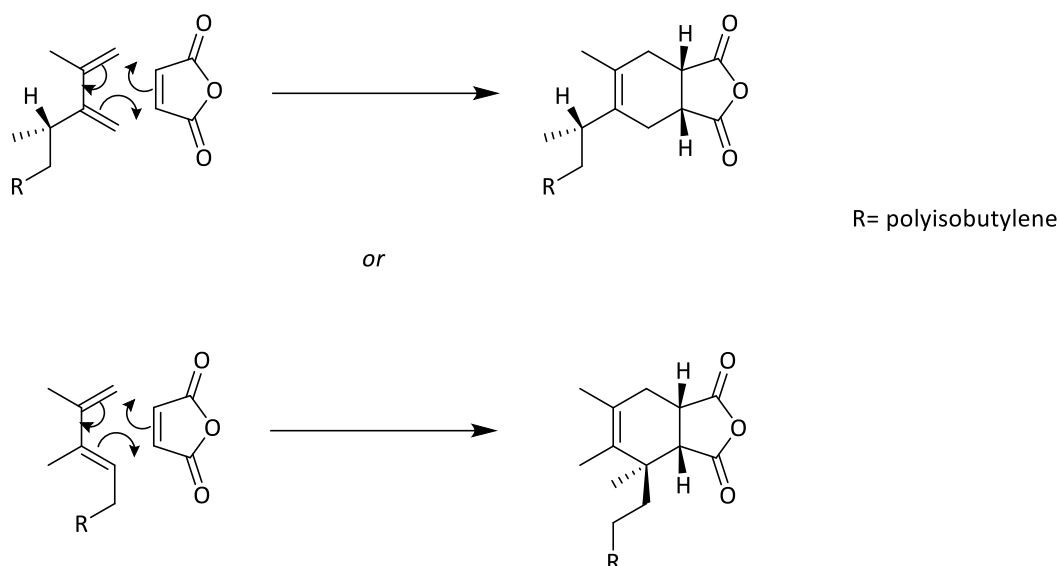
The formation of the succinic anhydride connecting group is achieved by reacting the polyisobutylene (PIB) hydrocarbon tail with maleic anhydride. This can be carried out thermally, such as was reported by Stuart *et al.* and the Chevron Research Company in the 1960s, with the two reactants being heated in excess of 200 °C to yield the desired alkenyl succinic anhydride.¹⁴⁷ It has been postulated that this reaction proceeds *via* an ene reaction (**Scheme 12**).



Scheme 12: Mechanism of alkenyl succinic anhydride formation

If the double bond in the product internalises as is shown in *reaction 1*, then the product cannot react with another molecule of maleic anhydride. However, if the double bond is external in the product, as shown in *reaction 2*, this can potentially react with another molecule of maleic anhydride. This was highlighted by Rense and the Lubrizol Corporation in 1965.¹⁴⁸ The major drawback of the thermal transformation is that it is not very energy efficient; high temperatures are required for it to proceed. Also, the reaction relies on the polyisobutylene having a high terminal olefin content, whereas work by Harrison *et al.* found that the choice of Lewis acid used during the polymerisation of isobutylene had a dramatic effect on the major isomer produced.¹⁴⁹ They reported that when using boron trifluoride one could produce a polyisobutylene that contained mainly terminal olefins, whereas if aluminium chloride was used then internal olefins predominated. This shows that the reliance on high terminal olefin contents can be overcome by tailoring the synthesis to use a catalyst that produce a polyisobutylene with predominantly terminal olefins.

The drawbacks of this transformation can also be overcome by using chlorine. Technologists from Lubrizol and the French Institute of Petroleum reported that a chlorine-mediated process required lower temperature and took less time for conversion to be complete.^{148,150,151} This process is also tolerant of internal olefins within the polyisobutylene. Weill, and others, have postulated that the chlorine assists in the formation of two possible dienes on the end of the polyisobutylene, followed by a facile Diels-Alder reaction (**Scheme 13**).^{138,152,153}



Scheme 13: Diels-Alder formation of alkenyl succinic anhydride

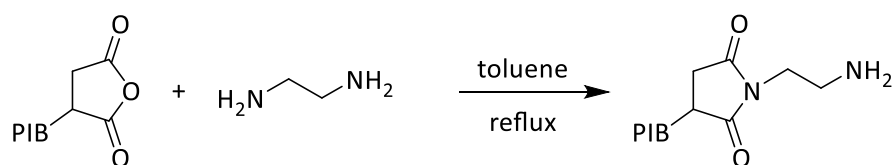
This process is far more economical because it can be carried out at much lower temperatures and can be completed in 30 minutes in some cases.¹⁴⁸ However, the resulting dispersants produced by this method have been reported to contain lingering chlorine in the form of organic chlorides which are of great environmental concern. In the late 1990s there was a push to produce dispersants with a low chlorine content.^{154–157} Baumanis *et al.* claimed¹⁵⁷ a process of treating the chlorine-containing product (in this case the polyisobutylene succinic anhydride) with either bromine or iodine, but preferably iodine, to remove any residual chlorine. The patent makes reference to a wide range of iodine-containing compounds which could be utilised, including but not limited to elemental iodine, I_3^- , I^- and organic iodides such as *t*-butyl iodide. Pudelski reported a method for removing chlorine from engine oil dispersants by reacting them with elemental sulfur at elevated temperatures.¹⁵⁴ While this reduced the chlorine content, it tended to lead to sulfur-based crosslinking of the polymer backbones which led to a detrimental increase in dispersant viscosity. Pleasingly, they reported that an amalgamation of the two processes outlined above produced succinic anhydrides with very low chlorine content indeed, with levels less than 100 ppm being reported.

The resultant alkenylsuccinic anhydrides can be reacted in different ways to impart functionality that produces the final dispersant. One may react them with polyamines to produce succinimides or react them with polyols to produce succinic esters.

1.19 Polyisobutylene Succinimides

By far the most common dispersants used in engine lubricants are those based on succinimides.¹⁴⁶ The PIB hydrocarbon tail with the succinic anhydride now in place is reacted with a polyamine. The polyamines most commonly encountered are produced *via* the reaction of chlorinated ethylene based species that have been reacted further with ammonia.^{138,153,158}

The first report of using succinimides as dispersants was disclosed by La Suer and his colleagues at The Lubrizol Corporation in 1965.¹⁵⁹ The PIB succinic anhydride was reacted with an ethylene polyamine, ethylene diamine being one such example, in toluene. Water is produced as a by-product, this being distilled off to drive the reaction to completion, affording the desired succinimide, as shown in **Scheme 14**.



Scheme 14: Polyisobutylene succinimide formation

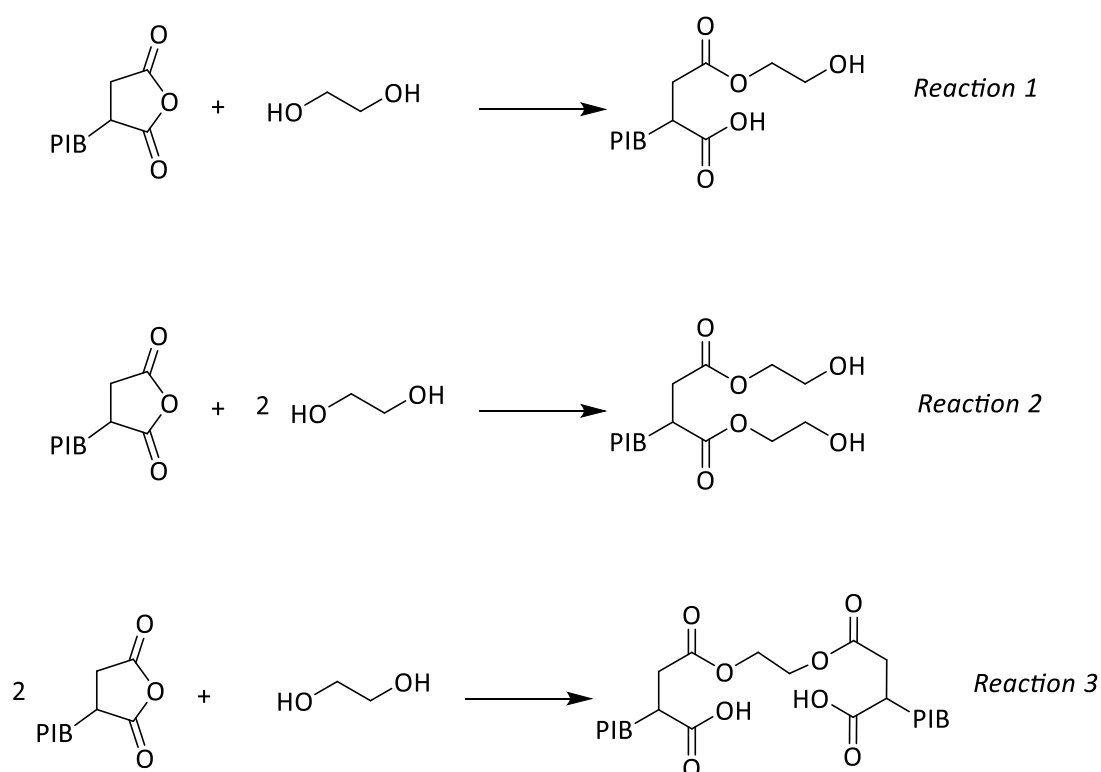
More recently, higher molecular weight amines have been prepared for the use in engine oil dispersants. Steckel *et al.* disclosed the preparation and use of polyalkylene amines such as triethylenetetramine as dispersants.¹⁶⁰ It was claimed that amines such as the tetramine produced dispersants that have a higher total base number than those prepared with more traditional polyamines. The total base number, or TBN, is a measure

of the dispersant's basicity and therefore its ability to neutralise harmful acidic species within the engine.

Researchers at Texaco also found that, after synthesis, PIB succinimides could be treated with borate esters in a drive to produce dispersants with improved performance.¹⁶¹ The borate ester containing succinimides patented by Texaco were claimed to have improved dispersant character and were also reported to inhibit engine wear, *i.e.* metal on metal contact.

1.20 Succinic Esters

Succinic, esters-based dispersants are synthesised by reacting the polyisobutylene succinic anhydride with an alcohol. This was first patented by La Suer *et al.* at the Lubrizol Corporation in 1968.¹⁶² It was disclosed that by varying the equivalents of anhydride and alcohol either the mono- (*reaction 1*) or di-ester (*reaction 2*) or indeed the coupled product (*reaction 3*), all exemplified in **Scheme 15** could be formed.

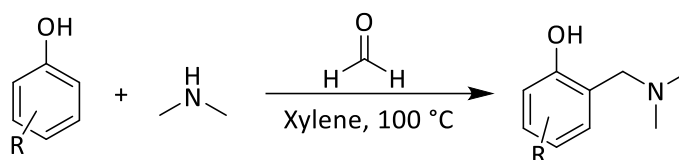


Scheme 15: Succinic ester formation

It was also noted that monohydric alcohols and other, much larger, polyols could be used in place of ethylene glycol. This was also demonstrated in the art some years later by researchers at the same company.¹⁶³

1.21 Mannich Dispersants

The last class of dispersant that will be examined are the so called 'Mannich dispersants', so named due to their being synthesised *via* a Mannich reaction. The first mention of this in the art was made in 1968 by a researcher at Mobil Oil Corporation.¹⁶⁴ Polypropylene was reacted with phenol to afford an alkyl phenol. The phenol was then reacted with an amine, dimethylamine was the first one to be used, and formaldehyde in xylene to produce the Mannich dispersant (**Scheme 16**).



Scheme 16: Mannich dispersant synthesis

Otto also reported the use of longer chain amines in the synthesis of these Mannich dispersants, as well as using diamines to prepare Mannich dispersants based on a long chain amine with an alkylphenol on either end.¹⁶⁴

Much research has been carried out in this area since Otto's seminal work.¹⁶⁵⁻¹⁶⁷ It has been reported in the literature that Mannich dispersants can be modified post-synthesis in a fashion similar to the succinimide dispersants discussed previously. Researchers at Standard Oil Company (since acquired by BP) reported the treatment of Mannich dispersants with boric acid to improve dispersant properties and viscometric properties.¹⁶⁸

Dispersants have been a main-stay of engine lubricants for more than half a century and notwithstanding the fact that dispersants can make up nearly 10% of the lubricant that

is present in the oil sump of an engine,¹³⁸ it can be seen that they are of the utmost importance in allowing the engine to perform efficiently and in some case for extended periods of time. However, while lubricant additives are incredible useful at dispersing oil and minimising the negative effects of it, they do not remove it completely. The soot and contaminants are still in contact with the oil where they can cause damage. Also, with fossil fuel reserves dwindling, more advanced engine hardware being produced and engine manufacturers pressing for higher mileages between oil changes, it is clear that new, innovative technologies will be needed. The result of this is that engine and lubricant technologists are investigating new engine lubricant paradigms that will isolate PAHs and other contaminants from the lubricant in an effort to better minimise the harm that they can cause.

1.22 ExBox: A PAH scavenger

Extensive work by Nobel laureate Sir Fraser Stoddart and his group at Northwestern University in Illinois has produced semi-rigid cyclophanes that can be used as very high-affinity scavengers of PAHs from crude oil samples.

First reported in 2012 was a tetracationic cyclophane salt called *Exbox*⁴⁺ (**Figure 9**), and this was reported to be a high affinity scavenger of PAHs in both aqueous and organic media.¹⁶⁹ It was also shown to be highly effective in the sorption of PAHs from a real crude oil sample.

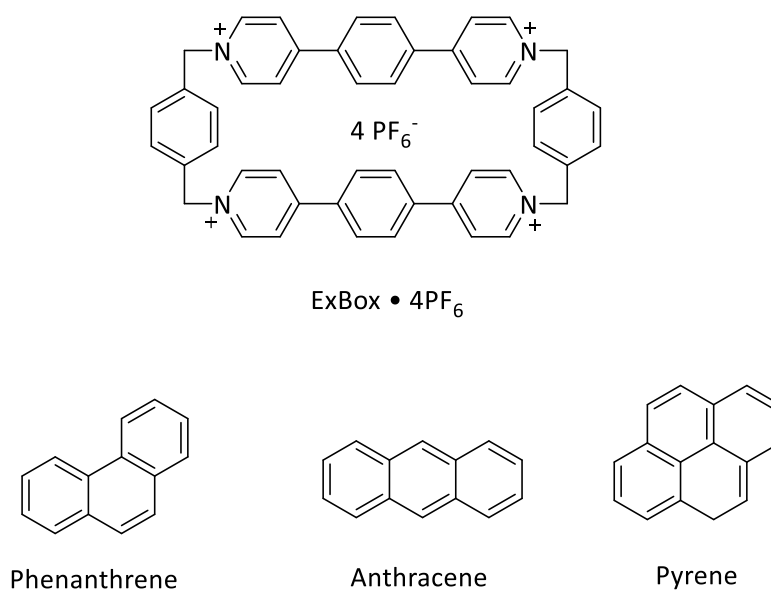


Figure 9: Electron deficient tetracationic cyclophane ExBox⁴⁺

Shown below the ExBox structure in **Figure 9** are three PAHs that it can bind. It was discovered that not only do the PAHs sit inside Exbox, but also on top and underneath it. It was noted that when the cyclophane was introduced to PAHs there was a dramatic colour change, indicative of a charge transfer reaction. Charge transfer bands appearing in the optical adsorption spectra confirmed this.

Stoddart *et al.* have also reported the synthesis of larger Exbox molecules. where the number of *para*-phenylene rings inserted between the pyridinium rings can be as high as three.¹⁷⁰ These allow for much larger PAHs to be bound.

Due to the rather complicated synthetic procedure and the costs associated with producing these materials, they will probably never be used within an engine to remove PAHs. However, it does highlight that favourable molecular interactions can be exploited to remove PAHs from a hydrocarbon fluid.

1.23 In Situ Soot and PAH Sorption

While dispersants are considered the norm in dealing with the problems that soot and PAHs can cause in an engine, the soot and PAHs are only dispersed, that is the particles/ molecules are still present in the lubricating oil and still able to cause harm. It should also be noted that dispersants will only work for a finite amount of time before the PAH and soot concentration becomes too high and the dispersant can no longer cope. In attempts to improve engine oil longevity and efficiency, Brownawell *et al.* at Exxon Research began to investigate using solid phase additives in the oil sump as sorption devices to remove soot and PAHs from the oil permanently. In the seminal work in this area they disclosed a lubrication device that embodied activated carbon as the sorption media.¹⁷¹ It was noted that between 50 and 150 g of activated carbon removed substantial amounts of the PAH content in an engine lubricant, with up to 90% removal being achievable. Lamentably, the activated charcoal, while working well as a sorbent, did not show a great deal of selectivity. The same patent also disclosed that the activated charcoal could be impregnated with lubricant additives, such as the dispersants discussed earlier. These

additives are able to leach slowly out of the carbon over time and replenish and replace additives in the lubricant as they are consumed.

In extending to this work, Brownawell disclosed an *in situ* filtration device that was able to rejuvenate engine lubricants.¹⁷² The patent describes a solid phase additive that contains both an oil insoluble chemically active filter media and a physically active filter media. The chemically active filter media, one example being calcium carbonate, reacts chemically with the lubricant to neutralise harmful acidic species. The physically active filter media is an activated carbon, and was claimed as before to show great promise in physically adsorbing PAHs and soot.

Brownawell has also patented lubricating systems that encompass a binder impregnated with oil additives, including but not limited to dispersants, antiwear and anti-corrosion additives, which are allowed to desorb from the binder into the lubricant over time to allow the lubricant to possess these beneficial properties for longer.^{173,174}

Suppressing the formation of PAHs, soot and other contaminants continues to be thoroughly researched, as does the removal of soot from the engine and lubricant system if it does form. It can be seen that there are a number of strategies that technologists have implemented that help in this regard, from engine control parameters to filtration. Something which, to the best of our knowledge, has never been attempted before is the use of polymer particles (both gel-type and macroreticular) to sorb PAHs, soot and other potential contaminants from an engine lubricant *in situ*.

1.24 Hypothesis and project aims

Within the Cormack Group, and elsewhere porous polymer particles have been shown to be highly useful in numerous applications, including sorption and capture of analytes of interest. Chemical modifications have also shown to enhance the selectivity of these materials when a particular analyte of interest is to be investigated.

One area of application where materials of this type have remained largely unexplored is in the sorption of soot and PAHs from an apolar media, such as engine oil.

Engine lubricants that are in use currently are incredibly complex mixtures. Lubricants contain an additive package that can make up more than 20% of a lubricant, containing numerous compounds, including: dispersants, detergents and surfactants, anti-foam agents, anti-wear agents and pour-point depressants, amongst others.

It is proposed that by using polymer particles (both gel-type and macroreticular) could be used as sequestration devices to remove, initially, PAHs from non-polar solvent. It was thought that these polymeric materials could be exploited further and used *in situ*, within an engine lubricant system, to remove soot precursors, soot and other potential contaminants from the lubricant. It is further believed that by including solid phase polymeric sorbents within engine oil to sequester harmful soot and PAHs, some of the compounds from the additive package may become obsolete and therefore can be removed. This could potentially have cost savings, as a less complicated lubricant needs to be formulated. It may also make recycling of lubricants, at the end of their useful life, a much simpler task as the lubricant would be a simpler mixture of compounds.

It may be the case that, in the future, solid phase polymeric sorbents could be utilised in conjunction with currently employed technologies to create a system that could aid sequestration of harmful contaminants within engine oil more effectively and efficiently than currently employed technologies alone.

It is therefore the aim of this study to investigate the synthesis and utilisation of solid-phase polymeric additives to sequester harmful species from lubricating oil *in situ*, where the undesirable species are soot particles or other harmful chemicals such as acids.

The overarching objective of the programme was to investigate whether the removal of PAHs and possibly soot from a hydrocarbon fluid (and potentially the lubricant of a diesel engine) using crosslinked, insoluble polymers was possible. To this end, the main aims have been:

1. To prepare a range of aromatic based polymers, with variations in functionality that are designed to exploit favourable interactions with aromatic contaminants (π - π stacking, hydrophobic interactions and charge transfer interactions, where appropriate).
2. To chemically modify, post-polymerisation, a selection of these polymers to prepare hypercrosslinked polymers to explore their potential in this area.
- 3 To investigate the polymeric materials potential as sorbents for polyaromatic hydrocarbon capture. It is proposed that GC should be utilised in these studies, with stock solutions of mixtures of PAH being dissolved in an apolar oil surrogate such as heptane.
4. Using the information gained in these sorption studies, prepare a range of analogous polymeric materials that would be appropriate for use in sorption studies of PAHs and soot from the lubricant system of a diesel engine.
5. Analyse these materials, post engine tests, to investigate their applicability as sorbents within a diesel engine lubricant.

2.0 Experimental

2.1 General

The reagents used for polymer synthesis, divinylbenzene-80 (DVB-80) (80% grade) and 4-vinylbenzyl chloride ($\geq 90\%$), were supplied by Fluka (Steinheim, Germany) and purified before use by passing through a short column of neutral alumina. 4-Vinyl pyridine (96%) was supplied by Alfa Aesar (Heysham, UK) and purified by distillation prior to use unless stated otherwise. Styrene (99%) and ethylene glycol dimethacrylate (EGDMA) (98%) were supplied by Sigma-Aldrich (Steinheim, Germany) and purified before use by passing through a short column of neutral alumina. The stabilisers poly(*N*-vinylpyrrolidone) (PVP) 360 (Mw 360,000) and Triton X-405 (a proprietary name for polyethylene glycol *tert*-octylphenyl ether) were supplied by Sigma Aldrich (Steinheim, Germany) and used as received. 2,2'-Azobis(isobutyronitrile) (AIBN) (97%) was supplied by BDH (Poole, UK) and was recrystallised from acetone at low temperature before drying *in vacuo* at room temperature prior to use. HPLC grade acetonitrile was supplied by Rathburn Chemicals (Walkerburn, Scotland) and used as received. Iron(III) trichloride, (97%), anhydrous 1,2-dichloromethane (DCE) (99.8%) and nitric acid (Riedel-de Haën, 65%) were supplied by Sigma-Aldrich (Steinheim, Germany) and used as received.

All other solvents used were of at least standard laboratory reagent grade, and were supplied by Sigma-Aldrich.

The analytes used in the PAH sorption studies presented herein were: acenaphthene, anthracene, 1-methylnaphthalene, 1-nitropyrene and pyrene. These were all supplied by Sigma-Aldrich (Steinheim, Germany) and were of GC grade and used as received. *n*-Heptane ($\geq 99\%$) used in these studies as an engine oil surrogate was supplied by Sigma-Aldrich (Steinheim, Germany) and used as received.

2.2 Equipment

Optical microscopy was carried out on an Olympus VANOX optical microscope (Olympus Corporation, Tokyo, Japan).

Elemental Microanalysis was performed by the University of Strathclyde Elemental Microanalysis Service. C, H and N elemental microanalyses were carried out simultaneously on a Perkin Elmer 2400 Series II analyser. Halogen contents were determined using standard titration methods.¹⁷⁵

Scanning Electron Microscopy (SEM) was carried out on a Cambridge Instruments Stereoscan 90. Samples were sputter coated with metal (platinum) prior to imaging.

IR spectra were obtained on a Shimadzu IRAffinity-1 Spectrophotometer machine by ATR.

BET and Langmuir surface areas and pore sizes were measured using a Micromeritics ASAP 2000 analyser. The methods for determining surface area, pore size and pore size distributions were based on procedures given by IUPAC¹⁷⁶ and the relevant British standards,¹⁷⁷⁻¹⁷⁹ as follows:

Approximately 300 mg of polymer sample was dried *in vacuo* (60 mbar, 40 °C) overnight. Prior to analysis the sample was degassed under vacuum at 100 °C until a constant pressure of < 0.006 mbar was achieved.

The specific surface area of the polymers was measured using nitrogen sorption at 77 K. The saturation vapour pressure, P_0 , of the adsorptive was determined and monitored directly using a pressure manometer. The free 'dead space' of the sample tube was measured with helium before the sample was immersed in liquid nitrogen. The static volumetric method was used for assessing how much gas was adsorbed. The BET¹⁸⁰ and Langmuir¹⁸¹ models were then applied to the data to determine specific surface areas. In the experimental data, the most appropriate specific surface area has been quoted based upon the calculated BET constant and isotherm data that was obtained for each polymer.

The mean pore size of the polymers was measured using nitrogen sorption. This method was conducted using the stepwise static method to obtain pore size data. 55 points were

recorded in total for the adsorption and desorption portions of the isotherm curve. Using data from the adsorption branch, the t-plot method, as proposed by Lippens and deBoer,¹⁸²⁻¹⁸⁴ was used for calculating micropore volume and surface area. Mesopore size distribution was also calculated from the adsorption branch of the isotherm, using the BJH method.¹⁸⁵

Gas Chromatography analyses were carried out on an Agilent 7890A Gas Chromatograph fitted with a flame ionising detector (FID). The optimised GC conditions are presented below:

Gas Chromatograph	Agilent 7890A
Analytical Column	30 m x 0.32 mm, 0.25 µm
Injection Temp (°C)	320 °C
Carrier Gas	Helium (6.5 mL/min)
Oven Program	90 °C held for 4 mins 90 – 250 °C at 20 °C/min held for 10 mins 250 – 320 °C at 30 °C/min held for 0 mins

2.3 Synthesis of 1st generation materials *via* precipitation polymerisation and NAD polymerisation and the hypercrosslinking of materials thereof

2.3.1 General Procedures

*General Procedure A – Preparation of polymer particles via Precipitation Polymerisation (PP).*⁵³

All of the monomer (including any comonomers if required) was added to a Nalgene[®] bottle, followed by the solvent (and any co-solvent if required) and initiator (AIBN unless stated otherwise). The bottle contents were ultrasonicated for 15 minutes. After ultrasonication, nitrogen gas was bubbled through the reaction mixture for 15 minutes at ice-bath temperature. After degassing, the Nalgene[®] bottle was sealed under nitrogen and placed on a low-profile roller (Stovall Life Sciences Inc., North Carolina, U.S.A) contained within an incubator (Stuart Scientific, Stone, U.K) and rotated about its long axis. The temperature inside the incubator was ramped from ambient temperature to 60 °C over a period of around two hours. The polymerisation was allowed to proceed for a further forty-six hours to give a milky suspension of polymer particles. The resulting particles were viewed *via* optical microscopy prior to filtration. The product was filtered by vacuum on a 0.22 µm nylon membrane filter. The particles were then washed with solvent to remove any unreacted monomer or initiator (~100 mL of acetonitrile followed by ~100 mL of toluene, methanol and finally acetone) before being dried overnight *in vacuo* (60 mbar, 40 °C).

*General Procedure B – Preparation of polymer particles via a Two-Stage Non-Aqueous Dispersion (NAD) Polymerisation.*⁶²

To a 150 mL 3-necked, round-bottomed flask, fitted with an overhead stirrer (2 bladed Teflon[™] stirrer), condenser and gas inlet was added stabiliser (PVP360, 1 g), co-stabiliser (Triton X-405, 0.35 g), all of the monomer, half of the functional co-monomer, half of the total solvent (ethanol in each case) and all of the initiator. The contents of the flask were stirred at 100 rpm and, once homogeneous, the resultant solution was degassed under

N₂ by bubbling nitrogen through the solution for 30 minutes (thereafter, the reaction was carried out under a blanket of nitrogen). The reaction was then heated to 70 °C for 1 hour. A solution of the crosslinker dissolved in the remaining functional co-monomer and the remaining solvent, heated to 70 °C was then added. The polymerisation was allowed to proceed for 24 hours. The resultant particles were centrifuged at 9000 rpm for 10 minutes. The liquid supernatant was then removed, and the particles were resuspended in ethanol and centrifuged again. This process was repeated once more in ethanol and a further twice in methanol. The particles were finally filtered by vacuum on a 0.22 µm nylon membrane filter before being dried to constant mass *in vacuo* overnight (60 mbar, 40 °C).

*General Procedure C – Hypercrosslinking of precursor polymer particles.*⁶⁴

To a 150 mL 3-necked round-bottomed flask, fitted with overhead stirrer, condenser and gas inlet was added precursor polymer particles and 1,2-dichloroethane (40 mL). The particles were left to swell for 1 hour at room temperature while the system was purged with N₂. Ferric chloride (1:1 mole ratio with respect to pendent chloromethyl groups present in the precursor particles) dissolved in 1,2-dichloroethane (40 mL) was added to the swollen polymer particles and the reaction heated to 80 °C for 18 hours. The particles were filtered by vacuum on a 0.22 µm nylon membrane filter then extracted overnight with acetone in a Soxhlet extractor. The particles were once again filtered as described above and washed with methanol and diethyl ether before drying *in vacuo* (60 mbar, 40 °C) to constant mass.

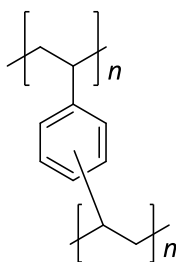
*General Procedure D – Partial hypercrosslinking followed by exhaustive hypercrosslinking of polymer particles.*⁶⁴

First Stage: To a 150 mL 3-necked round bottomed flask, fitted with an overhead stirrer, condenser and gas inlet was added precursor particles and hexane (40 mL) and the particles left to wet for 2 hours at ambient temperatures while the system was purged with N₂. The resultant mixture was cooled to -4 °C in an ice/brine slurry and ferric

chloride was added (11 mol % with respect to pendent chloromethyl groups present in the precursor particles) which was allowed to disperse for 2 hours before the mixture was heated to 80 °C and allowed to react for 18 hours. Mechanical stirring *via* an overhead stirrer was carried out for the duration of the reaction. The product was filtered by vacuum on a 0.22 µm nylon membrane filter and washed with methanol and aqueous HNO₃ (pH 1). The particles were then extracted overnight with acetone in a Soxhlet extractor. The particles were once again filtered, as described above, and washed with methanol and diethyl ether before drying *in vacuo* oven (60 mbar, 40 °C) to constant mass. **Second Stage:** These particles were then fully hypercrosslinked as per *General Procedure C*.

2.3.2 Preparation of Polymer Particles

Preparation of Poly(DVB-80) via Precipitation Polymerisation



Following *General Procedure A* results are reported as: a) amount of DVB-80; b) amount of AIBN; c) total volume of solvent (acetonitrile/toluene (75:25)); d) product yield

a) 2.0 g, 15.3 mmol; b) 0.045 g, 0.2 mmol; c) 100 mL; d) 0.54 g, 27%

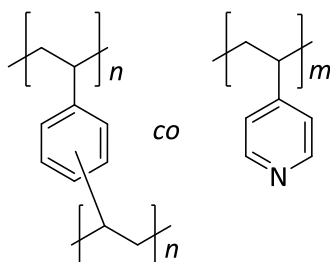
Appearance of product: White powder

FT-IR $\bar{\nu}/\text{cm}^{-1}$ (ATR): 3082 (aromatic C-H stretch), 3043 (unreacted vinyl group C-H stretch), 2920, 2358, 1975, 1602 (aromatic ring stretch), 1510 (aromatic ring stretch), 1487, 1444, 987, 902 (unreacted vinyl C-H out-of-plane stretch), 835 (1,4-disubstitution), 749 (1,3-disubstitution).

Elemental microanalysis: Expected 91.2% C, 8.1% H and 0.7% N; Found 89.6% C, 7.7% H and 0.5% N

Langmuir Specific Surface Area: 553 m²/g, Average pore diameter: 2.2 nm, Total pore volume (at saturation pressure): 0.2 cm³/g

Preparation of Poly(DVB-80-co-4-VP) via Precipitation Polymerisation



Following *General Procedure A* results are reported as: a) amount of DVB-80; b) Amount of 4-VP; c) amount of initiator (ABDV); d) total volume of solvent (acetonitrile/toluene (75:25)); e) product yield

a) 90 mol%, 0.9245 g, 7.1 mmol; b) 10 mol% 0.075 g, 0.7 mmol; c) 0.066 g, 0.4 mmol; d) 25 mL; e) 0.7 g, 66%

Appearance of product: White powder

FT-IR $\bar{\nu}/\text{cm}^{-1}$ (ATR): 3020 (aromatic C-H stretch), 2918, 1598 (pyridine ring stretch), 1510 (aromatic ring stretch) 1487, 1444, 1415 (aromatic C=N stretch), 989, 902, 827.

Elemental microanalysis: Expected 90.2% C, 8.1% H and 1.7% N; Found 90.1% C, 7.6% H and 1.4% N

Langmuir Specific Surface Area: 814 m²/g, Average pore diameter: 2.1 nm, Total pore volume (at saturation): 0.3 cm³/g.

Following *General Procedure A* results are reported as: a) amount of DVB-80; b) Amount of 4-VP; c) amount of initiator AIBN; d) total volume of solvent (acetonitrile/toluene (75:25)); e) product yield

a) 0.9258 g, 7.1 mmol; b) 0.0745g, 0.7 mmol; c) 0.0663 g, 0.4 mmol; d) 25 mL; e) 0.64 g, 86%

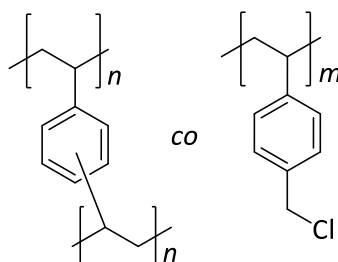
Appearance of product: White powder

FT-IR $\bar{\nu}/\text{cm}^{-1}$ (ATR): 3020 (aromatic C-H stretch), 2920, 1597 (pyridine ring stretch), 1510 (aromatic ring stretch), 1446, 1415 (aromatic C=N stretch), 1016, 989.

Elemental microanalysis: Expected 90.0 % C, 8.0% H and 2.0% N; Found 89.5% C, 7.6% H and 1.9% N

Langmuir Specific Surface Area: 729 m^2/g , Average pore diameter: 2.4nm, Total pore volume (at saturation): 0.33 cm^3/g .

Preparation of Poly(DVB-80-co-VBC) via Precipitation Polymerisation.



Following *General Procedure A* results are reported as: a) amount of DVB-80; b) amount of VBC; c) amount of initiator AIBN; d) volume of acetonitrile; e) product yield

a) 25 mol%, 0.889 g, 6.7 mmol; b) 70 mol% ,11.2 g, 20.3 mmol; c) 0.107 g, 0.6 mmol; d) 200 mL; e) 1.81 g, 47%

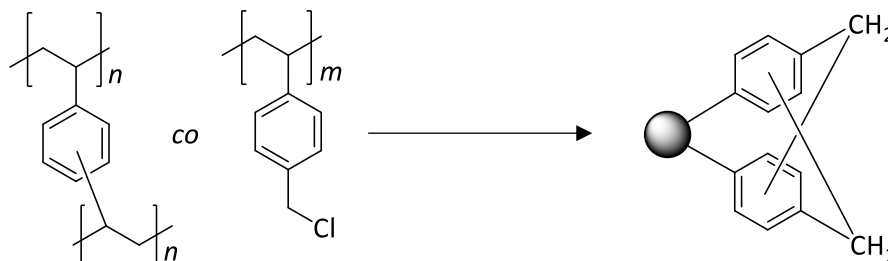
Appearance of product: pale yellow solid

FT-IR $\bar{\nu}/\text{cm}^{-1}$ (ATR): 3020, 3012, 2920, 2850, 1703, 1604, 1510, 1442, 1265 (C-H wag of $\text{CH}_2\text{-Cl}$) 825, 709(C-Cl str.)

Elemental microanalysis: Expected 75.4% C, 6.4% H, 0.5% N and 17.7% Cl; Found 77.0% C, 6.5% H, 0.7% N and 14.0 % Cl

BET Specific Surface Area: $< 5 \text{ m}^2/\text{g}$

Preparation of hypercrosslinked poly(DVB-80-co-VBC).



Following *General Procedure C* results are reported as: a) amount of precursor polymer particles (Poly(DVB-80-co-VBC)); b) mass of FeCl_3 ; c) Product yield

a) 0.5 g; b) 0.405 g, 2.5 mmol; c) 0.40 g, 93%

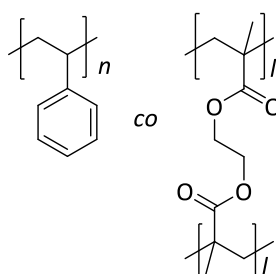
Appearance of product: Light brown powder

FT-IR $\bar{\nu}/\text{cm}^{-1}$ (ATR): 3026, 2920, 1700, 1599, 1491, 818, 756

Elemental microanalysis: Expected 91.8% C, 7.3% H, 0.9% N and 0% Cl; Found 85.5% C, 6.8% H, 0.9% N and 2.7% Cl

Langmuir specific surface area: $2034 \text{ m}^2/\text{g}$, Average pore diameter: 2.2 nm, Total pore volume (at saturation): $0.84 \text{ cm}^3/\text{g}$.

Preparation of Poly(styrene-co-EGDMA) via NAD polymerisation



Following *General Procedure B* results are reported as: a) total amount of styrene; b) amount of EGDMA; c) amount of AIBN; d) total volume of ethanol; e) product yield

a) 99 wt% 12.5 g, 0.12 mol; b) 1 wt%, 0.125 g, 0.63 mmol; c) 0.25 g, 1.5 mmol; d) 47.5 mL; e) 9.51 g, 77%

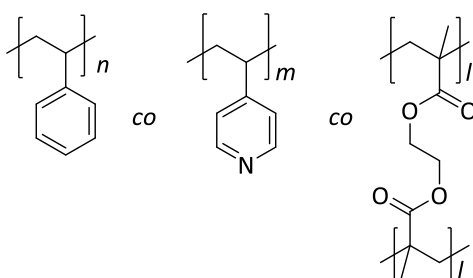
Appearance of product: white solid

FT-IR $\bar{\nu}/\text{cm}^{-1}$ (ATR): 3059, 3026, 2920, 1720 (C=O, ester str.), 1600, 1492, 1452, 756, 696

Elemental microanalysis: Expected 91.6% C, 7.8% H and trace N; found 91.7% C, 7.6% H and trace N

BET specific surface area: $< 5 \text{ m}^2/\text{g}$

Preparation of Poly(styrene-co-4-VP-co-EGDMA) via NAD polymerisation



Following *General Procedure B* results are reported as: a) total amount of styrene; b) total amount of 4-VP; c) amount of EGDMA; d) amount of AIBN; e) total volume of ethanol; f) product yield

a) 9.45 g, 0.09 mol; b) 0.55 g, 5.2 mmol; c) 1 wt %, 0.1 g, 0.5 mmol; d) 0.201 g, 1.2 mmol; e) 47.5 mL; f) 6.7 g, 68%

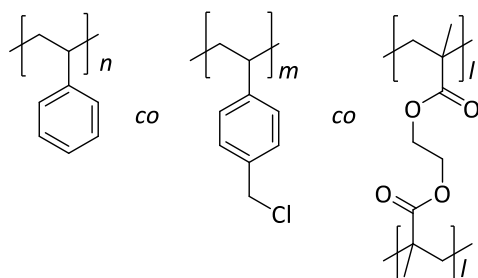
Appearance of product: Pale yellow solid

FT-IR $\bar{\nu}/\text{cm}^{-1}$ (ATR): 3024, 2920, 2848, 1720 (C=O, ester str.), 1580 (pyridine ring, str.), 1560 (pyridine ring, str.), 1492, 1452, 756, 696

Elemental microanalysis: Expected 90.9% C, 7.7% H and 1.1% N; Found 90.8% C, 7.7% H and 1.2% N

BET specific surface area: < 5 m²/g

Preparation of Poly(styrene-co-VBC-co-EGDMA) via NAD polymerisation.



Following *General Procedure B* results are reported as: a) total amount of styrene; b) total amount of VBC; c) amount of EGDMA; d) amount of AIBN; e) total volume of ethanol; f) product yield

a) 49.5 wt%, 5.025 g, 48 mmol; b) 49.5 wt%, 5.025 g, 33 mmol; c) 1 wt%, 0.1 g, 0.5 mmol; d) 0.201 g, 1.2 mmol; e) 47.5 mL; f) 7.1 g, 72%

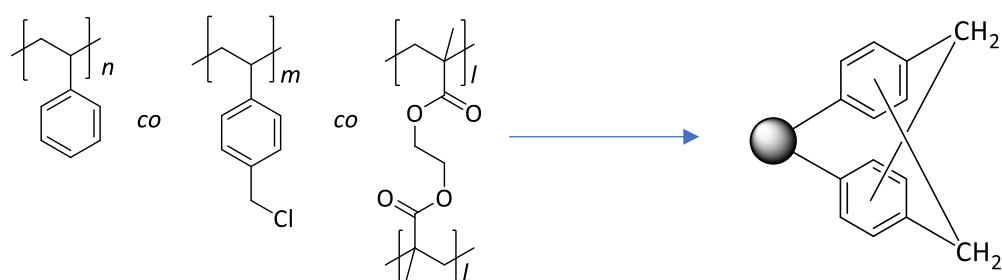
Appearance of product: Pale yellow powder

FT-IR $\bar{\nu}/\text{cm}^{-1}$ (ATR): 3024, 2922, 1724 (C=O, ester str.), 1600, 1492, 1452, 1265 (C-H wag of CH₂-Cl) 830, 699 (C-Cl str.)

Elemental microanalysis: Expected 81.2% C, 6.9% H, 0.3% N and 11.3% Cl; Found 85.3% C, 7.0% H, 0.4% N and 9.4% Cl

BET specific surface area: < 5 m²/g.

Preparation of hypercrosslinked poly(styrene-co-VBC-co-EGDMA) via a one stage process.



Following *General Procedure C* results are reported as: a) amount of precursor polymer particles; b) amount of FeCl₃; (c) Product yield

a) 2 g; b) 1.03 g, 6.35 mmol; c) 1.62 g, 89 %

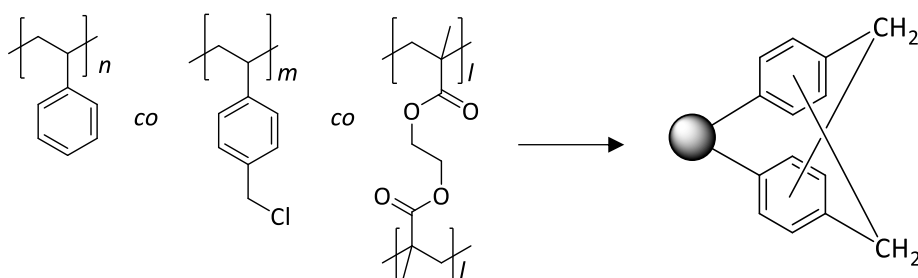
Appearance of product: Light brown powder

FT-IR $\bar{\nu}/\text{cm}^{-1}$ (ATR): 2920, 1722 (C=O, ester str.), 1508, 1494, 1452, 812, 758, 710 (weak. C-Cl str.) There appears to be no band at $\sim 1265 \text{ cm}^{-1}$ corresponding to the C-H wag of CH₂-Cl

Elemental microanalysis: Expected 92.2% C, 7.38% H, 0.4% N and 0% Cl; Found 89.2% C, 7.1% H, 0.7% N and 1.2% Cl.

Langmuir specific surface area: 788 m²/g, Average pore diameter: 2.5 nm, Total pore volume (at saturation): 0.36 cm³/g.

Preparation of hypercrosslinked poly(styrene-co-VBC-co-EGDMA) via a two-stage process.



Following *General Procedure D* results are reported as: a) mass of precursor polymer particles; b) mass of FeCl₃ in first stage; c) mass of FeCl₃ in second stage; d) Product yield

a) 1.5 g; b) 0.071 g, 0.3 mmol; c) 0.429 g, 2.64 mmol; d) 0.86 g, 63%

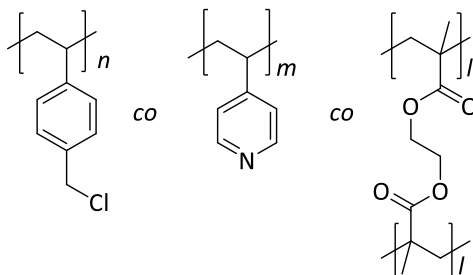
Appearance of product: Light brown powder

FT-IR $\bar{\nu}/\text{cm}^{-1}$ (ATR): 2920, 1722 (C=O, ester str.), 1508, 1494, 1452, 812, 758, 710 (weak. C-Cl str.) There appears to be no band at $\sim 1265 \text{ cm}^{-1}$ corresponding to the C-H wag of CH₂-Cl

Elemental microanalysis: Expected 92.2% C, 7.3% H, 0.5% N and 0% Cl; Found 90.2% C, 7.4% H, 0.4% N and 0.5% Cl

Langmuir specific surface area: 512 m²/g, Average pore diameter: 2.1 nm, Total pore volume (at saturation): 0.16 cm³/g.

Preparation of Poly(VBC-co-4-VP-co-EGDMA) via NAD Polymerisation



Following *General Procedure B* results are reported as: a) Total amount of VBC; b) total amount of 4-VP; c) amount of EGDMA; d) amount of AIBN; e) volume of ethanol; f) product yield

a) 93 wt%, 9.36 g, 61.3 mmol; b) 6 wt%, 0.65 g, 6.1 mmol; c) 1 wt%, 0.1 g, 0.5 mmol; d) 0.201 g, 1.2 mmol; e) 47.5 mL; f) 8.17 g, 81%

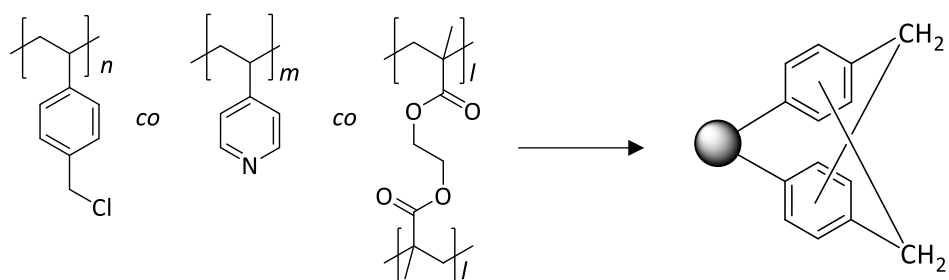
Appearance of product: Dull white powder

FT-IR $\bar{\nu}/\text{cm}^{-1}$ (ATR): 2924, 2854, 1720 (C=O, ester str.), 1635, 1560 (pyridine ring, str.), 1580 (pyridine ring, str.), 1265 (C-H wag of CH₂-Cl) 817, 707 (C-Cl str.)

Elemental microanalysis: Expected 71.3% C, 6.0% H, 1.2% N and 21.2% Cl; Found 71.3% C, 6.5% H, 1.4% N and 20.4% Cl

BET specific surface area: 14 m²/g, Average pore diameter: 16.2 nm, Total pore volume (at saturation): 0.06 cm³/g.

Preparation of hypercrosslinked Poly(VBC-co-4-VP-co-EGDMA) via a one stage process



Following *General Procedure C* results are reported as: a) amount of precursor polymer particles; b) amount of FeCl_3 ; c) Product yield

a) 1.5 g; b) 1.45 g, 8.9 mmol; c) 1.24 g, 96%

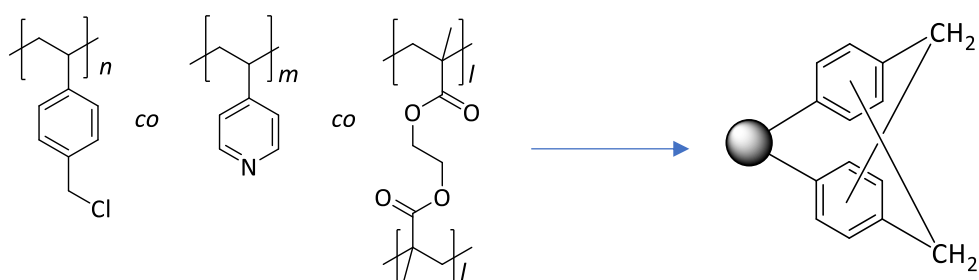
Appearance of product: Light brown powder

FT-IR $\bar{\nu}/\text{cm}^{-1}$ (ATR): 2922, 1720 (C=O, ester str.), 1683, 1550 (pyridine ring str.), 1446, 1265 (very weak), 902, 796

Elemental microanalysis: Expected 91.5% C, 7.0% H, 1.5% N and 0% Cl; Found 80.0% C, 6.6% H, 1.4% N and 6% Cl

Langmuir specific surface area: $780 \text{ m}^2/\text{g}$, Average pore diameter: 3.6 nm, Total pore volume (at saturation): $0.70 \text{ cm}^3/\text{g}$.

Preparation of hypercrosslinked Poly(VBC-co-4-VP-co-EGDMA) via a two-stage process



Following *General Procedure D* results are reported as: a) mass of precursor polymer particles; b) mass of FeCl_3 in first stage; c) mass of FeCl_3 in second stage; d) Product yield

a) 1.5 g; b) 0.098 g, 0.6 mmol; c) 0.429 g, 2.64 mmol; d) 1.14 g, 95%

Appearance of product: Light brown powder

FT-IR $\bar{\nu}/\text{cm}^{-1}$ (ATR): 2922, 1720 (C=O, ester str.), 1683, 1550 (pyridine ring str.), 1446, 1265 (very weak), 902, 796

Elemental microanalysis: Expected 90.6% C, 7.6% H, 1.8% N and 0% Cl; Found 79.7% C, 6.5% H, 1.6% N and 7.6% Cl

BET specific surface area: 513 m^2/g , Average pore diameter: 3.1 nm, Total pore volume (at saturation): 0.4 cm^3/g .

2.3.3 PAH Sorption Experiments using 1st generation materials

Small-scale sorption experiments

An 'equilibrium binding' type experiment was devised, in which 250 mg of each polymer was placed in a separate, closed syringe barrel. To each syringe barrel was added 500 μL of a heptane solution containing acenaphthene, anthracene and pyrene, each at a concentration of 30 $\mu\text{g}/\text{mL}$. This solution was left in contact with the polymer particles for a period of 24 hours at room temperature. After this time, a sample of the liquid portion was removed and analysed by GC. The percentage of each PAH removed from solution was then reported. Along with the polymer samples, a 'blank' experiment was also carried out, in which no polymer was included with the PAH/heptane solution. All sorption experiments were performed in triplicate.

Large-scale sorption experiments

The large-scale sorption experiments took a similar form as the small-scale sorption experiments. 250 mg of each polymer was placed into a glass jar. To the jar was added 20 mL of a heptane solution containing acenaphthene, anthracene, pyrene, nitropyrene and 1-methylnaphthalene, each at a concentration of 200 $\mu\text{g}/\text{mL}$. The jar was then sealed. The solution was left in contact with the polymer for a period of 24 hours at room temperature. After this time, a sample of the liquid portion was removed and analysed

by GC. The percentage of each PAH that was removed from solution was then reported. Along with the polymer samples, a 'blank' experiment was also carried out, in which no polymer was included with the PAH/heptane solution. All sorption experiments were performed in triplicate.

2.4 Synthesis of 2nd generation materials via suspension polymerisation and the hypercrosslinking of materials thereof

2.4.1 General Procedures

A. General procedure for the synthesis of non-porous polymers by suspension polymerisation⁶¹

All polymerisations were carried out on a 40 g monomer scale, using a common aqueous phase. The aqueous phase was prepared by dissolving PVA (7.5 g, 88% hydrolysed, \overline{M}_n 125000) in doubly distilled water (1000 mL). Some heat and stirring was required to fully dissolve the PVA. Once dissolved, NaCl (33 g) was then added and allowed to dissolve also. 700 mL of this solution was then used as the aqueous phase. This was added to a 1-litre, jacketed, parallel-sided, baffled, flange-topped reactor fitted with condenser, nitrogen inlet and a mechanical stirrer which possessed a double impeller.

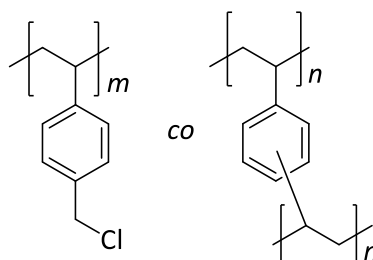
The organic phase was prepared in a separate round-bottomed flask, as follows: To a mixture of all monomers and crosslinker, was added 0.5 wt% of AIBN (0.2 g, 1.21 mmol). Nitrogen gas was then bubbled through this solution for 10 minutes to remove oxygen. The organic phase was then added to the reaction vessel containing the aqueous phase and suspended as spherical droplets by stirring at 425 r.p.m. The reaction mixture was heated to 80 °C for 6 hours, affording a white milky suspension of product. The reaction mixture was then cooled to room temperature and decanted onto a 25 µm sieve and washed with deionised water and methanol. The resultant particles were swollen in acetone for 10 – 15 mins and then Soxhlet extracted overnight with acetone. Finally, the polymer was filtered on a 0.45 µm nylon membrane filter. The polymer sample was sieved and the fraction greater than 106 µm was used in sorption tests.

B. General procedure to produce fully hypercrosslinked polymer particles.⁶⁴

To a flange-topped, 1 litre round-bottomed reactor fitted with a condenser, gas inlet and a 4 bladed PTFE stirrer was added the precursor polymer particles (all particles were >106 μm). *n*-Heptane (250 mL) was added and allowed to disperse among the polymer particles for 2 hours, with stirring at 200 r.p.m. Iron trichloride was then added to reaction mixture at 11 mol% relative to the chlorine that was expected to be present in the precursor particles. The reaction mixture was then heated rapidly to 60 °C for 18 hours. The partially hypercrosslinked polymer particles were filtered on a 0.45 μm nylon membrane filter and washed with methanol and 2M HNO_3 and then washed with acetone overnight in a Soxhlet extractor. The particles were then filtered once more and then dried overnight *in vacuo* (60 mbar, 40 °C). The resultant light brown particles were then fully hypercrosslinked: To a flange-topped, 1 litre round-bottomed reactor fitted with a condenser, gas inlet and a 4 bladed PTFE stirrer was added the precursor polymer particles (all particles were >106 μm). 1,2-Dichloroethane (125 mL) was added and allowed to swell the polymer particles for 1 hour, with stirring at 200 r.p.m. Iron trichloride was then added to the mixture in a 1:1 mol ratio of chloromethyl groups that were expected to be present in the non-hypercrosslinked precursor particles. The reaction mixture was then heated rapidly to 80°C for 18 hours. The resultant fully hypercrosslinked polymer particles were filtered on a 0.45 μm nylon membrane filter and washed with methanol and 2M HNO_3 , then washed with acetone overnight in a Soxhlet extractor. The particles were then filtered for the last time on a 0.45 μm nylon membrane filter with acetone and diethyl ether before drying *in vacuo* (60 mbar, 40 °C) overnight.

2.4.2 Preparation of Polymer Particles

Preparation of Poly(VBC-co-DVB-80) via suspension polymerisation



Following *General Procedure A*, results are reported as: a) Amount of VBC; b) Amount of DVB-80; c) Total Product Yield

a) 98 wt%, 39.2 g, 257 mmol; b) 2 wt%, 0.8 g, 6 mmol; c) 29.0 g, 72%

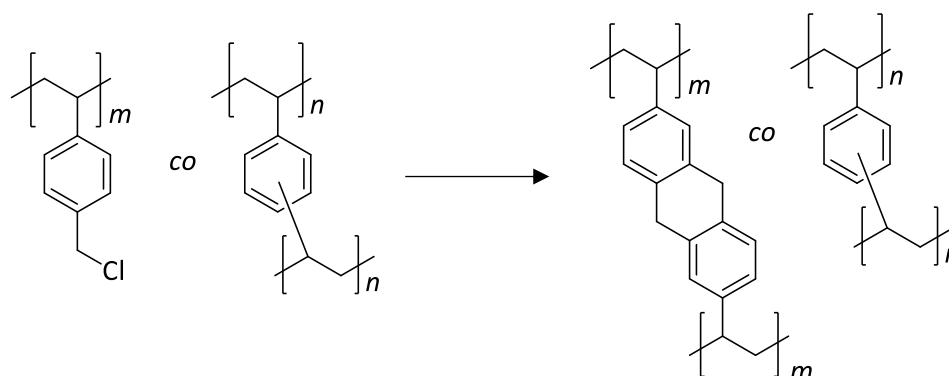
Appearance of product: White beads

FT-IR $\bar{\nu}/\text{cm}^{-1}$ (ATR): 3304 (broad O-H stretch), 3014 (aromatic C-H stretch), 2920 (aliphatic C-H stretch), 2914, 1512, 1419, 1265 (C-H wag of CH_2Cl), 1209, 1174, 1070, 1030, 810, 709 (C-Cl bond stretch)

Elemental microanalysis: Expected 71.3% C, 6.0% H, <0.3% N and 22.7% Cl; Found 73.6% C, 6.8% H, <0.3% N and 11.8% Cl.

BET surface area: < 5 m^2/g

Preparation of hypercrosslinked poly(VBC-co-DVB-80)



Following *General Procedure B*, results are reported as: a) Amount of polymer precursor particles; b) Amount of FeCl_3 in the first step; c) Amount of FeCl_3 in the second step; d) Total Product Yield

a) 19 g, expected to contain 120 mmol of chlorine; b) 2.17 g, 13.4 mmol; c) 19.46 g, 120 mmol; d) 15.12 g, 92%

Appearance of product: Dark brown beads

FT-IR $\bar{\nu}/\text{cm}^{-1}$ (ATR): 3014 (aromatic C-H stretch), 2920 (aliphatic C-H stretch), 2906, 1703, 1442, 1261 (broad, weak, C-H wag of CH_2Cl), 1168, 1085, 812, 709 (weak, C-Cl bond stretch).

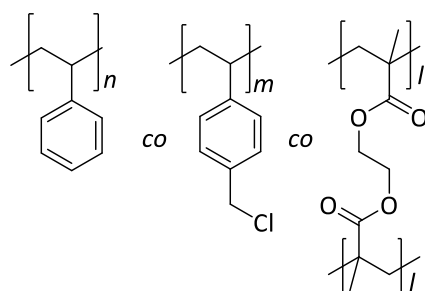
Elemental microanalysis: Expected 84.9% C, 7.1% H, <0.3% N and 0% Cl; Found 84.8% C, 6.6% H, <0.3% N and 2.3% Cl.

Langmuir Specific Surface area: 1320 m^2/g

Average pore diameter: 2.2 nm

Total pore volume (at saturation): 0.54 cm^3/g .

Preparation of Poly(Styrene-co-VBC-co-EGDMA) via suspension polymerisation



Following *General Procedure A*, results are reported as: a) Amount of Styrene; b) Amount of VBC; c) Amount of EGDMA; d) Total Product Yield

a) 49.5 wt%, 20.0 g, 192 mmol; b) 49.5 wt%, 20.0 g, 131 mmol; c) 1 wt% 0.4 g, 2 mmol; d) 32.9 g, 82%

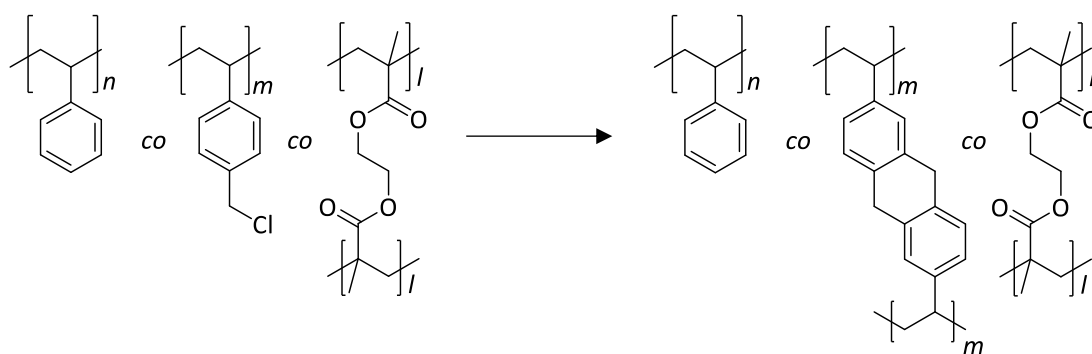
Appearance of product: White beads

FT-IR $\bar{\nu}/\text{cm}^{-1}$ (ATR): 3330 (broad O-H stretch), 3023 (aromatic C-H stretch), 1710 (ester C=O stretch), 1266 (C-H wag of CH_2Cl), 1214 (ester C-O stretch), 1113, 1098, 1015, 814, 760, 699 (C-Cl bond stretch).

Elemental microanalysis: Expected 81.3% C, 6.9% H, <0.3% N and 11.5% Cl; Found 81.2% C, 7.1% H, <0.3% N and 6.1% Cl.

Specific Surface area: <5 m^2/g

Preparation of HXL Poly(Styrene-co-VBC-co-EGDMA)



Following *General Procedure B*, results are reported as: a) Amount of polymer precursor particles; b) Amount of FeCl_3 in the first step; c) Amount of FeCl_3 in the second step; d) Total Product Yield

a) 9 g, expected to contain 27 mmol of chlorine; b) 0.52 g, 3.2 mmol; c) 4.45 g, 27 mmol; d) 7.7 g, 95%

Appearance of product: Dark Brown Beads

FT-IR $\bar{\nu}/\text{cm}^{-1}$ (ATR): 3021 (aromatic C-H stretch), 2917 (aliphatic C-H stretch), 1710 (ester C=O stretch), 1602, 1511, 1452, 1435, 1184, 1113, 1020, 812, 758.

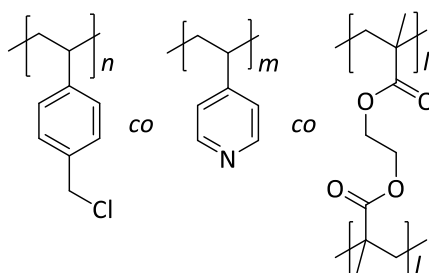
Elemental microanalysis: Expected 86.7% C, 7.4% H, <0.3% N and <0.3% Cl; Found 89.2% C, 6.9% H, <0.3% N and <0.3% Cl.

Langmuir Specific Surface area: 549 m^2/g

Average pore diameter: 2.4 nm

Total pore volume (at saturation): 0.24 cm^3/g .

Preparation of Poly(VBC-co-4-VP-co-EGDMA) via Suspension Polymerisation



Following *General Procedure A*, results are reported as: a) Amount of VBC; b) Amount of 4-VP; c) Amount of EGDMA d) Total Product Yield

a) 93 wt%, 37.4 g, 245 mmol; b) 6 wt%, 2.5 g, 25 mmol; c) 1 wt%, 0.4 g, 2 mmol; d) 26.4 g, 65%

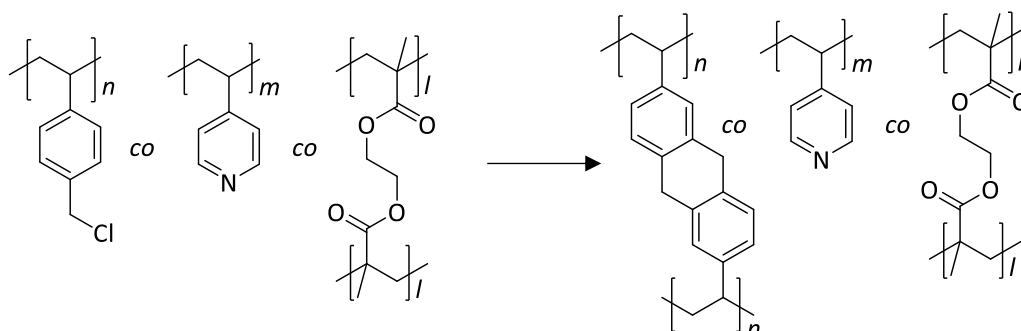
Appearance of product: White beads

FT-IR $\bar{\nu}/\text{cm}^{-1}$ (ATR): 3330 (broad O-H stretch), 2917 (aliphatic C-H bond stretch), 1705 (ester C=O stretch), 1422 (C-N bond stretch), 1208 (ester C-O bond stretch), 1250 (C-H wag of CH₂-Cl), 1009 and 814.

Elemental microanalysis: Expected 71.3% C, 6.0% H, 0.9% N and 21.5% Cl; Found 69.7% C, 6.8% H, 0.8% N and 12.2% Cl.

Specific Surface Area: <5 m²/g

Preparation of HXL Poly(VBC-co-4-VP-co-EGDMA)



Following *General Procedure B*, results are reported as: a) Amount of polymer precursor particles; b) Amount of FeCl₃ in the first step; c) Amount of FeCl₃ in the second step; d) Total Product Yield

a) 20 g, expected to contain 115 mmol of chlorine; b) 2.2 g, 13.3 mmol c) 18.54 g, 115 mmol; d) 16.2 g, 98%

Appearance of product: Dark Brown Beads

FT-IR $\bar{\nu}/\text{cm}^{-1}$ (ATR): 3056 (aromatic C-H stretch), 2919 (aliphatic C-H stretch), 2322, 1710 (ester C=O stretch), 1418 (pyridine C-N bond stretch), 1067, 1019, 812, 747.

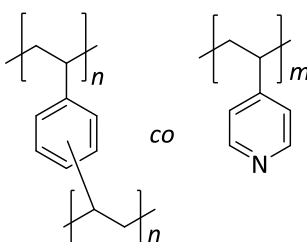
Elemental microanalysis: Expected 81.7% C, 7.1% H, 0.8% N and <0.3% Cl; Found 80.6% C, 6.1% H 1.1% N and 2.4% Cl.

Langmuir Specific Surface Area: 1392 m²/g.

Adsorption average pore diameter: 2.2 nm.

Total pore volume (at saturation): 0.56 cm³/g.

*Preparation of Poly(DVB-80-co-4-VP) via Suspension Polymerisation.*¹⁸⁶



The polymer beads were synthesised using a suspension polymerisation method⁶ in a 1-litre jacketed, parallel-sided, baffled, flange-topped reactor fitted with condenser, nitrogen inlet and a mechanical stirrer which possessed a double impeller. At room temperature, the reactor was charged with an aqueous phase consisting of 130 mL of distilled water and 2 wt% (2.6 g) of PVA.

The organic phase was prepared separately in a round-bottomed flask. An 80:20 mol ratio of DVB-80 (33.29 g, 254.9 mmol) to 4-VP (6.70 g, 63.7 mmol) was mixed with toluene (87 mL) as porogen. To this was added AIBN (0.67 g, 4.1 mmol) (1.3 mol% relative to moles of monomer). The total volume of the organic phase was 130 mL, therefore the ratio of organic phase to aqueous phase was 1:1. Nitrogen gas was then bubbled through this solution for 10 minutes to remove dissolved molecular oxygen.

This organic phase was then added to the aqueous phase and suspended by stirring at 425 r.p.m. The polymer suspension was heated to 80 °C for 24 hours affording a white milky suspension of product. The reaction mixture was then cooled, and the beads decanted onto a 25 µm sieve and washed with deionised water and methanol before

drying *in vacuo* (60 mbar, 40 °C) to constant mass. After drying, the beads were sieved and the fraction larger than 106 µm used in sorption tests.

Product yield: 39.5 g, 98%

Appearance of product: White beads

FT-IR $\tilde{\nu}/\text{cm}^{-1}$ (ATR): 2909 (aliphatic C-H stretch), 1693, 1597, 1558, 1416 (pyridine C-N stretch), 1260, 1071, 825, 795.

Elemental microanalysis: Expected 89.8% C, 7.8% H and 2.5% N; Found 87.8% C, 7.8% H, 2.2% N

Specific surface area (BET): 599 m²/g

Adsorption Average pore width: 7.8 nm

2.4.3 PAH sorption experiments

Sorption experiments of 2nd generation polymers synthesised via suspension polymerisation and the hypercrosslinked variants thereof

250 mg of each polymer was placed into a glass jar. To the jar was added 20 mL of a heptane solution containing acenaphthene, anthracene, pyrene, nitropyrene and 1-methylnaphthalene, each at a concentration of 200 µg/mL. The jar was then sealed. The solution was left in contact with the polymer for a period of 24 hours, with constant mixing by placing the jars on low-profile roller. After this time, a sample of the liquid portion was taken and analysed by GC. The percentage of each PAH that was removed from solution was then reported. Along with the polymer samples, a 'blank' experiment was also carried out, in which no polymer was included with the PAH/heptane solution. All sorption experiments were performed in triplicate.

2.5 Experimental for engine tests

The surface area analysis, FT-IR analysis, elemental microanalysis and SEM analysis were carried out at Strathclyde University.

2.5.1 Equipment

Engine tests were carried out at BP's Product Testing and Engineering facility by Robert Spragg, Thomas Peirson-Smith, Alistair Drury, and Mark Coakley.

A Ricardo diesel 'Hydra' test engine was used for all engine tests. This naturally aspirated, 0.5 L, single cylinder, light-duty engine is a bespoke research engine. It is of a modular design and has an 'open ECU' (Engine Control Unit). This allows for parameters including, *inter alia*, fuel/air mixture, ignition timing and engine idle speed to be controlled independently. This allows for specific soot loading in the engine lubricant to be achieved. The engine was fitted with an external oil circuit, as shown in **Figure 10**. Associated analytical analyses of the lubricants from the engine tests were carried out by BP's Formulated Products Technology Investigational Analysis facility.

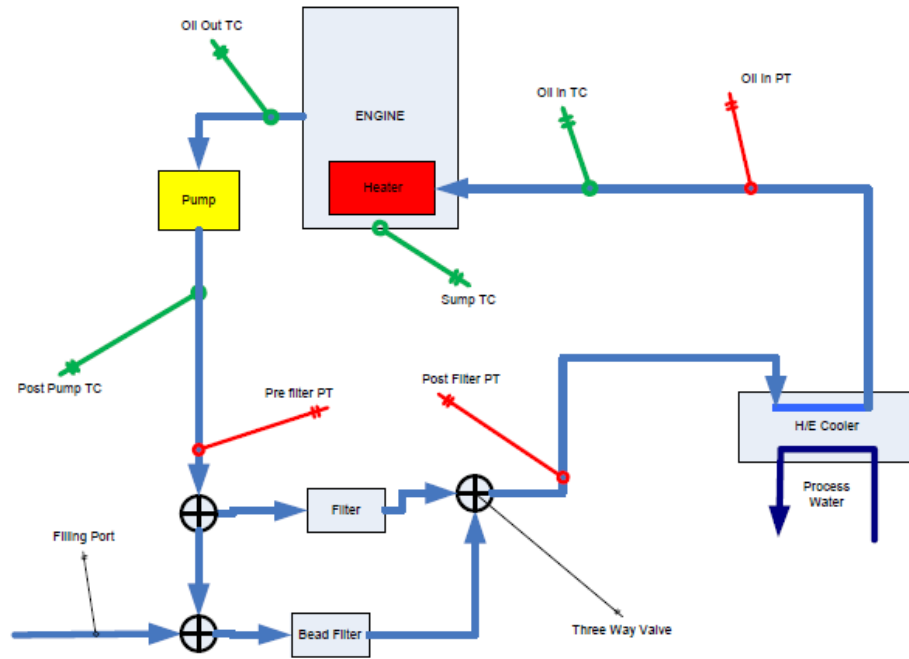


Figure 10 - Engine lubricant system circuit diagram

GC-MS/NDP/FPD was carried out on an Agilent 7890B Gas Chromatograph fitted with a mass spectrometer (MS), a nitrogen detector (ND) or a sulfur detector (FPD). Prior to the GC analysis the polymer samples were either thermally desorbed (heated to 350 °C) or pyrolysed (heated to 600 °C to break bonds) The polymers were analysed both neat and after washing with pentane. The pentane washing was to remove excess engine lubricant from the polymer sample. These analyses were carried out at BP's Formulated Products Technology Investigational Analysis facility by Chrissie Wicking and Sam Whitmarsh.

The elemental microanalysis, SEM analysis surface area analysis, FT-IR analysis and surface area analysis were carried out at Strathclyde University.

Procedures

Non – fired engine test

The non-fired engine test utilised only the oil pump to flow hot oil around the engine and lubricant circuit, without any engine combustion. The engine was flushed with the candidate lubricant for 30 minutes at 60 °C. The flushing lubricant was then removed, and the sump filled with more of the candidate lubricant, before heating to the test temperature (60 °C). For the non-fired engine test, the candidate lubricant was a used heavy-duty diesel engine lubricant that had been used in a field test. The polymer to be tested was then loaded into the ‘bead filter’ (see **Figure 46**) (a K&N lubricant and fuel filter). The hot lubricant was then pumped round the circuit for a total of 10 hours. A 100 mL sample of lubricant was taken every hour for analysis. To achieve this, the oil pump had to be stopped each time lubricant was to be removed.

Fired engine test

The fired engine test was run in much the same way as the non-fired engine test. The engine and lubricant circuit were flushed for 30 minutes with a strong detergent lubricant. The oil pump was used to perform this task. This lubricant was then removed and replaced with the candidate lubricant. For the fired engine test, the candidate lubricant was a bespoke diesel engine lubricant that did not contain any dispersant. The polymer beads were loaded in the ‘bead filter’. A small sample of engine lubricant was then taken for FT-IR and TGA-soot analyses to provide a base line.

The engine was then started. The engine was then run for either 8 hours or 16 hours, depending on the test being carried out. The engine was stopped every hour, 100 mL of oil was then sampled for analysis before the engine was restarted. To ensure a higher than normal soot loading in the lubricant, the test engine was run under the following conditions:

Injection pressure: 1800 bar

Number of fuel injections: One

Start of main injection: 10.5° Crank angle, beyond top dead centre.

Duration of main injection: 0.5 ms.

3.0 Results and Discussion

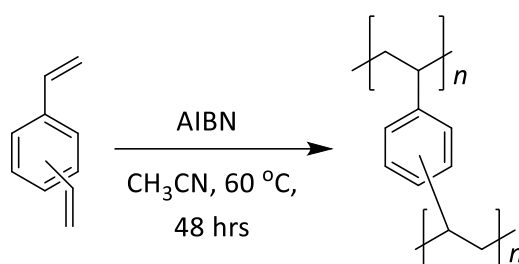
3.1 Synthesis of polymer microspheres by precipitation and non-aqueous dispersion polymerisation.

Porous polymer microspheres have found use in many sorption applications, with the sorption of contaminants from engine oil, *in situ*, being the focus of the work presented in this thesis. Methodologies that have been researched thoroughly within our group, and elsewhere, are utilised and built upon to synthesise materials that are envisaged to be of use within this area. The synthesis of a range of porous and non-porous polymer particles, prepared *via* both precipitation polymerisation (PP) and non-aqueous dispersion (NAD) polymerisation, to yield polymers containing varying ratios of comonomers, has been investigated. The investigation of ultra-high specific surface area materials has also been undertaken. These materials were produced using the previously discussed Friedel-Crafts chemistry developed by Davankov *et al.*⁶⁵

3.1.1 Synthesis of Poly(DVB-80)

Precipitation polymerisation is a robust and facile method of producing porous polymer microspheres. As a general rule, the higher the amount of crosslinker included the higher the yield of the polymerisation. Crosslinker also imparts more mechanical strength into the particles. Microspheres comprised entirely of crosslinker, *i.e.* divinylbenzene-80, were prepared in a usable yield (**Scheme 16**). The reaction was carried out on a 2 g monomer scale, using 100 mL of acetonitrile. In precipitation polymerisation, the growing microspheres capture growing oligomers and monomers onto their surface but due to the low monomer concentration, do not agglomerate with other growing microspheres. In more concentrated polymerisation systems these growing microspheres would merge together and form one interconnected polymer network (*e.g.* suspension polymerisation). A very low monomer concentration is therefore required in precipitation polymerisation, to avoid agglomeration of the polymer particles as they form. Acetonitrile is used as the polymerisation medium in precipitation polymerisation

as it is a near- θ solvent for poly(DVB). In precipitation polymerisation, if mono-disperse polymer particles are to be produced, near- θ solvents are required.⁴⁷ Carrying of the polymerisation of divinylbenzene allowed the author to gain experience in the methodology of precipitation polymerisation, it also allowed for the preparation of a material that had no functionality besides vinyl aromatic and hydrophobic character, which it was hoped would aid in π - π stacking interactions with PAHs.



Scheme 16: Synthesis of Poly(DVB-80) microspheres

An FT-IR spectrum of the product showed stretches at 3082, 835 and 749 cm⁻¹ indicative of: aromatic C-H stretching, 1,4 - and 1,3 di-substitution of the aromatic ring, respectively. Elemental microanalysis corroborated DVB being present in the product.

Nitrogen sorption analysis was used to investigate the surface area and porosity of the poly(DVB-80) particles. The specific surface area was found to be 413 m²/g, with an average pore diameter of 2.2 nm. A high surface area such as this may at first seem unusual as no potent pore forming solvent (such as toluene) was included in the synthesis. Indeed, when Li and Stöver carried out similar polymerisations of DVB-55 (which contains a mixture of 55% divinyl benzene and 45% ethylvinyl benzene), they found that when only acetonitrile was used as a solvent the resultant polymer beads had specific surface areas of less than 5 m²/g.⁴⁹ However, in the above synthesis DVB-80, which contains 80% divinylbenzene, was used. By increasing the amount of divinyl species in the crosslinker, a permanently porous material was produced due to an increase in crosslink density when compared to a poly(DVB-55). By increasing the number of crosslinks, upon removal of the solvent from the polymer, the material is more rigid and therefore able to retain a porous structure.

SEM was used to analyse the shape and size of the resultant particles. An SEM micrograph is shown in **Figure 11**.

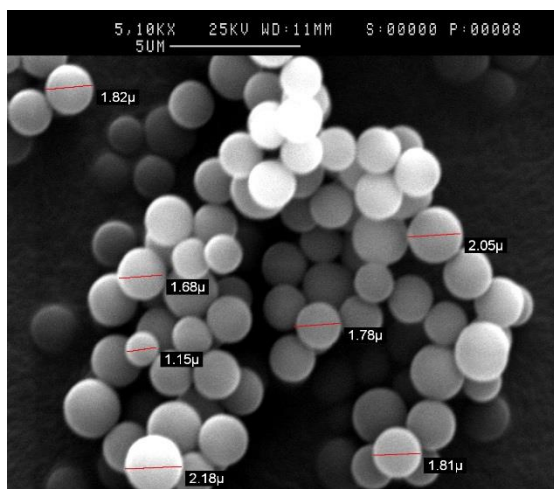


Figure 11 -SEM micrograph of poly(DVB-80)

The SEM image shows smooth spherical particles. As can be seen in the image, the particles are also discrete, that is they are a collection of individual particles. This is due to the very high level of crosslinker used which results in particles that do not aggregate together upon collision with one another. Most of the particles produced in this polymerisation were less than 2 μm in size, and are clearly polydisperse.

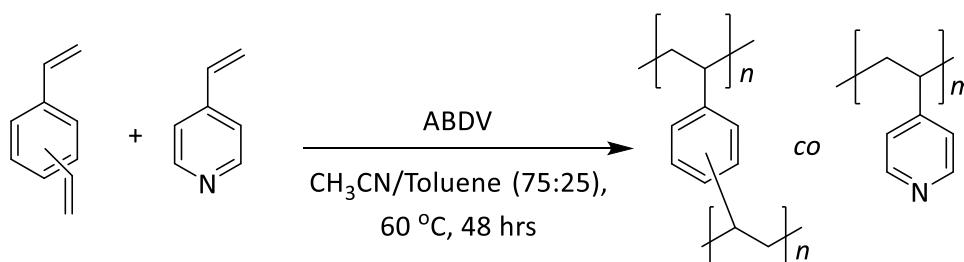
With proficiency in precipitation polymerisation now gained, attention turned to including co-monomers into the monomer feed to produce polymers that possess useful chemical functionality. It was believed that the inclusion of functional moieties may enhance the polymers capabilities in PAH sorption and capture, as well as allowing higher specific surface areas to be imparted through hypercrosslinking chemistry.

3.1.2 Synthesis of Poly(DVB-co-4-vinylpyridine)

Vinylpyridine has been used as a co-monomer in materials that are used in chromatographic columns for the separation of PAHs, specifically benzo[*a*]pyrene and

anthracene.¹¹⁰ With this information in hand it was deemed pertinent to this study to produce materials that were of a similar character.

In an analogous fashion to the poly(DVB-80) discussed above, poly(DVB-co-4-vinylpyridine) was synthesised from a 10:1 mole ratio of monomers (**Scheme 17**) in a 66% yield.



Scheme 17- Synthesis of poly(DVB-80-co-4-VP)

Toluene was used as a solvent in this polymerisation, with acetonitrile usually employed in addition. Toluene is considered a good solvent for aromatic polymers such as DVB. By including toluene, the solvency of the reaction medium is improved. This causes phase separation of the growing polymer to occur at a later stage. Some of the toluene will become trapped in the growing polymer particles, thereby forming small pores within the polymer particles.

To ensure both monomers were incorporated into the final polymer elemental microanalysis was employed and the values gained from this were compared with values expected for the elements present (**Table 2**).

	Elemental microanalysis (%)		
	C	H	N
Expected based on 10:1 mole ratio DVB-80:4-VP	90.2	8.1	1.7
Observed for poly(DVB-80-co-4-VP)	90.1	7.6	1.4

Table 2: Elemental microanalysis for poly(DVB-co-4-VP)

For context, elemental microanalysis has an approximate error of +/- 0.3%. The observed nitrogen content of 1.4% shows the incorporation of vinylpyridine into the polymer, with nitrogen being present only in 4-vinylpyridine and the initiator. The initiator, ABDV, does account for a small amount of the nitrogen present as it is combined into the polymer, but this was calculated as being in the region of 0.3%.

While the amount of 4-vinylpyridine in the polymer was rather low in comparison to the amount of divinylbenzene, the aromatic C-N bond stretch was visible at 1415 cm^{-1} .

In efforts to ensure the resultant material was indeed porous and of high specific surface area nitrogen sorption analysis was used to investigate the pore network of the resultant polymer particles. The poly(DVB-co-4-VP) was determined to have a rather higher surface area at $814\text{ m}^2/\text{g}$ with an average pore diameter of 2 nm indicating a microporous network. Stöver suggested that the growth mechanism of porous polymer particles in precipitation polymerisation (where a solvent is used as the porogen), is unlikely to form larger pores.⁴⁹ The isotherm produced, as seen in **Figure 12**, was a 'Type I', Langmuir isotherm. This indicates the presence of micropores predominantly.¹⁷⁸ The surface area is attributable to both the large amount of crosslinker present and the use of toluene as a porogenic solvent in the synthesis.

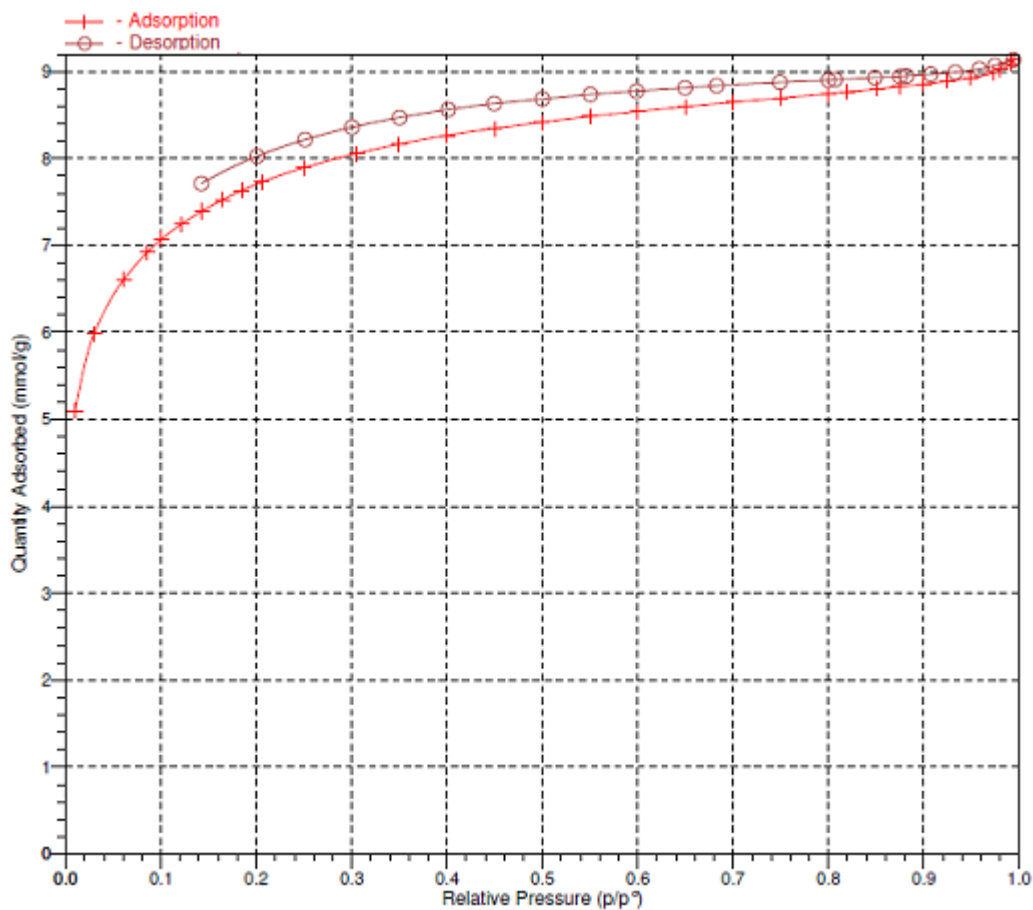


Figure 12 - Nitrogen sorption isotherm for ABDV initiated poly(DVB-80-co-4VP)

Spherical beads were formed as can be seen clearly from the SEM micrograph shown in Figure 13 - SEM micrograph of poly(DVB-co-4VP).

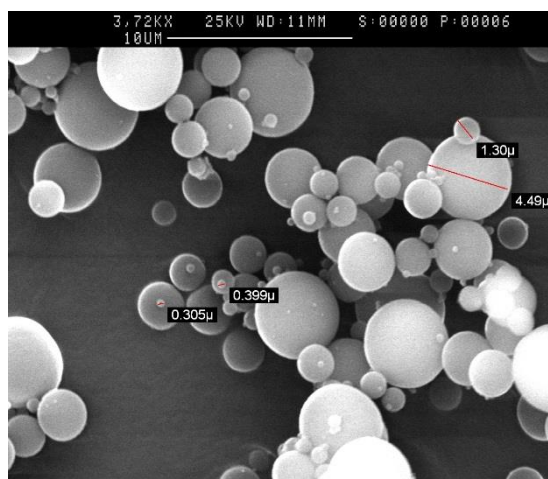


Figure 13 - SEM micrograph of poly(DVB-co-4-VP)

It is clear from this image that the particles are polydisperse, however while this may make the particles look somewhat unsightly, it should not hinder them in the intended application. As with the poly(DVB) discussed earlier, the high level of crosslinker present in this polymer would have imparted robustness into the particles leading to agglomeration of particles not being observed.

ABDV was used as an initiator in error. While this material was entirely suitable for the intended applications, the experiment was repeated using AIBN as this was the initiator of choice for all the other polymerisations presented herein. The material was produced in an otherwise identical precipitation polymerisation as detailed above, and was synthesised in a good 86% yield. As expected, the FT-IR data and elemental analysis data for the AIBN initiated polymer were very similar to the ABDV initiated polymer (see experimental section for details).

The nitrogen sorption analysis results for the AIBN initiated polymer showed a slightly lower specific surface area at 729 m²/g (compared to 814 m²/g for the ABDV initiated poly(DVB-80-co-4-VP)). However, the average pore size, pore volume and isotherm shape were very similar to the ABDV initiated polymer, indicating a pore structure dominated by micropores, as shown in **Figure 14**.

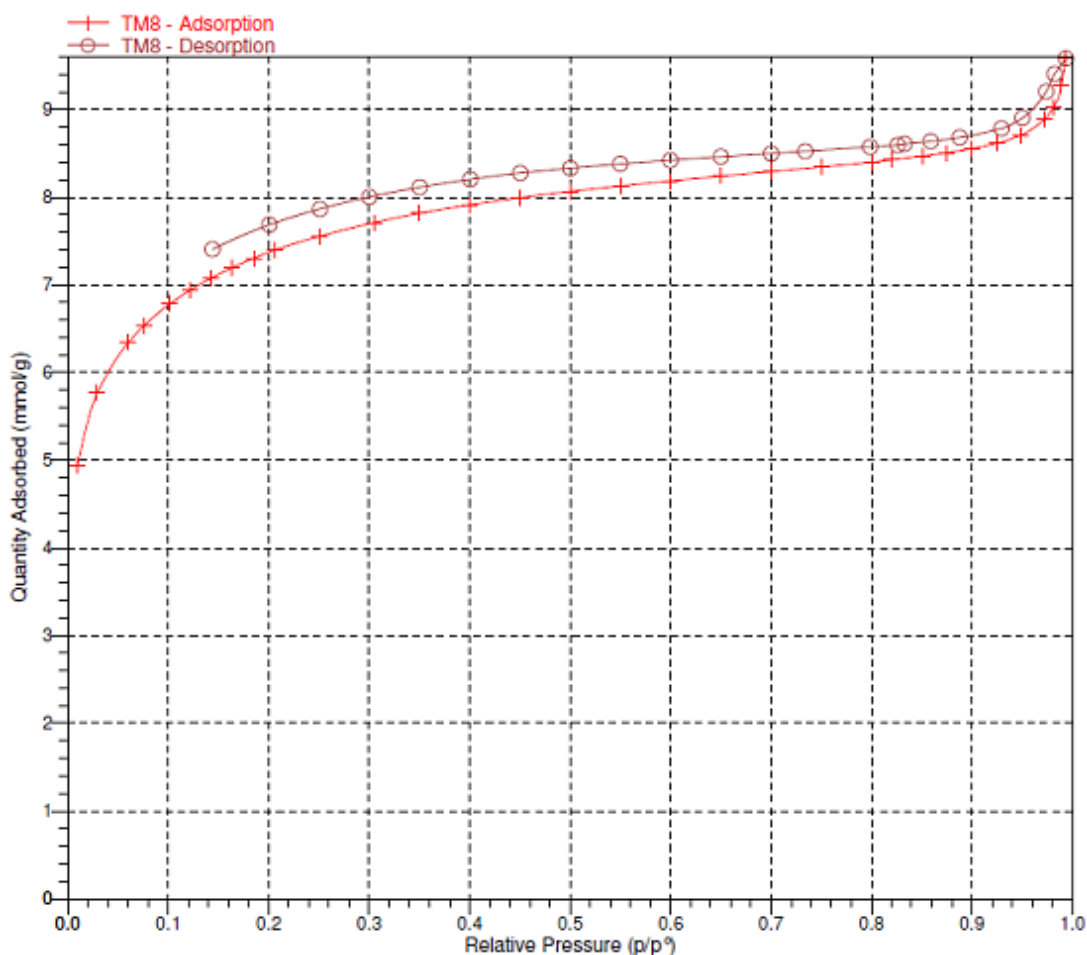


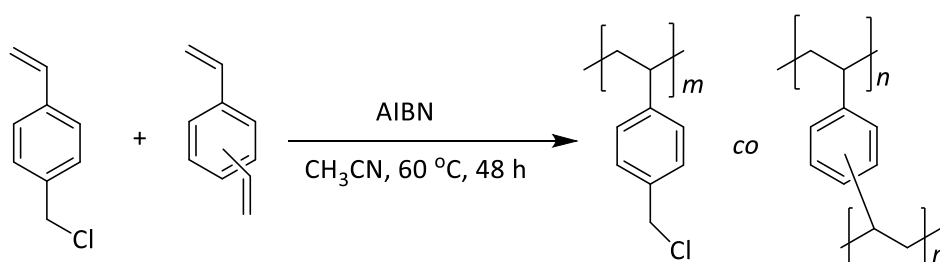
Figure 14 - Nitrogen sorption isotherm for AIBN initiated poly(DVB-80-co-4-VP)

The 'Type I' isotherm shown in **Figure 14**, for the AIBN initiated poly(DVB-80-co-4-VP) is very similar to that of the ABDV initiated poly(DVB-80-co-4-VP) shown in **Figure 12**. This indicates a very similar pore structure, with micropores (those less than 2nm) dominating. The main difference is in the region of 0.9 – 1.0 relative pressure. For the AIBN initiated polymer, the amount of nitrogen adsorbed in this region shows a large increase over a small change in pressure. This isotherm shape is commonly encountered in materials that contain macropores (those between 2 and 50 nm)¹⁷⁶ and is caused by a process called 'capillary condensation'. Capillary condensation occurs only in meso and macropores *via* a process of mono- and multilayer adsorption of gas. When analysing the surface of the material, analysis gas is admitted to the sample. It will fill the micropores first at lower partial pressures. Upon the micropores being filled with gas, the isotherm

will reach a plateau as no more gas is able to be admitted to the polymer. In materials that contain a mixture of micro- and mesopores, the micropores will be completely filled with gas but the gas in the mesopores will be one molecule thick, statistically. As more gas molecules enter the pores, they interact with the layer of gas molecules already present and produce a multilayer of adsorbed gas molecules. As the pore becomes filled with gas molecules, the Van der Waals forces between gas molecules increases due to the increasingly confined space of the pore, causing the gas to condense. This is accompanied by a rapid increase in the amount of gas adsorbed, as seen in the isotherm in **Figure 14** at an approximate partial pressure of 0.95. The AIBN initiated poly(DVB-80-*co*-4-VP) had a lower specific surface area, and this would indicate a slightly higher number of larger diameter pores.

3.1.3 Synthesis of Poly(DVB-80-*co*-VBC)

Porous polymer particles containing vinylbenzyl chloride (VBC) were prepared by precipitation polymerisation. Derived from a monomer mole ratio of 75:25 (VBC:DVB) the polymer was synthesised in a 47% yield (**Scheme 18**). This relatively low yield is not uncommon for polymers of this type and is generally attributed to losses in the filtration stage due to the formation of soluble polymer which was not recovered (in part due to the relatively low level of crosslinker that was used).



Scheme 18 - Synthesis of poly(VBC-*co*-DVB-80)

Elemental analysis was employed to probe the resultant polymer, and again these results were compared to expected values to ensure incorporation of both monomers into the resultant polymer (**Table 3**).

	Elemental microanalysis (%)			
	C	H	N	Cl
Expected for 25:75 mole ratio DVB:VBC	75.4	6.4	0.5	17.7
Observed	77.0	6.5	0.7	14.0

Table 3: Elemental microanalysis for poly(DVB-*co*-VBC)

The inclusion of VBC into the final polymer is confirmed by its presence in the elemental microanalysis results. While the chlorine content was lower than expected, it could only have arisen due to VBC. When the observed values were used to calculate the actual composition of the polymer, it was found that the mole ratio of DVB to VBC was 41:59. Using the reactivity ratios of the two monomers, DVB and VBC, the distribution of monomers in the polymer can be described.¹⁸⁷ With a mixture of two monomers, there are four different reactions that can occur at the reactive chain end. In the case of DVB and VBC. A propagating chain with a DVB radical can react with a VBC monomer or a DVB monomer. A propagating chain with a VBC radical can react with a DVB monomer unit, or a VBC unit. Each reaction has reaction rate constant, k . For each chain end, the reactivity ratio is the ratio of the rate constants for the addition of the same monomer as the reactive species already present on the chain to the rate constant for the addition of the other monomer present (**Figure 15**).

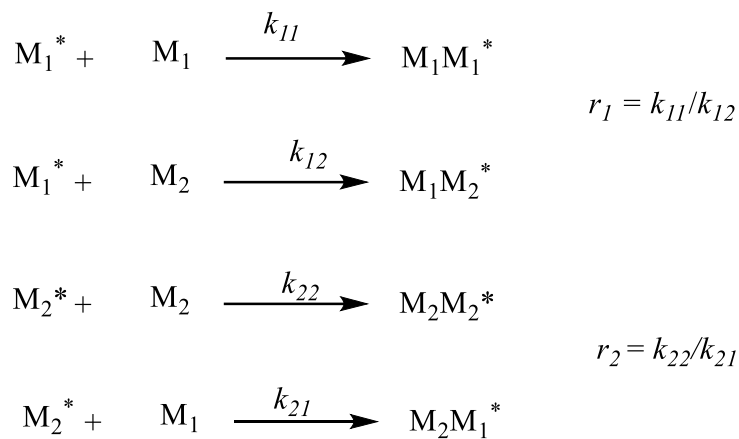


Figure 15 - Reaction schemes describing the propagation of polymer chains with two monomers present. Where M_1 is monomer 1. M_1^* is a reactive chain ending in M_1 . M_2 is monomer 2. M_2^* is a reactive chain ending in M_2 . r_1 is the reactivity ratio of monomer 1. r_2 is the reactivity of monomer 2.

The reactivity ratios for VBC and DVB are 0.27 and 1.24, respectively. What this indicates is, that propagating chains terminating in either VBC or DVB are more inclined to react with DVB monomers than they are with VBC monomers. This may explain why the mole ratio of DVB to VBC found in the polymer was higher than the mole ratio of DVB to VBC in the monomer feed.

The small amount of nitrogen present was attributed to incorporation of the nitrogen containing initiator into the polymer.

FT-IR analysis of the polymer showed bands at 1265 cm^{-1} , indicative of the C-H wag of the chloromethyl moiety, and 709 cm^{-1} , indicative of a carbon-chlorine bond stretch. A band at 1018 cm^{-1} was attributed to unreacted (pendent) vinyl bonds derived from divinyl benzene.

The polymerisation yielded spherical particles that had a relatively narrow size distribution with most particles being between 2 and 5 μm in size. **Figure 16** shows a typical SEM micrograph of poly(VBC-co-DVB-80).

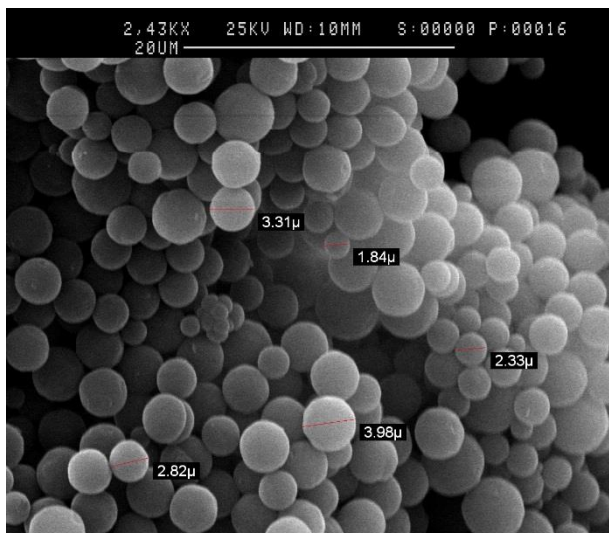


Figure 16 - SEM micrograph of poly(VBC-co-DVB-80)

$$\bar{d} = 3.13 \mu\text{m} \text{ CV} = 26\%$$

Nitrogen sorption analysis was employed to probe the surface area of this material. Due to low levels of crosslinker (25%) and a lack of a porogenic solvent, the poly(VBC-co-DVB-80) was found, as expected, to have a very low specific surface area of less than 5 m²/g. When the solvent is removed from the polymer particles at the end of the synthesis, the polymer chains have enough crosslinks to create an insoluble, infinite network. However, the number of crosslinks is not high enough to produce a well-defined pore structure

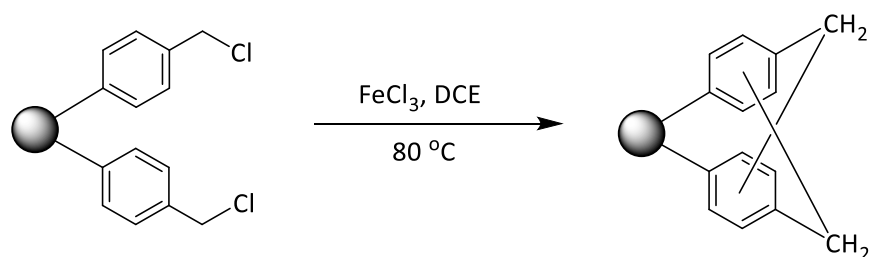
VBC containing polymers were of particular interest to the current work since not only does it yield polymers that contain a functional handle that can be reacted further to install useful functionality into the polymer, but it also allows for post-polymerisation, Davankov-type, hypercrosslinking reactions to be performed on the materials, to yield ultra-high specific surface area polymers.

3.1.4 Synthesis of hypercrosslinked (HXL) poly(VBC-co-DVB-80)

The poly(VBC-co-DVB-80) was modified *via* a Friedel-Crafts reaction to introduce porosity into the polymer. By reacting chloromethyl groups that are located close to one another, methylene bridging (crosslinks) between aromatic rings within the polymer can be achieved. By introducing many crosslinks between polymer chains in the swollen state, a

highly porous architecture can be created. The introduction of these crosslinks is accompanied by a dramatic increase in the polymer's specific surface area, in some cases this can be from only a few m^2/g to over $1000 \text{ m}^2/\text{g}$. Due to high surface areas; polymers of this type were hypothesised to be appropriate and work well for the sorption of contaminants from engine lubricants. It was also hypothesised that the high surface area could potentially reduce the contact time required between the polymer and the contaminated engine lubricant for sorption to occur.

Microporosity was introduced into the polymer microspheres by reacting them with a suitable Friedel-Crafts reagent, FeCl_3 in this case (**Scheme 19**). The polymer beads are allowed to swell in an appropriate solvent to allow access to the pendant chloromethyl groups to create methylene bridges between adjacent aromatic rings. Iron trichloride is used to catalyse the reaction in a 1:1 molar ratio with respect to the chlorine content of the polymer. These reactions are generally very high yielding. The hypercrosslinking of poly(VBC-co-DVB-80) was completed in a 92% yield (based on conversion of chloromethyl groups to methylene groups).



Scheme 19 - Hypercrosslinking of poly(VBC-co-DVB-80)

It should be noted that **Scheme 19** is a highly schematic representation of the crosslinking of two adjacent chloromethyl moieties. In reality, the hypercrosslinking occurs throughout the swollen polymer bead between chloromethyl groups that are located near each other in space, and not just at the bead surface.

Elemental microanalysis was used to monitor the hypercrosslinking reaction. The elemental content of both the hypercrosslinked polymer (HXL) and the swellable precursor are shown in **Table 4**.

Polymer	Elemental microanalysis (%)			
	C	H	N	Cl
Poly(DVB-co-VBC)	77.0	6.5	0.7	14.0
HXL poly(DVB-co-VBC)	85.5	6.8	0.9	2.7

Table 4 - Elemental microanalysis for HXL poly(VBC-co-DVB-80) and the swellable precursor poly(VBC-co-DVB-80)

Being highly strained in the dry state made polymers of this type very hygroscopic, therefore they readily sorb any solvent they came into contact with, be it moisture present in the air or any residual solvent from the hypercrosslinking reaction itself. This can make analysis of these polymers *via* elemental microanalysis somewhat tricky and can lead to discrepancies in the observed elemental content. In spite of this, it was clearly evident that there was a significant reduction in the chlorine content of the hypercrosslinked polymer as compared to its non-hypercrosslinked precursor, indicative of successful hypercrosslinking. The small amount of chlorine which remained is not necessarily a bad thing. This indicates that there are a small number of chloromethyl groups that remain. These chloromethyl groups can be utilised for further chemical modification, such as the inclusion of different functionality.^{74,75}

Nitrogen sorption analysis was used to analyse the surface area and pore morphology of the beads after having been hypercrosslinked. The data obtained is shown in **Table 5**

Polymer	BET c Value	Specific surface area (m ² /g)		Specific pore volume (cm ³ /g)	Average pore diameter (nm)
		BET	Langmuir		
		HXL poly(VBC-co-DVB-80)	549		

Table 5 - Nitrogen sorption analysis data for HXL poly(VBC-co-DVB-80)

The 'BET c value' is a number which varies from solid to solid, however in all cases it relates to the heat of adsorption of nitrogen gas onto the solid surface and the heat of liquefaction of the adsorbate. 'C' can be calculated from the gradient and y-intercept of the linear BET plot. If the BET plot is negative, then the calculated 'C' value will also be negative and is considered to be out with the valid range of the BET equation; in these cases the Langmuir value is more plausible and should therefore be used. In the above case, the BET value is positive, however it is considered very high and should not be used in this case, with the Langmuir value being more appropriate. Also, the adsorption isotherm was 'Type I' in shape, indicative of the adsorption of nitrogen gas following Langmuir rather than BET theory. A 'Type I' adsorption isotherm is also typical of materials where micropores dominate, which was corroborated by the average pore diameter measurement. In any event, it was clear that the hypercrosslinking was successful as the specific surface area of the HXL polymer had increased dramatically, to over 2000 m²/g.

FT-IR data showed the disappearance of the chloromethyl band at 1265 cm⁻¹, further evidence of successful hypercrosslinking due to the transformation of the chloromethyl groups into methylene bridges.

SEM analysis was utilised to investigate the morphology of the hypercrosslinked polymer microspheres. An SEM image is shown in **Figure 17** (right), with an SEM image of the polymer before hypercrosslinking shown on the left for comparison.

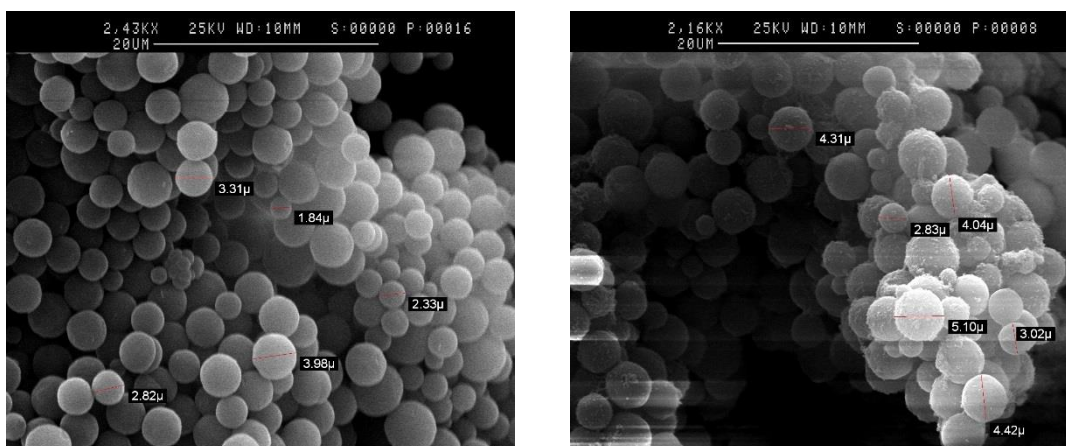


Figure 17 - SEM micrographs of poly(VBC-co-DVB-80) before (left) and after (right) hypercrosslinking

Despite high temperatures (80 °C) and very powerful Lewis acidic FeCl_3 being present, the particle's appearance remained relatively unchanged by hypercrosslinking. Small deposits on the surfaces of the hypercrosslinked particles was noticed, possibly being residual catalyst that was left behind during the reaction. These deposits may also have been oligomeric material which was trapped within the polymer network. When the polymer particles were swollen in 1,2-dichloroethane, at the beginning of the hypercrosslinking reaction, this may have allowed some of the oligomeric material to be released and it may then have deposited onto the polymer beads.

With a firm grasp on synthesising materials using precipitation polymerisation and the hypercrosslinking of appropriately functionalised polymers, attention turned to utilising non-aqueous dispersion polymerisation to produce polymer microspheres.

3.2 Non-Aqueous dispersion (NAD) polymerisation

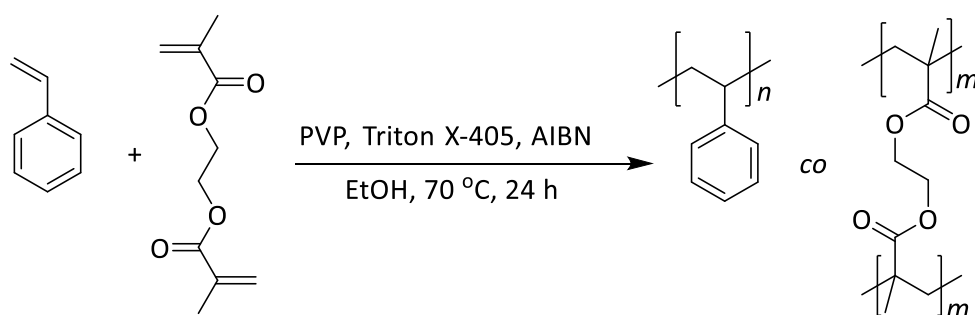
NAD polymerisation was investigated for the synthesis of materials that were to be applied in the sorption of contaminants from engine lubricants.

NAD polymerisations, like precipitation polymerisations, begin as homogenous mixtures but are usually classed as a heterogeneous polymerisation as polymer begins to fall out

of solution rather early in the synthesis. Mechanistically, NAD polymerisation is very similar to precipitation polymerisation, with both processes following a nucleation and growth pathway. Where NAD polymerisation differs from precipitation polymerisation is in the use of polymeric stabilisers. In NAD polymerisation, because no crosslinkers or low levels of crosslinker are used (typically as low as 1% of the monomer feed) polymeric stabilisers must be used to ensure that stable microspheres are synthesised. This contrasts with precipitation polymerisations which do not require stabilisers and surfactants. In precipitation polymerisations, the growing polymer microspheres possess a solvent-swollen layer which aids steric stabilisation of the polymer microspheres. Also, the rather dilute systems in precipitation polymerisations help with stabilisation. In contrast, NAD polymerisations are carried out in a far more concentrated reaction system.

3.2.1 Synthesis of Poly(Styrene-co-ethylene glycol dimethacrylate (EGMDA))

In order for the experimenter to gain proficiency in non-aqueous dispersion polymerisation procedures (which is outlined in detail in the Experimental of this thesis) it was decided to prepare poly(styrene-co-EGDMA) in the same fashion as had been reported by Winnik *et al*, **Scheme 20**.⁶² In this process half of the styrene monomer was allowed to nucleate, and after the very short nucleation stage (~ 1 hr) the other half of styrene was mixed with the crosslinking agent (EGDMA) and this was added to the polymerisation mixture. Winnik and co-workers found that by delaying the addition of crosslinker until after the highly sensitive nucleation phase, very narrow size distributions could still be prepared. If monomer and crosslinker were added together at the outset, it was reported that flocculation and coagulation occurred, with little control over particle size or indeed the formation of polymer particles at all.



Scheme 20 - Synthesis of poly(styrene-co-EGDMA)

Carried out on a 12.875 g monomer scale, as Winnink and co-workers had described, the synthesis proceeded successfully in a 77% yield. Elemental microanalysis of the product, **Table 6**, showed very good correlation to the expected values for this polymer, with the trace nitrogen present coming from AIBN which was used as the initiator.

	Elemental microanalysis (%)		
	C	H	N
Expected based on 99/1 (w/w) styrene/EGDMA	91.6	7.8	<0.3
Observed for poly(styrene-co-EGDMA)	91.7	7.6	<0.3

Table 6 - Elemental microanalysis data for poly(styrene-co-EGDMA)

FT-IR analysis was employed to investigate the composition of the polymer. The band at $\sim 1725 \text{ cm}^{-1}$ was the most significant, indicative of a C=O stretch of the ester moiety contained within the crosslinker, confirming its presence in the polymer.

The polymer incorporated a very small amount of crosslinker, approximately 1 wt%. This very low amount of crosslinker together with the fact that no porogenic solvent was used, meant that in the dry state the polymer chains would have collapsed and there would be no discernible specific surface area, as confirmed by the nitrogen sorption analysis ($\text{SSA} < 5 \text{ m}^2/\text{g}$).

SEM imagery showed a highly mono-disperse polymer with most particles being approximately 1.5 μm in diameter. Interestingly, the polymer also exhibited some hexagonal packing. **Figure 18** shows a typical micrograph of poly(styrene-*co*-EGDMA).

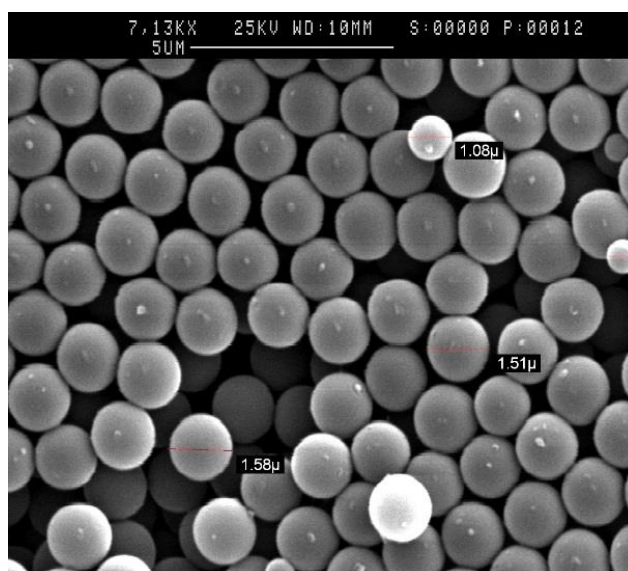


Figure 18 - SEM micrograph of poly(styrene-*co*-EGDMA)

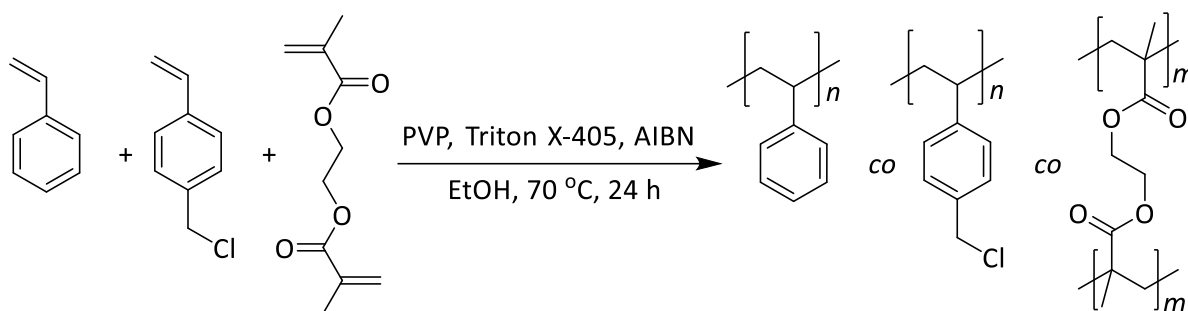
$$\bar{d} = 1.50 \mu\text{m} \text{ CV} = 7.1 \%$$

3.2.2 Synthesis of poly(styrene-*co*-VBC-*co*-EGDMA)

Winnink and co-workers also described the synthesis by NAD polymerisation of other styrene-based polymers with the inclusion of other functional monomers, namely VBC. The NAD polymerisation of poly(styrene-*co*-VBC-*co*-EGDMA) was carried out as outlined by Winnink in 2005.⁶²

The particles were derived from a 50/50 (w/w) ratio of styrene/VBC in the monomer feed together with 1 wt% of EGDMA. The same delayed addition procedure as for the poly(styrene-*co*-EGDMA) was used, where half of the styrene and VBC was allowed to nucleate for approximately one hour. After this, the remaining monomer and all the crosslinker was then added. The particles were synthesised in a gratifying 72% yield (**Scheme 21**). The amount of VBC relative to styrene was kept high to ensure that the

resultant particles possessed a sufficiently high chloromethyl content so that the particles could be further reacted further in hypercrosslinking reactions.



Scheme 21 - Synthesis of poly(styrene-co-VBC-co-EGDMA)

Elemental microanalysis results for the product showed very close agreement to the expected values for this polymer, **Table 7**.

	Elemental microanalysis (%)			
	C	H	N	Cl
Expected for 50/50 (w/w) styrene/VBC	81.2	6.9	0.3	11.3
Observed	85.3	7.0	0.4	9.4

Table 7 - Elemental microanalysis results for poly(styrene-co-VBC-co-EGDMA)

The successful incorporation of VBC into the polymer was also confirmed spectroscopically. Bands in the FT-IR spectrum at $\sim 1265\text{ cm}^{-1}$ and $\sim 700\text{ cm}^{-1}$ were indicative of the C-H wag and the C-Cl stretch of the chloromethyl group.

As with all the NAD polymers synthesised, the very low crosslink density resulted in a specific surface of less than $5\text{ m}^2/\text{g}$ being observed for poly(styrene-co-VBC-co-EGDMA) in the dry state.

SEM microscopy revealed aesthetically pleasing, highly monodisperse, spherical particles, **Figure 19**. Due to the use of small amounts of crosslinker, the NAD polymer

microspheres tended to be less robust and more malleable than microspheres with increased crosslinker density. This was evident from the slight deformations observed in the micrograph below.

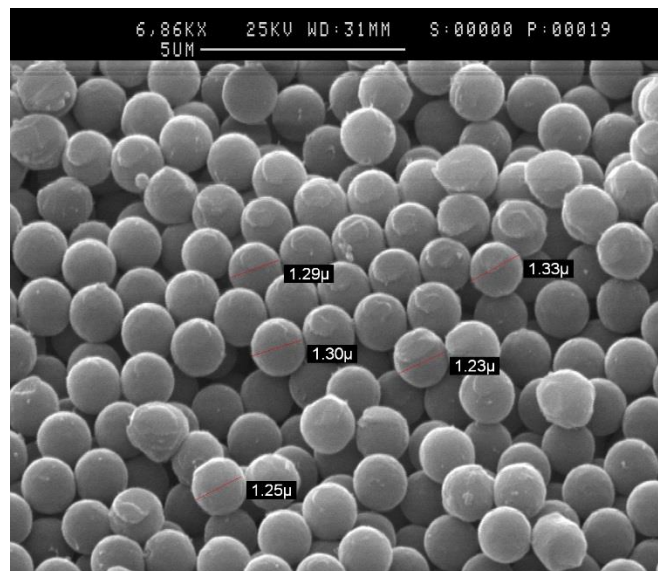
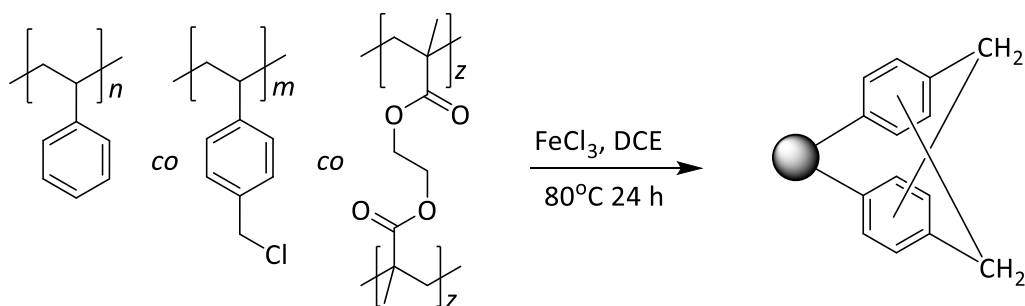


Figure 19 - SEM micrograph of poly(styrene-co-VBC-co-EGDMA)

$$\bar{d} = 1.3 \mu\text{m} \text{ CV} = 5.9\%$$

3.2.3 Synthesis of hypercrosslinked (HXL) poly(styrene-co-VBC-co-EGDMA)

The poly(styrene-co-VBC-co-EGDMA) was synthesised with the objective to react it further through post-polymerisation chemical modification, namely hypercrosslinking. It was hypothesised that the increase in specific surface area would increase the potential for sorption of PAHs and potentially other contaminants in a lubricant. Through a Friedel-Crafts reaction, the chloromethyl groups present in the polymer were reacted with appropriately located aromatic rings. This reaction was carried out successfully in an 89% yield. (Scheme 22)



Scheme 22 - Synthesis of HXL poly(styrene-co-VBC-co-EGDMA)

The main indicator of successful hypercrosslinking is the large increase in specific surface area that occurs during the reaction. The nitrogen sorption analysis data is presented in **Table 8**

Polymer	BET c Value	Specific surface area (m ² /g)		Specific pore volume (cm ³ /g)	Average pore diameter (nm)
		BET	Langmuir		
Poly(styrene-co-VBC-co-EGDMA)	129	4	6	0.0058	5.39
HXL poly(styrene-co-VBC-co-EGDMA)	549	576	788	0.355	2.47

Table 8 - Nitrogen sorption analysis for HXL poly(styrene-co-VBC-co-EGDMA) and its precursor

The isotherm that was produced by the HXL polymer was 'Type I' in shape, suggesting the Langmuir specific surface area to be the more appropriate value for this material. The very large BET 'c' value that was produced for the HXL polymer also suggests that BET theory is not appropriate for this material. The adsorption of a monolayer of nitrogen molecules, on which Langmuir theory is based, is entirely plausible for this material given the fact that it has a small average pore diameter, nearing the micropore range. With smaller pores, it may be more difficult for more nitrogen molecules to access these pores.

In any event, the success of the hypercrosslinking was clearly evident, with a very large increase in specific surface area to 788 m²/g post hypercrosslinking.

Evidence of successful hypercrosslinking was also provided by elemental microanalysis. As the chloromethyl moieties are transformed into methylene bridges, there is a large drop in the chlorine content of the polymer. The chlorine content dropped from nearly 10% before hypercrosslinking, to 1.2% after (**Table 9**).

Polymer	Elemental microanalysis (%)			
	C	H	N	Cl
Poly(styrene-co-VBC-co-EGDMA)	85.3	7.0	0.4	9.4
HXL poly(styrene-co-VBC-co-EGDMA)	89.2	7.1	0.7	1.2

Table 9 - Elemental microanalysis of HXL poly(styrene-co-VBC-co-EGDMA)

It is not unusual to observe some remaining chlorine in the HXL polymers. This may be due to some chloromethyl groups not being in an appropriate location for hypercrosslinking to occur. For example, some VBC units may be located in very small pores where it is not possible for them to freely move when solvated or for the reagents to access these sites.

The FT-IR data showed the band attributed to the C-H wag of the chloromethyl group at 1265 cm⁻¹ was no longer present in the spectrum. The band at 710 cm⁻¹, due to C-Cl stretching, was also greatly reduced. The FT-IR data therefore further supported the successful hypercrosslinking reaction.

SEM data showed that, as expected, the hypercrosslinking process had not disrupted the integrity of the particles, despite the rather harsh temperatures and reagents used, (**Figure 20**).

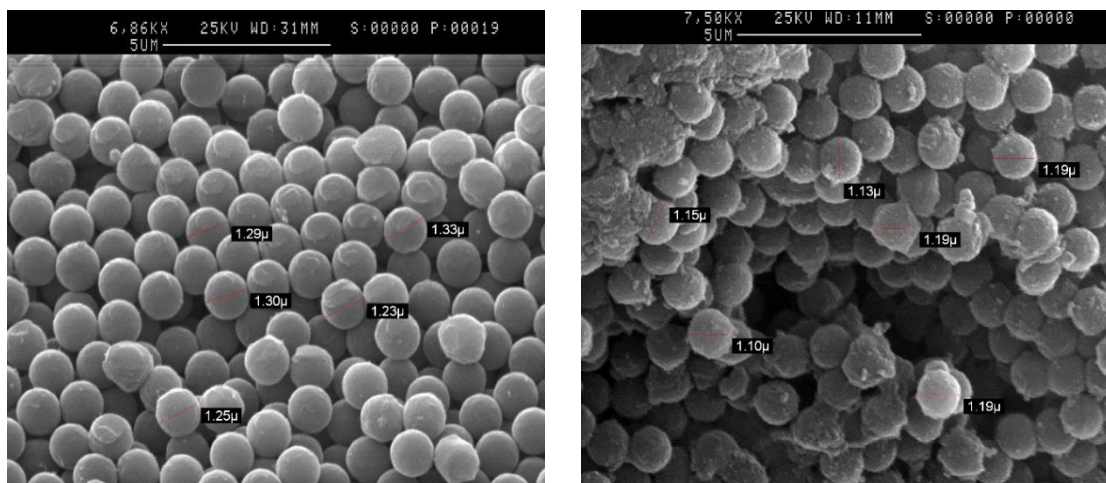


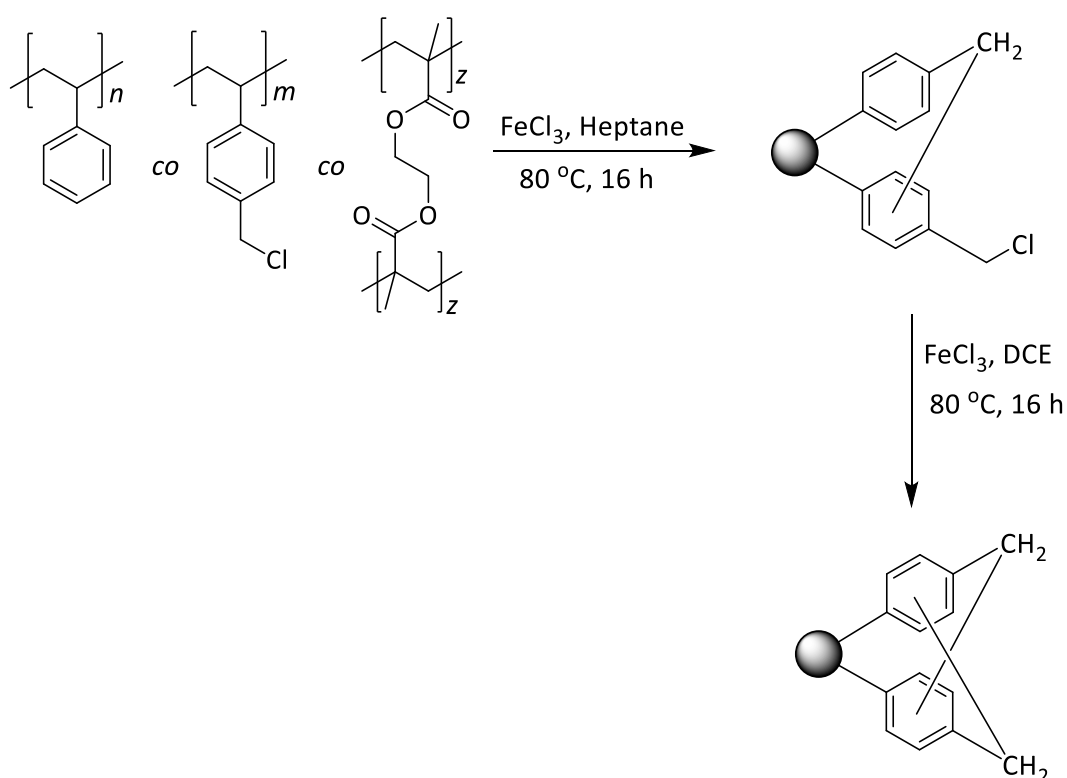
Figure 20 - SEM micrographs of poly(styrene-co-VBC-co-EGDMA) (left) and the HXL product (right)

The precursor showed smooth, soft discrete particles of about 1 μm in diameter and a very narrow particle size distribution. Upon hypercrosslinking, the particles were observed to not change a great deal, despite forcing reaction conditions. While the particles did not appear to be damaged in any way, it was noted that the hypercrosslinked product particles appeared to have roughened, contaminated surfaces. This phenomenon has been encountered by other researchers within our research group in the hypercrosslinking of gel-type, non-porous particles, with it being proposed that it was due to the precursor particles containing some soluble polymer within their pore networks. Upon swelling in solvent, this soluble portion is released and free to interact with the polymer particles as they are hypercrosslinked creating a roughened surface.

In order to address this issue, the hypercrosslinking reaction was repeated using the same precursor particles but using a modified protocol reported by Abdullah.⁶⁴

3.2.3 Synthesis of HXL poly(styrene-co-VBC-co-EGDMA) via a two-stage hypercrosslinking process

The gel-type polymer precursor particles were contacted with a non-swelling solvent, heptane in this case, and a sub-stoichiometric amount of Friedel-Crafts catalyst added (10 mol% relative to the chlorine content) and allowed to disperse throughout the polymer. This allowed for the particles to be partially hypercrosslinked and thus add stability to the particles. These partially hypercrosslinked were then fully hypercrosslinked in a thermodynamically good solvent using a 1:1 molar ratio of FeCl_3 relative to the chlorine of the precursor particles, **Scheme 23**.



Scheme 23 - Partial hypercrosslinking followed by exhaustive hypercrosslinking of poly(styrene-co-VBC-co-EGDMA)

This reaction was completed in a 63% yield, which was slightly lower than the one-step HXL reaction, reported earlier. The lower yielding reaction can be attributed to losses in

the transfer of material due to additional drying and transfer steps being involved in the two-step synthesis.

Pleasingly, the two-stage reaction was shown to be successful, with a large increase in specific surface area being observed; increasing from less than 5 m²/g before hypercrosslinking to 512 m²/g afterwards.

The elemental microanalysis and FT-IR data were both very similar for the two-step HXL polymer were very similar to the data reported for the product form the one-step HXL synthesis. In the FT-IR spectrum, the bands indicative of the VBC units were no longer present, and in the elemental microanalysis, the chlorine level had dropped significantly from 9.2% before hypercrosslinking to 0.5% post hypercrosslinking.

SEM was utilised to investigate whether or not the two-stage HXL process helped to prevent contamination of the surfaces of the polymer beads. Shown in **Figure 21** are SEM images of the polymer beads after the one- and two-stage HXL processes.

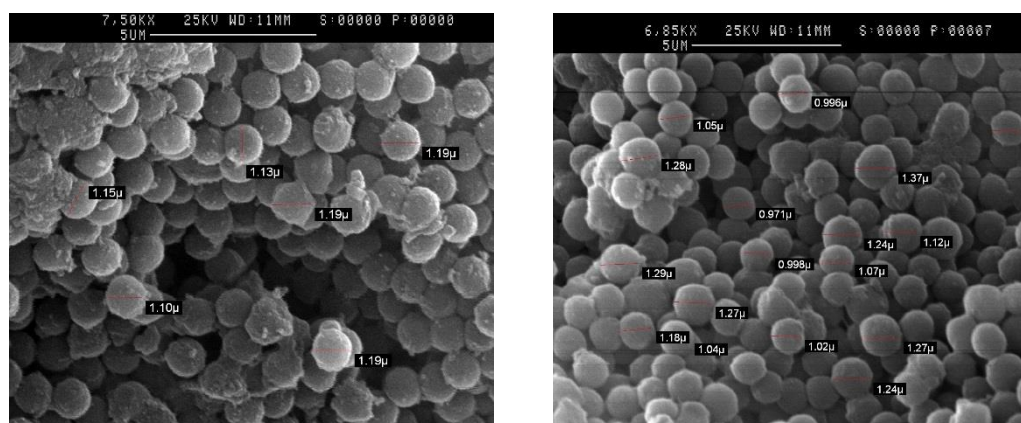
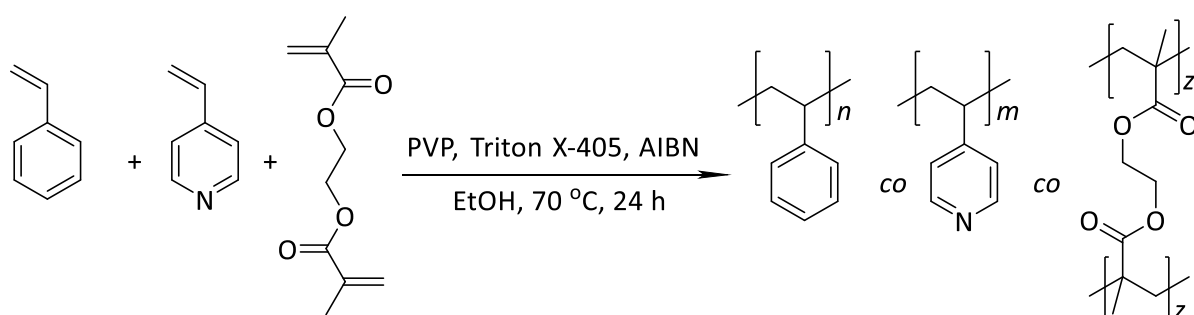


Figure 21 - SEM micrographs of HXL poly(styrene-co-VBC-co-EGDMA) after the one-step (left) and two-step (right) hypercrosslinking process

It is clearly evident that after the two-stage hypercrosslinking, (image shown on the right of **Figure 21**) the polymer microspheres surfaces appeared much less rough and there appeared to be less contamination, compared to the product from the one-step process.

3.2.5 Synthesis of poly(styrene-co-4-VP-co-EGDMA)

With the replication of Winnik's work being successful, attention turned to preparing NAD polymers that included some other useful functionality. To this end, 4-vinylpyridine was utilised as a functional monomer in other NAD polymerisations (**Scheme 24**). It has been reported that pyridine-based polymers have been used in the adsorption of PAHs from aqueous samples.¹⁸⁸ Due to the sensitive nucleation stage, 4-VP and half of the styrene were allowed to nucleate for 1 hour before adding the remaining styrene and the crosslinker (1 wt% of monomer feed) and allowing the polymerisation to progress to completion. The polymerisation, being carried out on a 10.1 g monomer scale, was successful and gave the desired product in a 68% yield.



Scheme 24 - Synthesis of poly(styrene-co-4-VP-co-EGDMA)

Due to very sensitive nucleation stage in NAD polymerisations, only 6 wt% of 4-VP could be incorporated into the final polymer. When attempts were made to include higher amounts of 4-VP into the polymer, the polymerisation product would coagulate and agglomerate.

Successful incorporation of 4-VP was confirmed *via* elemental microanalysis, **Table 10**, with the observed nitrogen content of the polymer being as expected.

	Elemental microanalysis (%)		
	C	H	N
Expected	90.9	7.7	1.1
Observed for poly(styrene-co-4-VP-co-EGDMA)	90.8	7.7	1.2

Table 10 - Elemental microanalysis data for poly(styrene-co-4-VP-co-EGDMA)

The presence of bands in the FT-IR spectrum at 1580 and 1560 cm^{-1} were indicative of pyridyl ring stretching. A band was also observed at $\sim 1420 \text{ cm}^{-1}$, and this was attributed to a C-N bond stretch. This infrared data confirmed the successful incorporation of 4-VP into the polymer microspheres. A very small C=O bond stretch, appearing at $\sim 1700 \text{ cm}^{-1}$, indicated the successful incorporation of the crosslinker into the polymer.

As before, low levels of crosslinking within the polymer resulted in a network that was expected to collapse upon drying and exhibit no discernible surface area. This was confirmed experimentally *via* nitrogen sorption analysis, which indicated a specific surface area of $< 5 \text{ m}^2/\text{g}$.

SEM was used to analyse the morphology and surfaces of the polymer particles. A typical SEM micrograph is shown in **Figure 22**.

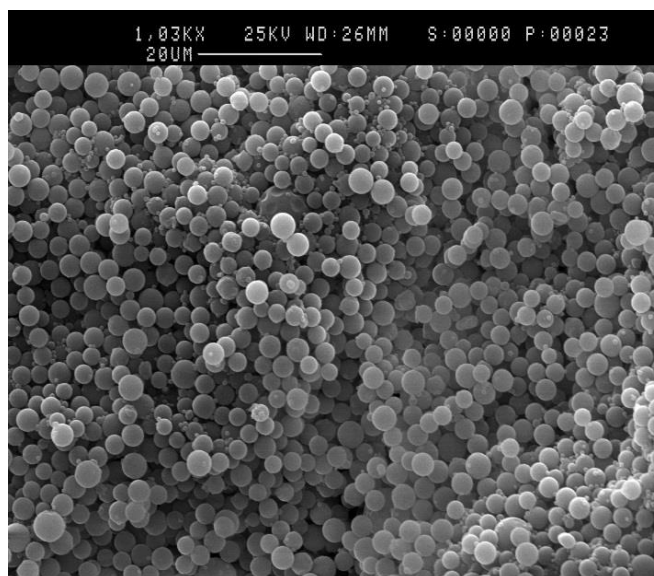


Figure 22 - SEM micrograph of poly(styrene-co-4-VP-co-EGDMA)

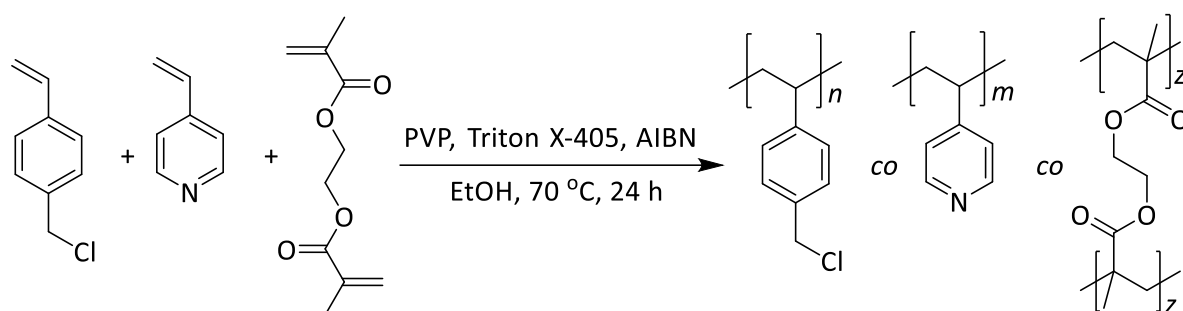
$$\bar{d} = 5.5 \mu\text{m} \text{ CV} = 5.8 \%$$

The particles appeared somewhat polydisperse, with some particles being much larger in diameter than others. It is though tthat the inclusion of small amounts of 4-VP into the polymer has disrupted the nucleation of some of the growing particles. Work by Winnik *et al*^{62,63,189} and work carried out in the Cormack Lab at Strathclyde⁶⁴ has indicated that even very small changes to the NAD polymerisation process can have very large effects on the outcome of the polymerisation and the resultant particles.

This polymer, while having some functionality that was expected to create favourable interactions with the target analytes, was of very low specific surface area. It was proposed that by increasing the specific surface area, higher levels of sorption of PAHs from lubricants and hydrocarbon fluids would be possible. To this end, a polymer that included 4-vinyl pyridine and VBC was synthesised. The inclusion of VBC would allow for hypercrosslinking chemistry to be utilised to deliver a polymer that exhibited very high specific surface areas, and functionality that would maximise PAH/polymer interactions.

3.2.4 Synthesis of poly(VBC-co-4-VP-co-EGDMA) *via* NAD polymerisation

Non-porous particles comprising a 10:1 mole ratio of VBC:4-VP in the monomer feed and 1 wt% of crosslinking agent, EGDMA, were synthesised *via* NAD polymerisation, in a gratifying 81% yield (**Scheme 25**). Following a similar protocol so that which had been adopted for all the other NAD polymers discussed, half of the VBC and all the 4-VP was reacted for approximately one hour. After the nucleation step the remaining VBC and all the crosslinker were added to the reaction vessel and the polymerisation was allowed to proceed for the allotted time.



Scheme 25- Synthesis of poly(VBC-co-4-VP-co-EGDMA)

Elemental microanalysis showed very close correlation between the expected values for the NAD polymer and those that were found experimentally (**Table 11**).

	Elemental microanalysis (%)			
	C	H	N	Cl
Expected	71.3	6.0	1.2	21.2
Observed for poly(VBC-co-4-VP-co-EGDMA)	71.3	6.5	1.4	20.4

Table 11 - Elemental microanalysis data for poly(VBC-co-4-VP-co-EGDMA)

The FT-IR data also provided evidence of incorporation of 4-VP and VBC into the final polymer. C-N bond stretching was apparent at $\sim 1420\text{ cm}^{-1}$, as well as C-Cl and the C-H wag of the chloromethyl groups at 700 and 1265 cm^{-1} , respectively.

As with the other NAD polymers synthesised, poly(VBC-co-4-VP-co-EGDMA) exhibited a very low dry-state specific surface area of $19\text{ m}^2/\text{g}$, as determined by nitrogen sorption analysis. The isotherm was of a 'Langmuir' or 'Type I' shape, also indicative of very low porosity, or indeed non-porous, materials.

Unfortunately, when this polymer was examined *via* SEM microscopy it became apparent that severe polymer agglomeration had occurred. Agglomeration and coagulation had been experienced by other researchers when the system was disrupted.⁶⁴ It was believed that by replacing all the styrene with other monomers, the nucleation of the polymer had been disturbed to the extent that agglomeration and coagulation occurred. **Figure 23** shows an image of such a poly(VBC-co-4-VP-co-EGDMA) where the agglomeration is clearly apparent. Some polymer microspheres that nucleated successfully are also shown.

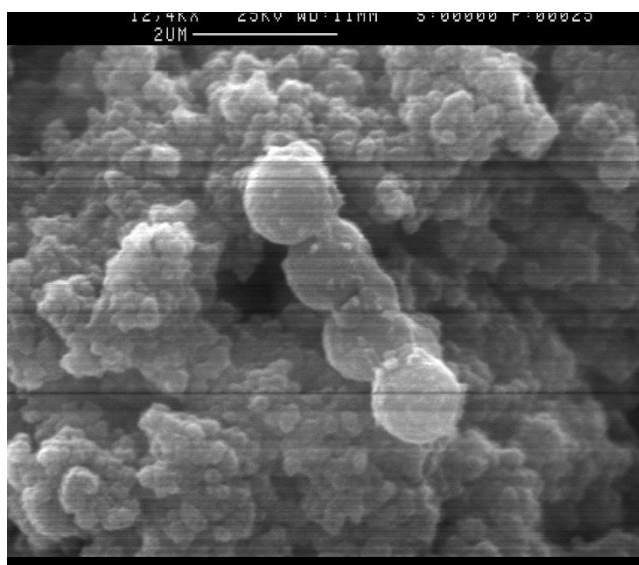


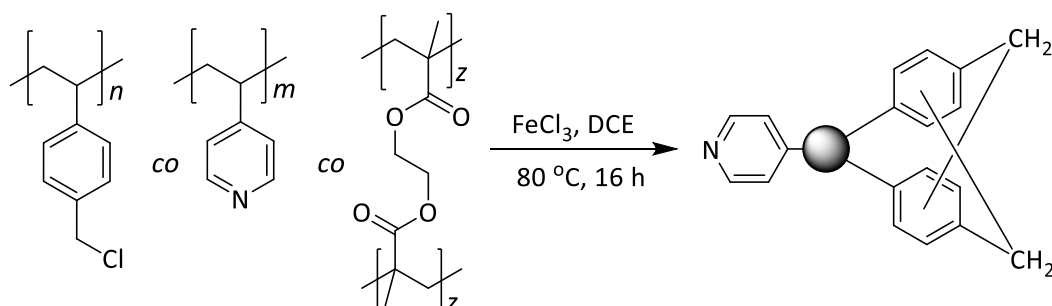
Figure 23 - SEM micrograph of poly(VBC-co-4-VP-co-EGDMA)

While this polymer had agglomerated and coagulated together, and the formation of microspheres had been somewhat unsuccessful, the spectroscopic and elemental

analysis provide corroborating evidence of the incorporation of 4-VP, VBC and EGDMA into the polymer. It was therefore believed that this polymer would still be of value since it possessed the correct functionality. This polymer was taken onwards to hypercrosslinking, to install permanent porosity to increase the sorption capabilities for the potential capture of PAHs and other contaminants from a hydrocarbon fluid.

3.2.5 Hypercrosslinking of poly(VBC-co-4-VP-co-EGDMA)

As per other hypercrosslinking reactions presented herein, poly(VBC-co-4-VP-co-EGDMA) was reacted in a Friedel-Crafts alkylation in the presence of stoichiometric amounts of FeCl_3 as a catalyst. This is exemplified schematically in **Scheme 26**. The polymer was swollen in DCE for one hour before the addition of FeCl_3 . After this addition, the hypercrosslinking was allowed to precursor for 18 hours. The synthesis was completed in a yield of 96% based on the transformation of chloromethyl groups to methylene bridges.



Scheme 26 - Hypercrosslinking of poly(VBC-co-4-VP-co-EGDMA)

Scheme 26 suggests that only VBC units are involved in the formation of methylene bridges. It may be envisaged that hypercrosslinking can occur and create methylene bridges between VBC units and the nitrogen on 4-VP residues, creating n -alkylated pyridinium ions. FT-IR data, shown in **Figure 24**, suggested that this was not the case.

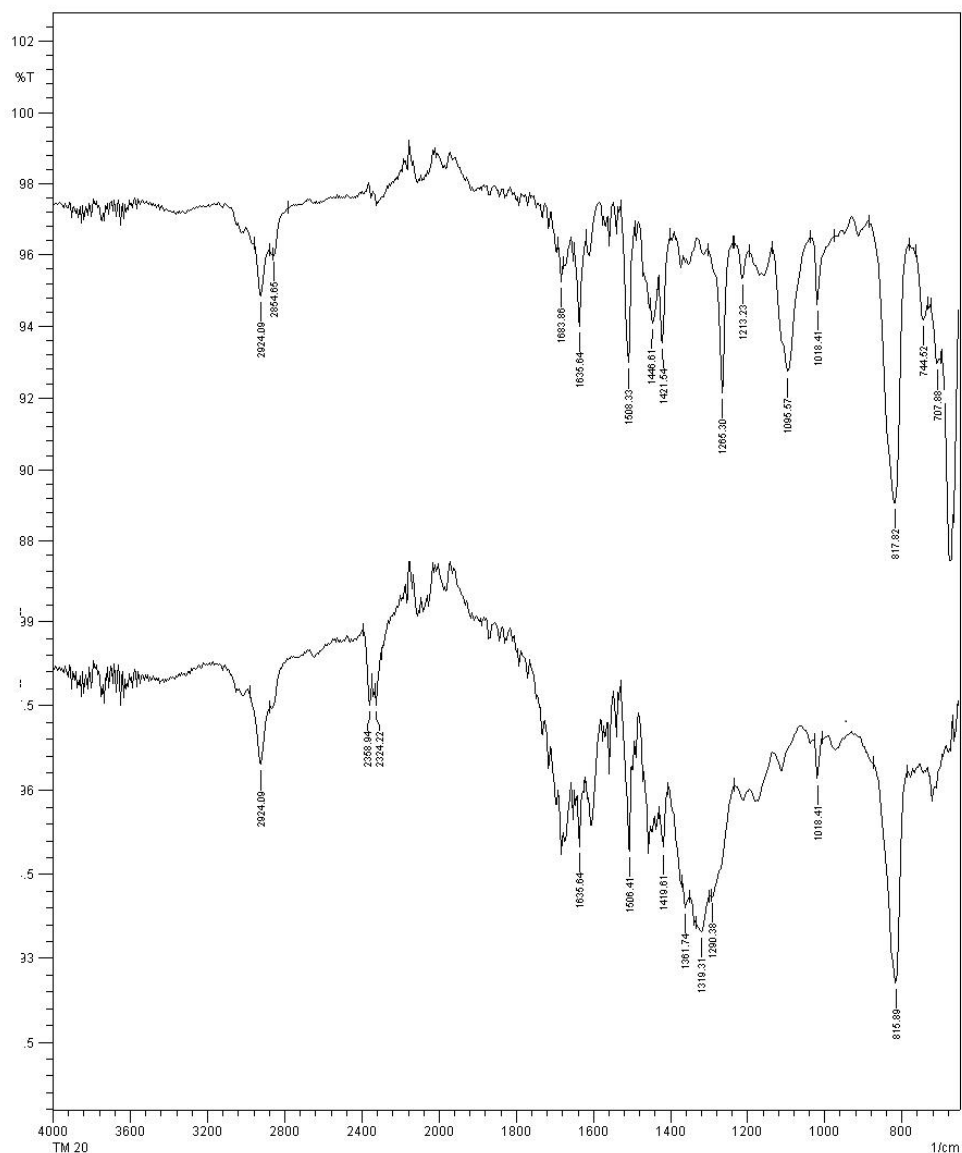


Figure 24 - FT-IR spectra of HXL poly(VBC-co-4-VP-co-EGDMA) (bottom) and gel-type precursor polymer (top)

FT-IR bands which are characteristic of the C-N bond stretching of a quaternary nitrogen atom in a heterocyclic ring have been reported to be in the region of $1631\text{-}1625\text{ cm}^{-1}$.^{190,191} It was clearly evident that in this region of the spectrum there was little change after the hypercrosslinking reaction, indicating that the formation of quaternary pyridium moieties had not occurred. It may also be the case that, due to a large excess (approximately 10 times as much) of VBC being present compared to 4-VP, the likelihood

of a hypercrosslink forming between a chloromethyl group and the pyridine nitrogen was greatly reduced.

The FT-IR spectra did show that the bands characteristic of VBC had changed after hypercrosslinking. The band at 1265 cm^{-1} (C-H wag of $\text{CH}_3\text{-Cl}$) had become reduced in intensity and the band at 700 cm^{-1} (C-Cl bond stretch) was no longer visible.

Elemental microanalysis showed a drastic reduction in the chlorine content after hypercrosslinking, indicating a successful reaction, **Table 12**.

Polymer	Elemental microanalysis (%)			
	C	H	N	Cl
Poly(VBC-co-4-VP-co-EGDMA)	71.3	6.5	1.4	20.4
HXL poly(VBC-co-4-VP-co-EGDMA)	89.2	6.6	1.4	6.0

Table 12 - Elemental microanalysis data for HXL poly(VBC-co-4-VP-co-EGDMA)

Successful hypercrosslinking was also corroborated by the nitrogen sorption analysis data, shown in **Table 13**.

Polymer	BET c Value	Specific surface area (m^2/g)		Specific pore volume (cm^3/g)	Average pore diameter (nm)
		BET	Langmuir		
Poly(VBC-co-4-VP-co-EGDMA)	83	14	19	0.0	16.2
HXL poly(VBC-co-4-VP-co-EGDMA)	549	780	1069	0.70	3.5

Table 13 - Nitrogen sorption analysis data for HXL poly(VBC-co-4-VP-co-EGDMA)

HXL poly(VBC-co-4-VP-co-EGDMA), exhibited a Langmuir-shaped isotherm and an unusually high BET C value, suggesting that the application of Langmuir theory over BET theory was most appropriate in this case. Due to the pore network of all the hypercrosslinked polymers synthesised being either predominantly made up of micropores or, in the case of HXL poly(VBC-co-4-VP-co-EGDMA), being very close to the micropore region (3.5 nm) BET theory (which generally applies to materials that contain a large proportion of pores in the meso pore range) was not applied in any case.

It can be noted from **Table 13** that upon hypercrosslinking the Langmuir specific surface area increased to over 1000 m²/g indicating successful application of the hypercrosslinking chemistry.

SEM microscopy revealed that hypercrosslinking appeared to have no obvious effect on the morphology of the polymer. The overall agglomeration observed in the precursor material was observed in the hypercrosslinked material. Shown in **Figure 25** are typical SEM micrographs of the polymer before and after hypercrosslinking.

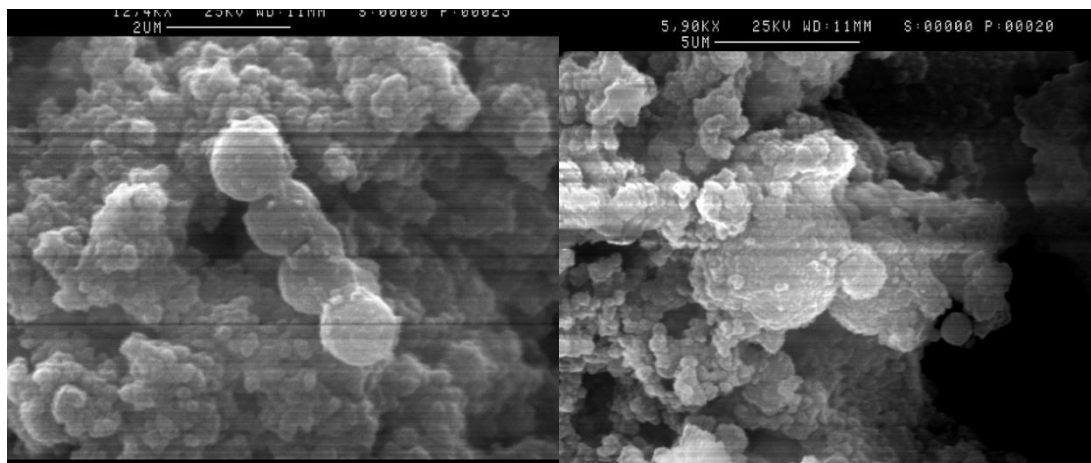
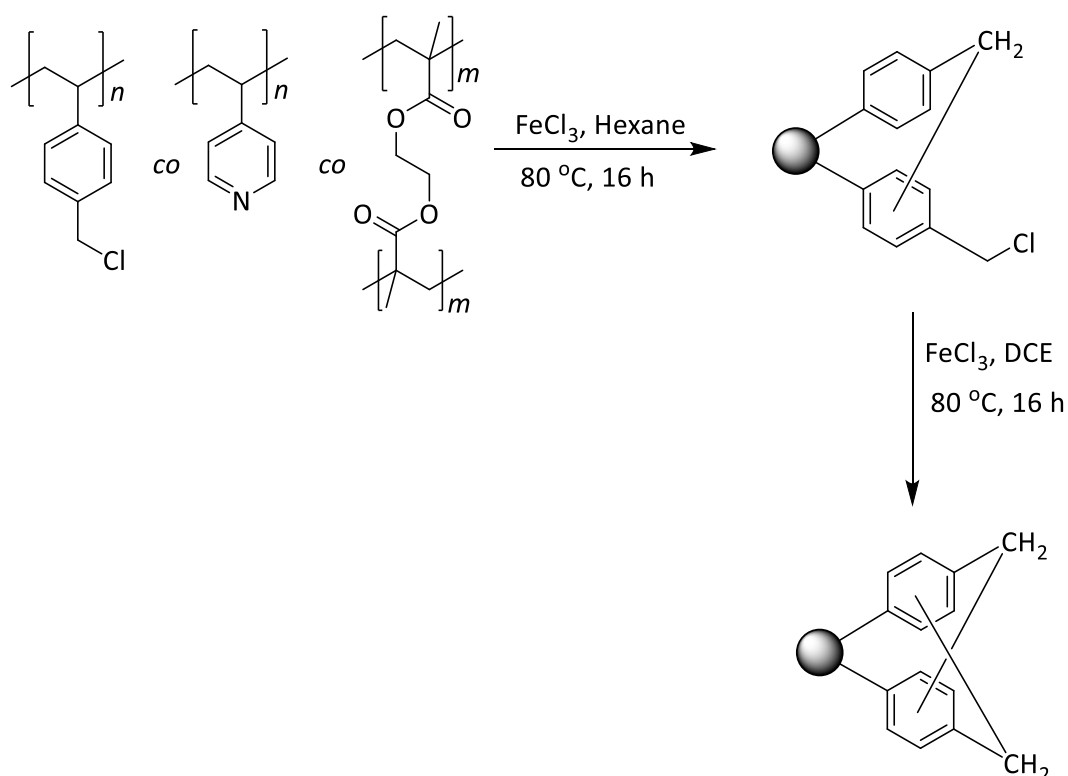


Figure 25 - SEM micrograph of poly(VBC-co-4-VP-co-EGDMA) (left) and its HXL variant (right).

Even though HXL poly(VBC-co-4-VP-co-EGDMA) and its precursor polymer exhibited very high levels of agglomeration and coagulation, it was decided to investigate the two-step hypercrosslinking process with poly(VBC-co-4-VP-co-EGDMA).

3.2.6 Hypercrosslinking of poly(VBC-co-4-VP-co-EGDMA) *via* a two-stage hypercrosslinking process

As before, the precursor particles were treated with a sub-stoichiometric amount of FeCl_3 in a non-swelling solvent and allowed to react for 18 hours. This installed some methylene bridges between adjacent aromatic rings, in a drive to add stability into the polymer particles. The now partially hypercrosslinked material was then treated with stoichiometric amounts of FeCl_3 catalyst in 1,2-dichloroethane to yield fully hypercrosslinked poly(VBC-co-4-VP-co-EGDMA) in a 95 % yield, **Scheme 27**.



Scheme 27 - Partial hypercrosslinking followed by exhaustive hypercrosslinking of poly(VBC-co-4-VP-co-EGDMA)

Utilising the usual suite of analytical techniques that have been used on all the polymers presented, namely: FT-IR spectroscopy, elemental microanalysis, nitrogen sorption analysis and SEM, it was evident that the HXL poly(VBC-co-4-VP-co-EGDMA) produced *via* the two-step hypercrosslinking process was very similar to the polymer synthesised by the one-step process.

Upon exhaustive hypercrosslinking, the chlorine content was observed to drop from 21% to below 8%. Similarly, the FT-IR data indicated a dramatic reduction in the intensity of the bands associated with the C-Cl bond stretch at 700 cm^{-1} and the $\text{CH}_2\text{-Cl}$ wag at 1265 cm^{-1} .

Nitrogen sorption analysis showed a very large increase in specific surface area, after exhaustive hypercrosslinking, to $513\text{ m}^2/\text{g}$. The increase in specific surface area was not as large as the increase observed for the HXL polymer that was synthesised *via* the one-step hypercrosslinking. In the material synthesised *via* a one-step process, there was a lower amount of chlorine (6%) remaining in the polymer post-hypercrosslinking when compared to the material produced in the two-step synthesis.

3.3 Application of Polymers in Sorption and Capture of PAHs

3.3.1 Smaller-scale sorption study

With a small suite of polymeric materials prepared successfully, attentions moved to utilising these materials in the sorption and capture of contaminants, namely PAHs, from a hydrocarbon fluid. The materials were prepared with a range of functionalities and specific surface areas, to gain insight into the effect that these variables may have on the removal of PAHs. At these early stages of the investigation, it was deemed appropriate to make the sorption tests as simple as possible. It was envisaged that, eventually, the hydrocarbon fluid of choice would be a lubricant from a diesel engine. However, for the initial lab-based experiments, in the interests of simplicity, the hydrocarbon fluid that was chosen was heptane. As model contaminants, three of the simplest PAHs, pyrene, anthracene and acenaphthene, were selected. These are shown in **Table 14**.

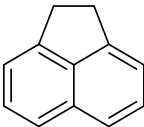
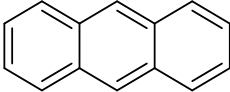
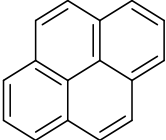
Compound	Structure
Acenaphthene	
Anthracene	
Pyrene	

Table 14 - PAHs to be used in the initial sorption experiments

The three PAHs were dissolved in heptane to give a solution where the concentration concentration of the PAHs was 30 µg/mL .

A simple and reproducible method of sorption and analysis was required. To achieve this, a method somewhat similar to solid-phase extraction was used. 250 mg of polymer was packed into a small tube called a cartridge which resembles a syringe barrel as, shown in **Figure 26**. The heptane solution was then contacted with the polymer and the solution allowed to mix for 24 hours with continuous agitation of the cartridges to ensure equilibration. The liquid was then removed from the polymer by drawing the liquid through a syringe filter using vacuum. The filtrate was then analysed by gas chromatography and the percentage of each PAH removed from solution calculated.



Figure 26 - SPE cartridge used for the smaller-scale sorption and capture of PAHs

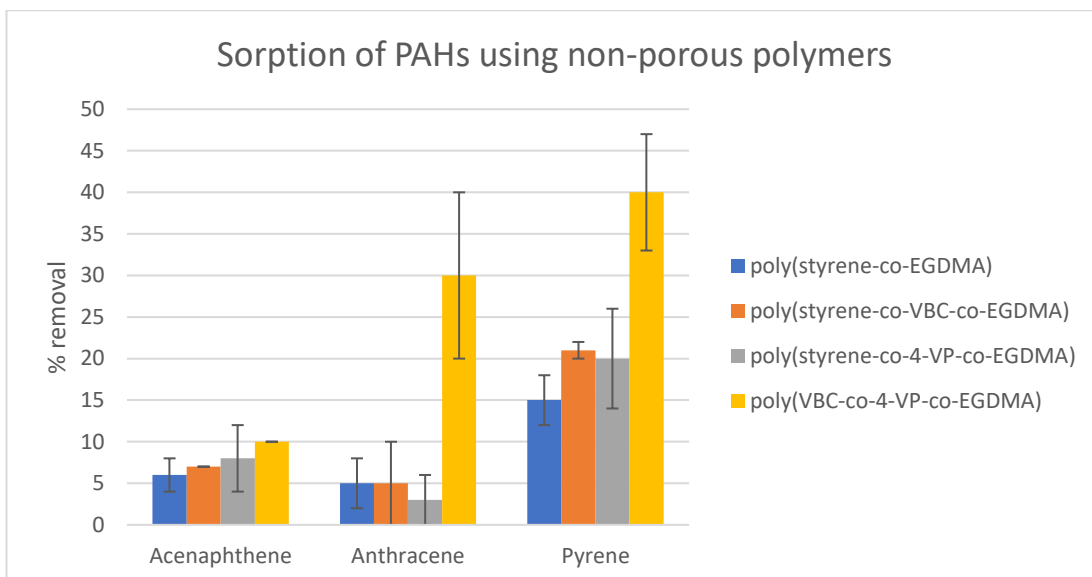
3.3.2 PAH Sorption using Non-Porous Polymers

The non-porous polymers prepared by non-aqueous dispersion polymerisation were the first polymers to be applied to the sorption and capture of PAHs. Due to their very low specific surface area, it was expected that these materials would not perform particularly well in this regard, but were tested anyway. 250 mg of polymer was placed in the cartridge as described above and incubated for 24 hours with a heptane solution containing the PAHs at a concentration of 30 $\mu\text{g}/\text{mL}$. After 24 hours the liquid was separated from the polymer by filtration and the filtrate analysed by GC. The results were reported as the percentage of PAH that was removed from the solution. Alongside each polymer being analysed a cartridge containing no polymer was also put through the same regime to ensure that the cartridge or filtration method was having no effect on the

apparent sorption capability of the polymers. The results for the sorption experiments using the non-porous polymers is shown in **Table 15**. *N.B.* All figures are presented as the percentage of PAH that has been *removed* from solution

Polymer	Acenaphthene (% removed)	Anthracene (% removed)	Pyrene (% removed)
Control – no polymer	0	0	0
Poly(styrene- co-EGDMA)	6 ±2	5 ±3	15 ±3
Poly(styrene- co-VBC-co- EGDMA)	7 ±0	5 ±5	21 ±1
Poly(styrene- co-4-VP-co- EGDMA)	8 ±4	3 ±3	20 ±6
Poly(VBC-co- 4-VP-co- EGDMA)	10 ±0	30 ±10	40 ±7

Table 15 - Sorption of PAHs using non-porous polymers. n=3



Graph 1 – Sorption of PAHs using non-porous polymers

Pleasingly, when no polymer was included it appeared that no PAHs were removed. As expected with materials of very low specific surface area, the sorption capabilities were rather low – with less than 10% of each PAH being removed in most cases. It was observed that pyrene was sorbed more readily than acenaphthene or anthracene. Pyrene is less soluble in heptane than the other two PAHs and this may explain why higher levels of sorption were observed for this PAH.

The polymer with functionality were observed to remove a greater proportion of PAHs than the materials that were mainly styrene-based. Of particular note was the 4-VP containing polymer, which was able to sorb much higher amounts of PAHs compared to the other polymers. This was a rather surprising result given the low specific surface area of these materials.

Modest PAH removal using non-porous polymers was not unexpected as heptane, the medium used in this study, is a non-solvent for polystyrene-based polymers. This would mean that none of the polymers presented in **Table 15** would swell to any extent in the presence of heptane. Therefore, very little of the inner surface of the polymer microspheres would be available for PAH capture. By moving to permanently porous

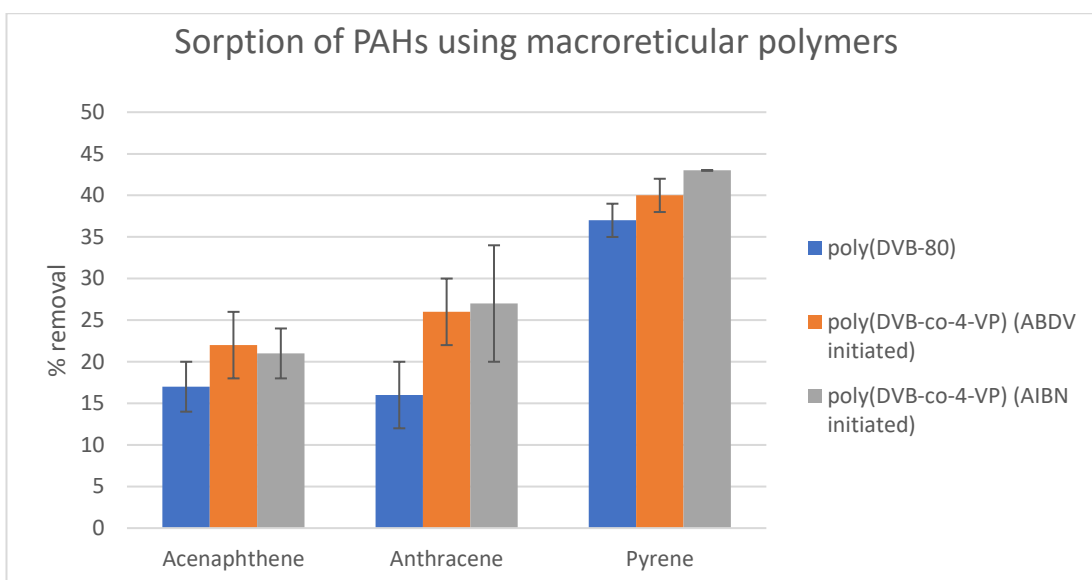
polymers, which do not require swelling in appropriate solvent to reveal their inner surface, it was hoped that higher levels of PAH removal could be realised.

3.3.3 PAH Sorption Using Porous Polymers

The non-porous polymers showed positive signs that the sorption of PAHs from a hydrocarbon fluid was possible. In this regard, the permanently porous materials were expected to perform even better. Due to having higher specific surface areas, there is more surface available on which to capture PAHs. The regime employed to examine the porous materials was the same as that used for the examination of the non-porous materials. The % of each PAH removed by each polymer is shown in **Table 16**.

Polymer	Acenaphthene (% removed)	Anthracene (% removed)	Pyrene (% removed)
Control – no polymer	0	0	0
Poly(DVB-80)	17 ±3	16 ±4	34 ±2
Poly(DVB-80-co- 4-VP) (Initiated with ABDV)	22 ±4	26 ±4	40 ±2
Poly(DVB-80-co- 4-VP) (Initiated with AIBN)	21 ±3	27 ±7	43 ±0

Table 16 - Sorption of PAHs using macroreticular polymers. n=3



Graph 2 – Sorption of PAHs using macroreticular polymers

As with the non-porous polymers, the sorption of PAHs by the porous materials exhibited some obvious trends. The sorption level of PAHs when using a material that was unfunctionalised, *i.e.*, poly(DVB-80), were modest but not insignificant. This would suggest that as well as the functionality possessed by the material playing a role, the specific surface area also has an influence of the sorption capabilities. For example, poly(styrene-*co*-EGDMA) (**Table 15**), is a largely aromatic polymer which is somewhat comparable to poly(DVB-80) with respect to functionality. The biggest difference between these two materials is the high specific surface area exhibited by poly(DVB-80). Poly(styrene-*co*-EGDMA) removed only small amounts of PAH (generally less than 5%, with the exception of pyrene, where 15% was removed), whereas poly(DVB-80) was able to remove upwards of 30% of pyrene.

As was observed in the sorption experiments using the non-porous materials, when 4-VP was included, the amount of PAH removed increased. It was also evident that when different initiators were used, the overall sorption capability of the material was unaffected, as can be seen in the poly(DVB-80-*co*-4-VP).

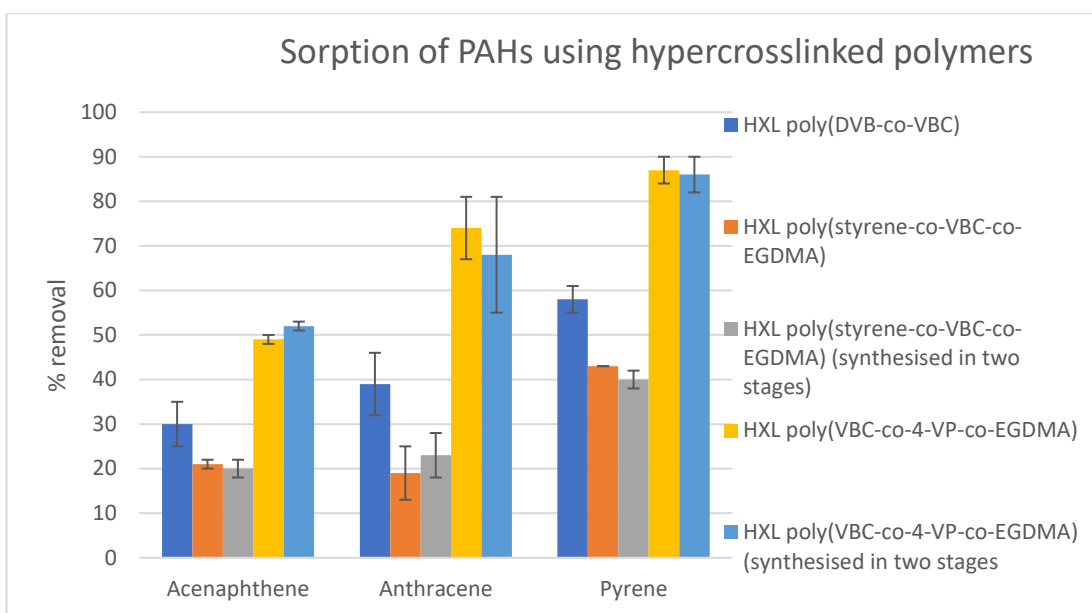
3.3.4 PAH sorption Using Ultra-High Specific Surface Area-Hypercrosslinked Polymers

The removal of PAHs from heptane using the porous materials proved to be effective. It was hypothesised that by using materials that exhibited even higher specific surface areas, higher levels of PAH removal could be achieved. The porous polymers discussed above all have a specific surface area of $\sim 500 \text{ m}^2/\text{g}$, whereas the hypercrosslinked (HXL) materials have a specific surface from $\sim 800 \text{ m}^2/\text{g}$ up to more than $1000 \text{ m}^2/\text{g}$. Shown in **Table 17** is the % of each PAH removed by each hypercrosslinked polymer.

Polymer	Acenaphthene (% removed)	Anthracene (% removed)	Pyrene (% removed)
Control – no polymer	0	0	0
HXL poly(DVB-co-VBC)	30 \pm 5	39 \pm 7	58 \pm 3
HXL poly(styrene-co-VBC-co-EGDMA)	21 \pm 1	19 \pm 6	43 \pm 0
HXL poly(styrene-co-VBC-co-EGDMA)*	20 \pm 2	23 \pm 5	40 \pm 2
HXL poly(VBC-co-4-VP-co-EGDMA)	49 \pm 1	74 \pm 7	87 \pm 3
HXL poly(VBC-co-4-VP-co-EGDMA)*	52 \pm 1	68 \pm 13	86 \pm 4

Table 17 - Sorption of PAHs using hypercrosslinked polymers. n=3

****** denotes hypercrosslinked polymers synthesised *via* a two-stage hypercrosslinking process



Graph 3 – Sorption of PAHs using hypercrosslinked polymers

As expected, the large increase in specific surface area for the HXL polymers resulted in much higher amounts of PAHs being removed from the heptane solution. As had been observed in the PAH sorption experiments using materials of lower specific surface area (**Table 15** and **Table 16**), the hypercrosslinked polymers appeared to remove more of pyrene than the other PAHs. However, due to much increased specific surface areas the HXL polymers were able to remove much more acenaphthene and anthracene than the lower specific surface area materials.

The HXL poly(VBC-co-4-VP-co-EGDMA) was the best performing of the HXL polymers, being able to sorb nearly 90% of the pyrene present in the heptane solution. The materials marked with a '*' in **Table 17** were the HXL materials that were prepared *via* the two-step hypercrosslinking process. They proved just as effective for the removal of PAHs from heptane as the equivalent material synthesised in a one-step hypercrosslinking reaction. The HXL polymers synthesised through a two-step hypercrosslinking process had lower specific surface area and specific pore volume than the corresponding polymer prepared through a one-stage hypercrosslinking process. However, both polymers removed very similar amounts of PAHs. This suggests that while increased specific surface area improves sorption ability, functionality of the polymer has a larger influence. This was also demonstrated by HXL poly(DVB-80-co-VBC), which had

the largest specific surface area (2034 m²/g) in this study, but performed less effectively than the 4-VP containing polymers which had specific surface areas more than half that of HXL poly(DVB-80- *co*-VBC).

While these early sorption studies proved to be both insightful and successful it was deemed important to further investigate the removal of PAHs from a simple heptane solution as the heptane solutions were both low volume and low concentration. For example, the best performing polymer, HXL poly(VBC-*co*-4-VP-*co*-EGDMA), was able to remove 52%, 68%, and 86% of acenaphthene, anthracene and pyrene, respectively. This corresponds to a total of 31 µg of PAH removed from solution (the total amount of PAH in each sample was 45 µg). So, while proving that PAHs could be removed from a hydrocarbon fluid, due to only very small amounts of PAHs being present, further investigation was deemed necessary. To this end, a new set of sorption experiments was undertaken, with a more concentrated heptane solution to be used along with larger volumes of the heptane solution being contacted with the polymers.

3.4 Large-scale sorption study

After the successful application of the polymers in the removal of small amounts of PAHs from a heptane solution, further investigation was required. It was proposed that, to fully evaluate the sorption capabilities of the polymeric materials, two functionalised PAHs were to be included in this study, in addition to the three PAHs studied already. Nitropyrene and methyl naphthalene were chosen as evidence suggests that both are formed in the exhaust stream of heavy-duty diesel engines.¹⁹² 20 mL samples of a more concentrated (200 µg/mL of each PAH) heptane solution was to be contacted with 250 mg of each polymer in the new larger scale sorption study. This would mean that a total of 4 mg of each PAH would be contacted with the polymers. Due to the low solubility of PAHs in heptane, 200 µg/ mL was reaching the upper limits of solubility for these compounds

The sorption study was carried out in a very similar manner to the small-scale sorption study, discussed previously. 20 mL of the heptane solution was contacted with 250 mg

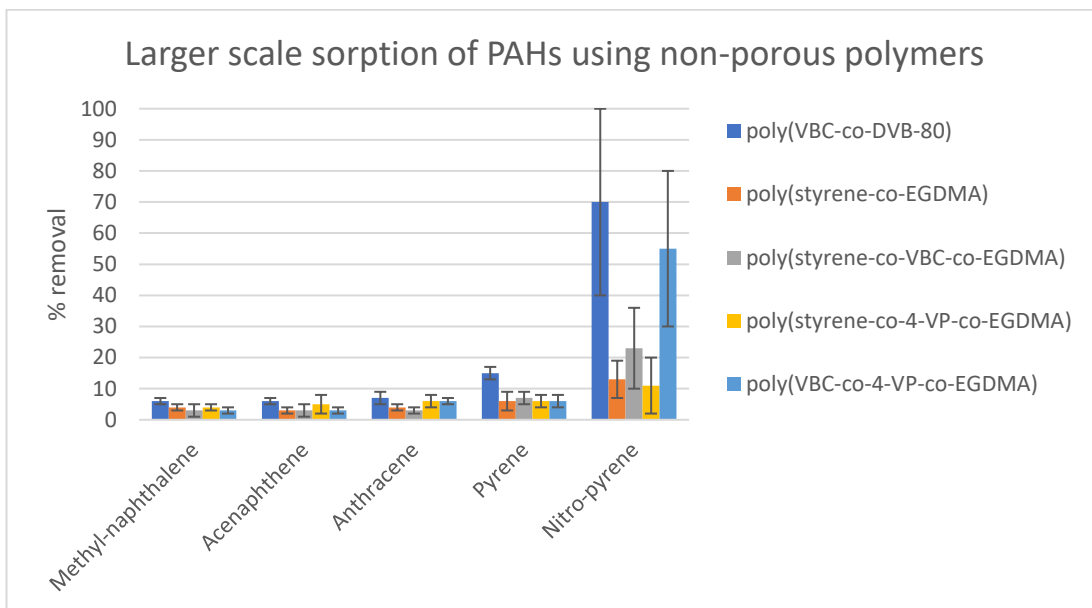
of each polymer in a glass jar, and allowed to incubate for 24 hours, with continuous agitation of the mixture. After this time, the solid was separated from liquid and the liquid portion analysed by GC. The % of each PAH that the polymer removed was then calculated. All sorption experiments were repeated three times and an average value reported.

3.4.1 Larger-scale PAH capture using non-porous polymers

The first polymers to be examined in the sorption of PAHs from the more concentrated heptane solution were the gel-type, non-porous materials. As had been proposed in the smaller scale study, these materials were not expected to prove as effective for the removal of PAHs when compared to the higher specific surface area materials. Shown in **Table 18** are the % removal of each PAH from the heptane solution by each non-porous polymer.

Polymer	Methyl-naphthalene (% removed)	Acenaphthene (% removed)	Anthracene (% removed)	Pyrene (% removed)	Nitropyrene (% removed)
Control – no polymer	0	0	0	0	0
Poly(VBC-co-DVB-80)	6 ±1	6 ±1	7 ±2	15 ±4	70 ±30
Poly(styrene-co-EGDMA)	4 ±1	3 ±1	4 ±1	6 ±3	13 ±6
Poly(styrene-co-VBC-co-EGDMA)	3 ±2	3 ±2	3 ±1	7 ±2	23 ±13
Poly(styrene-co-4-VP-co-EGDMA)	4 ±1	5 ±3	6 ±2	6 ±2	11 ±9
Poly(VBC-co-4-VP-co-EGDMA)	3 ±1	3 ±1	6 ±1	6 ±2	55 ±25

Table 18 - Larger-scale sorption of PAHs using non-porous polymers. n=3



Graph 4 – Larger scale sorption of PAHs using non-porous polymers

In this larger scale sorption study, the overall trend was very similar to the smaller scale sorption study; the non-porous materials removed low levels of PAH from the heptane solution. While the overall extent of removal of PAH was low for the larger-scale sorption study (**Table 18**) when compared to the smaller scale sorption study (**Table 15**), the actual amount of PAH removed was much larger. For example, poly(styrene-co-EGDMA), in the smaller scale sorption study, this polymer was able to remove 6%, 5%, and 15% of acenaphthene, anthracene and pyrene, respectively. This amounts to 3.9 μg of PAH removal in total. However, in the larger scale sorption study this polymer removed 3%, 4% and 6% of acenaphthene, anthracene and pyrene. This equates to a total of 540 μg of PAH, a much larger amount than for the smaller-scale study. This increase in PAH removal may be attributed to the fact that the heptane solution used in the larger-scale sorption study was over six times more concentrated than the solution used in the smaller-scale study. An increase in concentration would mean there were more PAH molecules available for removal. It was also thought that the removal of PAHs onto the surfaces of the polymer may have encouraged more PAH removal through favourable interactions between PAHs removed and those still residing in solution.

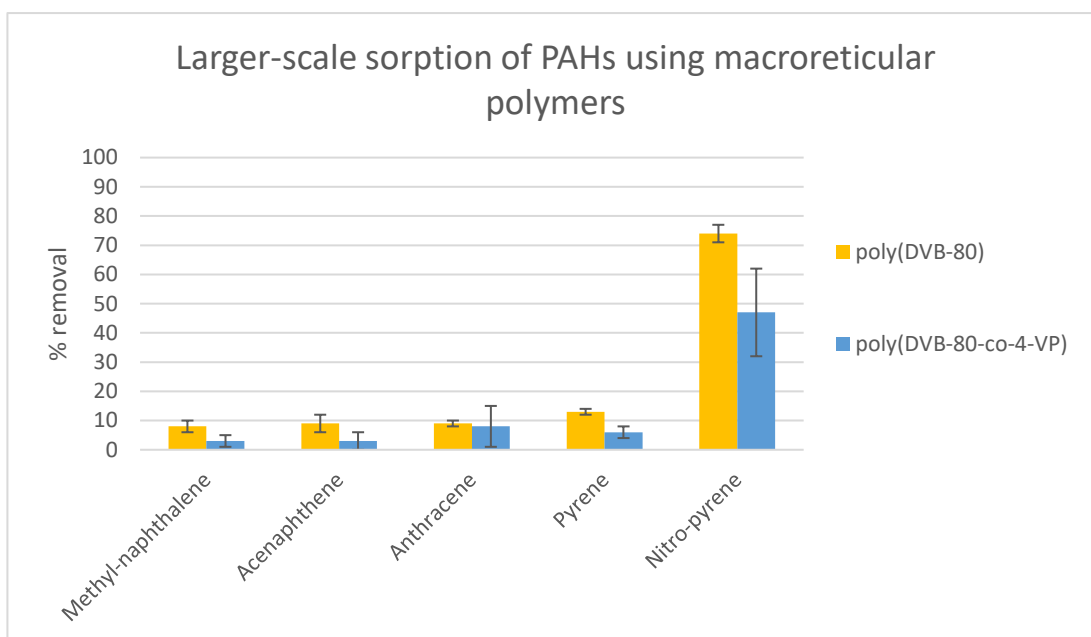
For the two other PAHs that were included in this sorption study, methylnaphthalene and nitropyrene, methylenaphthalene was poorly retained by all of the polymers, with 6% or less being removed in all cases. In heptane, methylnaphthalene is the most soluble of all the PAHs which were studied, and it was believed that this led to increased difficulty in removing it from the heptane solution. Conversely, very high levels of removal of nitropyrene was observed. Nitropyrene was the least soluble PAH in heptane, and it was believed that this was aiding removal from the test solution. Also, it was observed that the functionalised polymers, containing VBC and 4-VP residues, were able to remove even greater amounts of nitropyrene. It is thought that the relatively electronegative VBC moiety and the lone pair of 4-V were interacting favourably with the electron-deficient π -system of nitropyrene. Favourable interactions between 4-VP and nitrated PAHs in studies investigating the separation of PAHs *via* gas chromatography has been reported.¹¹⁰ Pyridine lone pair – π interactions have also been implicated in the stabilisation of DNA-protein interactions.¹⁹³ Moreover, computational studies have suggested that the inclusion of electron-withdrawing groups onto the π -system, resulting in a more electron-deficient π -system, may enhance lone pair- π interactions.¹⁹⁴

3.4.2 Larger-scale sorption using macroreticular polymers

The two permanently porous, macroreticular materials were also subjected to the same testing regime. The % removal of each PAH by poly(DVB-80) and poly(DVB-80-*co*-4-VP) is shown in **Table 19**.

Polymer	Methyl-naphthalene (% removed)	Acenaphthene (% removed)	Anthracene (% removed)	Pyrene (% removed)	Nitropyrene (% removed)
Control – no polymer	0	0	0	0	0
Poly(DVB-80)	8 ±2	9 ±3	9 ±1	13 ±1	74 ±3
Poly(DVB-80-co-4-VP)	3 ±2	3 ±3	8 ±7	6 ±2	47 ±15

Table 19 - Larger-scale sorption of PAHs using macroreticular polymers. n=3



Graph 5 –Larger-scale PAH removal using macroreticular polymers

Very similar trends were appearing when using macroreticular materials in the removal of PAHs from heptane. While the overall % recovery of PAH was still rather low, a general trend was still evident. The heavier, less soluble PAH, nitropyrene, was removed much more readily than the other PAHs. The lighter and more soluble PAHs, were retained in the heptane solution.

Poly(DVB-80) had a specific surface area of 553 m²/g, slightly lower than that of poly(DVB-80-co-4-VP) at 729 m²/g. **Table 19** shows that both materials removed similar amounts of each PAH from the heptane solution. The levels of sorption exhibited by both polymers may be explained when the pore structure of each material is considered. Both polymers showed similarly small pores, nearing 2 nm in diameter, and similar pore size distribution, displaying a larger proportion of mesopores (between 2 and 50 nm in diameter). It may be the case that due to the small size of the pores in these materials, once a small amount of PAH has been removed the smaller pores become blocked, hindering the sorption of more PAHs from solution. (*Note: measuring the pore size distribution of pores less than 2 nm and greater than approx. 100 nm cannot be achieved*)

using nitrogen sorption methods, therefore only the pore size distributions between 2 and 100 nm has been analysed in this body of work)

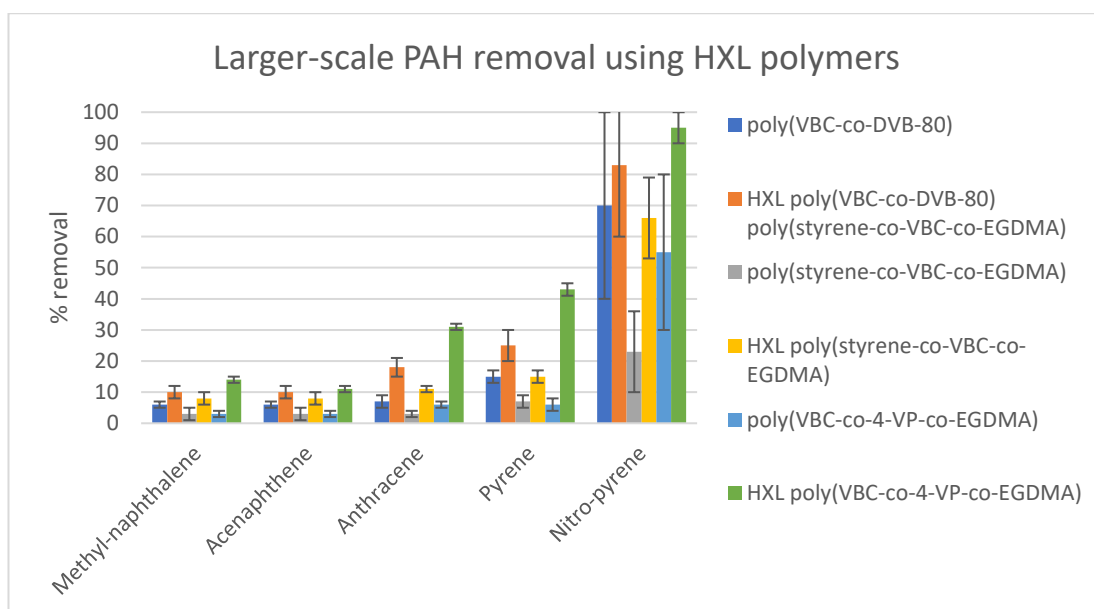
Only poly(DVB-80-co-4-VP) which had been initiated with AIBN was included in this study. Polymer initiated with ABDV was included in the smaller scale sorption study, but both polymers showed very similar sorption efficacy in the removal of PAHs therefore only one was included in this larger scale study.

3.4.3 Larger-scale sorption of PAHs using hypercrosslinked polymers

It was expected that by moving to materials with a much-increased specific surface area, the % removal of PAHs from heptane would increase. Shown in **Table 20** are the results of the experiments to remove the five PAHs from heptane.

Polymer	Methyl-napthalene (% removed)	Acenaphthene (% removed)	Anthracene (% removed)	Pyrene (% removed)	Nitro-pyrene (% removed)
Control – no polymer	0	0	0	0	0
Poly(VBC-co-DVB-80)	6 ±1	6 ±1	7 ±2	15 ±4	70 ±30
HXL Poly(VBC-co-DVB-80)	10 ±2	10 ±2	18 ±3	25 ±5	83 ±23
Poly(styrene-co-VBC-co-EGDMA)	3 ±2	3 ±2	3 ±1	7 ±2	23 ±13
HXL Poly(styrene-co-VBC-co-EGDMA)	8 ±2	8 ±2	11 ±1	15 ±0	66 ±22
Poly(VBC-co-4-VP-co-EGDMA)	3 ±1	3 ±1	6 ±1	6 ±2	55 ±25
HXL Poly(VBC-co-4-VP-co-EGDMA)	14 ±1	11 ±1	31 ±1	43 ±1	> 95

Table 20 - Larger-scale PAH sorption using HXL polymers. Includes pre-hypocrosslinked material for comparison. n=3



Graph 6 – Larger-scale PAH removal using HXL polymers

The sorption of the corresponding pre-hypercrosslinked materials are also shown in **Table 20** along with the results for the HXL material. In all cases, an increase in sorption of PAH was observed, especially the removal of anthracene, pyrene and nitropyrene. In the case of HXL poly(VBC-co-4-VP-co-EGDMA), a marked increase in PAH removal was noted. **Graph 6** highlights that while increasing specific surface area does improve overall PAH removal, the functionality of the material is just as important. HXL poly(VBC-co-4-VP-co-EGDMA) both had a specific surface area of approximately 700m²/g, one of the lowest specific surface areas observed in the hypercrosslinked materials, and significantly less than that of HXL poly(VBC-co-DVB-80) which was approx. 2000 m²/g. Yet, the 4-VP containing polymer was able to remove as much as 25% more pyrene and anthracene. . The differences in average pore size may also offer insight into the observed levels of PAH removal. The other HXL materials in this study, HXL poly(DVB-80-co-VBC) and HXL poly(styrene-co-VBC-co-EGDMA), both had very similar average pore diameters of 2.2 and 2.4 nm, respectively, as measured by nitrogen sorption analysis. Both also possessed similar pore size distributions, with most pores being less than 5 nm. However, HXL poly(VBC-co-4-VP-co-EGDMA) had an average pore diameter of 3.5 nm. Pore size distribution data also highlighted that while a significant amount of the pore structure was in the micropore region, there was a small but significant amount of

porosity that was in the mesopore region. It is suggested that by possessing predominantly micropores and having a smaller pore diameter on average, both HXL poly(DVB-80-co-VBC) and poly(styrene-co-VBC-co-EGDMA) were less effective at removing PAHs from the heptane solution. The HXL poly(VBC-co-4-VP-co-EGDMA) was able to remove more of each PAH due to having larger diameter pores. It is believed that by possessing larger pores, more PAH molecules would be accommodated within the pore network. The materials possessing larger numbers of smaller pores may not have been able to remove as much of the PAHs due to accessing the pore network being more challenging. It may also be that the smaller pores become saturated or blocked with PAH quicker and stop more PAH from being sorbed. This larger scale sorption study highlighted that, while in general sorption will be increased with increasing specific surface area, there is some tuning that is required with these materials in terms of functionality, pore size, pore volume and specific surface area. While there were some materials that possessed very high specific surface areas, they tended to have smaller average pore diameters, potentially hindering the adsorbance of PAH molecules. Also, by including certain functionalities, *i.e.*, 4-VP, favourable interactions between this molecule and nitrated PAHs could be realised.

3.5 Conclusion

In this chapter, the successful synthesis of a small library of polymers has been demonstrated. This was achieved utilising facile polymerisation techniques, namely precipitation polymerisation, and non-aqueous dispersion polymerisation. These materials have ranged from simple homopolymers, such as poly(DVB-80), to the more complex terpolymers produced *via* NAD polymerisation. Inclusion of more elaborate functionalities was also included in these materials, with vinylbenzyl chloride and 4-vinylpyridine being used extensively.

The morphology of the polymers was varied systematically. By avoiding porogenic solvents, and using low levels of crosslinker during polymerisation, all the NAD polymers were gel-type in nature and therefore had very low specific surface areas in the dry state. Conversely, poly(DVB-80) and poly(DVB-80-co-4-VP), prepared *via* precipitation

polymerisation were macroreticular and therefore had appreciable specific surface areas even in the dry state.

By including VBC in the gel-type materials, Fried-Crafts alkylation chemistry was exploited to produce Davakov-type materials that exhibit very high specific surface areas of 1000 m²/g, or more. By solvating the gel-type polymers in a suitable solvent, methylene bridging (created *via* the VBC moieties) between appropriately located phenyl rings 'locked in' the swollen architecture. This process exposed the pore structure of these materials, leading to the high specific surface areas observed.

The main aim of this work was the investigation of the ability of the solid-phase polymers to aid in the capture and removal of soot and its precursors from the lubricant system of a diesel engine. Before being used within an engine, the polymers described above were elucidated in a simplified, lab-based test remove PAHs (the main precursors to soot) from a hydrocarbon fluid. Indeed, the studies showed the successful removal of five candidate PAHs from a heptane solution. Unsurprisingly, the polymers with lower specific surface area, such as the gel-type materials, generally removed less PAH (**Table 15** and **Table 18**) than the higher specific surface area, macroreticular materials (**Table 16** and **Table 19**). Moving to the hypercrosslinked materials, which had even higher specific surface areas, the removal of PAHs from heptane was increased further.

The sorption studies highlighted not only the desirability of high specific surface areas for the removal of PAHs but also the need for pores which were of an appropriate size to remove contaminants. HXL poly(4-VP-*co*-VBC-*co*-EGDMA) proved more successful in the removal of PAHs from heptane than the other HXL materials. Not only did this polymer have a high specific surface area, it also possessed pores which were slightly larger in diameter than the other HXL materials.

Lastly, the sorption studies provided some insights into the effects of sorption of PAHs from heptane using polymers with differing functionalities. The inclusion of 4-vinylpyridine within the polymer appeared to assist in the removal of PAHs, especially nitropyrene. This information was deemed useful for work in the future, where polymeric materials could be tailored to interact with contaminants that bear functional groups, such as excess acids or bases within an engine.

3.6 Synthesis of polymers *via* suspension polymerisation

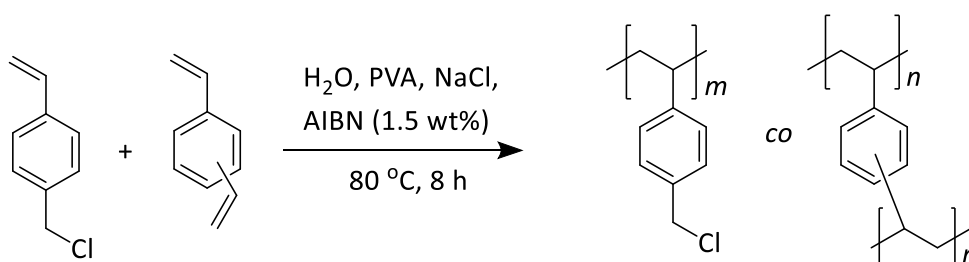
In the previous chapter, the synthesis of a small library of aromatic, vinyl polymers and the examination of these materials as potential sorbents for contaminants in hydrocarbon fluids was described. These materials were synthesised by precipitation polymerisation and NAD polymerisation processes, both of which are facile and relatively easy to perform. This allowed for materials to be synthesised and screened in the sorption studies in rather short time frames. However, the polymer particles produced *via* NAD polymerisation and precipitation polymerisation are generally less than 10 microns in diameter. Within the lubricant system of an engine, the filters involved generally have a pore size of no less than 40 microns.¹⁹⁵ It had been decided in the early stages of the current study that the simplest way of screening any materials within the lubricant system of an engine was to allow contact with the lubricant, *via* the oil filter. The oil filter provided a locus where the polymer particles could be held in place and the lubricant would then be able to flow through, over and around the polymer, maximising potential interactions between the two. When it came time to use the polymeric materials within an engine, if the polymer bead diameter was too small, beads would be able to pass through the oil filter causing damage to high-precision engineered parts. In order to ensure that the polymer particles had a large enough diameter such that they would be held against the oil filter and not pass through, suspension polymerisation was utilised as a synthetic strategy to produce materials which were similar in structure to the most successful candidate polymers identified in the previous chapter, as well as producing polymer particles with much larger diameters.

3.6.1 Synthesis of poly(VBC-*co*-DVB-80) *via* suspension polymerisation

The production of polymer resins by suspension polymerisation can be a difficult task. As was discussed in the introduction of this thesis, reactor design, stirrer type, monomer concentration, continuous phase concentration and suspending agents used can all influence the success, or failure, of a suspension polymerisation.

In the previous chapter, poly(VBC-co-DVB-80) was one of the materials that was able to remove some of the PAHs from a heptane solution. Pleasingly, synthesis of such a material by suspension polymerisation had already been studied extensively within both the Sherrington and latterly the Cormack research groups at Strathclyde.⁶¹ This meant that there was already a synthetic strategy in place to be followed. Due to following a synthetic protocol that was already in place, the ratio of monomers used in the suspension polymerisation was different to that used in the precipitation polymerisation discussed in the previous chapter. In the suspension polymerisation, a 98:2wt% ratio of VBC: DVB-80 was used, while in the precipitation polymerisation a 75:25 mol% ratio of VBC:DVB-80 was used. While these materials were different, they were deemed to be somewhat comparable and it was therefore considered that this material could be accessed more readily than if a new synthetic strategy was to be devised.

An aqueous phase of 1000 mL of water and 7.5g of PVA acting as a suspension stabiliser was prepared, and 700 mL of this solution was used as the aqueous phase. To this was added 33g of NaCl to minimise any dissolution of the monomer phase into the aqueous phase. The synthesis was carried out on a 40 g monomer scale, with a 98:2 wt% ratio of VBC to DVB-80. The reactor used was a 1 L flange-top, jacketed, baffled reactor, identical to that presented in Sherrington's discussion of polymeric supports.¹⁴ The poly(VBC-co-DVB-80) was synthesised in a high 72% yield (29 g), **Scheme 28** .



Scheme 28 - Synthesis of poly(VBC-co-DVB-80) by suspension polymerisation

Elemental microanalysis was used to ensure the successful incorporation of both VBC and DVB-80 into the final polymer. Shown in **Table 21** is the elemental composition of the polymer along with the expected composition for this material.

	Elemental microanalysis (%)			
	C	H	N	Cl
Expected	71.3	6.0	<0.3	22.7
Observed for poly(VBC-co-DVB-80)	73.6	6.8	<0.3	11.8

Table 21 - Elemental microanalysis for poly(VBC-co-DVB-80) synthesised by suspension polymerisation

The carbon, nitrogen and hydrogen content of poly(VBC-co-DVB-80) showed a close correlation to the values that were expected. However, the chlorine content was more than 50% lower than the theoretical value for this polymer. This result was not surprising since it has been discussed in the literature, by Fontanals *et al.*⁹² The low levels of chlorine were explained by the partial hydrolysis of the chloromethyl group of VBC. This would be expected to proceed *via* an S_N1 reaction through the generation of a highly stabilised carbocation followed by nucleophilic attack by a water molecule. Given the fact that suspension polymerisation involves elevated temperatures and large quantities of water, it was not surprising to observe this side reaction.

Spectroscopically, one would expect that this side reaction would be very easy to identify. Indeed, the infra-red spectrum of poly(VBC-co-DVB-80) showed a very distinct, broad peak at ~3300 cm⁻¹, indicative of -OH bond stretching. The bands indicative of the chloromethyl group (the C-H wag of CH₂Cl and the C-Cl bond stretch) were clearly visible at 1265 and 709 cm⁻¹, respectively. Shown in **Figure 27** is a typical FT-IR spectrum of the poly(VBC-co-DVB-80) prepared by suspension polymerisation.

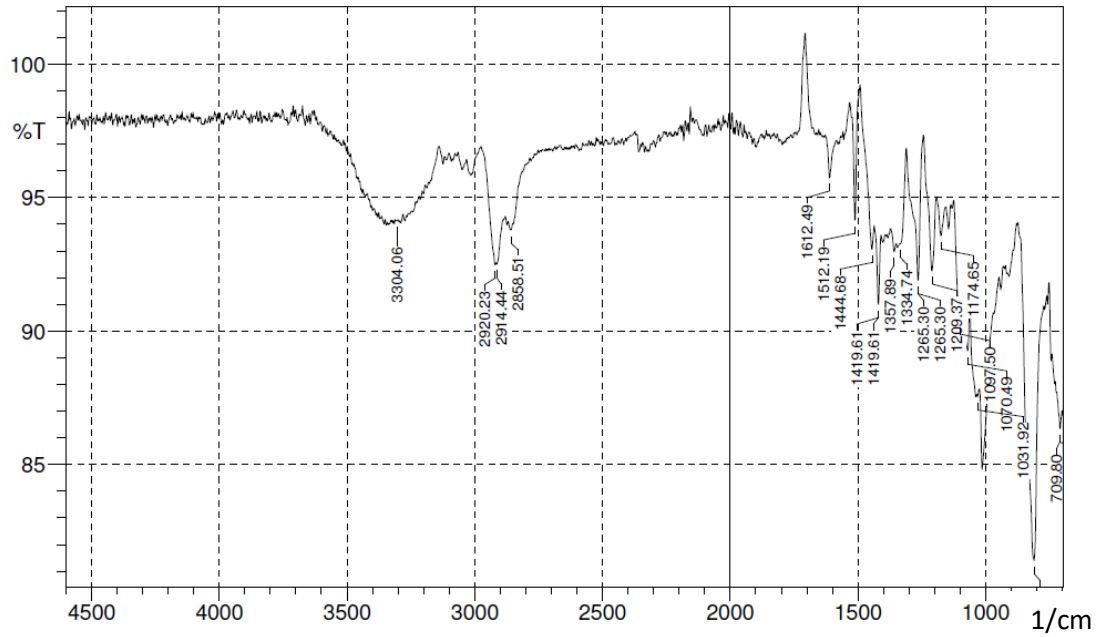


Figure 27 - FT-IR spectrum of poly(VBC-co-DVB-80) synthesised by suspension polymerisation

The polymer beads produced by suspension polymerisation are much larger in diameter than those produced by either NAD or precipitation polymerisation. Therefore, successful production of a beaded polymer in the above synthesis was evident almost immediately, as the beads were visible to the naked eye. SEM microscopy was used to investigate the surfaces of the beads more closely. Shown in **Figure 28** is an SEM micrograph of a typical polymer bead from this batch.

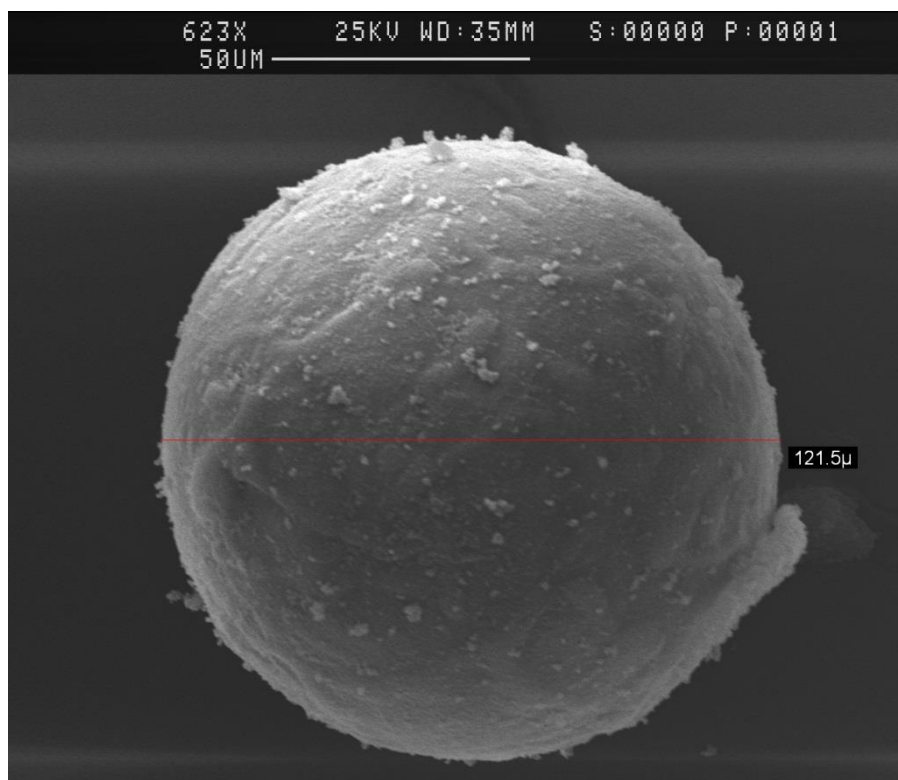


Figure 28 - SEM micrograph of poly(VBC-co-DVB-80) synthesised by suspension polymerisation

The bead shown has a diameter of 121 microns, and this allowed for much more detail of the surface to be observed. Upon further, closer inspection the roughness observed upon the surface was discerned to be microgel (the large collection of much smaller particles (approx. 1000 Å, or so, in diameter) that constitute the overall bead presented in **Figure 28**). **Figure 29** shows the microgels in some detail.

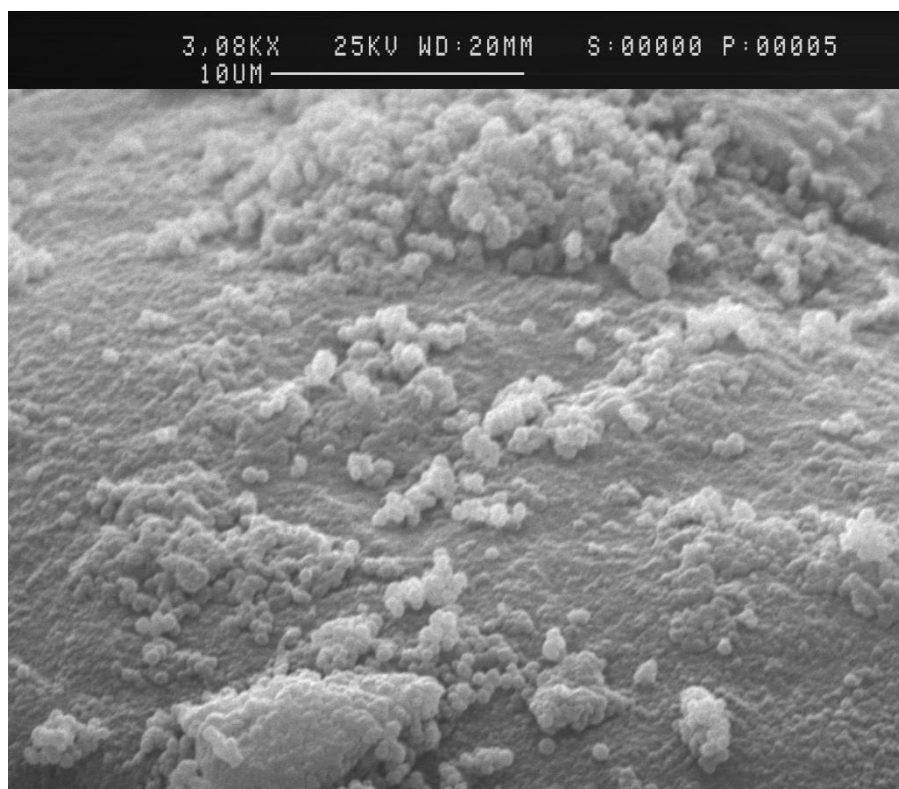


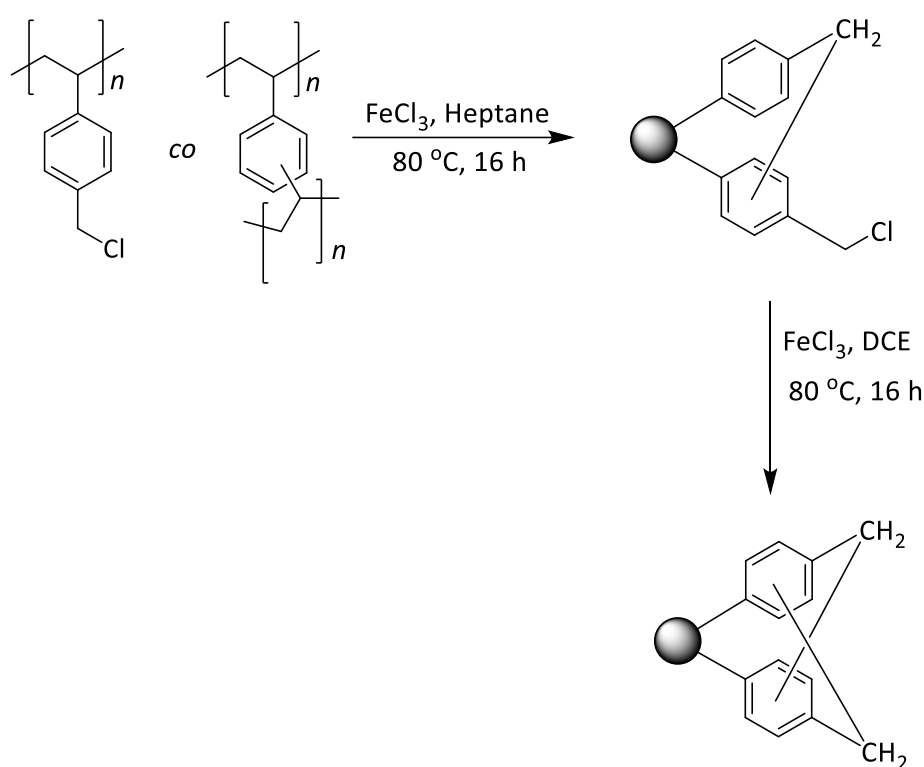
Figure 29 - SEM micrograph showing detail of the microgel particles in poly(VBC-co-DVB-80)

Due to the very low levels (2 wt%) of crosslinker, as well as the lack of any porogenic solvents used in the synthesis of this material, it was expected that this material would be gel-type in nature and therefore have a very low specific surface area in the dry state. Nitrogen sorption analysis confirmed this; the surface area was measured to be less than 5 m²/g.

3.6.2 Synthesis of hypercrosslinked (HXL) poly(VBC-co-DVB-80)

The HXL variant of poly(VBC-co-DVB-80) having a very large specific surface area also performed very well in the sorption studies discussed in the previous chapter. It was therefore, also chosen to be used in the larger engine-based sorption studies. The hypercrosslinking reaction that was carried out on the polymers synthesised by suspension polymerisation was very similar to that carried out both the precipitation and

NAD polymerisation materials. The suspension polymerisation particles were partial hypercrosslinked in heptane, using 11 mol% (relative to chlorine present in the precursor) of FeCl_3 to facilitate Friedel-Crafts alkylation, to stabilise the particles. These particles were recovered then immediately taken forward and fully hypercrosslinked by swelling in dichloroethane and locking in the swollen structure by installation of methylene bridges between aromatic moieties. In this second step, 100 mol% (relative to chlorine in the non-hypercrosslinked precursor) of FeCl_3 was used. The full hypercrosslinking of poly(VBC-co-DVB-80) was successfully carried out in a high 92% (15 g) yield, **Scheme 29**.



Scheme 29 - Exhaustive hypercrosslinking of poly(VBC-co-DVB-80)

Shown in **Table 22** is the elemental microanalysis of the fully hypercrosslinked polymer. The chlorine content was observed to fall, from 11.8% to 2.3%, indicative of successful hypercrosslinking.

Polymer	Elemental microanalysis (%)			
	C	H	N	Cl
Poly(VBC-co-DVB-80)	73.6	6.8	<0.3	11.8
HXL poly(VBC-co-DVB-80)	84.8	6.6	<0.3	2.3

Table 22 - Elemental microanalysis data for HXL poly(VBC-co-DVB-80), produced from a precursor synthesised by suspension polymerisation

FT-IR spectroscopic analysis also indicated a successful hypercrosslinking reaction. A drop in intensity of bands corresponding to the VBC moieties was observed, with both the chloromethyl C-H wag band at 1265 cm^{-1} and the C-Cl bond stretching band at 709 cm^{-1} appearing lower in intensity.

Another major piece of evidence that proved the success of the hypercrosslinking reaction was nitrogen sorption analysis. The specific surface area of the HXL material was noted to have increased from $<5\text{ m}^2/\text{g}$, before hypercrosslinking, to $1320\text{ m}^2/\text{g}$ afterwards. As with many materials that exhibit such high specific surface areas, the HXL poly(VBC-co-DVB-80) possessed a small average pore diameter of 2.2 nm. The presence of a large number of pores very close to, or indeed in, the micropore region was corroborated by the isotherm displaying a 'Type I' or Langmuir shape, characteristic of porous materials which have predominantly micropores.

SEM microscopy was used to inspect the surface morphology of the material after hypercrosslinking. Shown in **Figure 30** is a micrograph of the HXL poly(VBC-co-DVB-80), both before and after hypercrosslinking.

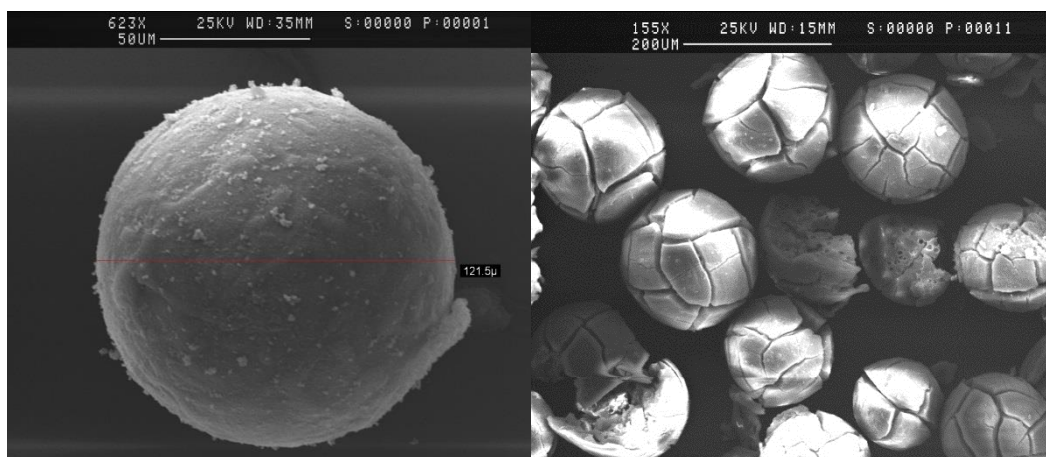


Figure 30 - SEM micrographs of poly(VBC-co-DVB-80) before (left) and after (right) hypercrosslinking.

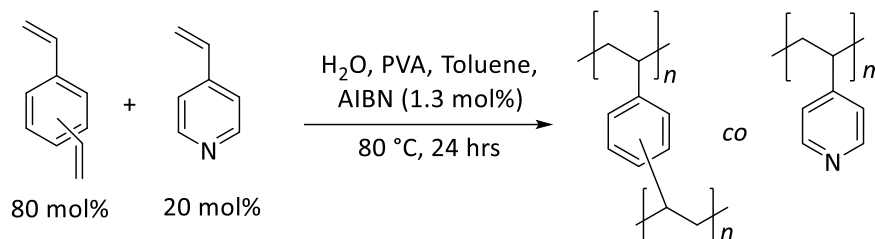
N.B. The beads in both images are of approximately the same diameter. The scale bar in each image is different.

After hypercrosslinking, the polymer particles exhibited interesting surface features, such as fractures. It has not been ascertained what the exact cause of this phenomenon is. It may be related to the swelling of the precursor particles in solvent before hypercrosslinking which causes the beads to fatigue and crack when dried. However, this was not observed in the hypercrosslinking of the materials that were synthesised *via* either precipitation or NAD polymerisation. While the hypercrosslinking reaction had changed the particles' appearance, it was still successful in producing robust, high surface area materials that were usable in the engine based, PAH-removal studies.

3.6.2 Synthesis of poly(DVB-80-co-4VP) via suspension polymerisation

In the smaller scale PAH sorption studies, the macroreticular poly(DVB-80-co-4VP) was shown to successfully remove PAHs from a heptane solution. This was therefore a material that was to be carried forward to be studied within the engine based sorption studies. Fortuitously, the synthesis of a macroreticular poly(DVB-80-co-4VP) by suspension polymerisation had been reported by Fontanals *et al.*¹⁸⁶ This synthesis was followed to produce a polymer using a 80:20 mole ratio of DVB-80:4-VP in the monomer feed. This compared to a 10:1 mole ratio of DVB-80 to 4-VP in the monomer feed that was utilised in the preparation of this material by precipitation polymerisation. As with

the precipitation polymerisation, in the suspension polymerisation toluene was included in the monomer phase, to induce the formation of a porous network in the material. In this way, a poly(DVB-80-co-4-VP) was successfully synthesised in a very high 98% (39.5 g) yield, **Scheme 30**.



Scheme 30 - Synthesis of poly(DVB-80-co-4-VP) by suspension polymerisation

Elemental microanalysis indicated a 2.2% nitrogen content (the theoretical value was 2.5%), highlighting the successful incorporation of 4-vinylpyridine. Shown in **Table 23** is the elemental microanalysis data for poly(DVB-80-co-4-VP), along with the theoretical values for this material.

	Elemental microanalysis (%)		
	C	H	N
Expected based on 80:20 monomer mole ratio DVB-80:4-VP	89.8	7.8	2.5
Observed for poly(DVB-80-co-4-VP)	87.8	7.8	2.2

Table 23 – Elemental microanalysis data for poly(DVB-80-co-4-VP) synthesised by suspension polymerisation

A clear indication of successful incorporation of 4-vinylpyridine in the polymer came from the FT-IR spectroscopic analysis; the spectrum showed an intense peak at 1599 cm^{-1} , attributed to pyridine ring stretching. Also, a band at 1416 cm^{-1} was ascribed to a C=N bond stretch.

Nitrogen sorption analysis showed a 'type IV' isotherm, **Figure 31**, typical of a permanently porous, macroreticular material.

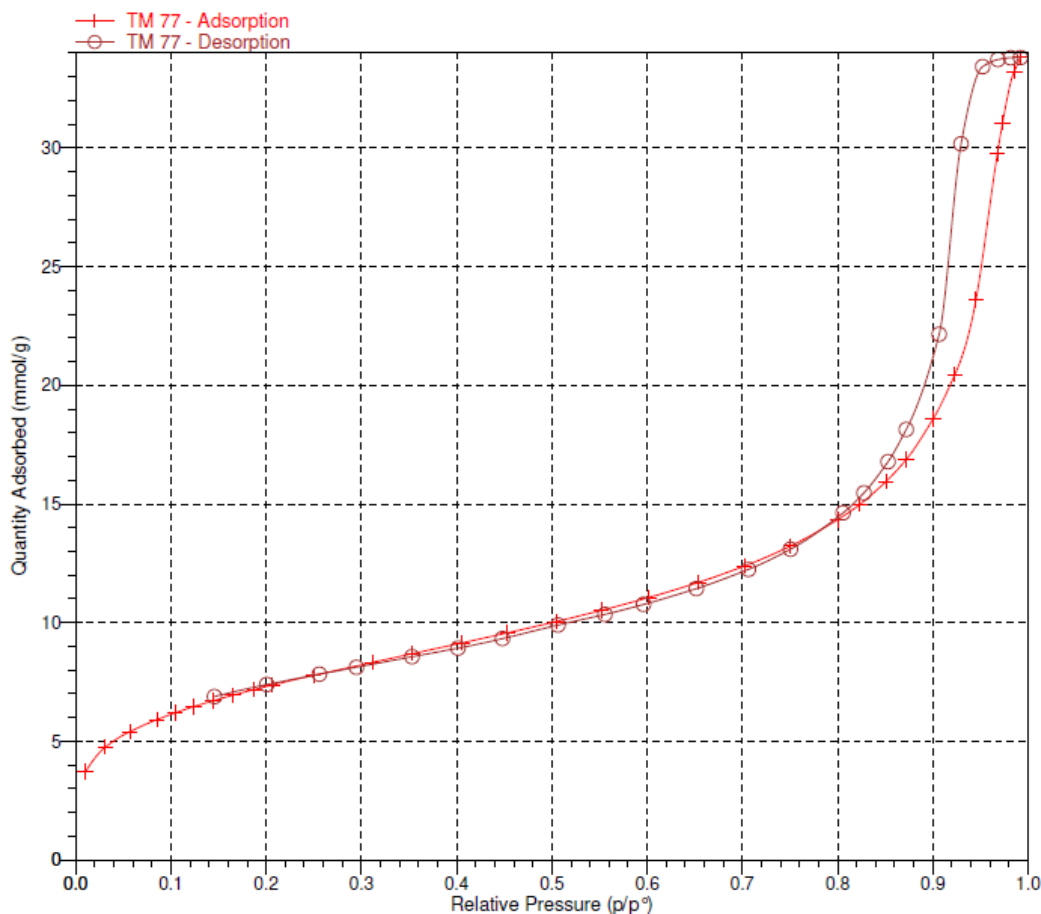


Figure 31 - Adsorption isotherm for poly(DVB-80-co-4-VP)

The specific surface area, calculated by BET theory, was found to be 599 m²/g. At 7.8 nm, this synthesis also produced pores that were much larger in diameter than those observed in the HXL polymers. In this poly(DVB-80-co-4-VP), the average pore diameter was found to be somewhat misleading. Shown in **Figure 32**, is the pore size distribution of mesopores (*i.e.*, those of diameter greater than 2 nm) within the material. As can be noted from this distribution graph, the average diameter of 7.8 nm was found to sit in a well between a larger number of smaller pores, and many pores of larger diameter. This material was, therefore, bi-modal in its pore size distribution, possessing pores that were both small in diameter and large in diameter. Unfortunately, due to the physical mechanism by which gas is adsorbed into micropores it is not possible to measure the pore size distribution of pores which are approximately less than 2nm in diameter. Therefore, it was challenging to get a full view of the pore size distribution across all the

pores present in this material. Indeed, this was true of all of the porous materials which were encountered in this work.

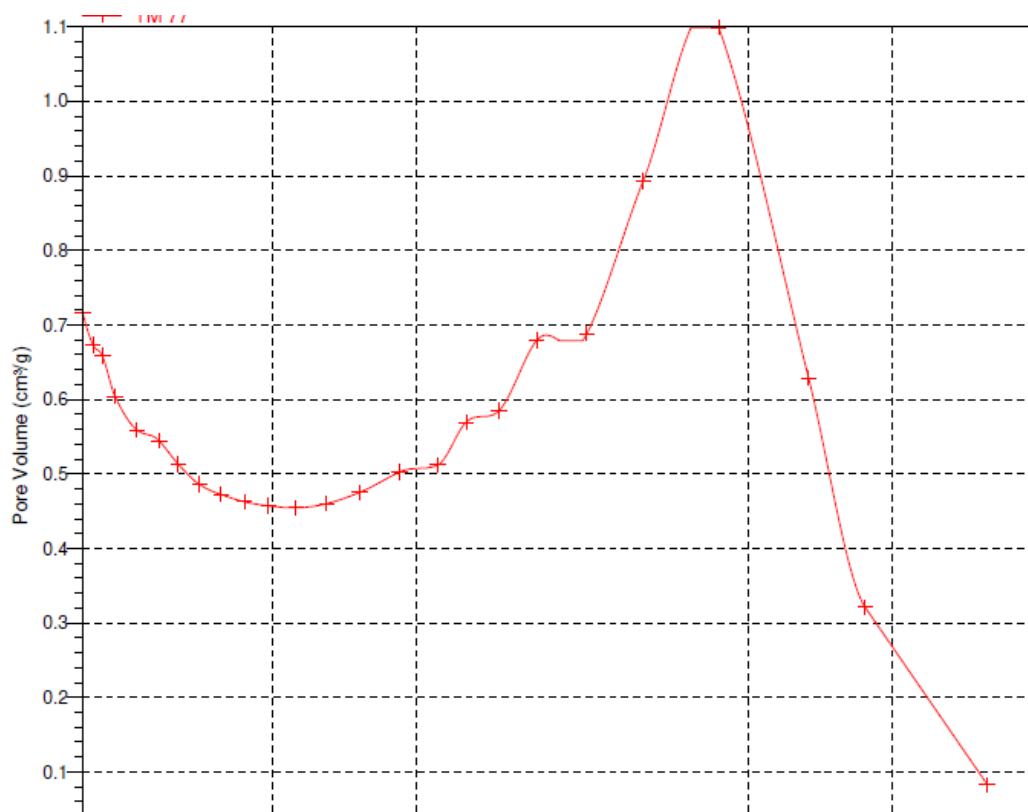


Figure 32 - Pore size distribution data for poly(DVB-80-co-4-VP) of pores between 2 and 100 nm in diameter.

As with the other materials, the surface morphology of the poly(DVB-80-co-4-VP) was examined using SEM microscopy. Shown in **Figure 33** is a typical SEM micrograph of the polymer particles.

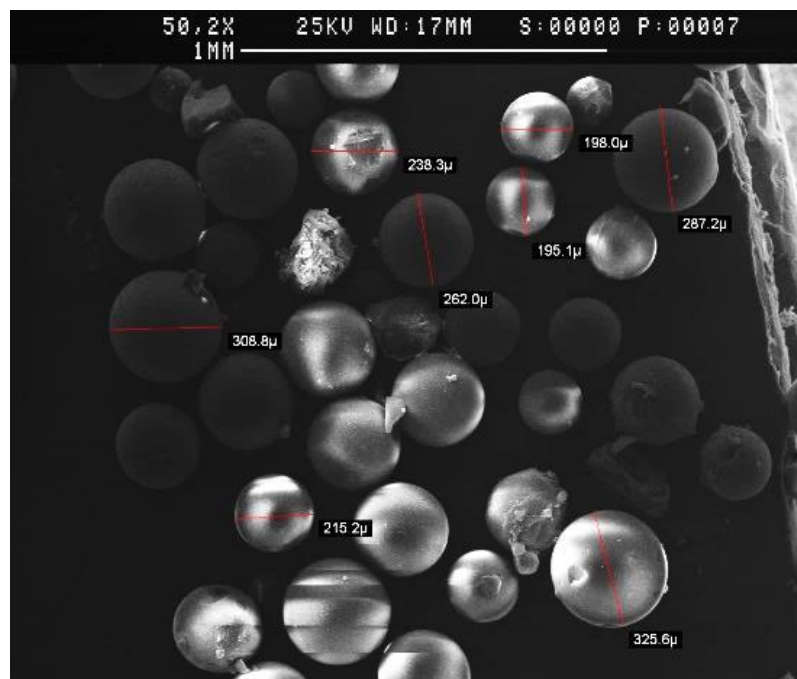


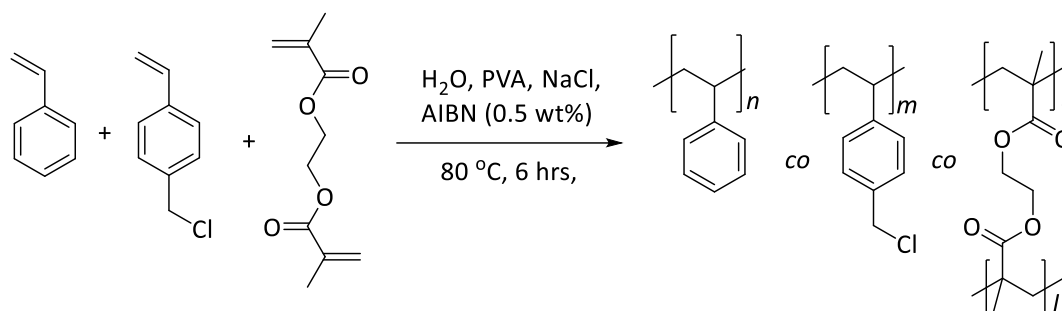
Figure 33 - SEM micrograph of poly(DVB-80-co-4-VP) synthesised by suspension polymerisation

Smooth, spherical particles were shown to have been successfully synthesised. Most of the particles in **Figure 33** are between approximately 195 and 325 μm in diameter. From the micrograph, there is some evidence of particle breakage, which may have occurred in the washing steps, post polymerisation. It may also have occurred in preparing the samples to be examined under the SEM.

3.6.3 Synthesis of poly(styrene-co-VBC-co-EGDMA) *via* suspension polymerisation

Following the success in PAH removal from heptane by some of the materials that were synthesised by NAD polymerisation, suspension polymerisation was employed to investigate the synthesis of similar materials. It was envisaged that, as is the case for all the suspension polymerisation polymers presented in this chapter, these materials would also be studied in the removal of PAHs from heptane and in engine-based contamination removal studies.

The synthesis of poly(styrene-*co*-VBC-*co*-EGDMA) by suspension polymerisation utilised the same ratio of monomers as the NAD polymerisation synthesis, namely 49.5 wt% styrene, 49.5 wt% VBC, and 1 wt% EGDMA acting as crosslinker. The aqueous phase employed was the same as that used in the synthesis of poly(VBC-*co*-DVB-80): 700 mL taken from a 1000 mL mixture of water, 7.5 g of PVA and 33 g of NaCl. The synthesis was completed in a pleasing 89 % yield (32.9 g) (**Scheme 31**).



Scheme 31 - Synthesis of poly(styrene-*co*-VBC-*co*-EGDMA) via suspension polymerisation

Elemental microanalysis data, shown in **Table 24**, indicated clearly the incorporation of VBC into the final polymer, from the Cl content. As was observed in poly(VBC-*co*-DVB-80) (**Table 21**), the amount of chlorine that was found to be present in the polymer was lower than the expected value. Owing to the presence of water in the synthesis, the lower levels of chlorine were hypothesised to be due to hydrolysis of pendent chloromethyl groups, as had been observed previously. The sum-total of all the elements analysed was noted to not equal 100%. This was believed to be due to the presence of oxygen in the hydroxyl groups.

	Elemental microanalysis (%)			
	C	H	N	Cl
Expected	81.3	6.9	<0.3	11.3
Observed for poly(styrene-<i>co</i>-VBC-<i>co</i>-EGDMA)	81.2	7.1	<0.3	6.3

Table 24 - Elemental microanalysis data for poly(styrene-*co*-VBC-*co*-EGDMA) synthesised *via* suspension polymerisation

Further evidence of hydrolysis was clear in the FT-IR spectrum of poly(styrene-co-VBC-co-EGDMA). A broad band present at 3300 cm^{-1} was ascribed to -OH stretching. The stretching frequencies attributable to VBC were also present at 1266 (the C-H wag of the chloromethyl group) and 699 cm^{-1} (C-Cl bond stretching). A very weak band was also present at 1710 cm^{-1} . This was due to C=O bond stretching and therefore indicated the successful incorporation of the crosslinker, EGDMA.

As was expected for the gel-type material, nitrogen sorption analysis showed that, in the dry state, poly(styrene-co-VBC-co-EGDMA) was non-porous with a very low specific surface area of less than $5\text{ m}^2/\text{g}$. The low surface area can be attributed to a lack of porogen used during synthesis and the very low levels of crosslinker that were employed. Upon removal of the reaction medium and drying, post-polymerisation, the polymer network would collapse upon itself, therefore presenting a very low surface area devoid of pores.

SEM microscopy revealed interesting information about the polymer particles' surfaces (**Figure 34**). The microspheres appeared to be 'deflated', as if the polymer beads had collapsed. This appearance somewhat corroborates the nitrogen sorption analysis data that showed the material to be non-porous. It is believed that what was observed in the SEM image was this same phenomenon; upon drying, the low-crosslinking density of the material means that the polymer chains are unable to support themselves and collapse, giving the beads a deflated appearance.

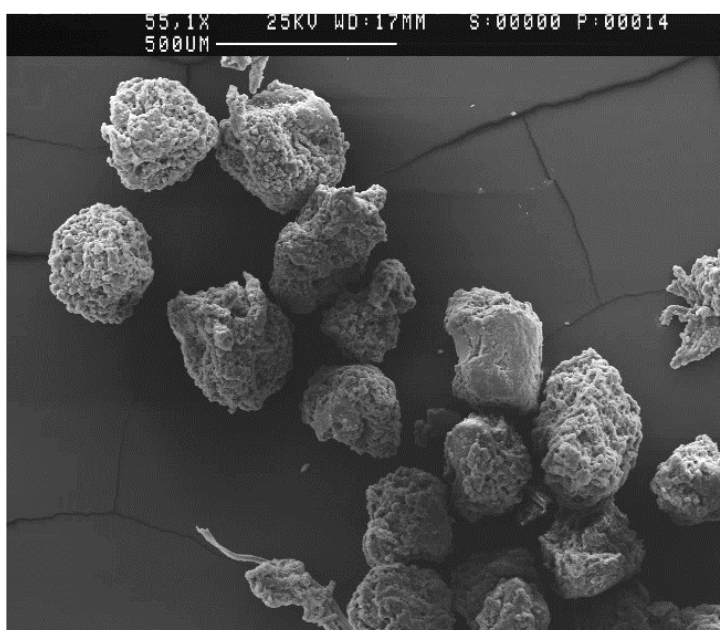
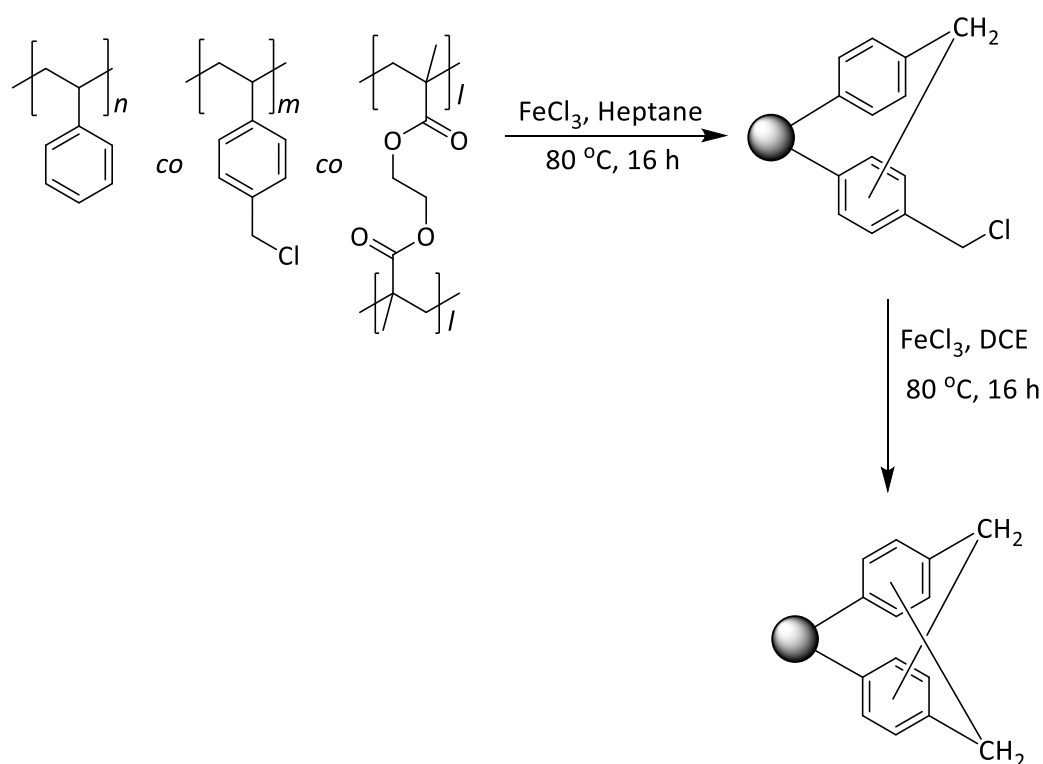


Figure 34 - SEM micrograph of suspension polymer poly(styrene-co-VBC-co-EGDMA)

3.6.4 Synthesis of HXL poly(styrene-co-VBC-co-EGDMA)

As with other polymers studied in this work, the presence of VBC in poly(styrene-co-VBC-co-EGDMA) allowed for the material to be hypercrosslinked to induce porosity and install a very high specific surface area within the polymer. The HXL poly(styrene-co-VBC-co-EGDMA) was synthesised in the usual two-step hypercrosslinking process, using the VBC moieties to install methylene bridges between appropriately located aromatic groups. This was completed in a high 95 % yield (**Scheme 32**).



Scheme 32- Hypercrosslinking of poly(styrene-co-VBC-co-EGDMA) via a two-stage hypercrosslinking process

As with all the HXL materials presented, the success of the reaction was first investigated using elemental microanalysis. **Table 25** shows the elemental microanalysis data for the HXL poly(styrene-co-VBC-co-EGDMA). The drop in chlorine content, from 6.3% before hypercrosslinking to <0.3% after hypercrosslinking, was indicative of a successful reaction.

Polymer		Elemental microanalysis (%)			
		C	H	N	Cl
Poly(styrene- <i>co</i> -VBC- <i>co</i> -EGDMA)		81.2	7.1	<0.3	6.3
HXL	poly(styrene-<i>co</i>-VBC-<i>co</i>-EGDMA)	89.2	6.9	<0.3	<0.3

Table 25 - Elemental microanalysis data for HXL poly(styrene-*co*-VBC-*co*-EGDMA) synthesised from a suspension polymer precursor

The lowering of chlorine content was also evident in the FT-IR data. The two bands at 1266 (C-H wag of CH₂Cl) and 699 (C-Cl bond stretch) cm⁻¹ that were present in the polymer before hypercrosslinking were no longer present, due to the consumption of almost all the chloromethyl groups.

Nitrogen sorption analysis was utilised to demonstrate the specific surface area increase, which is observed in HXL materials. Poly(styrene-*co*-VBC-*co*-EGDMA) exhibited an isotherm that was predominantly 'Type I' in shape, indicative of a larger specific surface area, predominated by pores which are around the micropore region (a diameter of less than 2 nm), **Figure 35**. Indeed, the Langmuir specific surface area was calculated at 529 m²/g. The specific surface area of this material was lower when compared to some of the other HXL materials synthesised; for example, the poly(VBC-*co*-DVB-80), **Scheme 29**, had a specific surface area of 1320 m²/g. The disparity in specific surface areas is due to the fact that HXL poly(styrene-*co*-VBC-*co*-EGDMA) had only 49.5 wt% VBC, whereas the HXL poly(VBC-*co*-DVB-80) had 98 wt% VBC, allowing for many more methylene bridges to be installed and a larger specific surface area to be achieved.

The open hysteresis, observed on the desorption branch of the isotherm, is often observed in hypercrosslinked materials and is possibly linked to the presence of pores with very small diameters, whereupon the gas can be admitted to these pores with greater ease than removing it.¹⁷⁶ Another possible explanation of the open hysteresis is the presence of an interconnected pore network. After the pores have filled with gas, it

requires more vacuum to draw the gas out as it must meander through the network before removal.

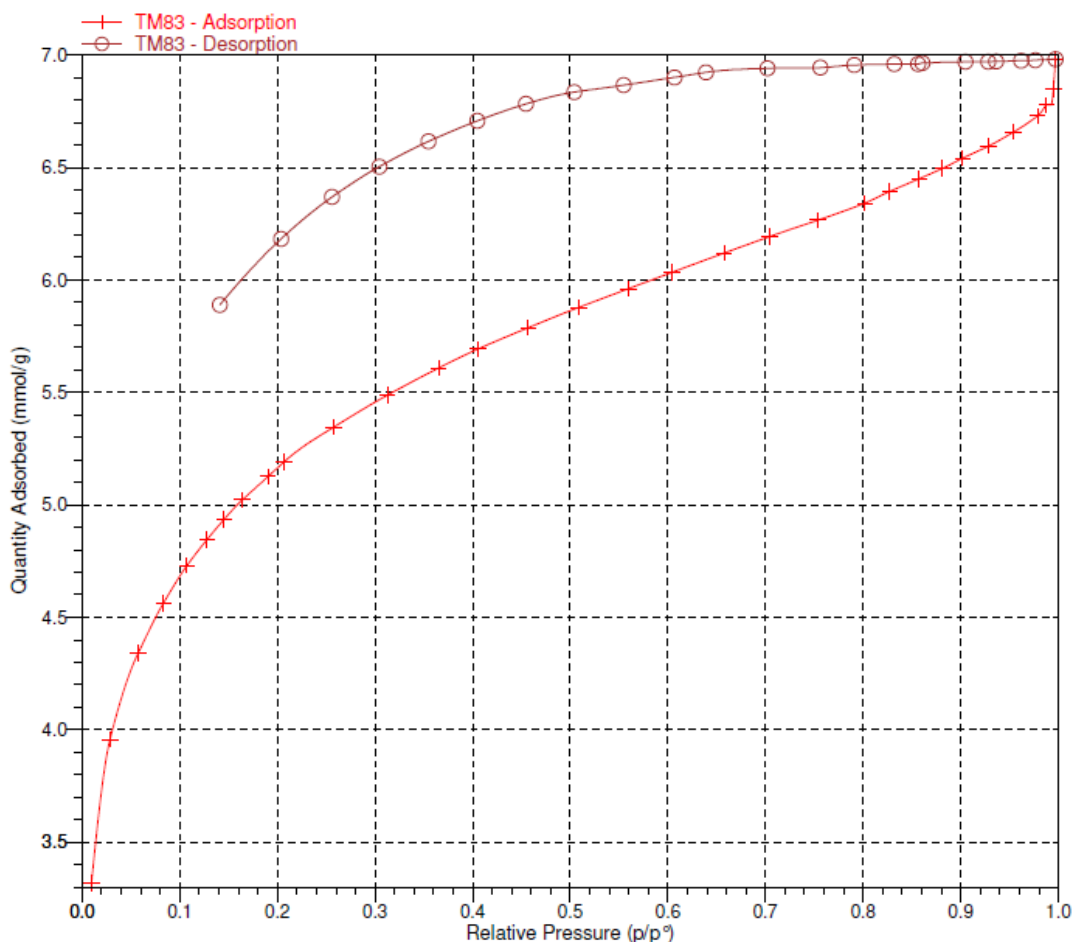


Figure 35 - Nitrogen sorption isotherm for HXL poly(styrene-co-VBC-co-EGDMA) synthesised from a suspension polymerisation precursor

The sharp increase in adsorption, observed at saturation (at a relative pressure of 1), was a particularly interesting feature of the isotherm. This sharp increase is often encountered in 'Type IV' isotherms and was attributed to pore condensation, the phenomenon by which pores in the mesopore region fill with gas. The presence of pore condensation in the isotherm corroborated the presence of a small amount of mesopores in the pore size distribution graph (Figure 36).

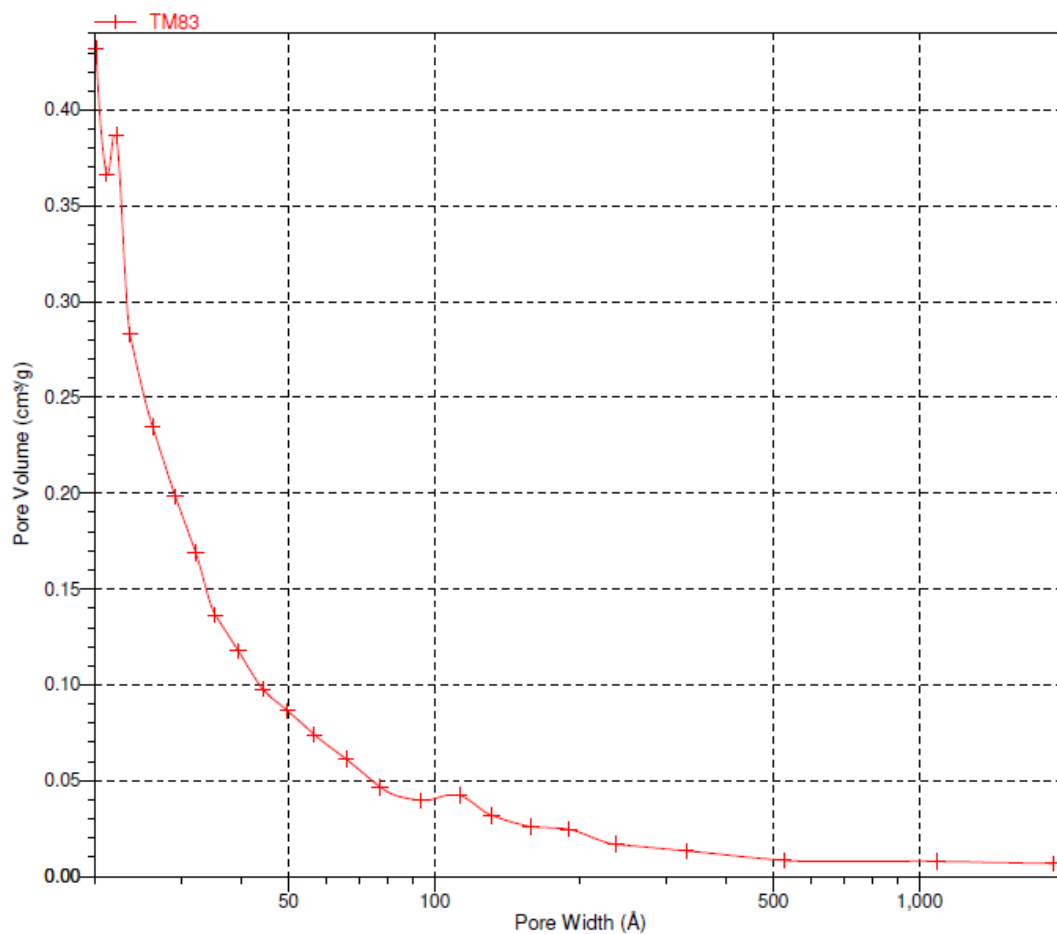


Figure 36 - Pore size distribution for mesopores present in HXL poly(styrene-co-VBC-co-EGDMA) synthesised from a suspension polymerisation precursor

SEM microscopy was employed to study the morphology of the beads after hypercrosslinking. Shown in **Figure 37** is a typical SEM image showing the polymer both before and after hypercrosslinking.

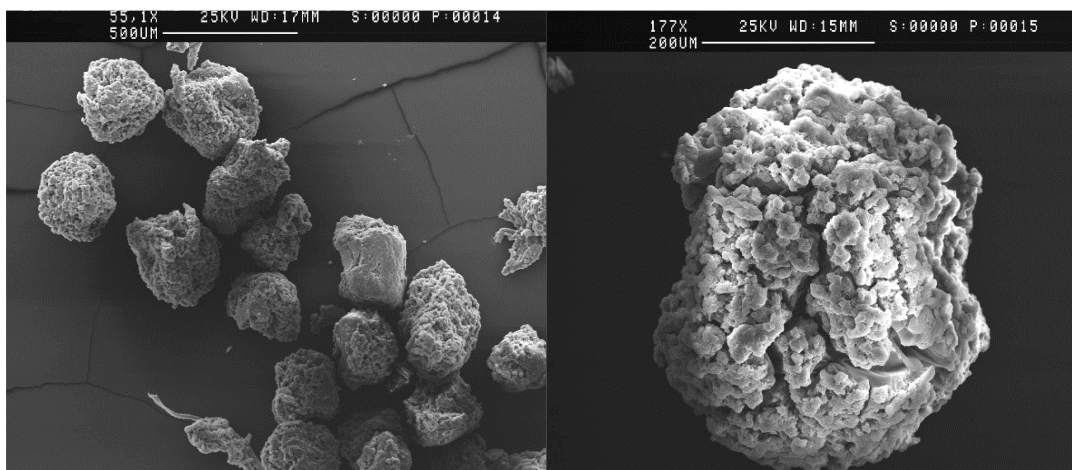
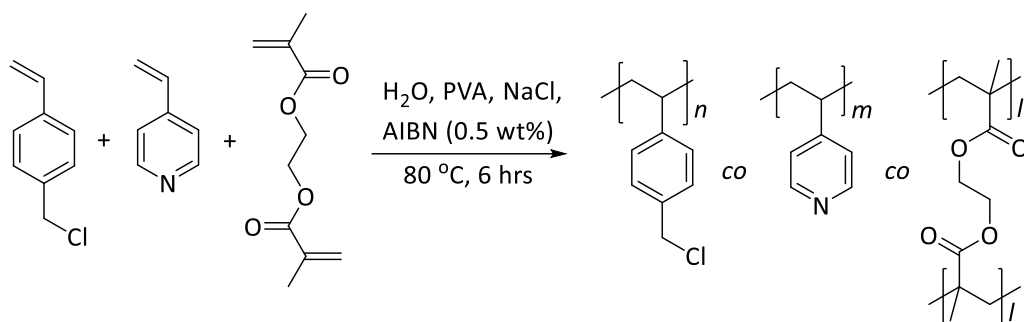


Figure 37 - SEM micrograph of HXL poly(styrene-co-VBC-co-EGDMA) before (left) and after (right) hypercrosslinking

The beads remained largely unchanged in appearance after hypercrosslinking. However, as had been observed with HXL poly(VBC-co-DVB-80), **Figure 30**, there appeared to be a fracturing of the surfaces of the polymer beads after hypercrosslinking. It is still unclear as to why this occurs. It may have been due to the swelling procedure as this polymer, before hypercrosslinking, had a very low crosslinking density and it was therefore expected to swell significantly in 1,2-dichloroethane. Another possible cause may have been that upon drying the polymer surfaces become cracked.

3.6.5 Synthesis of poly(VBC-co-4-VP-co-EGDMA) via suspension polymerisation

The other successful 4-VP containing polymer was also re-synthesised using suspension polymerisation to produce a material that would be usable in an potential engine based sorption test. Using the same suspension polymerisation protocol that had been employed for the synthesis of the other gel-type materials presented in this chapter, a poly(VBC-co-4-VP-co-EGDMA) (comprising 96 wt% VBC, 3 wt% 4-VP and 1 wt% EGDMA in the monomer feed) was produced in a usable 65 % (26.4 g) yield (**Scheme 33**).



Scheme 33 - Synthesis of poly(VBC-co-4-VP-co-EGDMA) via suspension polymerisation

Elemental microanalysis was particularly useful for the analysis of the product as both of the major monomers, *i.e.* VBC and 4-VP, contained an element that was not present elsewhere in the monomer feed (the amount of nitrogen contributed by AIBN to the total was negligible). **Table 26** shows the elemental microanalysis data for poly(VBC-co-4-VP-co-EGDMA) as well as the expected values for this material. The presence of large amounts of chlorine and nitrogen confirmed the incorporation of both VBC and 4-VP into the polymer. As with other polymers which contained VBC and were synthesised by suspension polymerisation, the lower than expected amount of chlorine was due to partial hydrolysis of the VBC during the preparation of the polymer.

	Elemental microanalysis (%)			
	C	H	N	Cl
Expected	71.3	6.0	0.9	21.5
Observed for poly(VBC-co-4-VP-co-EGDMA)	69.7	6.8	0.8	12.2

Table 26 - Elemental microanalysis data for poly(VBC-co-4-VP-co-EGDMA)

FT-IR analysis indicated the inclusion of both VBC and 4-VP. The usual bands associated with VBC were present at 1250 cm^{-1} (C-H wag of $\text{CH}_2\text{-Cl}$) and 702 cm^{-1} (C-Cl bond stretch).

A band present at 1422 cm^{-1} was ascribed to a C=N bond stretch due to the presence of 4-VP. As expected, due to the VBC content being much higher than 4-VP, 93 wt% and 6 wt% of the monomer feed, respectively, the bands associated with VBC slightly more pronounced than the band associated with 4-VP. Proof of the hydrolysis of VBC units within the polymer was shown by a large OH stretching band at 3300 cm^{-1} . A small band present at 1701 cm^{-1} (C=O bond stretch), indicated the successful inclusion of the diester crosslinker. The spectrum FT-IR of poly(VBC-co-4-VP-co-EGDMA) is shown in **Figure 38**.

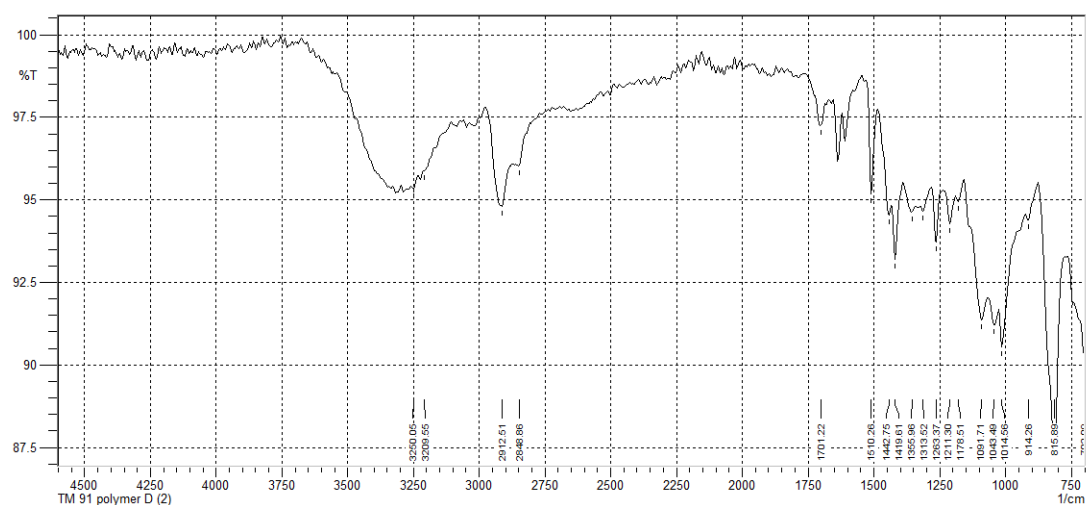


Figure 38- FT-IR spectrum of poly(VBC-co-4-VP-co-EGDMA) synthesised by suspension polymerisation

With only 1 wt% of crosslinker used in the monomer feed for this polymerisation, and the lack of an porogenic solvent, poly(VBC-co-4-VP-co-EGDMA) was expected to be non-porous in the dry state and exhibit a very low specific surface area. To corroborate this theory nitrogen sorption analysis was undertaken. This analysis showed that this material had a specific surface area of less than $5\text{ m}^2/\text{g}$ and was non-porous in the dry state.

The use of SEM microscopy proved invaluable in the analysis of the morphology and surfaces of all the materials that were synthesised throughout this study. Shown in **Figure 39** is a typical SEM micrograph of poly(VBC-co-4-VP-co-EGDMA). The image shows spherical particles that exhibit roughened surfaces and what appeared to be

agglomerated material. This material may be smaller particles that have coalesced onto the surfaces of the larger particles thereby producing a rough surface to the beads.

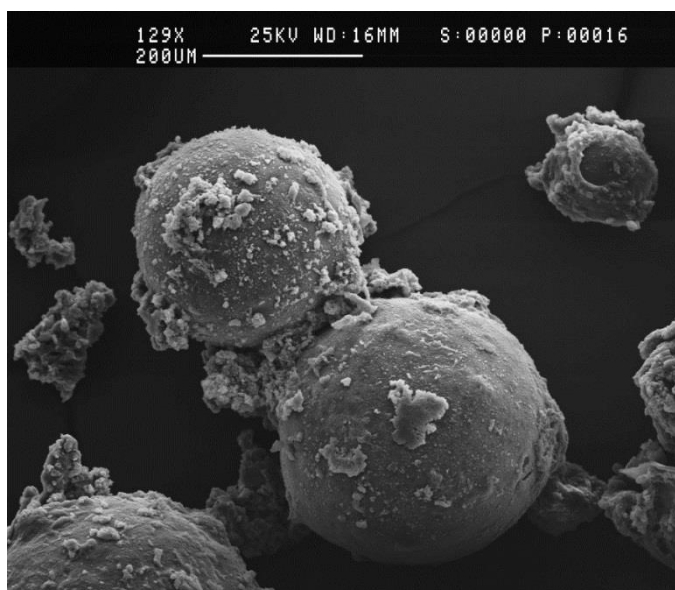
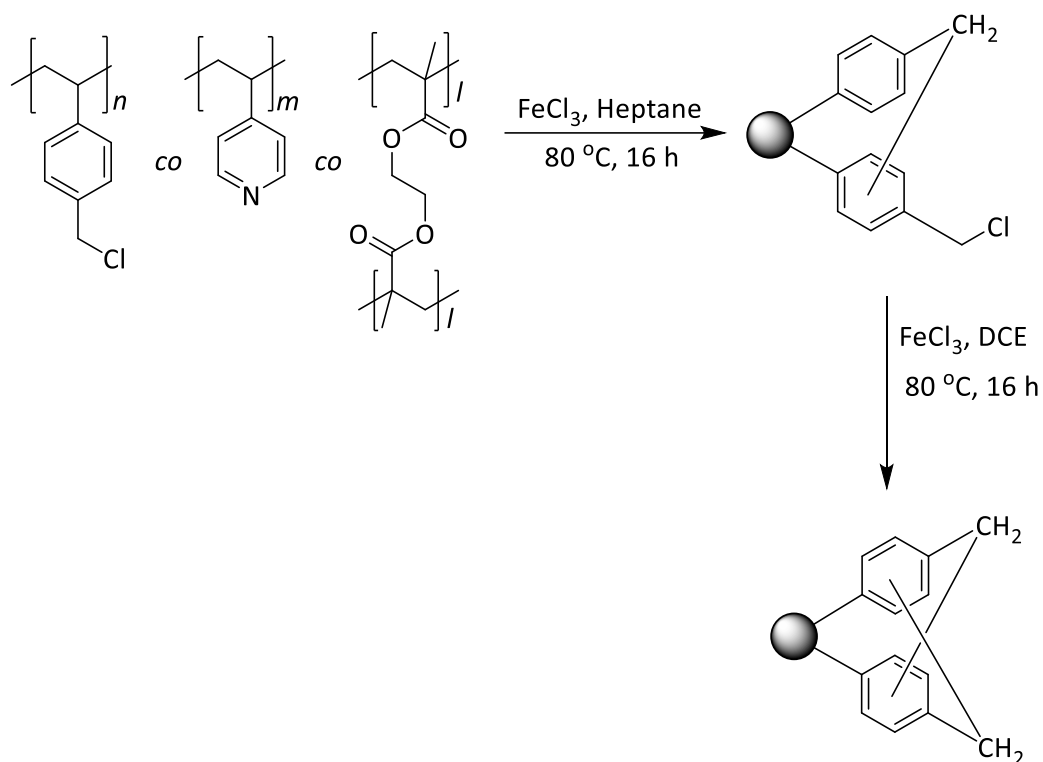


Figure 39 - SEM micrograph of poly(VBC-co-4-VP-co-EGDMA) synthesised by suspension polymerisation

3.6.6 Synthesis of HXL poly(VBC-co-4-VP-co-EGDMA) via a two-stage hypercrosslinking process

Due to high levels of VBC being present within the polymer, poly(VBC-co-4-VP-co-EGDMA) provided a material that could also be put under the hypercrosslinking protocol to produce a high specific surface area material. This material would allow for comparison, as with previously discussed polymers, between materials that exhibited similar chemistries but very different porous morphologies. Following the same hypercrosslinking reaction as described previously, HXL poly(VBC-co-4-VP-co-EGDMA) was successfully synthesised in a high 98 % yield (**Scheme 34**).



Scheme 34 - Hypercrosslinking of poly(VBC-co-4-VP-co-EGDMA) via a two-stage hypercrosslinking process

The first evidence to indicate successful hypercrosslinking was the large decrease in chlorine content of the material after hypercrosslinking. Shown in **Table 27** is the elemental microanalysis data for HXL poly(VBC-co-4-VP-co-EGDMA) along with the elemental composition of the precursor material for comparison.

Polymer	Elemental microanalysis (%)			
	C	H	N	Cl
Poly(VBC-co-4-VP-co-EGDMA)	69.7	6.8	0.8	12.2
HXL poly(VBC-co-4-VP-co-EGDMA)	80.6	6.1	1.1	2.4

Table 27 - Elemental microanalysis data for HXL poly(VBC-co-4-VP-co-EGDMA) produced from a suspension polymerisation precursor

FT-IR spectroscopic data displayed the expected drop in intensity of the bands at 1263 and 702 cm^{-1} as evidence of the consumption of VBC in the hypercrosslinking process. Also, a band at 1408 cm^{-1} (C=N bond stretch) indicated that the nitrogen of 4-VP had been unaffected by the reaction process.

Nitrogen sorption analysis was again undertaken to investigate the porosity and specific surface area of the HXL polymer. Before hypercrosslinking, poly(VBC-co-4-VP-co-EGDMA) had a specific surface area of less than 5 m^2/g . After hypercrosslinking, this had increased to 1392 m^2/g . This ultra-high specific surface area was explained due the VBC content of the precursor material. As the hypercrosslinks are installed using the VBC moieties, the larger VBC content in the precursor would result in a higher specific surface area. Poly(VBC-co-4-VP-co-EGDMA) contained 93 wt% of VBC in the monomer feed. Therefore, the hypercrosslinking of this material was expected to yield a very high specific surface area, due to the larger proportion of VBC present in the precursor. The adsorption isotherm (**Figure 40**), like most of the other HXL materials, was mostly 'Type I' in shape, with a sharp increase in adsorption at lower partial pressure as the smallest pores filled with adsorptive gas. As the partial pressure was increased towards 1, the rate of adsorption was noted to slow down as there was room for gas to be admitted (as all the smaller pores have been filled). The slower rate of adsorption in this region (between approximately 0.2 and 0.9 partial pressure) was also attributed to gas adsorbing in a much smaller number of mesopores that were present in the material. The presence of mesopores was also observed in the isotherm at saturation where pore condensation was observed. The large, open hysteresis observed upon desorption was attributed to both a large number of micropores and an interconnected pore structure, creating an environment where desorption of the nitrogen gas is more challenging than its adsorption.

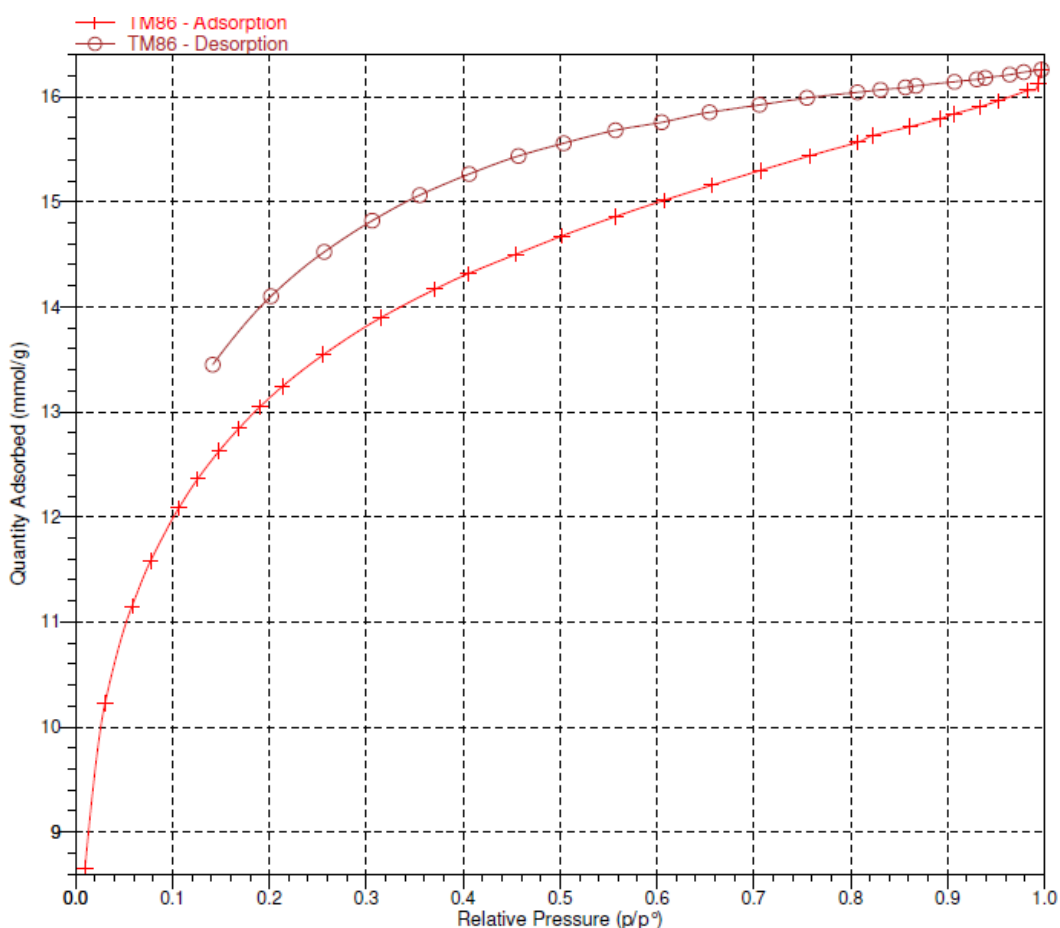


Figure 40 - Adsorption isotherm of HXL poly(VBC-co-4-VP-co-EGDMA)

The presence of micropores predominantly was noted from both the average pore diameter, of 2.2 nm, as well as the pore size distribution of mesopores within the polymer. The pore size distribution showed that there was a far greater number of smaller pores of around 2 nm in diameter and below. This data also corroborated the evidence of pore condensation observed in the isotherm, with a small but not insignificant amount of mesopores, especially at approximately 10 nm in diameter. Shown in **Figure 41** is the pore size distribution data for mesopores present in HXL poly(VBC-co-4-VP-co-EGDMA).

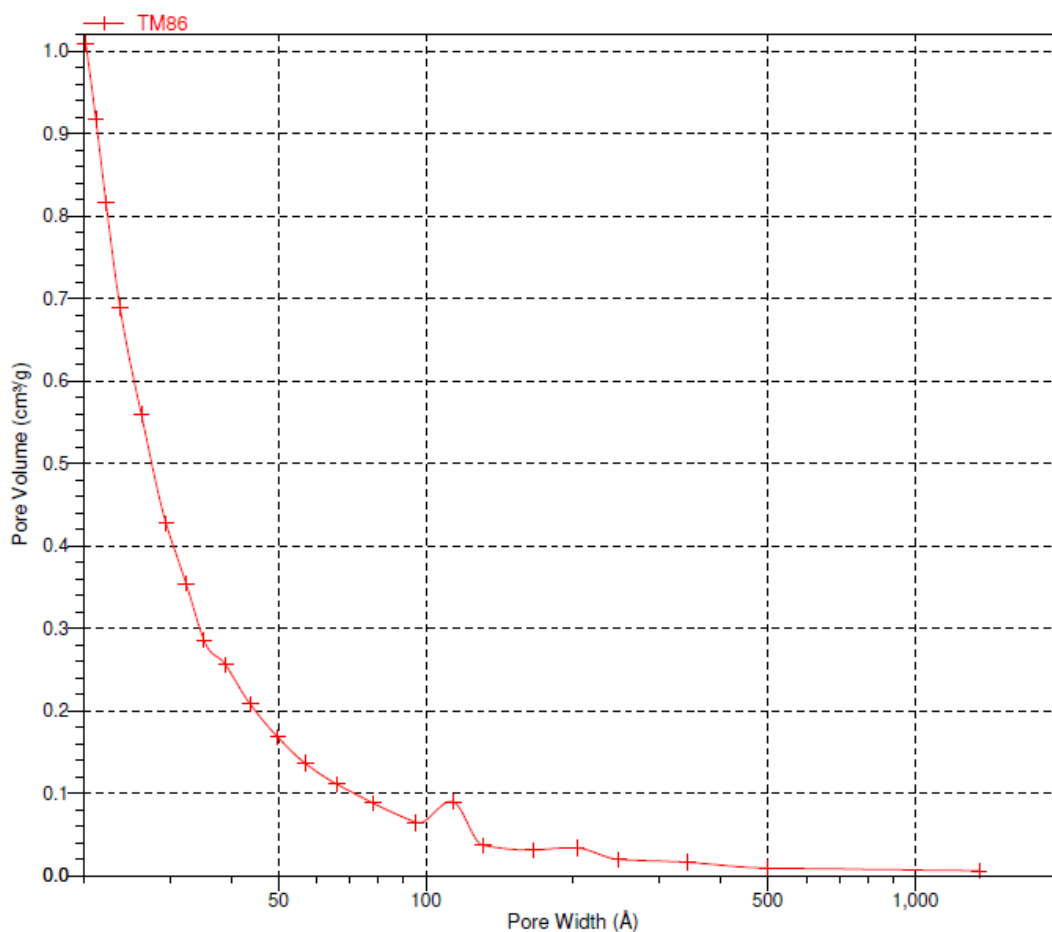


Figure 41 - Pore size distribution of mesopores in HXL poly(VBC-co-4-VP-co-EGDMA)

SEM was used to visually compare the polymer particles both before and after hypercrosslinking. Shown in **Figure 42** is an SEM image of the polymer before (left) and after (right) hypercrosslinking. Interestingly, the HXL material, shown on the right of **Figure 42**, did not exhibit the same level of fracturing as appeared on the surface of other HXL polymer beads.

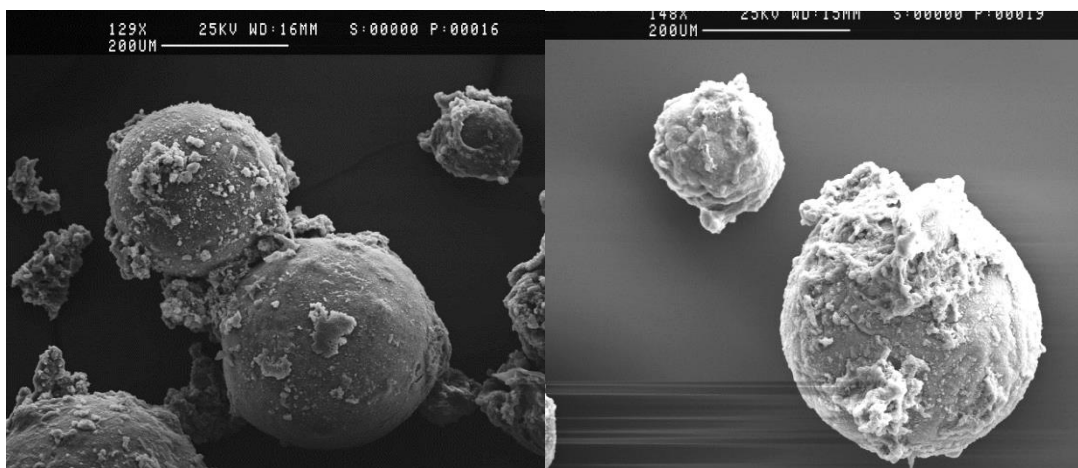


Figure 42 - SEM micrographs of poly(VBC-co-4-VP-co-EGDMA) before (left) and after (right) hypercrosslinking

3.7 Larger-scale sorption studies

By utilising suspension polymerisation, polymer microspheres of much larger diameters could be produced, when compared to microspheres synthesised by either precipitation polymerisation or NAD polymerisation. This was of the utmost importance, as it was envisaged that the materials presented in this chapter could then be investigated as potential contaminant removal devices within a diesel engine, since the polymer microspheres need to be large enough such that they could be contained within one area of the engine so as not to cause damage.

Having successfully synthesised a small library of polymers using suspension polymerisation and, in some cases, a hypercrosslinking protocol, it was deemed necessary to investigate the potential of these materials in the sorption and capture of PAHs from a hydrocarbon fluid, before testing within a diesel engine could commence. The materials synthesised in this chapter were exposed to a sorption and capture-based experiment which was the same as that described in the previous chapter: 250 mg of each polymer was contacted with a heptane solution containing five PAHs (namely methylnaphthalene, acenaphthene, anthracene, pyrene and nitropyrene), at a concentration of 200 µg/mL of each PAH (this gave a total PAH concentration of 1000 µg/mL). By using the same sorption and capture experiment as before, the polymers

presented in this chapter could be compared to the polymers studied in the previous chapter and upon which the new polymers are based.

3.7.1 PAH sorption using gel-type polymers synthesised by suspension polymerisation

The first polymers to be tested were the gel-type, non-porous polymers that had been synthesised by suspension polymerisation. The gel type polymers tested were: poly(VBC-co-DVB-80), which contained 98 wt% VBC and 2 wt% of DVB-80 in the monomer feed, poly(styrene-co-VBC-co-EGDMA), containing 49.5 wt% of both styrene and VBC in the monomer feed, and poly(VBC-co-4-VP-co-EGDMA), containing 93 wt% VBC and 6 wt% of 4-VP in the monomer feed. EGDMA was present as 1 wt% of the monomer feed in both EGDMA containing polymers. The sorption experiment was carried out in triplicate and included a blank for reference.

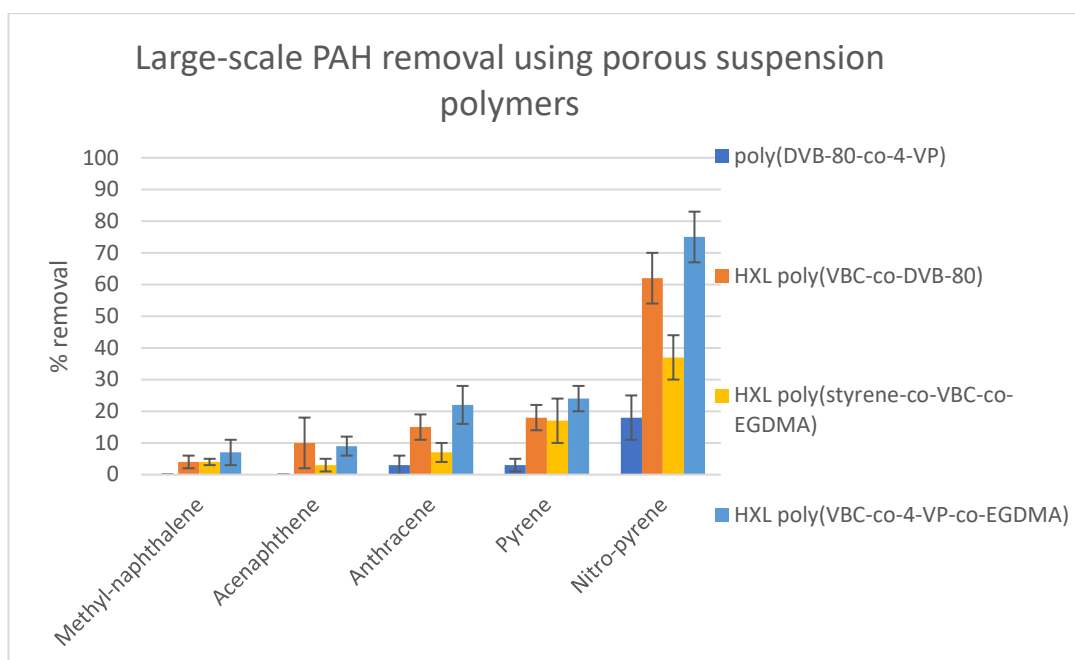
Unfortunately, it was found that all the gel-type polymers were unsuccessful in removing any of the PAHs from the heptane solution. The gel-type polymers synthesised by precipitation polymerisation and NAD polymerisation were able to remove up to 14 % (2.92 mg) of the total PAH content of a 20 mL sample (see poly(VBC-co-4-VP-co-EGDMA) synthesised by NAD polymerisation in **Table 20**) (five PAHs present at a concentration 200 µg/mL each in a 20 mL samples means there is 20 mg of PAH in total, in each sample). Due to the gel-type polymer presented in the last chapter proving fruitful in the removal of PAHs, and the gel-type materials synthesised by suspension polymerisation proving less so, it was determined that the low specific surface area of these materials could not be the reason for the low levels of sorption observed. However, all the materials that were synthesised by suspension polymerisation did contain VBC. Hydrolysis of some of the VBC units within these polymers was evident from FT-IR spectra and has been previously discussed in this chapter. Therefore, the suspension polymerisation polymers were much more hydrophilic in character, meaning that failure in removing hydrophobic PAHs from a hydrophobic medium (heptane) was not surprising.

3.7.2 PAH removal using porous polymers synthesised by suspension polymerisation

The porous polymers described in this chapter were also examined in the sorption and capture of PAHs from heptane. Both a permanently porous poly(DVB-80-co-4-VP) which had an 80:20 mole ratio of DVB-80 to 4-VP in the monomer feed, and the HXL variants of the three gel-type materials described in the previous section. Shown in **Table 28** is the % of each PAH removed from a 20 mL solution of heptane containing each of the five PAHs each at a concentration of 200 µg/ mL.

Polymer	Methylnaphthalene (% removed)	Acenaphthene (% removed)	Anthracene (% removed)	Pyrene (% removed)	Nitropyrene (% removed)
Control – no polymer	0	0	0	0	0
Poly(DVB-80-co-4-VP)	0 (3 ±2)	0 (3 ±3)	3 ±3 (8 ±7)	3 ±2 (6 ±2)	18 ±7 (47 ±15)
HXL poly(VBC-co-DVB-80)	4 ±2 (10 ±2)	10 ±8 (10 ±2)	15 ±4 (18 ±3)	18 ±4 (25 ±5)	62 ±8 (83 ±23)
HXL Poly(styrene-co-VBC-co-EGDMA)	4 ±1 (3 ±2)	3 ±2 (3 ±2)	7 ±3(3 ±1)	17 ±7(7 ±2)	37 ± 7 (23 ±13)
HXL Poly(VBC-co-4-VP-co-EGDMA)	7 ±4 (3 ±1)	9 ±3 (3 ±1)	22± 6 (6 ±1)	24 ±4 (6 ±2)	75 ± 8 (55 ±25)

Table 28 - Large-scale sorption of PAHs from heptane using a permanently porous polymer and HXL materials produced from gel-type precursors. n=3



Graph 7 – Larger-scale PAH removal using porous suspension polymers

In **Table 28** the bracketed values shown in italics are the proportion of each PAH that was removed from heptane by a comparable material that was discussed in the previous chapter. For the HXL materials this data is reproduced from **Table 20** and, in the case of poly(DVB-80-co-4-VP), **Table 19**. These values are included to allow comparison between the materials that were synthesised by precipitation polymerisation and NAD polymerisation, and the materials which were synthesised by suspension polymerisation.

In general, the trend observed in the sorption studies discussed in the previous chapter is noted again. Namely, as the molecular weight (and hydrophobicity) of the PAH increases the more of that PAH was retained by the polymer. For example, nitropyrene was removed from the heptane far more readily than the lighter methylnaphthalene.

The poly(DVB-80-co-4VP) synthesised by suspension polymerisation was similar in composition and specific surface area to the material that was synthesised by precipitation polymerisation. The nitrogen content of these materials was 2.2% and 1.9%, respectively, indicating very similar amounts of 4-VP in the polymer. This would explain the similarities in sorption observed in these materials.

In the case of HXL poly(styrene-*co*-VBC-*co*-EGDMA), both the material that had been synthesised from a suspension polymerisation precursor and from a NAD polymerisation precursor showed very similar levels of sorption across all five PAHs.

From the data presented in **Table 28** it was observed that specific surface area has a pronounced bearing on the amount of PAH that is removed from heptane. For example, both HXL poly(VBC-*co*-DVB-80) and HXL poly(VBC-*co*-4-VP-*co*-EGDMA), synthesised from precursors made *via* suspension polymerisation, had specific surface areas of more than 1300 m²/g and removed far more of the PAHs from heptane than either poly(DVB-80-*co*-4-VP) or HXL poly(styrene-*co*-VBC-*co*-EGDMA). Both poly(DVB-80-*co*-4-VP) and HXL poly(styrene-*co*-VBC-*co*-EGDMA) had lower specific surface areas, of approximately 500 m²/g, resulting in less PAH being removed

3.8 Conclusions

Using materials synthesised from NAD polymerisation and precipitation polymerisation in successful sorption and capture of PAHs from a hydrocarbon fluid has been demonstrated in the last chapter. However, the format of these materials was unsuitable for use within a combustion engine as the microspheres possessed too small a diameter to be contained effectively. Therefore, work in this chapter demonstrated the successful synthesis of a small library of polymer microspheres synthesised by suspension polymerisation using previously disclosed protocols. By replicating the monomer composition of the materials that were able to remove high levels of PAH from heptane in the previous chapter, large polymer microspheres with similar chemistries were obtained. Most of these materials were gel-type in nature and devoid of a porous architecture in the dry state. To induce porosity and increase specific surface area, the gel-type materials were subjected to hypercrosslinking chemistry. A macroreticular material, poly(DVB-80-*co*-4VP) was also synthesised. This material possessed a high specific surface area but had an average pore diameter which was much higher than those observed for microporous materials, such as the HXL polymers. By having materials which spanned a range of specific surface areas, porous structures as well as differing chemistries, the effect of these properties on PAH removal could be investigated.

To ensure that the suspension polymerisation-based materials and HXL derivatives were effective in the removal of PAHs from heptane, as the previously discussed materials had been, the same sorption and capture experimental procedure was used. The polymers were exposed to a heptane solution containing five PAHs of known concentration and allowed to interact for 24 hours, after which time the total amount of PAH removed by each polymer was determined. From this study it was found that, unfortunately, the gel-type, non-porous materials were not effective in PAH removal. Partial hydrolysis of VBC within the polymer had rendered the materials more hydrophilic in nature and therefore the removal of hydrophobic PAHs within a hydrophobic environment (heptane) was not achieved.

By increasing the specific surface area through hypercrosslinking, it was found that much more PAH could be removed from the heptane. With respect to the HXL materials produced from suspension polymerisation precursors, it was found that the specific surface area of the material had the greatest bearing on the amount of PAH that could be removed; the chemistry of the material appeared to have less of an effect on the removal of PAH from heptane. Both HXL poly(VBC-co-DVB-80) and HXL poly(VBC-co-4-VP-co-EGDMA) had specific surface areas of 1300 m²/g and were able to achieve much higher levels of PAH removal than the other porous materials which had much lower specific surface areas of around 500 m²/g..

3.9 Use of polymeric materials as soot and contaminant sorbents within a diesel engine

In the previous chapter, the hypothesis that solid-phase polymers could be used to remove contaminants from a hydrocarbon fluid was demonstrated and a proof of concept achieved.. With this information in hand, attention turned to evaluating the viability of using these materials within the lubricant system of a diesel engine as sequestration devices for PAHs, and soot amongst other contaminants.

Currently, lubricant technology relies upon cellulosic filters to remove soot and larger contaminants from the engine lubricant. To ensure smooth running of the engine,

lubricants also contain additives, in the form of dispersants and detergents, to assist in the suspension of small PAHs and soot particles within the lubricant. Not only is this costly to achieve, but the additives allow for the contaminants to build up within the lubricant whereupon damage can still be done to the internal parts of the engine.

It is believed that by moving to solid-phase additives, such as the polymers described herein, that PAHs, soot and potentially other contaminants could be removed from the lubricant system entirely. In the future these materials may supersede, or indeed work in conjunction with currently employed technologies to provide a more cost effective lubricant system that does not rely upon costly and complex additive packages, as well as a more environmentally friendly one which could be recycled with greater ease and more control than is currently available.

3.9.1 Initial engine test using a non-fired, research engine

All of materials described in the previous chapter, synthesised either by suspension polymerisation or through the hypercrosslinking of these materials, were to be used in the engine-based studies. The logistics surrounding the implementation of this investigation were not straightforward as all the engine-based studies were carried out at Castrol's Technology Centre in Berkshire, England by Robert Spragg, Thomas Peirson-Smith, Alistair Drury and Mark Coakley.

For the initial engine-based studies, it was decided that due to both practical and safety concerns, the engine would not be fired, and the lubricant would be heated *in situ* and circulated around the engine, simulating its flow in normal engine operations. The Ricardo, diesel 'Hydra' research engine that was used for these studies is shown in **Figure 43**.

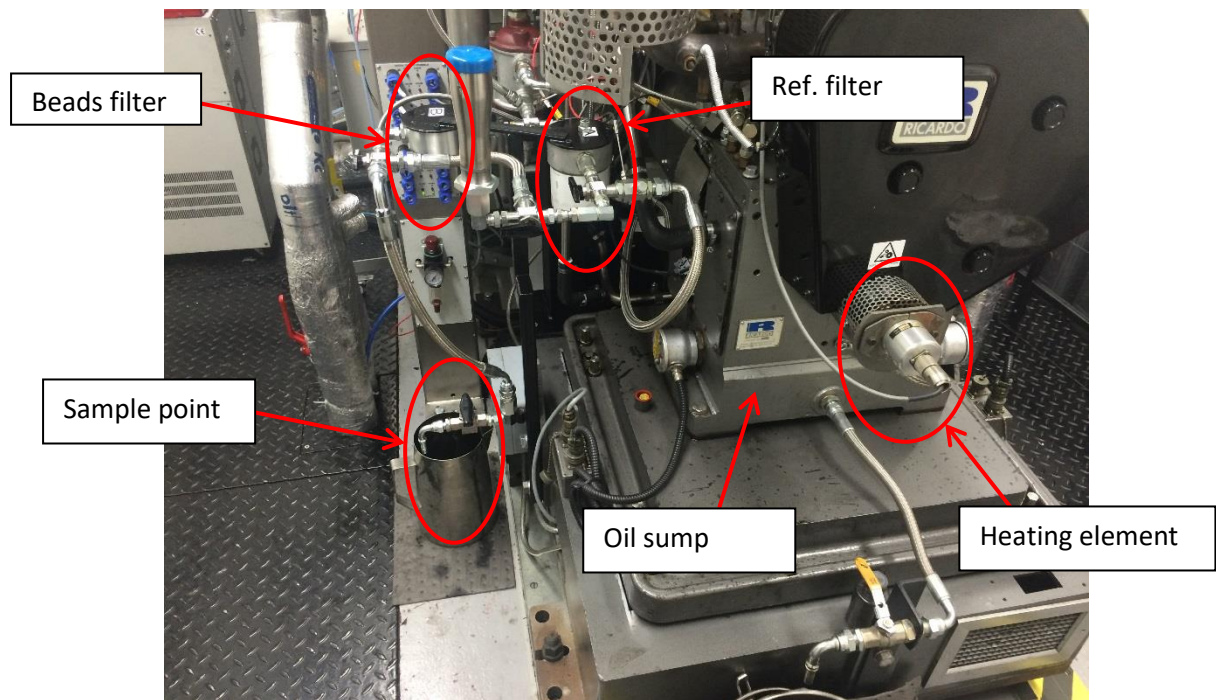
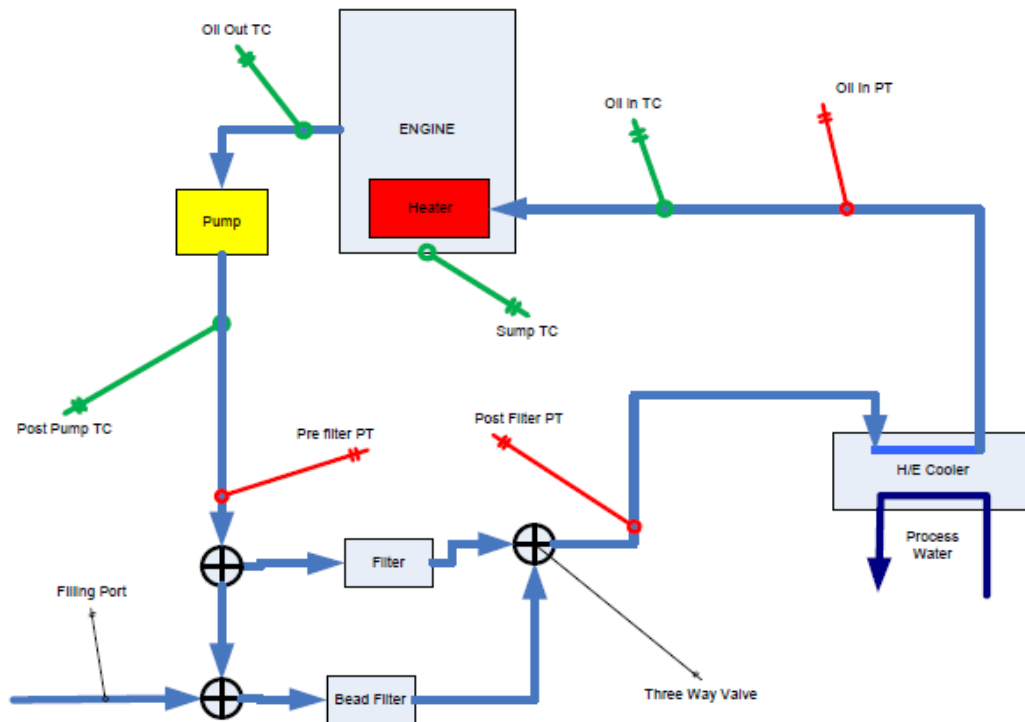


Figure 43 - Photograph of the Ricardo 'Hydra' diesel research engine

Before sending to Castrol for testing, all of the polymer samples were sieved on a 100 μm sieve to ensure that all particles were large enough to be contained within the lubricant system. To ensure the polymer particles were contained and not allowed to flow around the lubricant system they were inserted against the filter element of a 'K&N' fuel filter (10 g of polymer was used in each engine test). A fuel filter was used as the pores within the filter element are smaller than those found within an oil filter. Also, fuel filters do not contain a by-pass valve, whereas oil filters do have this feature. If an oil filter was to be used and became blocked, the by-pass valve would open and allow polymer particles to flow around the engine causing damage. These steps were taken to ensure the integrity of the engine, ensuring that the polymer particles were contained and were not allowed to cause damage to the engine. The lubricant system design is shown schematically in **Figure 44**. The 'beads filter' was where the polymer particles were contained. Pressure transducers and thermocouples were placed at various points throughout the system. This allowed the pressure across the filters to be monitored, to ensure no blockages occurred. Thermocouples facilitated the control of lubricant temperature throughout the experiments.



**Figure 44 - A schematic diagram of the engine lubricant system.
(PT – pressure transducer. TC – thermocouple)**

Once the polymer particles were in place, the engine was flushed with the candidate lubricant. As the engine was not running during these tests, a lubricant that had already been used in a heavy-duty diesel engine field trial was chosen. This lubricant was at the end of its service life and therefore contained high levels of soot and contaminants. By using a heavily sooted, contaminated lubricant it was thought that this would provide the best opportunity for the polymers to remove PAHs and soot as there were very high levels of soot present. **Figure 45** shows a photograph of the candidate lubricant before use in the engine-based sorption studies (a fresh sample of engine lubricant is shown in the left of the image for reference).



Figure 45 - Photograph of the pre-sooted engine lubricant (right) to be used in initial engine-based sorption studies (a sample of fresh lubricant is shown on the left for reference)

The candidate lubricant was used to flush the engine for 30 minutes to prepare the lubricant system and engine for testing. After flushing, a new sample of pre-sooted lubricant was introduced into the engine and the testing commenced.

The lubricant was circulated around the engine and contacted with the polymer for 10 hours at 60 °C. A sample of lubricant was removed every hour for testing at Castrol's testing facility. Upon completion of each test the polymer was removed from the filter and returned to the Cormack Lab for further analysis. The polymer particles were washed with heptane in a Soxhlet extraction apparatus for 24 hours and dried overnight *in vacuo* at 40 °C. Within the Cormack Lab the polymer particles returned from the engine test were subjected to SEM analysis, FT-IR analysis and nitrogen sorption analysis to allow comparison with samples of the polymer before testing. Shown in **Figure 46** is an example of polymer particles being prepared for testing within the lubricant system and an image of the same filter element after the 10 hour engine test. It is clearly evident that the blackened and dirty oil had adhered to filter element and the polymer particles.



Figure 46 - Photographs of filter element and polymer particles before (left) and after (right) engine based sorption test

Unfortunately, due to time constraints and limited availability of the research engine used in these studies, both poly(VBC-co-DVB-80) and its hypercrosslinked variant HXL poly(VBC-co-DVB-80) were not able to be tested.

3.9.2 Engine-based sorption study using poly(DVB-80-co-4-VP) as sorption media

The first polymer to be analysed post-engine test was the macroreticular poly(DVB-80-co-4-VP). The blackened particles were first washed in heptane for 24 hours in a Soxhlet extraction apparatus before drying overnight. The polymer particles were then imaged using SEM. Shown in **Figure 47** are micrographs of the polymer before the engine test (left) and after Soxhlet extraction, *post-engine* testing.

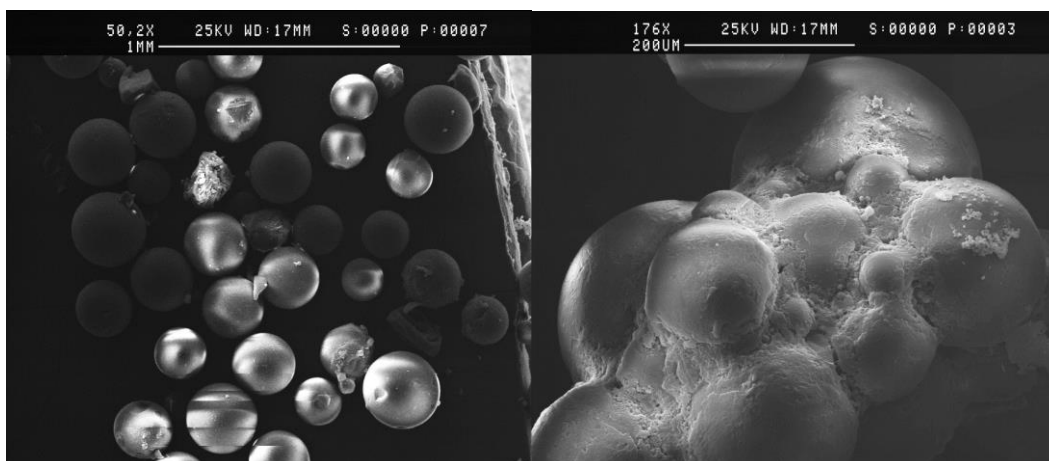


Figure 47 - SEM images of poly(DVB-80-co-VBC) before (left) and after (right) engine testing

After engine testing, it was evident that agglomeration of the polymer particles had occurred. It was believed that this agglomeration may have been due to soot or other contamination being captured on the surfaces of the microspheres. The temperature of the lubricant as it was flowing over the polymer was 60 °C, 20 °C lower than the reaction temperature at which the polymer was synthesised. Therefore, temperature was not believed to be causing the agglomeration. FT-IR spectroscopic analysis of the polymer beads after the engine testing was undertaken and compared to an infrared spectrum of the material before the engine test to investigate any changes that may have occurred. Spectra of poly(DVB-80-co-4-VP) before and after the engine testing are shown in **Figure 48**. FT-IR spectroscopic analysis of the lubricant that was used in the engine-based studies was also carried out. It was anticipated that this would allow for any potential observations in the FT-IR spectra of the materials to be rationalised, by the observation of bands in the lubricant, that were attributable to soot, PAHs or contaminants being observed in the FT-IR spectrum of the polymer, *post* engine test. The FT-IR spectrum of the lubricant is shown in **Figure 49**.

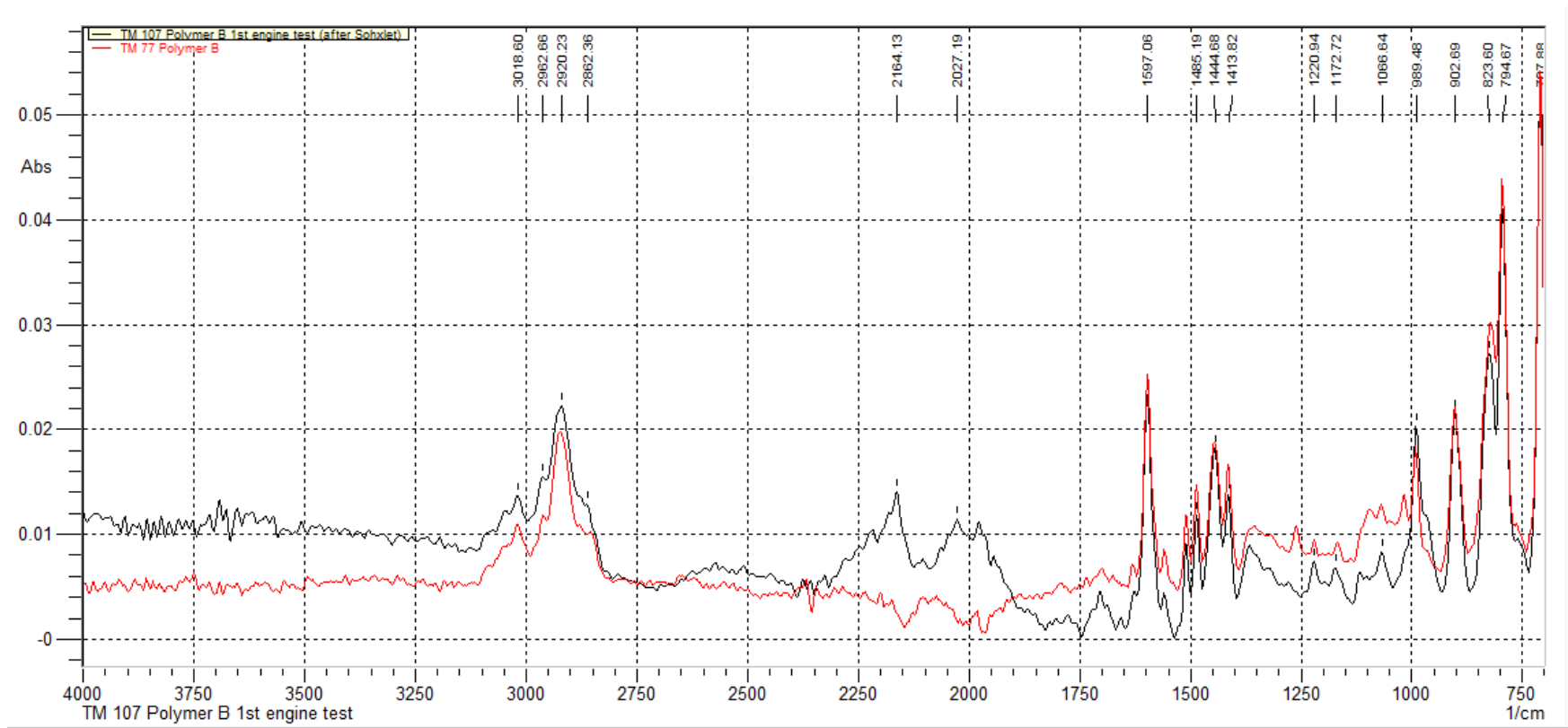


Figure 48 - FT-IR spectra of poly(DVB-80-co-4-VP), synthesised by suspension polymerisation, before (red) and after the first engine test (black)

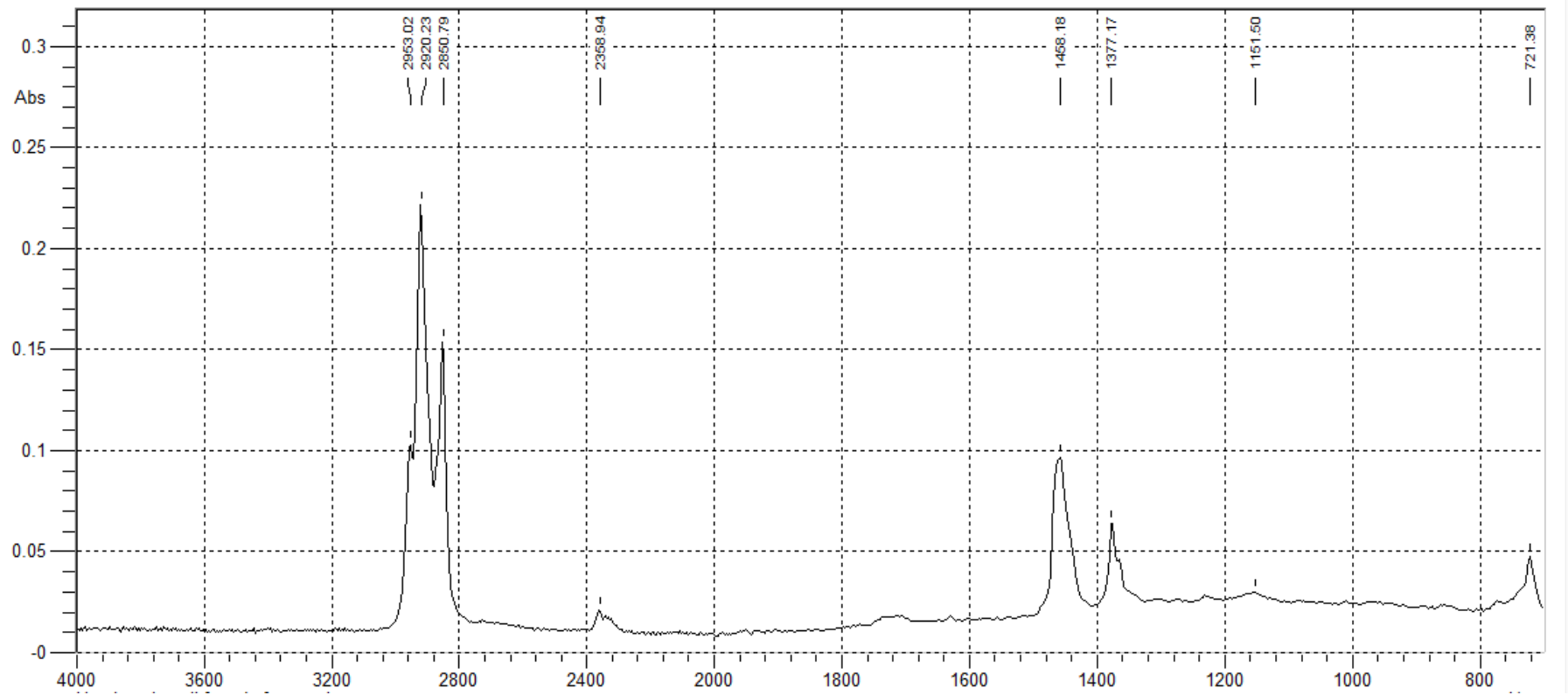


Figure 49 - FT-IR spectrum of the lubricant used in engine-based testing.

The presence of aliphatic hydrocarbons, which constitute the majority of compounds encountered in engine lubricants, dominated the FT-IR spectrum of the lubricant and made the identification of any contaminants (PAHs, soot or otherwise) that were present, in much smaller quantities, impossible. The C-H stretching bands at 2850-2950 cm^{-1} and C-H bending bands at 1377-1458 cm^{-1} were clearly visible.

Analysing the polymer particles after the engine test (**Figure 48**) was rather challenging, especially *via* infra-red spectroscopy. The species that were to be removed by the polymers, PAHs, were aromatic in nature. This aromatic character was very similar to the structure of the polymers, which were almost entirely based on styrene and divinyl benzene as the main constituent in each material. Therefore, looking for changes in the aromatic region of the IR spectra provided no positive indications of successful PAH removal. However, in the spectral region of approximately 2150 to 1900 cm^{-1} there were some notable differences between the polymer before and after the engine-based sorption test. The main family of compounds that absorb in this region are acetylenes.¹⁹⁶ While PAHs are seen to be the beginnings of soot particle nuclei (when PAHs are being formed most often during the pyrolysis of the engines fuel), acetylenes, polyacetylenes and unsaturated hydrocarbons are also known to be formed during soot formation.^{117,119} The surface growth of soot particles is known to proceed through the acceptance of gas-phase molecules, mainly acetylenes, onto the growing surfaces of the soot particles¹¹⁹ Modelling using the premise of soot growth *via* capture of acetylene species on growing soot particles have given good correlation to *in situ* observations of soot formation.¹⁹⁷

With the presence of acetylene and polyacetylenes being observed in different stages of the soot growth process, it was believed that the FT-IR data presented in **Figure 48** was positive and indicated the possible removal of acetylene-based material from the lubricant.

Nitrogen sorption analysis of the polymer particles allowed for specific surface area, average pore size and information regarding the pore size distribution present in the material to be gained. It was believed that if the polymers had proved successful in the removal of contaminants from the lubricant during the engine test, this may have affected and changed the specific surface area and the pore structure of the material. By carrying out nitrogen sorption analysis of the materials after the engine tests it was

believed that some indication of the removal of contaminants from the lubricant may be possible. This sorption analysis data was then compared to sorption data for the same material before the engine test to observe possible changes. Shown in **Figure 50** are the isotherms of poly(DVB-80-co-4VP) before and after the engine-based sorption test.

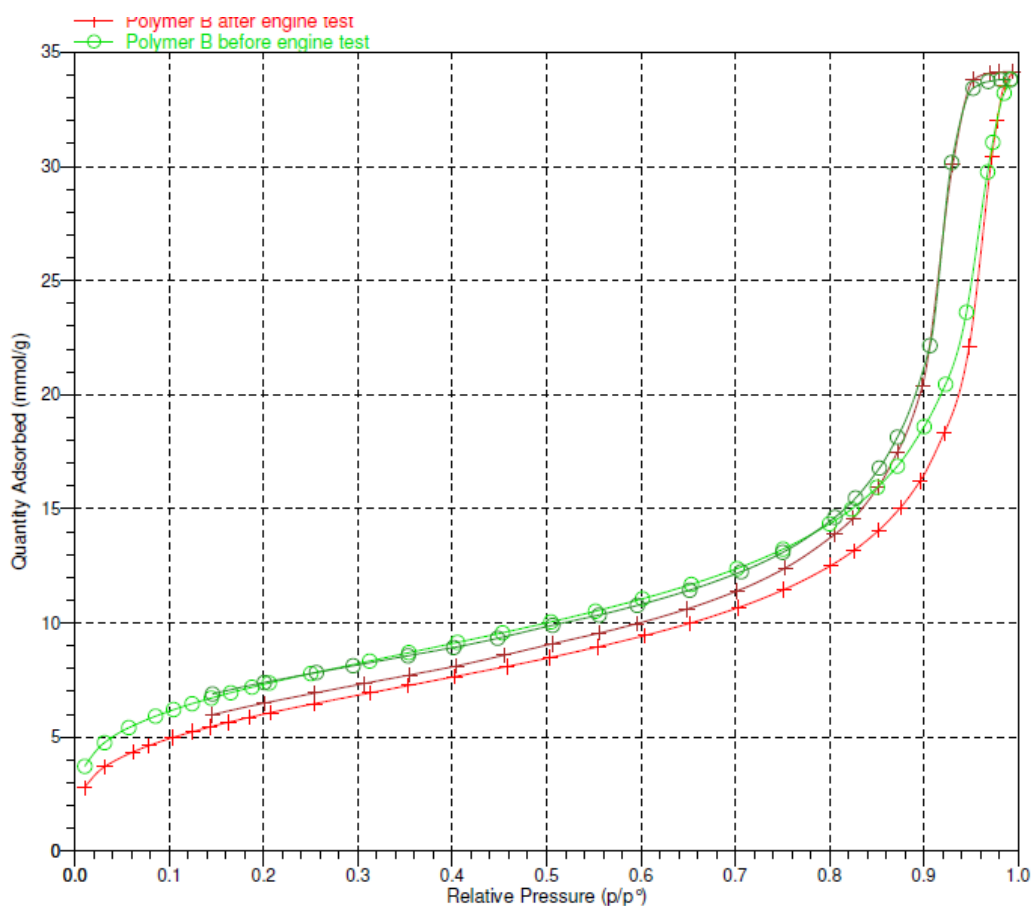


Figure 50 - Nitrogen sorption isotherms of poly(DVB-80-co-4-VP) before (green) and after (red) the engine-based sorption test

The overall shape of the isotherms, before and after the engine testing, were noted to be the same with a large increase in adsorption in the region between approximately 0.8 and 1.0 relative pressure being attributed to pore condensation of gas in larger mesopores. The hysteresis loop, created by the adsorption and desorption of analysis gas being admitted and removed from the sample at different pressures, was noted to have changed in the polymer *post* engine test. In poly(DVB-80-co-4-VP) before the engine test, this hysteresis loop was noted to close in the region of 0.8 relative pressure. However, in

the material that was tested after the engine test, this hysteresis loop was noted to remain open until the end of the analysis. It has been suggested that hysteresis which extends to such low pressures may be associated with uptake of molecules within the very smallest pores, present in a material.¹⁷⁶ Thommes *et al.* have also suggested that blocking of the pore network, whereupon access to the pore network is restricted by the entrance to the pores being narrowed (*e.g.*, 'ink bottle pores') can lead to analysis gas desorption extending to much lower pressures.¹⁹⁸ In these cases, the adsorptive gas will not empty from the main body of the pore until the gas from the narrow neck has emptied, which occurs at much lower pressures.

With regards to the poly(DVB-80-co-4-VP), it was thought that contaminants in the lubricant may have been removed by the polymer and located in the smallest pores of the material, as well as potentially blocking some of the entrances to the pore network. This was seen as a reasonable explanation of the difficulties in desorption observed in the isotherm data, showing the hysteresis loop extending to much lower relative pressures than had been observed in the materials before the engine test. The observation of potential pore blocking, contamination of the polymer surface after engine testing (**Figure 47**) and the presence of new bands in the FT-IR spectrum after the engine test, suggested the successful removal of contaminants from the lubricant.

3.9.3 Engine-based sorption study using poly(styrene-co-VBC-co-EGDMA) as sorption media

The gel-type non-porous poly(styrene-co-VBC-co-EGDMA) was also investigated in the engine-based sorption study, in the exact same manner as poly(DVB-80-co-4-VP). 10 g of the polymer was contacted with the hot lubricant, circulated around the research engine, for 10 hours. The polymer particles were then washed with heptane in a Soxhlet extraction apparatus for 24 hours prior to analysis.

To investigate the surface morphology of the polymer particles, SEM was used. Shown in **Figure 51** is an SEM Image of the particles before (left) and after (right) the engine-based sorption test.

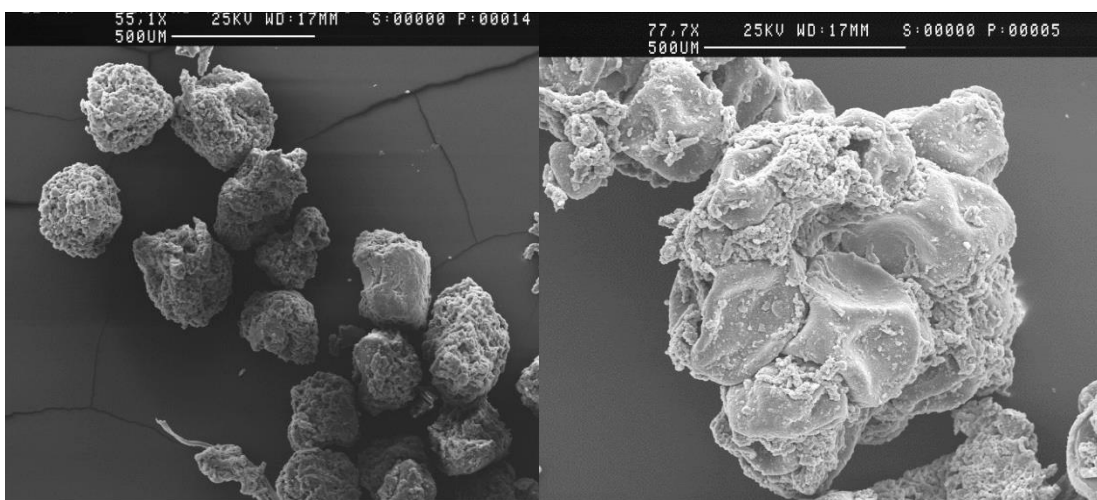


Figure 51 - SEM images of poly(styrene-co-VBC-co-EGDMA) before (left) and after (right) the engine-based sorption study

After the engine test, the polymer particles were noted to look quite different to how they had appeared before the engine test. Poly(styrene-co-VBC-co-EGDMA) exhibited the same agglomeration of primary polymer particles that had been observed in the engine test when using poly(DVB-80-co-4-VP) as the solid-phase. This agglomeration was ascribed to contamination from the lubricant aggregating on the polymer surfaces and causing polymer particles to stick together. The polymer particles shown in **Figure 51** were noted to appear deflated and collapsed. This was attributed to the low level of

crosslinker present in this material, which caused the pore network , in the dry state, to be totally collapsed.

FT-IR analysis was also undertaken to investigate the chemical composition of the polymer particles after the engine test. Shown in **Figure 52** are the FT-IR spectra of poly(styrene-*co*-VBC-*co*-EGDMA) before (red) and after (black) the engine test.

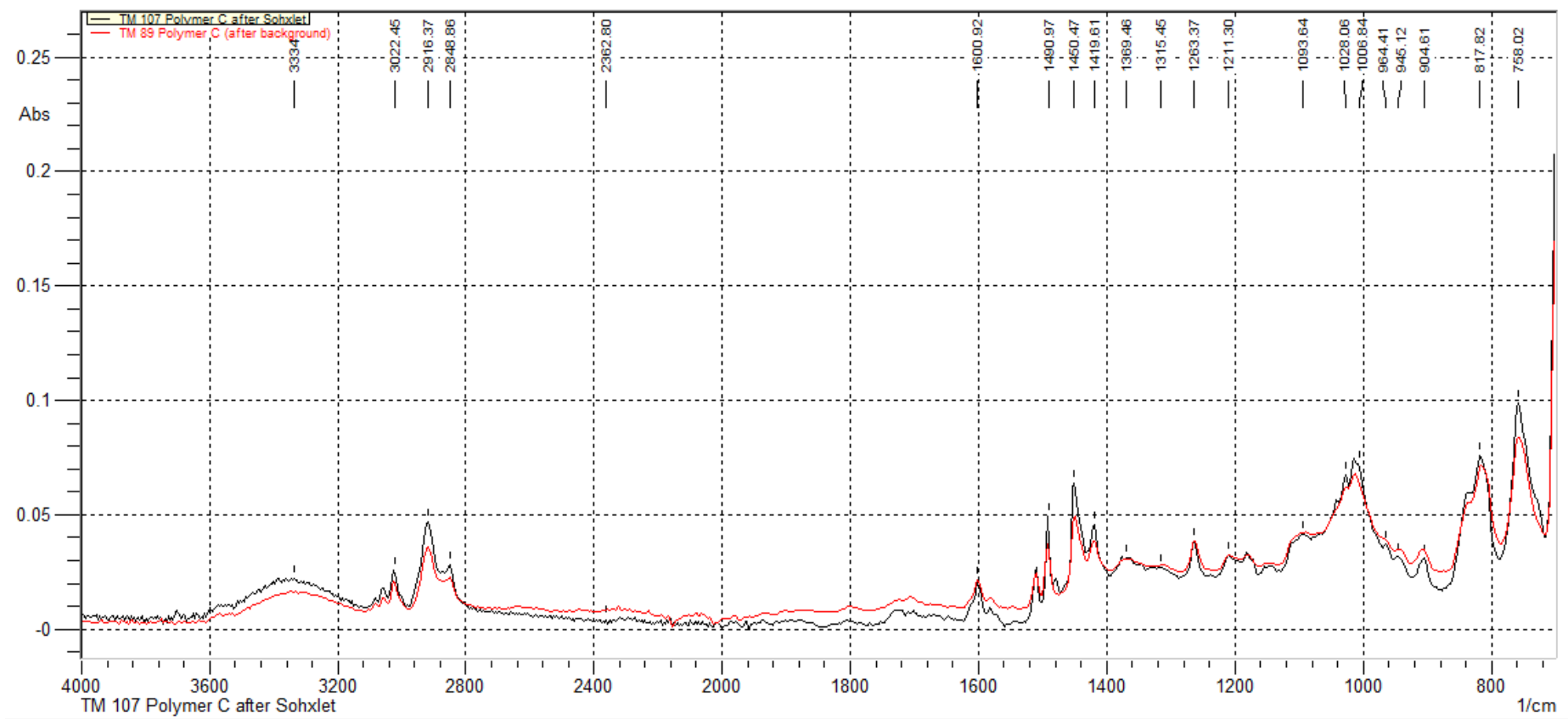


Figure 52 - FT-IR spectra of poly(styrene-co-VBC-co-EGDMA) before (red) and after (black) the engine test

There were no changes apparent in the IR spectrum of the polymer after the engine test, when compared to the material before the engine test. While soot and PAHs may have adhered to polymer surfaces and explain the agglomeration of primary polymer particles that was observed *via* SEM, PAH and soot removal would not have been apparent in any FT-IR analysis due to the similarities between them and the mainly aromatic constituents of the polymer.

Due to the very low specific surface area of this polymer, nitrogen sorption analysis was not carried out. Nitrogen sorption, especially in low specific surface area materials can be unreliable and give inconsistent results. The inconsistent results arise from the way in which isotherms, and therefore specific surface areas, are measured. Each point on an adsorption isotherm is measured by calculating the difference between the amount of gas admitted to the sample and the amount that remains in the vapour phase (dead space) after the sample has been allowed to equilibrate. Therefore, in materials with very low specific surface areas, this difference between the amount of gas admitted to the sample and the amount that has not been adsorbed by the material will be very small leading to greater errors in the measurement of each point on the isotherm.

3.9.4 Engine-based sorption study using HXL poly(styrene-co-VBC-co-EGDMA) as sorption media

It was envisaged that with a higher specific surface area, HXL poly(styrene-co-VBC-co-EGDMA) would be better able to remove contaminants from the lubricant during the engine-based sorption tests. The polymer, after the engine test, was washed in heptane (using a Soxhlet extraction apparatus) for 24 hours and then imaged using SEM. Shown in **Figure 53** are images of the HXL poly(styrene-co-VBC-co-EGDMA) before (left) and after (right) the engine test.

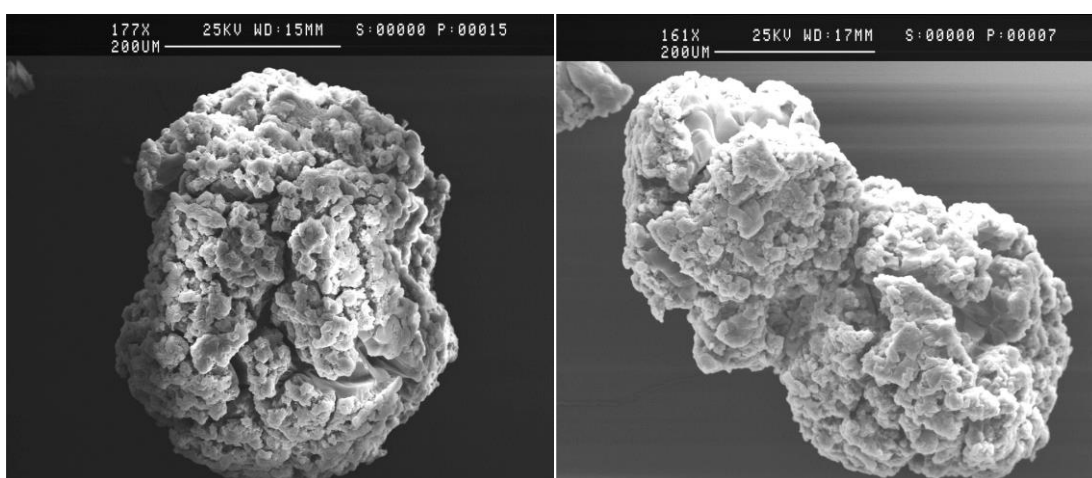


Figure 53 - SEM micrographs of HXL poly(styrene-co-VBC-co-EGDMA) before (left) and after (right) the engine-based sorption study

The HXL poly(styrene-co-VBC-co-EGDMA) showed some signs of agglomeration, although it did not appear to be to the same extent as some of the previous samples (*c.f.* **Figure 47** and **Figure 51**). The fracturing of the surfaces of the polymer particles, which had been caused by the hypercrosslinking process, while still present in the polymer after the engine test, is less apparent. It may be the case that some of these fractures were in-filled in with sorbed contaminants from the lubricant.

To investigate the possible sorption of contaminants from the lubricant, FT-IR analysis was undertaken. FT-IR spectra of the polymer before and after the engine test were compared in an attempt to observe any changes in the materials. Shown in **Figure 54** is

an FT-IR spectrum of HXL poly(styrene-co-VBC-co-EGDMA) before the engine test. Overlaid upon this spectrum is an FT-IR spectrum of the material afterwards.

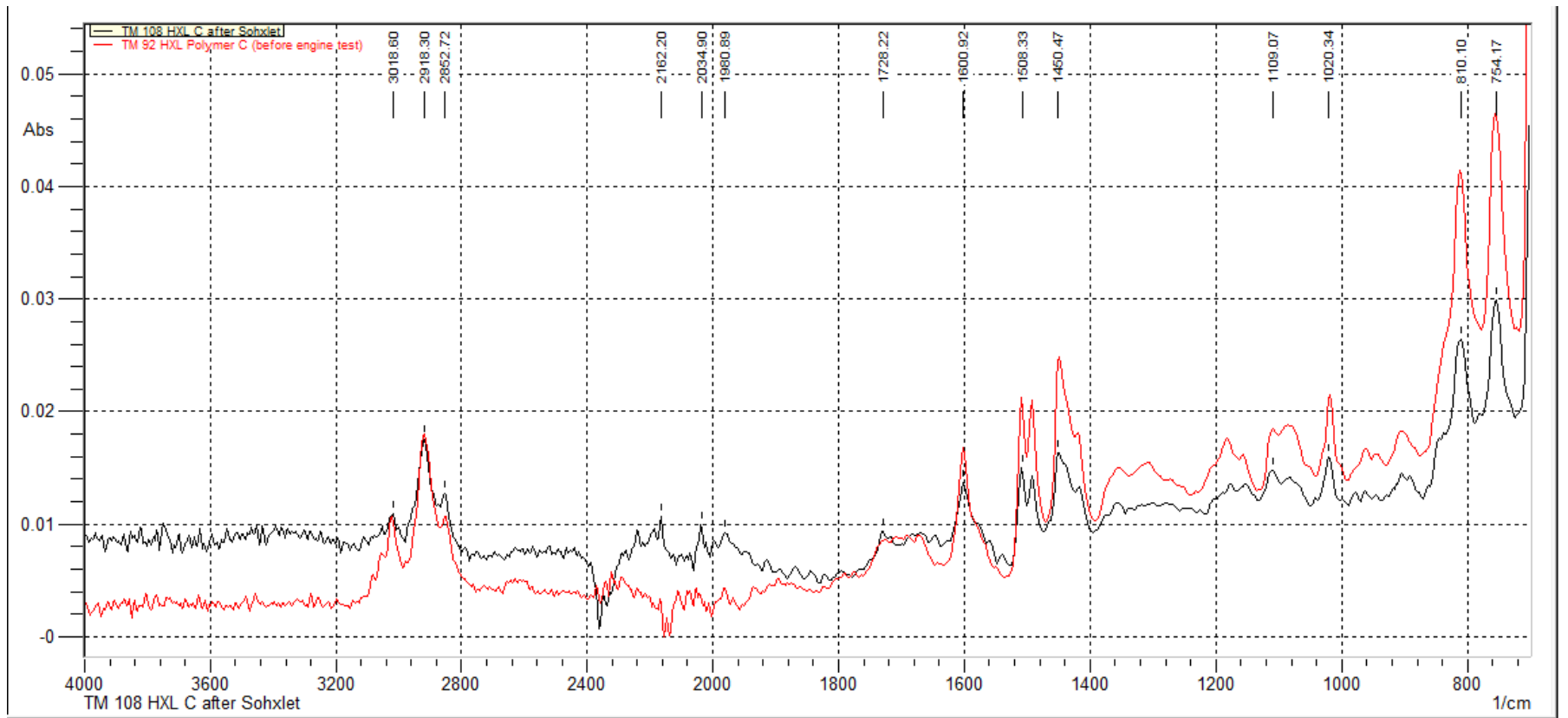


Figure 54 - FT-IR spectra of HXL poly(styrene-co-VBC-co-EGDMA) before (red) and after (black) the engine-based sorption test

After the engine test, much of the FT-IR spectrum remained unchanged. However, two bands, present at 2034 and 2162 cm^{-1} , had appeared in the spectrum of the polymer after the engine test. Both of these bands may be attributed to the presence of acetylene-based material being removed by the polymer during the engine test, which has previously been discussed. These bands were almost identical to the bands that were present in poly(DVB-80-co-4-VP) after the engine test using this polymer, and suggested that both materials were successful in the removal of polyacetylenes or acetylene-based materials from the lubricants.

To further study the surface area and porosity of the material after the engine testing, nitrogen sorption analysis was undertaken, and the results compared to data obtained before the engine test. Shown in **Figure 55** is the isotherm produced by HXL poly(styrene-co-VBC-co-EGDMA) before and after the engine-based sorption study.

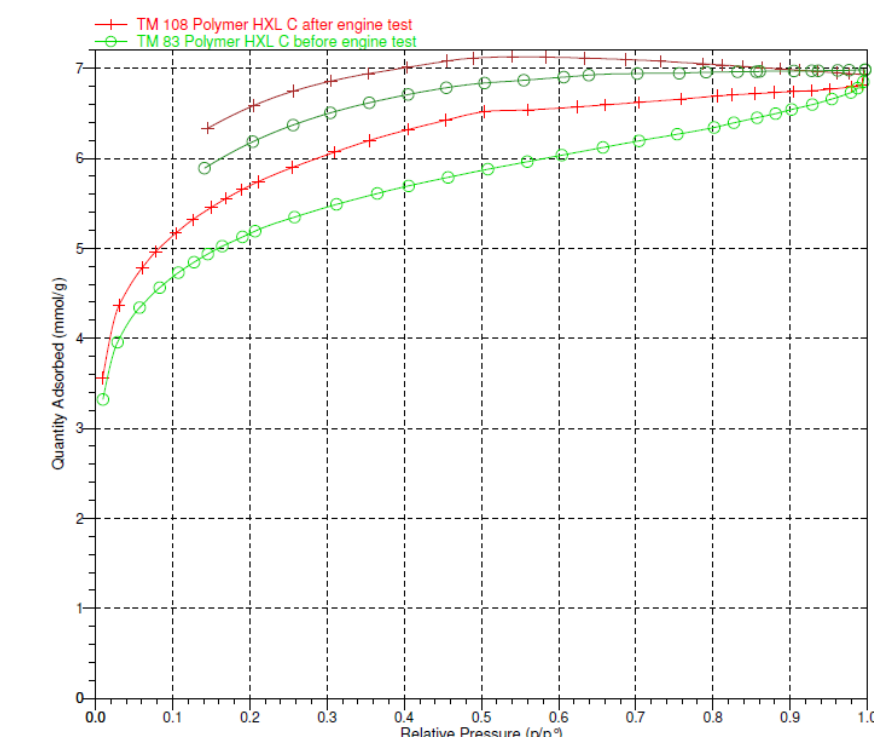


Figure 55 - Nitrogen sorption analysis isotherms produced by HXL poly(styrene-co-VBC-co-EGDMA) before (green) and after (red) the engine test.

The overall shape of the isotherms remained constant before and after the engine test. Large, open hysteresis loops present in both isotherms give an indication of a larger number of very small pores. There was one slight difference however: the adsorption branch of the polymer after the engine test (shown in red) was noted to plateau and remain almost constant up to saturation pressure. This plateauing of the isotherm indicated a reduction in adsorption in this region which would mean that there was less surface for the nitrogen molecules to adsorb on to. This reduction in adsorption was corroborated by the mesopore size distribution data, **Figure 56**.

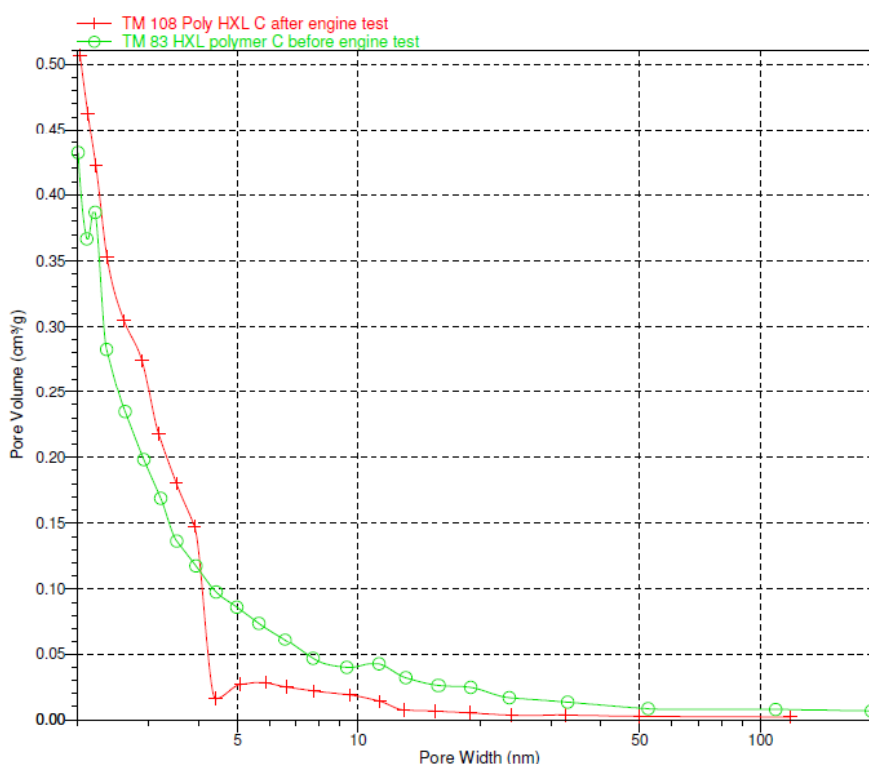


Figure 56 - Mesopore size distribution graph for HXL poly(styrene-co-VBC-co-EGDMA) before (green) and after (red) the engine test

After the engine test there appeared to be a large drop in the pore volume from pores of 4 to 50 nm, indicating that these pores were no longer accessible to the probe gas. The lack of access to the pores in this region may have been due to the blocking of these pores. Unfortunately, the other main indicator of pore blocking is open hysteresis, which was already present in this polymer before the engine test due to the presence of very

small pores. Therefore, the hysteresis phenomenon could not be used to indicate the removal of contaminants from the lubricant. In spite of this difficulty, the FT-IR data showing the removal of acetylene-based materials and the loss of pore volume in certain mesopores did positively indicate the successful removal of contaminants from the lubricant during the engine test.

3.9.5 Engine-based sorption study using poly(VBC-co-4-VP-co-EGDMA) as sorption media

With successes being evident in the removal of contaminants from the used engine lubricants, poly(VBC-co-4-VP-co-EGDMA) was exposed to the same engine test regime, where hot, used engine lubricant was contacted with the polymer for 24 hours within the engine. The polymer samples returned for analysis were washed with heptane for 24 hours before all analysis was undertaken. Firstly, SEM analysis was performed to inspect the polymer particles' surfaces after the engine test in order to observe any possible changes. Shown in **Figure 57** is an SEM image of poly(VBC-co-4-VP-co-EGDMA) after the engine test (right). Shown on the left is an SEM image of the same material before the engine test.

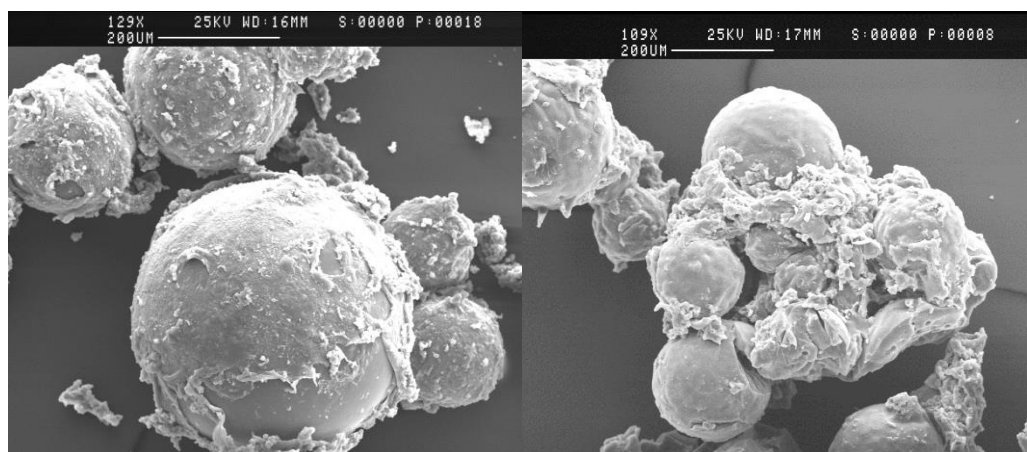


Figure 57 - SEM images of poly(VBC-co-4-VP-co-EGDMA) before (left) and after (right) the engine-based sorption test

As with most of the previous materials, poly(VBC-co-4-VP-co-EGDMA) showed the same agglomeration of the polymeric material after the engine test. To investigate the surface agglomeration further, FT-IR analysis was undertaken in the hope of observing changes in the chemical composition after the engine test. Shown in **Figure 58** is the FT-IR spectrum of poly(VBC-co-4-VP-co-EGDMA) before (red) and after (black) the engine test.

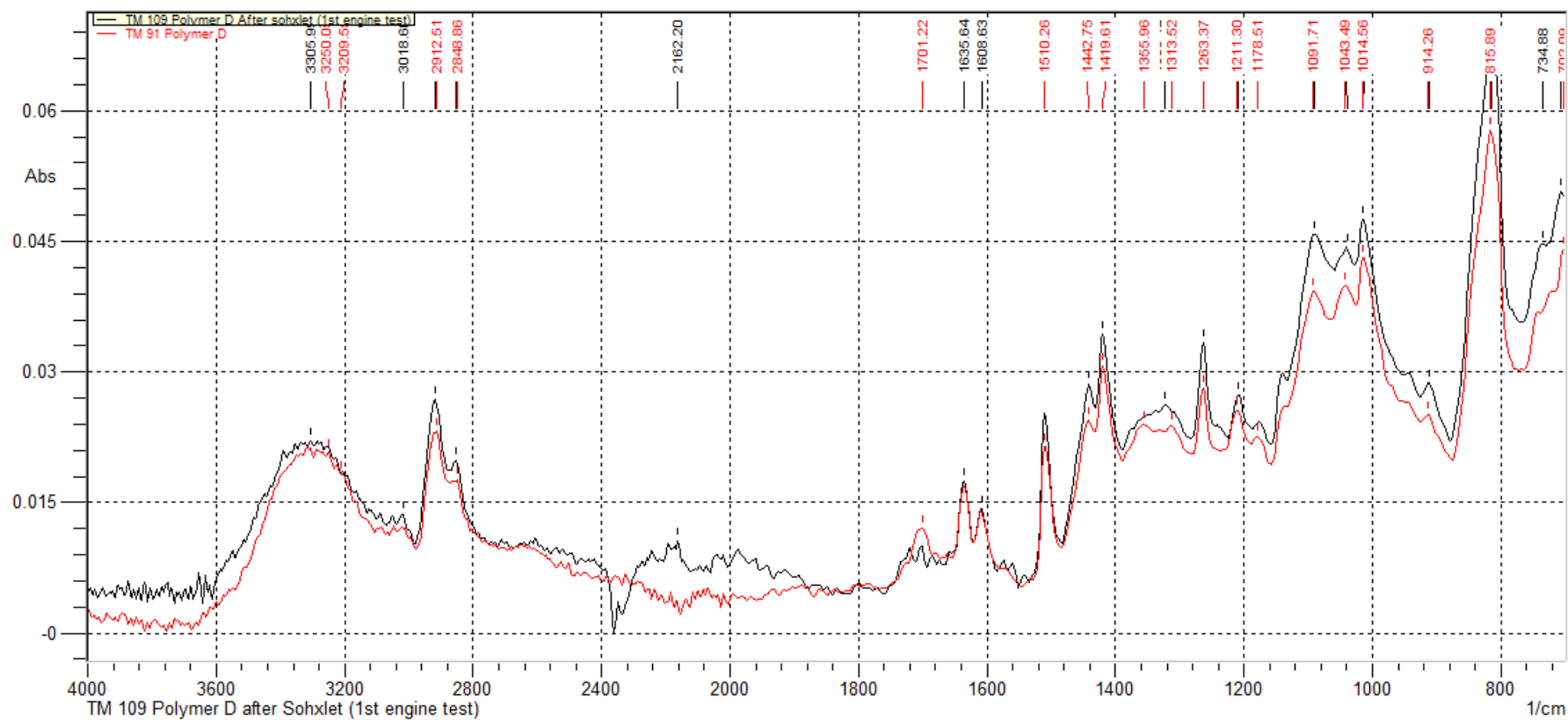


Figure 58 - FT-IR spectra of poly(VBC-co-4-VP-co-EGDMA) before (red) and after (black) the engine-based sorption test

Many of the features present in the polymer before the engine test were still present afterwards. The large -OH stretching band at about 3300 cm^{-1} , due to partial hydrolysis of VBC units within the polymer during synthesis, was still clearly visible. Interestingly, after the engine testing, similar bands that had appeared in previous materials also became apparent in poly(VBC-co-4-VP-co-EGDMA). The main area of interest was in the region of approximately $2000\text{-}2170\text{ cm}^{-1}$. As has been discussed with previous polymers, the presence of bands in this region indicate the possible presence of polyacetylenes in the material after contact with the lubricant.

As poly(VBC-co-4-VP-co-EGDMA) was of very low specific surface area, no nitrogen sorption analysis was carried out on the material after the engine testing. As has been discussed previously, nitrogen sorption on materials of low surface area can provide inconsistent results and it was therefore believed doing so would not provide any useful information.

3.9.6 Engine-based sorption study using HXL poly(VBC-co-4-VP-co-EGDMA) as sorption media

The final polymer to be tested in the non-fired engine test was the hypercrosslinked variant of the previous polymer, namely HXL poly(VBC-co-4-VP-co-EGDMA). This material was of a very high specific surface area, owing to the high proportion of VBC units present in the precursor material, by which the methylene bridges and therefore surface area is installed. To inspect the surfaces of the material after the engine testing regime, SEM was used. **Figure 59** shows SEM images of the material before (left) and after (right) the engine test.

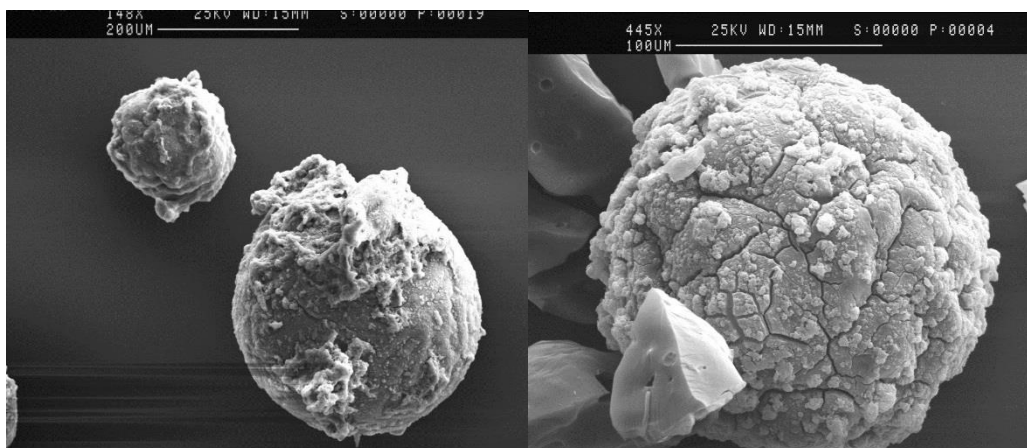


Figure 59 - SEM images of HXL poly(VBC-co-4-VP-co-EGDMA) before (left) and after (right) engine testing

Surprisingly, unlike all the previous materials, HXL poly(VBC-co-4-VP-co-EGDMA) did not display any agglomeration of polymer particles. The surface cracks on the surfaces of the beads were still clearly visible. Further to this SEM analysis, FT-IR analysis was carried out to observe if any chemical changes had occurred after the engine test. **Figure 60** shows the comparison of the FT-IR spectra of HXL poly(VBC-co-4-VP-co-EGDMA) before (red) and after (black) the engine test.

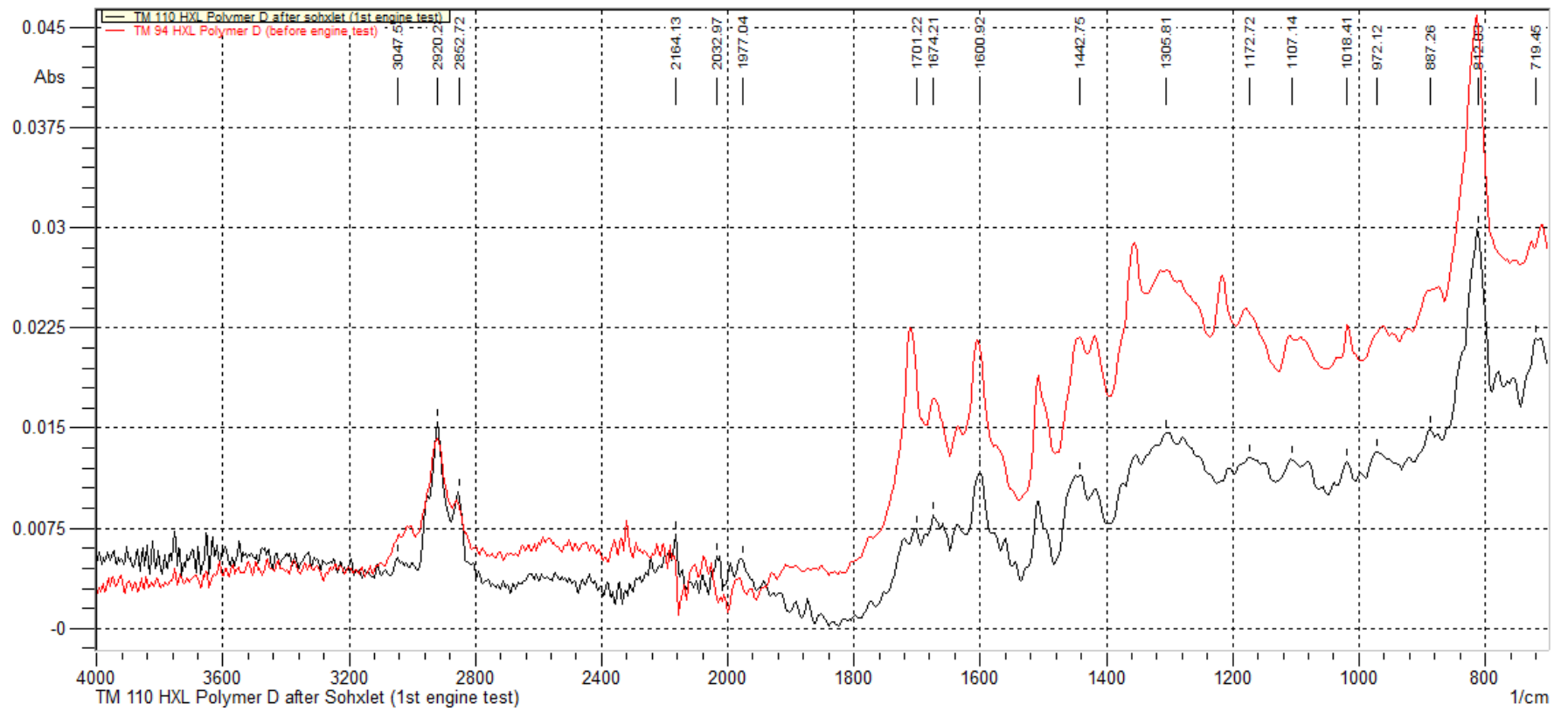


Figure 60 - FT-IR spectra of HXL poly(VBC-co-4-VP-co-EGDMA) before (red) and after (black) the engine-based sorption test

Overall, the spectrum of the material before the engine test was very similar to the material after the engine test. There did appear to be some bands in the region just above 2000 cm^{-1} that had appeared in most of the other materials after contact with the lubricant. However, the FT-IR spectra of this material both before and after appeared to have much more noise in the base line which made confidently discerning bands in this region much more difficult. Two very small bands at 2032 and 2164 cm^{-1} , were tentatively identified in this region after the engine test, both of these were identical to bands that had appeared in the other materials after the respective engine tests.

Further analysis was carried out, in the form of nitrogen sorption analysis, to inspect the porosity and specific surface area of the material after the engine test. Isotherm data is shown in **Figure 61** for the material after the engine test. Also shown is the isotherm of the polymer before the engine test, included for comparison.

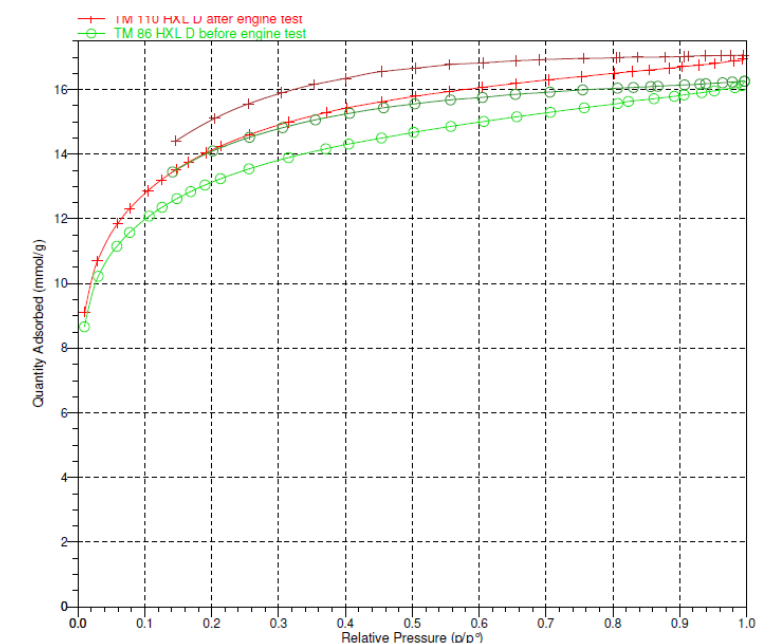


Figure 61 - Nitrogen sorption isotherms of HXL poly(VBC-co-4-VP-co-EGDMA) before (green) and after (red) engine testing

The isotherm shape was very similar with open hysteresis being observed in the material both before and after. The open hysteresis was present due to a large proportion of very small pores in the material. The difference observed in overall adsorption was quite small, and most likely due to experimental error. The pore size distribution was also noted to be unchanged after the engine test.

Due to very little changes being observed in the SEM images and FT-IR spectra, as well as no changes being observed in the nitrogen sorption analysis data, It was concluded that HXL poly(VC-co-4-VP-co-EGDMA) was unsuccessful in removing contaminants from the lubricant.

3.10 Conclusions

At the start of this section it was noted that during the engine test a sample of lubricant was taken every hour for analysis. This analysis took the form of TGA-soot analysis. TGA-soot analysis is an industry-standard technique that allows the soot content of engine lubricants to be determined. Unfortunately, the lubricant used in these engine tests was already heavily sooted, making analysis very troublesome. Also, technologists at Castrol highlighted the fact that this lubricant had been used in America (for field-based engine trials), transported back to the United Kingdom and was kept in storage for some time, before use in the engine-tests disclosed herein. It was believed that leaving the lubricant for long lengths of time may have caused soot to settle out of the lubricant, further compromising any results that were obtained. Two other major issues were raised during the course of these engine studies:

1. The lubricant used in this test was fully formulated, *i.e.*, it contained a full additive package, including dispersants. Therefore, any soot which had formed in the lubricant before it was used in the above sorption tests would have been dispersed by the additive package, making removal by the solid-phase polymer particles very difficult.
2. The lubricant in this test was at the end of its useful life. While this provided high levels of soot and PAHs to hopefully remove during the test, the polymers were never designed to work in this way. The polymers were designed to be contacted with fresh lubricant and remove contaminants, PAHs and soot, as they were formed over time.

These test which utilised a used, dirty lubricant were useful and provided evidence that it was possible to remove contaminants from a lubricant. However, as described above, the engine-based test did not really reflect the true, end-use of the polymeric materials.

To fully investigate the thesis of this work and to address some of the issues highlighted above, a new engine-based experiment was investigated. In this engine-based test, the engine would be fired. Also, a bespoke, dispersant-free lubricant was to be used. It was

envisaged that, by using a fired engine, PAHs and soot could be generated quickly *in situ* and the lack of dispersant in the lubricant would allow for a clearer investigation of the polymers' potential as PAH and soot removal devices, without the possibility of dispersants hindering this process.

3.11 Fired engine tests

The fired engine tests used the same diesel 'Hydra' research engine, that was used in the non-fired engine tests. The engine was flushed with lubricant for 30 minutes prior to each test to ensure it was clean. The candidate lubricant (containing no dispersant) was then loaded into the engine. Next, the polymer beads used in the test were then loaded into a fuel filter, in the exact same manner as was described for the non-fired engine test. The engine was then started, and the lubricant was contacted with polymer for the duration of the test. A sample of lubricant was taken every hour to investigate the soot level present in the lubricant over time. After each test the polymer samples were returned to Strathclyde for testing.

3.11.2 Fired, engine-based sorption study using poly(DVB-80-co-4-VP) as sorption media

The first polymer to be tested in the fired engine test was poly(DVB-80-co-4-VP). This permanently porous, macroreticular material had shown positive signs of removing contaminants from the used lubricant in the non-fired engine test. The polymer beads were placed in the filter element and contacted with the lubricant for 8 hours. The engine was running for the duration of this test, with soot being built up within the lubricant over this time, as would be experienced in a real engine. After the engine test, the polymers were returned to Strathclyde and, as with all the polymers in the previous tests, washed with heptane for 24 hours *via* Soxhlet extraction to remove excess lubricant and assist with analysis. Shown in **Figure 62** are images of the filter element after the engine test and an image of some of the polymer particles *post* testing.



Figure 62 - Photograph of filter element after fired engine test (left) and image of poly(DVB-80-co-4-VP) after fired engine test (right)

Due to soot building up during the engine test, the lubricant had become somewhat black in colour. As expected, however, the lubricant was not as black (and therefore contained less soot) than the lubricant that had been used in the non-fired engine test (*c.f.* **Figure 46**)

Interestingly, agglomeration and discolouration (going from white before the test to grey afterwards) had occurred to the polymer particles during the engine test. This was believed to be due to lubricant adhering to the surface of the polymer particles.

To investigate further the effects of the engine test on the polymer particles, SEM analysis was used. SEM had been used successfully in previous tests to show the agglomeration of polymer particles. Shown in **Figure 63** is an SEM image of poly(DVB-80-co-4-VP) after the fired engine test, and reproduced for reference is the SEM image of the same material after the non-fired engine test (left).

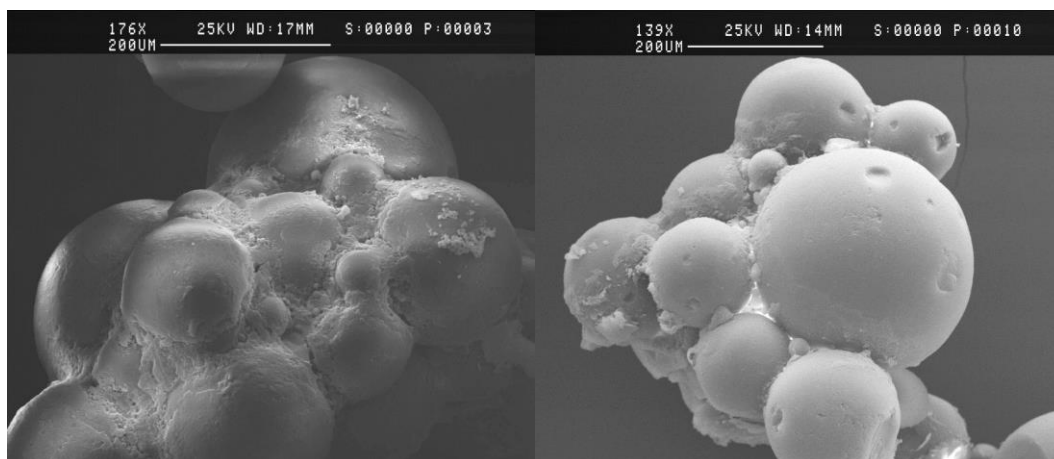


Figure 63 - SEM images of poly(DVB-80-co-4-VP) after the non-fired engine test (left) and after the fired engine test (right)

Pleasingly, the SEM image of the polymer after the fired engine test showed the same signs of agglomeration that had been evident after the non-fired engine test. It can be seen from the images that due to less soot being present in the fired engine test, the material in between the polymer particles, which is causing the agglomeration, is less. Whereas, in the non-fired engine test there was a much higher amount of soot in the lubricant, therefore there appears to be more material agglomerating the polymer particles together.

As with the non-fired engine tests, FT-IR spectroscopy was employed to examine the agglomeration further and investigate any chemical changes in the polymer particles. **Figure 64** shows the FT-IR spectra of poly(DVB-80-co-4-VP) before the engine test (red) and after the fired-engine test (black).

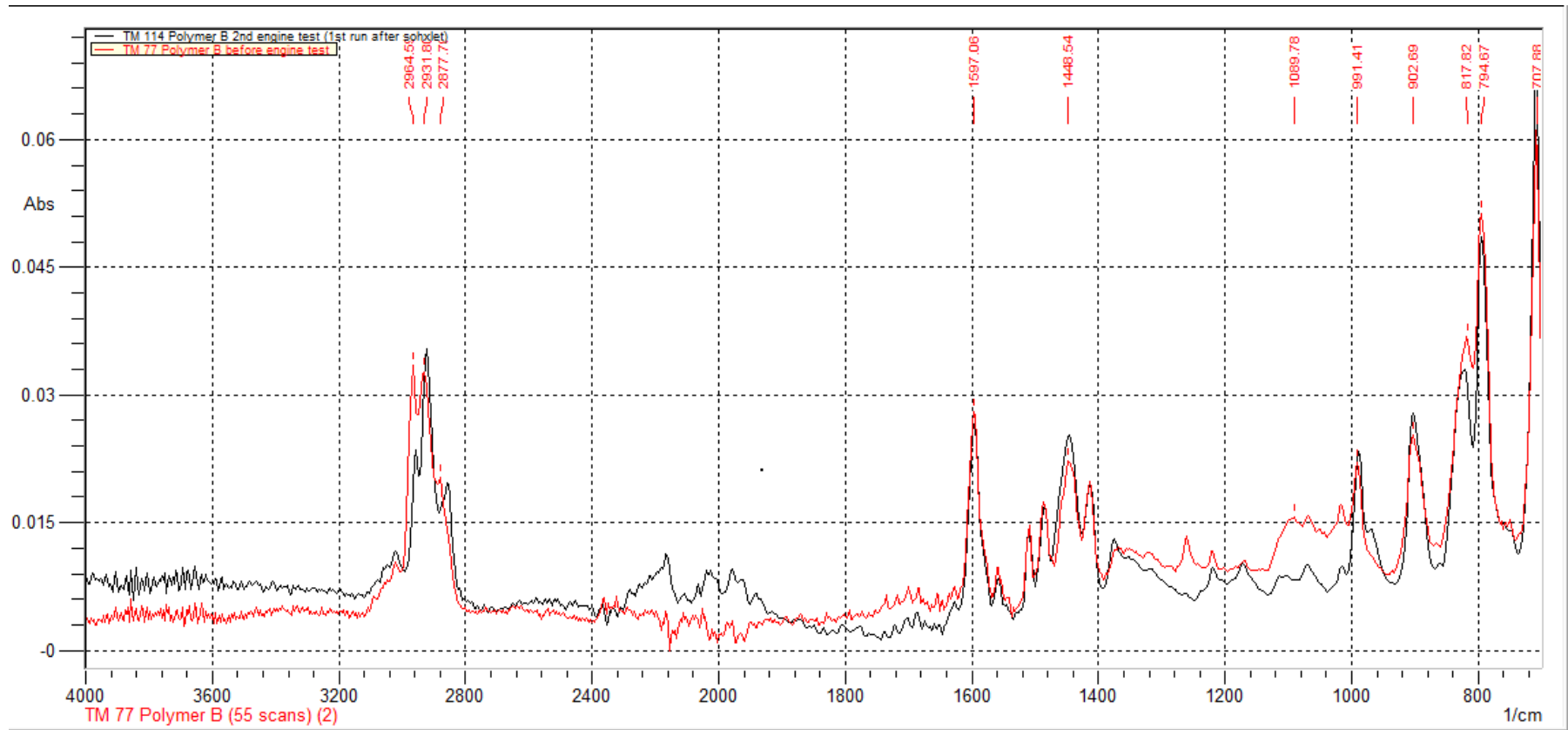


Figure 64 - FT-IR spectra of poly(DV-80-co-4-VP) before (red) and after (black) the fired engine test

Whilst both spectrum remained largely unchanged after the engine test, evidence of small bands appearing in the region of 2200 – 2000 cm^{-1} were observed. As had been observed in the earlier non-fired engine test, these peaks were attributed to the presence of polyactylenes or possibly growing soot species bearing acetylene functionality, both of which are present in the soot inception and growth processes. As has been discussed previously, due to the aromatic character of the polymer, deducing the presence of PAHs from the FT-IR spectrum alone was not possible.

To further investigate the possibility of contaminant removal, nitrogen sorption analysis was undertaken in the hopes of observing changes to the pore network and specific surface area after the fired engine test. Displayed in **Figure 65** is the nitrogen sorption isotherm produced by poly(DVB-80-co-4-VP) before (green) and after the fired engine test (shown in red). The area within the blue rectangle has been enlarged to show detailed differences between the two isotherms.

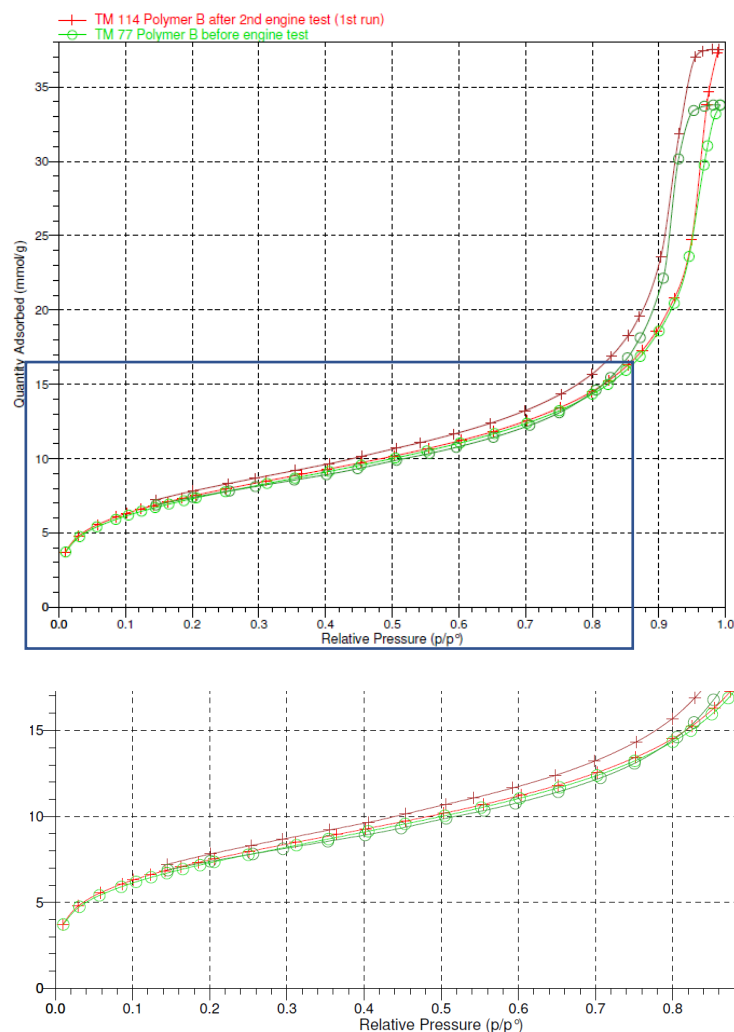


Figure 65 - Nitrogen sorption isotherms of poly(DVB-80-co-4-VP) before (green) and after (red) the fired engine test. Area between 0 and 0.8 relative pressures has been enlarged for clarity.

It was evident that the hysteresis, present in both isotherms, closed much sooner (at an approximate partial pressure of 0.8) before the engine test. Afterwards, this hysteresis, shown in red in the enlarged section, extended and was still open at a relative pressure of 0.2. Low pressure hysteresis suggested the presence of blockages in much smaller pores present in the material. Other data collected during the nitrogen sorption analysis experiment indicated very little change to the polymer after the fired engine test. The average pore diameter of the material was 7.8 nm before the test and 8.2 nm afterwards. Also, the pore size distribution data indicated the same features of the mesopores that

had been present in the material before, with a large number of pores in the region of 50 nm in diameter being present

With some promising results in the fired engine test (agglomeration of polymer particles, new species appearing in FT-IR data and some indication from the nitrogen sorption analysis that pore blockages had appeared) it was agreed that further investigation was warranted. To this end, the fired engine test was repeated with poly(DVB-80-co-4-VP). However, this time the engine test was run for 16 hours rather than the 8-hour long test that had been carried out previously. It was believed that by leaving the engine running for longer, more PAHs and soot could be produced and hopefully more would be removed by the polymeric sorbent, thereby facilitating their analysis.

After the 16 hour long fired engine test, the polymer particles were washed overnight with heptane and inspected (**Figure 66**).

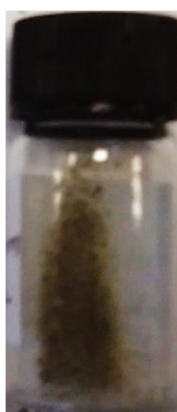


Figure 66 - Photograph of poly(DVB-80-co-4-VP) particles after 16 hour fired engine test

The particles isolated, after the 16 hour test were observed to be darker in colour than the particles after the 8 hour test (**Figure 62**). This may have indicated a larger amount of soot present on the particles, as it is the soot content within the lubricant that gives it the blackened colour.

SEM was used to examine the surfaces of the particles more closely. Shown in **Figure 67** are SEM micrographs of poly(DVB-80-co-4-VP) after the 16 hour test (right). A micrograph

of the same material after the 8-hour test is also shown on the left, to allow comparison between the two.

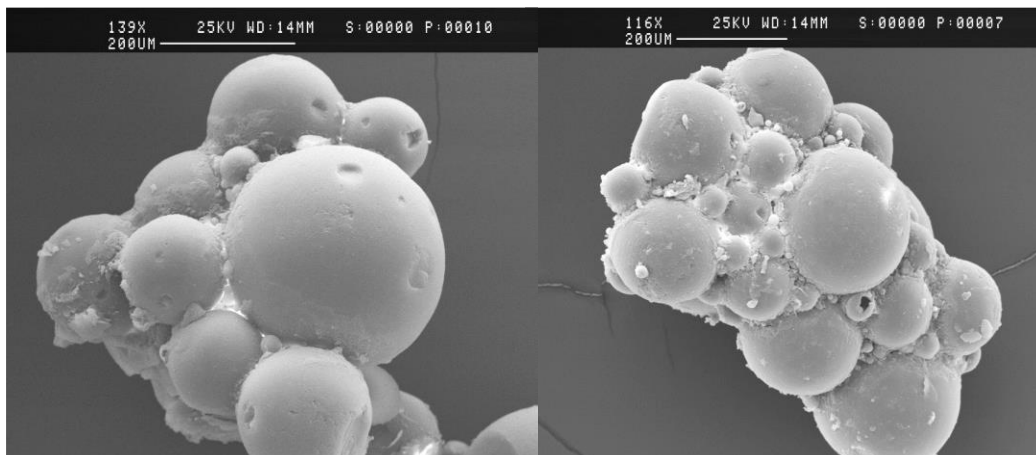


Figure 67 - SEM micrographs of poly(DVB-80-co-4-VP) after the 8 hour fired engine test (left) and after the 16 hour test (right)

It was apparent that after the longer engine test there was more agglomerating material holding the polymer particles together. If the material that was causing agglomeration was indeed soot, one would expect to observe more soot if the engine test was run for longer. Unfortunately, SEM was not able to prove the composition of this material.

FT-IR spectroscopy was again utilised to investigate any possible chemical changes in the material. Shown in **Figure 68** are the FT-IR spectra of poly(DVB-80-co-4-VP) after the 16 hour engine test (black) as well as the material before the engine test (red).

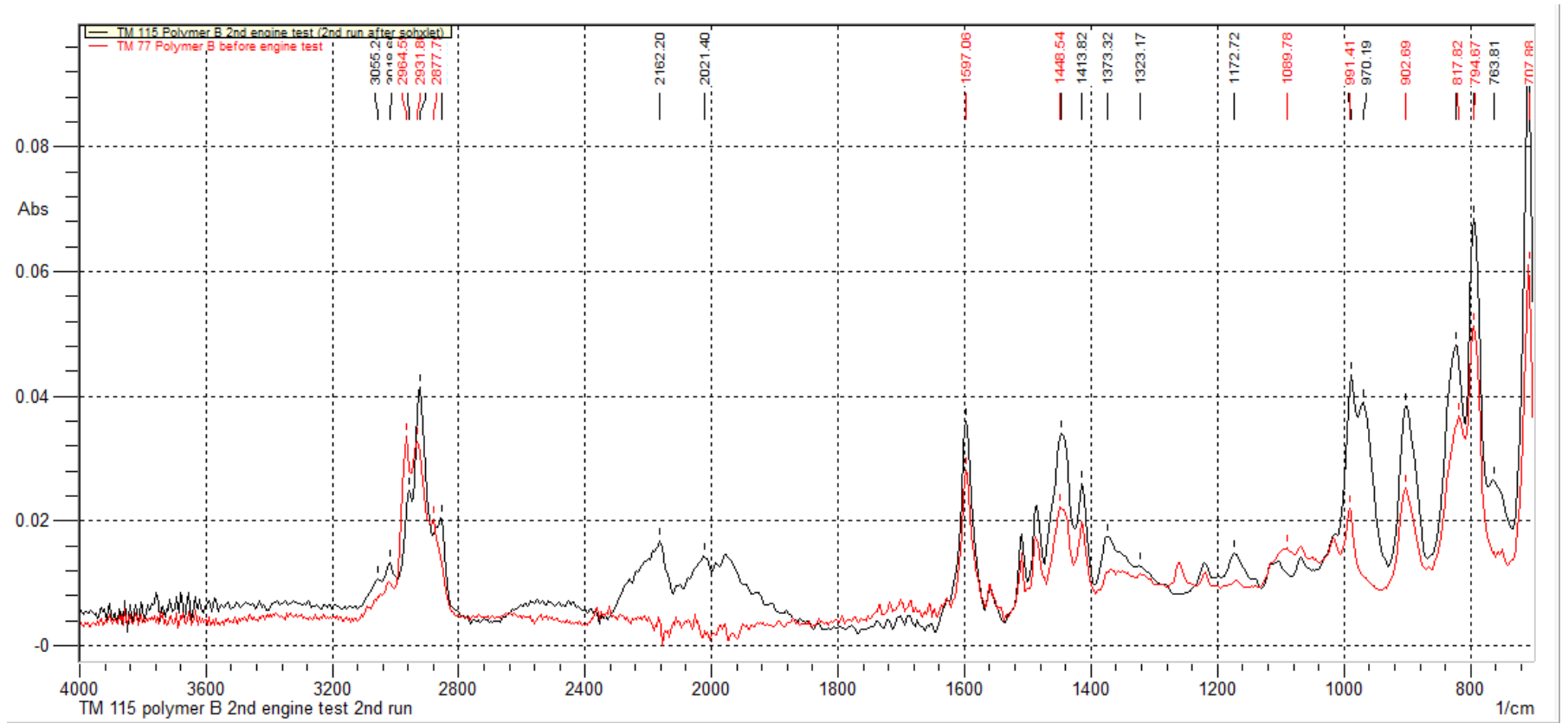


Figure 68 - FT-IR spectra of poly(DVB-80-co-4-VP) before (red) and after (black) the 16 hour fired engine test

The spectral from region of 2200-2000 cm^{-1} again showed the presence of acetylene-based material being present after the engine test, potentially indicating its removal during the engine test. While PAHs had proved notoriously difficult to detect *via* IR, due to the aromatic character of the polymeric sorbents being used, it was interesting to note that after the 16 hour engine test a shoulder at 3055 cm^{-1} had appeared. This could indicate the presence of more aromatic material which could be attributed to the removal of PAHs.

As with all of the other materials, nitrogen sorption analysis was used to investigate differences in pore structure and surface area before and after the engine test. Shown in **Figure 69** are the nitrogen sorption isotherms of poly(DVB-80-co-4-VP) before and after the engine test.

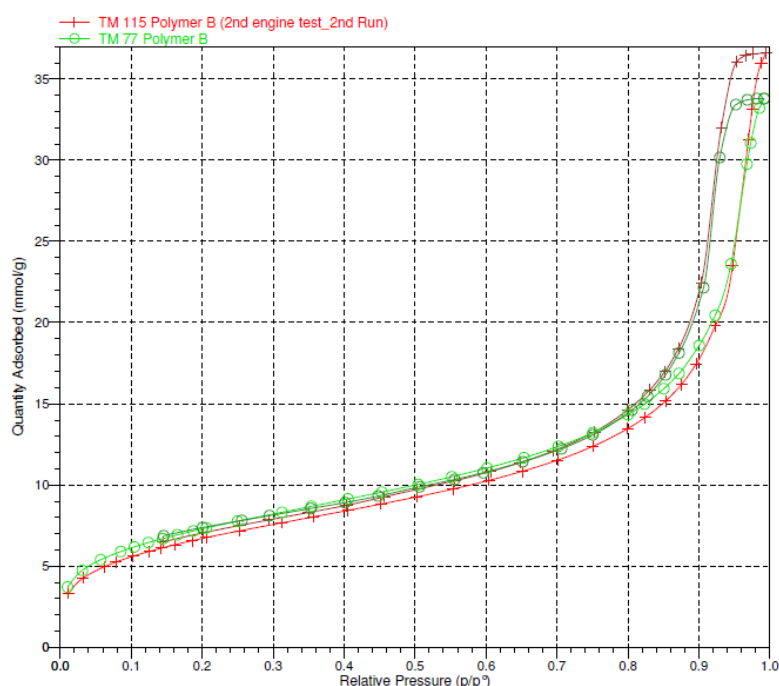


Figure 69 - Nitrogen sorption isotherms of poly(DVB-80-co-4-VP) before (red) and after (green) the 16-hour fired engine test

After the 16-hour engine test, the material presented a very similar isotherm to that which had been produced after the 8- hour engine test (**Figure 65**). As had been observed before, the hysteresis remained open and extended to a much lower partial pressure after the engine test, indicative of pore blocking.

3.11.2 Fired, engine-based sorption study using poly(styrene-co-VBC-co-EGDMA) as sorption media

In furtherance of this work, a material that had proven less successful in the first engine test was also tested in the fired engine test. Poly(styrene-co-VBC-co-EGDMA) had shown less of promise of contaminant removal as judged from FT-IR data after the first engine test. Also, due to its very low specific surface area, testing this material would allow for the comparison between a low specific surface area material and the high specific surface area encountered in poly(DVB-80-co-4-VP). The poly(styrene-co-VBC-co-EGDMA) was run for 8 hours in the fired engine. After testing, the polymer particles were returned to Strathclyde and put through the usual testing regime. Shown in **Figure 70** is a photograph of the darkened polymer particles after washing in heptane *post* engine test.



Figure 70 - Photograph of poly(styrene-co-VBC-co-EGDMA) after the 8-hour fired engine test

After the engine test, the polymer particles were noted to be blackened, even after washing, potentially indicating the presence of soot on the beads. SEM analysis was used to scrutinise the surfaces of the polymer in more detail. Shown in **Figure 71** are SEM micrographs of the poly(styrene-co-VBC-co-EGDMA) after the first, non-fired engine test (left) and after the 8-hour fired engine test.

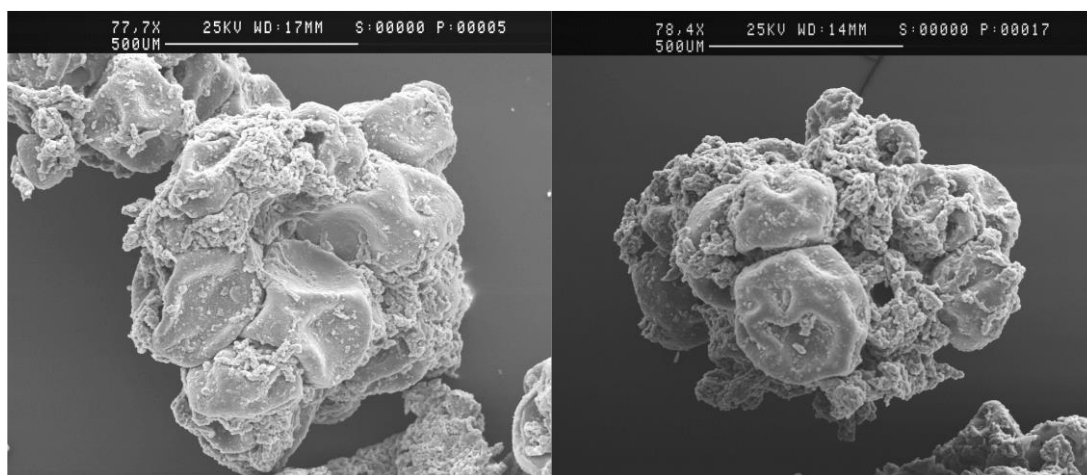


Figure 71 - SEM micrographs of poly(styrene-*co*-VBC-*co*-EGDMA) after the non-fired engine test (left) and after the 8-hour fired engine test (left)

The polymer particles, again, showed signs of agglomeration and were very similar in appearance to how they appeared after the non-fired engine test. The polymer particles also exhibited a deflated appearance, as they had done after the non-fired engine test.

FT-IR analysis was used to investigate the agglomeration phenomenon further. Shown in **Figure 72** is the FT-IR spectra of poly(styrene-*co*-VBC-*co*-EGDMA) before (red) and after the fired engine test.

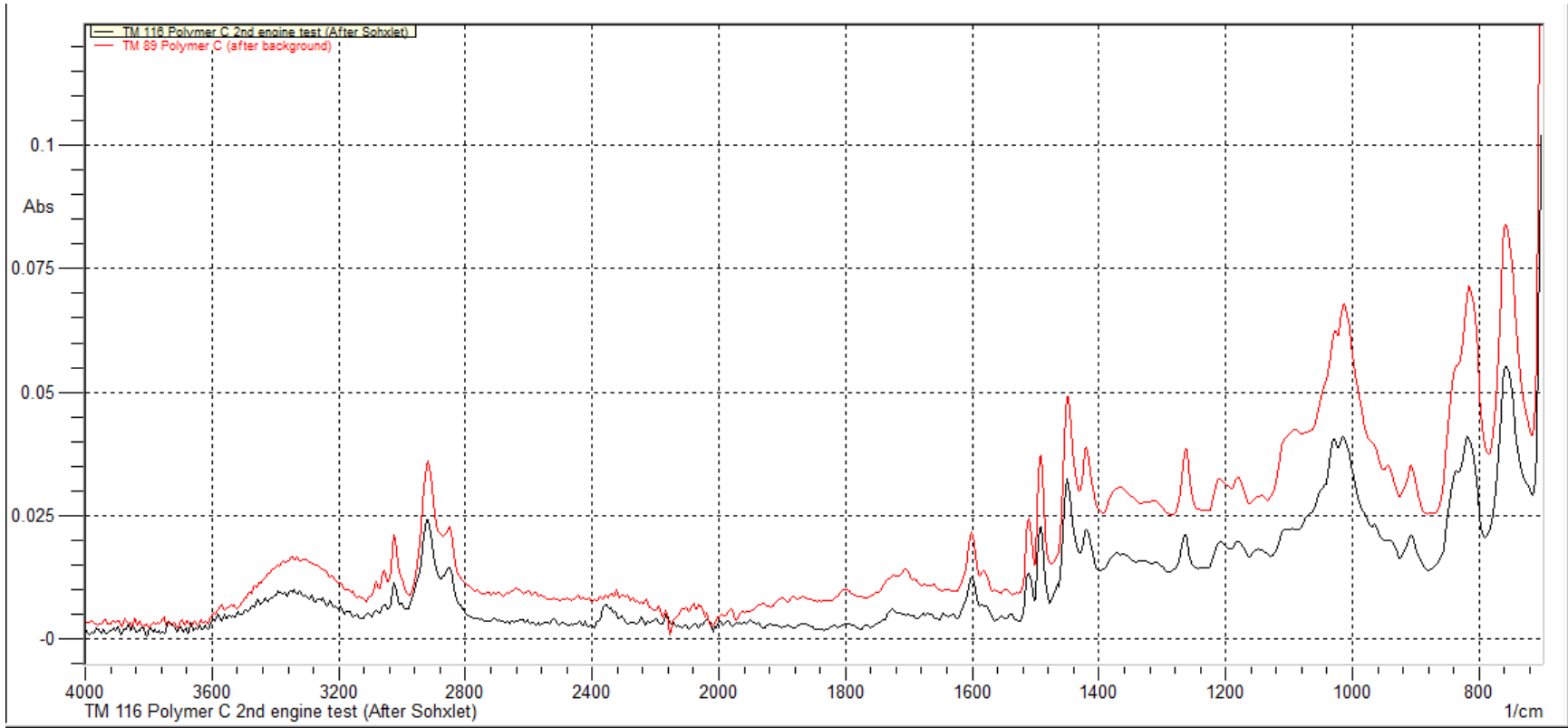


Figure 72 - FT-IR spectra of poly(styrene-co-VBC-co-EGDMA) before (red) and after (black) the fired engine test

The FT-IR spectra exhibited the same features before and after the engine test. The -OH stretching at 3300 cm^{-1} was still apparent, due to hydrolysis of VBC units within the polymer during synthesis. There was very little change, if any, in the region $2200\text{--}2000\text{ cm}^{-1}$, as had been seen in some of the other materials.

It was therefore believed that this material had been somewhat unsuccessful in the removal of any contaminants from the lubricant during the engine testing.

During the fired engine testing, technologists at Castrol removed a sample of lubricant every hour to be tested for soot content. This was done during a 'blank run' wherein no polymer was present in the engine, as well as during the tests on poly(DVB-80-co-4-VP) and poly(styrene-co-VBC-co-EGDMA). Shown in **Figure 73** is some of the data that was collected during these analyses.

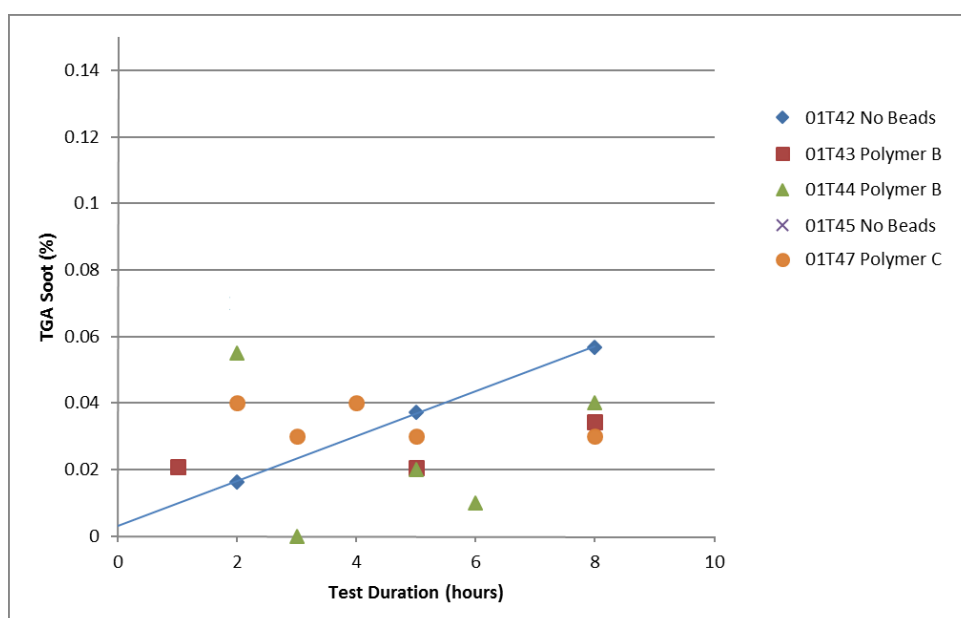


Figure 73 - TGA-soot analysis of lubricant after engine testing

The blue diamonds (01T42) are TGA-soot analysis of the lubricant without any polymer present and it produced a linear increase in soot over time, as would be expected, *i.e.*, the longer the lubricant is used in the engine the more soot is produced. Interestingly when a polymer sorbent was added, the initial amount of soot was seen to be higher

than without. This was thought to be due to the polymer beads surface producing a nucleation site for soot to begin forming. However, as the test progressed the level of soot observed was noted to remain static for the duration of the test, indicating the removal of soot by the polymeric material. For example, test 01T43 (red squares) was the 8-hour, fired engine test of poly(DVB-80-co-4-VP). After two hours, 0.02 % of soot was present in the lubricant, and after 8 hours this had risen to nearly 0.03%. This was only half the amount of soot present in the oil after 8 hours when no polymer was present.

Therefore, the TGA-soot analysis proved that the removal of soot as it was formed in the lubricant, using solid phase polymeric materials, was possible. The significance of the findings from the fired engine testing should not be overlooked. The removal of soot and other potential contaminants from an engine lubricant system, while running, using solid-phase polymeric material is something which to the best of our knowledge has not been successfully carried out before. This work was incorporated into a patent filing and is currently under examination.¹⁹⁹

4.0 Conclusions

With ever stricter legislation governing emissions from fossil-fuel powered engines, global concerns over fossil fuels impact on the environment, and the volatility of dependence on a finite resource, researchers are having to use novel approaches to ensure that fossil fuels (and their derivatives) are able to last longer and are as environmentally friendly as they possibly can be.

In pursuit of engine lubricants that last longer and are cleaner, presented in this thesis is research into the application of solid-phase polymeric sorbents as *in situ* contaminant removal devices for combustion engines.

Precipitation polymerisation and non-aqueous dispersion polymerisation were both employed successfully to synthesise a small library of aromatic, vinyl-based polymers. Some of these materials were functionalised using co-monomers, including VBC and 4-VP. By including porogenic solvents in the synthesis, porosity was installed and produced materials with specific surface areas in the region of 500 m²/g. Porosity was also installed in some of the polymers *post*-polymerisation. By using the VBC units as functional handles; porosity was induced *via* Friedel-Crafts alkylation, methylene bridges between appropriately located phenyl moieties were installed, creating hypercrosslinked polymers. By utilising this chemistry, polymers with specific surface areas in excess of 1500 m²/g were achieved.

In order to investigate and understand the possibility of using porous materials for contaminant removal from engine lubricants, lab-based sorption and capture experiments were carried out. It was hypothesised that, through π - π stacking and other non-covalent interactions, the polymer particles would be able to sorb PAHs from a heptane solution containing up to five different PAHs. PAHs are one group of compounds which are known to be precursors to engine soot, and were utilised in these studies for this reason. The effects of PAH size and functionality were investigated by including PAHs of differing ring size and two which had functionality. It was demonstrated that even the simplest polymer synthesised, poly(DVB-80), with a specific surface area of 550 m²/g, was able to remove significant amounts of PAH. At this early stage of the investigation, some trends in PAH removal, using polymer microspheres, were able to be deduced; the

specific surface area of the polymer had a large bearing on the overall sorption of PAHs, with a large specific surface area (possessed by the hypercrosslinked materials) allowing for more PAH to be removed from the heptane (**Table 19** and **Table 20**). Polymers possessing lower specific surface area were found to remove much less PAH (**Table 18**). The functionality included in the polymer was also found to influence the amount of PAH removed. 4-VP containing polymers were found to be the most effective, especially for the removal of the nitropyrene. It was believed that favourable interactions between the electron deficient phenyl rings of nitropyrene and the lone-pair of electrons in 4-VP were responsible, at least in part, for the favourable removal of nitropyrene from heptane. It was also believed that the solubility of each PAH in heptane had an influence on the ability of the polymers to remove it from the heptane solution. The larger PAHs (such as anthracene and nitropyrene) were removed more readily by all of the polymers, whereas the smaller PAHs (such as methylnaphthalene), were retained in the heptane solution, rather than being removed by the polymer.

These initial studies proved that it was indeed possible to remove contaminants (PAHs) from a hydrocarbon fluid (heptane). To further investigate this hypothesis, attention turned to producing materials which could be used within the lubricant system of an engine. Polymer particles which were of a large enough diameter such that they could be contained with relative ease within the lubricant system, when compared to the much smaller diameter materials produced *via* precipitation polymerisation and NAD polymerisation, were required. Using previously disclosed synthetic strategies, suspension polymerisation was employed successfully to produce a small library of aromatic, vinyl-based polymers, chemically similar to the best-performing lab-based sorption tests but which possessed much larger particle diameters. Again, a mixture of functionalities was included, both to enhance polymer-PAH interactions (in the case of 4-VP) and, in the case of VBC, to facilitate the introduction of porosity into the material through previously discussed hypercrosslinking chemistry. The suspension polymerisation polymers containing VBC were found to have been partially hydrolysed due to the use of an aqueous phase during the polymer synthesis. Upon attempts to remove PAHs from heptane, the low specific surface area, partially hydrolysed, polymers were found to perform particularly poorly. Both the low surface area and the increased

hydrophilicity of the polymers were believed to have been the cause. In the heptane-based sorption and capture experiments, the permanently porous and HXL materials (synthesised from suspension polymerisation precursors) were found to perform in a similar fashion to the NAD and precipitation polymer particles (**Table 28**). In this study, again, polymers having higher specific surface areas were found to remove more (upwards of 75% in the case of nitropyrene) PAHs from the heptane solution than those materials with a lower specific surface area.

With evidence of successful removal of PAHs from heptane, the suspension polymerisation polymer particle, and the HXL derivatives, were passed to colleagues at Castrol for engine-based sorption studies. Upon contact with a hot, used engine lubricant in a non-fired engine test, SEM data, FT-IR spectroscopic data and nitrogen sorption analysis all indicated the removal of contaminants from the lubricant. In all cases the polymer particles were agglomerated together after the engine tests. Apart from the gel-type poly(styrene-*co*-VBC-*co*-EGDMA), all polymers exhibited bands attributable to acetylene or polyacetylenes after the engine test in the respective FT-IR spectra. Polyacetylenes are believed to play a role in the formation of soot and their presence in the polymers indicated successful soot removal. Unfortunately, due to the degraded nature of the lubricant used in these tests, further analysis proved fruitless in providing any further information regarding the lubricant after the engine tests.

To investigate the potential application of solid-phase polymers as contamination removal devices in lubricant systems, a further round of engine testing was undertaken, whereupon the engine would be running throughout the test. The porous poly(DVB-80-*co*-4-VP) and the non-porous gel-type poly(styrene-*co*-VBC-*co*-EGDMA) were chosen to be investigated. In these engine tests a clean, new, dispersant-free lubricant was used, and soot built up within the lubricant over time, as would be observed in a 'real-world' engine lubricant. In these tests, all polymers displayed the agglomeration of polymer particles and FT-IR data of poly(DVB-80-*co*-4-VP) displayed evidence of soot precursors, in the form of acetylene functionality or polyacetylenes, being present in the polymers after the engine test. The lubricant itself was also scrutinised, by technologists at Castrol. It was found that, soot builds up over time within the lubricant. When the tests were repeated in the presence of the polymer sorbent, the amount of soot in the lubricant

increased at a slower rate, or remained steady (**Figure 73 - TGA-soot analysis of lubricant after engine testing**), demonstrating the polymers' ability to aid in the removal of the soot contamination.

At the outset of this body of work it was hypothesised that through favourable, non-covalent interactions, aromatic, vinyl polymers would be able to remove PAHs and possibly other contaminants from a hydrocarbon fluid. Through lab-based tests it has been demonstrated that this was indeed possible. Further engine-based studies have also shown that the removal of soot-based contamination from diesel engine lubricants is feasible.

There are a few examples in the patent literature of the use of a porous medium to remove contamination from engine lubricants and the use of porous polymers (specifically bearing 4-VP) as stationary phases for the separation of PAHs.^{171-174,188,200} However, the use of polymer microspheres for the *in-situ* removal of PAHs, soot and other contaminants from engine lubricants is, to the best of our knowledge, something that has not, until now, been demonstrated.

5.0 Future work

Further research in this area is on-going. Polymer samples have been sent to a testing facility in Germany for further, long-term engine-based testing. By running longer engine tests, a better understanding of the longer-term effects of the polymer sorbents presence within the lubricant will be gained. By testing for longer, better comparison between solid-phase sorbents and currently employed dispersant technology can be realised. The comparison between the materials produced during this work and commercially available materials may also be achievable. By investigating already available polymers, potentially high costs associated with the synthesis of bespoke materials could be avoided.

Further imaging analysis, in the form of SEM and TEM, is being undertaken at Reading University to gain insight into the nature and structure of contaminants that have been removed by the polymers during engine-based tests. Some preliminary work in this area has suggested that the structure of the agglomerating material on the surface of the polymer beads appears to be ordered carbon, similar to that observed in TEM analysis of engine soot.

Another fruitful outcome from this body of work is collaboration between research groups. Researchers at Lancaster University are currently employing computational based methods to better understand the polymer-PAH interactions. It is hoped that by gaining a better understanding of how the polymers remove the PAHs from solution, better insight into the design and synthesis of the materials could be realised. This offers up the potential for future collaborative efforts, whereupon the polymer sorbent could be designed and tailored using computational chemistry to enhance specific polymer-contaminant interaction. It is hoped that by using computational methods, costly syntheses could be minimised, where specific characteristics of a potential material have already been devised before the synthesis even begins, allowing for a polymer displaying the correct functionality and porosity characteristics to be made for the specific sorption application in mind.

Related work in this area, within the Cormack Group, is also on-going. Solid-phase, polymer particles bearing functionality observed in currently used lubricant dispersants

(specifically amine-based functionality), is being investigated. It is envisaged that polymer particles bearing dispersant functionality could potentially be used in conjunction with polymer sorbents to extend the useful life of engine lubricants even further.

One final area of interest for the use of solid-phase polymers, like those discussed in this body of work, is Castrol's Nexcel system.²⁰¹ Nexcel is a revolutionary technology whereupon the engine lubricant and filter are housed in a unit which can be removed and replaced with ease. This technology is currently employed in the Aston Martin Vulcan, a track-only hypercar. It is envisaged that the technology employed by Nexcel will reduce CO₂ and other emissions, as well as easing the process by which engine lubricant is changed. Also, due to Nexcel being a sealed unit, used engine lubricant can be collected both safely and easily at the end of its useful life, thereby improving the environmental impact and recyclability of engine lubricants. It is thought that this disruptive technology would be the ideal system with which to implement a solid-phase, polymer sorbent into the lubricant system. Due to being a contained unit, Nexcel would make the containment of any polymer particles much simpler. Also, disposal or recycling of the polymeric material after use would be more straightforward, for the same reason.

6.0 References

1. <http://www.dupont.co.uk/products-and-services/fabrics-fibres-nonwovens/fibres/brands/kevlar.html> Accessed 15th September 2017
2. L. R. Rudnick, *Lubricant Additives Chemistry and Applications*, CRC Press, Second Edition., 2009.
3. W. H. Carothers, *J. Am. Chem. Soc.*, 1929, **51**, 2548–2559.
4. P. J. Flory, *Principles of Polymer Chemistry*, Cornell University Press, Ithaca, New York, 1953, vol. 1.
5. M. P. Stevens, *Polymer Chemistry An Introduction*, Oxford University Press, Oxford, UK, Third Edition., 1999.
6. W. H. Carothers, *Trans. Faraday Soc.*, 1936, **32**, 39–49.
7. J. M. Cowie and V. Arrighi, *Polymers: Chemistry and Physics of Modern Materials*, CRC Press, Florida, U.S.A, Third Edition., 2008.
8. *Market Study: Polypropylene*, Ceresana Market Intelligence Consulting, 2010.
9. B. G. Frushour, J. R. Kontoff, H. Eichenauer, J. Maul, K.-H. Ott and C. Schade, in *Ullmann's Encyclopedia of Industrial Chemistry*, 2007.
10. P. W. Atkins and J. De Paula, *Atkins' Physical Chemistry*, Oxford University Press, New York, 9th Edition., 2014.
11. D. Walton and P. Lorimer, *Polymers*, Oxford University Press, Oxford, UK, 2001.
12. H. Bakeland U.S Pat., 942699, 1907.
13. C. Goodyear, U.S Pat., 3635, 1844.
14. D. C. Sherrington, *Chem. Commun.*, 1998, 2275–2286.
15. M. P. Tsyurupa and V. A. Davankov, *React. Funct. Polym.*, 2006, **66**, 768–779.
16. C. Garcia-Diego and J. Cuellar, *Ind Eng Chem Res*, 2005, **44**, 8237–8247.
17. Q. Liu, L. Wang, A. Xiao, H. Yu, Q. Tan, J. Ding and G. Ren, *J Phys Chem C*, 2008, **112**, 13171–13174.
18. M. J. Beneš, D. Horák and F. Sveč, *J. Sep. Sci.*, 2005, **28**, 1855–1875.
19. D. Horak, J. Labsky, J. Pilar, M. Bleha, Z. Plezbauer and F. Sveč, *Polymer*, 1993, **34**, 3481–3489.
20. A. Ferreira, N. Bigan and D. Blondeau, *React. Funct. Polym.*, 2003, **56**, 123–126.
21. F. S. MacIntyre and D. C. Sherrington, *Macromolecules*, 2004, **37**, 7186–7193.

- 22 K. Kanamori, J. Hasegawa, K. Nakanishi and K. Hanada, *Macromolecules*, 2008, **41**, 7186–7193.
- 23 O. Okay, *Prog. Polym. Sci.*, 2000, **25**, 711–779.
- 24 M. T. Gokmen and F. E. Du Prez, *Prog. Polym. Sci.*, 2012, **37**, 365–405.
- 25 R. Arshady, *Colloid Polym. Sci.*, 1992, **270**, 717–732.
- 26 B. W. Brooks, *Chem. Eng. Technol.*, 2010, **33**, 1737–1750.
- 27 K. W. Pepper, *J. Appl. Chem.*, 1951, **1**, 124–132.
- 28 F. de Dardel and T. V. Arden, in *Ullmann's Encyclopedia of Industrial Chemistry*, 2008.
- 29 F. Hoffmann, K. Delbruk, German Pat., 250690, 1909.
- 30 F. Hoffmann, K. Delbruk, German Pat., 254672, 1912.
- 31 W. P. Hohenstein and H. Mark, *Journal. Polym. Sci.*, 1946, **1**, 127–145.
- 32 P. J. Blythe, A. Klein, J. A. Phillips, E. D. Sudol and M. S. El-Aasser, *J. Polym. Sci. Part A. Polym. Chem.*, 1999, **37**, 4449–4457.
- 33 R. Arshady, *Colloid Polym. Sci.*, 1990, **268**, 948.
- 34 M. Zefra and B. W. Brooks, *Colloids Surf.*, 1998, **132**, 267.
- 35 R. P. Borwanker, S. I. Chung and D. T. Wasan, *J. Appl. Polym. Sci.*, 1986, **32**, 5749.
- 36 Z. Wang and B. W. Brooks, *Polym Int*, 1992, **28**, 239.
- 37 D. Wolters, W. Meyer-Zaika and F. Bandermann, *Macromol Mater Eng*, 2001, **286**, 94.
- 38 L. I. Atanase and G. Riess, *Colloids Surf.*, 2010, **355**, 29.
- 39 M. Zefra and B. W. Brooks, *Chem Eng Sci*, 1996, **51**, 3591.
- 40 S. Ormondroyd, *Br. Polym. J.*, 1988, **20**, 353.
- 41 Y. Z. Bao, *J. Appl. Polym. Sci.*, 2002, **185**, 1544.
- 42 F. Lerner and S. Nemet, *Plast. Rubbers Compos.*, 1999, **28**, 100.
- 43 J. M. Church, *Chem Eng*, 1966, **73**, 79.
- 44 J. Haginaka, *J. Chromatogr. B.*, 2008, **866**, 3–13.
- 45 K. Li and D. H. Stöver, *J. Polym. Sci. Part A. Polym. Chem.*, 1993, **31**, 3257–3263.
- 46 C. H. Bamford, A. Ledwith and P. K. Gupta, *J. Appl. Polym. Sci.*, 1980, **25**, 2559–2566.
- 47 J. S. Downey, R. S. Frank, W.-H. Li and H. D. H. Stöver, *Macromolecules*, 1991, **32**, 2838–2844.

- 48 S. E. Shim, S. Yang, H. H. Choi and S. Choe, *J. Polym. Sci. Part A. Polym. Chem.*, 2004, **42**, 835–845.
- 49 L. Wen-Hui and D. H. Stöver, *J. Polym. Sci. Part A. Polym. Chem.*, 1998, **36**, 1543–1551.
- 50 W.-H. Li and H. D. H. Stöver, *Macromolecules*, 2000, **33**, 4354–4360.
- 51 P. A. G. Cormack, A. Davies and N. Fontanals, *React. Funct. Polym.*, 2012, **72**, 939–946.
- 52 N. Fontanals, P. A. G. Cormack and D. C. Sherrington, *J. Chromatogr. A*, 2008, **1215**, 21–29.
- 53 N. Fontanals, P. Manesiotis, D. C. Sherrington and P. A. G. Cormack, *Adv. Mater.*, 2008, **20**, 1298–1302.
- 54 D. Cabooter, A. Fanigliulo, G. Bellazzi, B. Allieri, A. Rottigni and G. Desmet, *J. Chromatogr. A*, 2010, **1217**, 7074–7081.
- 55 Y. Zhao, H. D. H. Stöver and N. A. D. Burke, *J. Polym. Sci. Part Polym. Chem.*, 2016, **54**, 1159–1161.
- 56 J. M. Tobin, T. J. D. McCabe, A. W. Prentice, S. Holzer, G. O. Lloyd, M. J. Paterson, V. Arrighi, P. A. G. Cormack and F. Vilela, *ACS Catal.*, 2017, **7**, 4602–4612.
- 57 S. Pardeshi and S. K. Singh, *RSC Adv*, 2016, **6**, 23525–23536.
- 58 V. A. Davankov, M. P. Tsyurupa and N. N. Alexienko, *J. Chromatogr. A*, 2005, **1100**, 32–39.
- 59 L. Tan and B. Tan, *Chem Soc Rev*, 2017, **46**, 3322–3356.
- 60 B. Li, R. Gong, Y. Luo and B. Tan, *Soft Matter*, 2011, **7**, 10910.
- 61 N. Fontanals, J. Cortés, M. Galià, R. Maria Marcé, P. A. G. Cormack, F. Borrull and D. C. Sherrington, *J. Polym. Sci. Part Polym. Chem.*, 2005, **43**, 1718–1728.
- 62 J.-S. Song and M. A. Winnik, *Macromolecules*, 2005, **38**, 8300–8307.
- 63 J.-S. Song, F. Tronc and M. A. Winnik, *J. Am. Chem. Soc.*, 2004, **126**, 6562–6563.
- 64 N. Abdullah, PhD Thesis, University of Strathclyde, 2013.
- 65 V. A. Davankov, S. V. Rogozhin, M. P. Tsjurupa, U.S Pat., 3729457, 1973.
- 66 R. Law, D. C. Sherrington, C. Snape, J. Ando and H. Kurosu, *Molecules*, 1996, **29**, 6284–6293.
- 67 R. Joseph, W. T. Ford, S. Zang, M. P. Tsyurupa, A. V. Pastukhov and V. A. Davankov, *J. Polym. Sci. Part Polym. Chem.*, 1997, **35**, 695–701.

- 68 D. Wu, C. M. Hui, H. Dong, J. Pietrasik, H. J. Ryu, Z. Li, M. Zhong, H. He, E. K. Kim, M. Jawoniec, T. Kowalewski and K. Matyjaszewski, *Macromolecules*, 2001, **44**, 5846–5849.
- 69 B. Gawdzik and J. Ospiuk, *Chromatographia*, 2001, **54**, 323–328.
- 70 A. Li, Q. Zhang, G. Zhang, J. Chen, Z. Fei and F. Liu, *Chemosphere*, 2002, **47**, 981–988.
- 71 V. A. Davankov and M. P. Tsyurupa, *React. Funct. Polym.*, 1990, **13**, 27–42.
- 72 C. D. Wood, B. Tan, A. Trewin, H. Niu, D. Bradshaw, M. J. Rosseinsky, Y. Z. Khimiyak, N. L. Campbell, R. Kirk, E. Stockel and A. I. Cooper, *Chem Mater*, 2007, **19**, 2034–2048.
- 73 J.-H. Ahn, J.-E. Jang, C.-G. Oh, S.-K. Ihm, J. Cortez and D. C. Sherrington, *Macromolecules*, 2006, **39**, 627–632.
- 74 D. Bratkowska, R. M. Marcé, P. A. G. Cormack, D. C. Sherrington, F. Borrull and N. Fontanals, *J. Chromatogr. A*, 2010, **1217**, 1575–1582.
- 75 N. Fontanals, P. A. G. Cormack, D. C. Sherrington, R. M. Marcé and F. Borrull, *J. Chromatogr. A*, 2010, **1217**, 2855–2861.
- 76 V. A. Davankov and M. P. Tsyurupa, *React. Funct. Polym.*, 2002, **53**, 193–203.
- 77 C. D. Wood, B. Tan, A. Trewin, F. Su, M. J. Rosseinsky, D. Bradshaw, Y. Sun, L. Zhou and A. I. Cooper, *Adv. Mater.*, 2008, **20**, 1916–1921.
- 78 S. Bhunia, B. Banerjee and A. Bhaumik, *Chem. Commun.*, 2015, **51**, 5020–5023.
- 79 W. Chaikittslip, M. Kubo, T. Moteki, A. Sugawara-Narutaki, A. Shimojima and T. Okubo, *J Am Chem Soc*, 2011, **133**, 13832–13835.
- 80 S. Yuan, D. White, A. Mason and D. J. Liu, *Int. J. Energy Res.*, 2013, **37**, 732–740.
- 81 B. Li, R. Gong, W. Wang, X. Huang, W. Zhang, H. Li, C. Hu and B. Tan, *Macromolecules*, 2011, **44**, 2410–2414.
- 82 M. Errahali, G. Gatti, L. Tei, G. Paul, G. A. Rolla, L. Canti, A. Fraccarollo, M. Cossi, A. Comotti, P. Sozzani and L. Marchese, *J Phys Chem C*, 2014, **118**, 28699–28710.
- 83 P. Cui, X. F. Jing, Y. Yuan and G. S. Zhu, *Chin Chem Lett*, 2016, **27**, 1479–1484.
- 84 C. Zhang, P. C. Zhu, L. Tan, J. M. Liu, B. Tan, X. L. Yang and H. B. Xu, *Macromolecules*, 2015, **48**, 8509–8514.
- 85 T. L. Zhai, L. Tan, Y. Luo, J. M. Liu, B. Tan, X. L. Yang, H. B. Xu and Zhang C., *Chem-Asian J*, 2016, **11**, 294–298.

- 86 T. Ravijitvech, M. Barrow, A. I. Cooper and D. J. Adams, *Polym. Chem*, 2015, **6**, 7280–7285.
- 87 F. Maya and F. Svec, *Polymer*, 2014, **55**, 340–346.
- 88 L. J. Abbott, K. E. Hart and C. M. Colina, *Theor. Chem. Acc.*, 2013, **132**, 1334
- 89 L. J. Abbott, J. E. Hughes and C. M. Colina, *J. Phys. Chem. B*, 2014, **118**, 1916–1924.
- 90 L. J. Abbott and C. M. Colina, *Macromolecules*, 2014, **47**, 5409–5415.
- 91 G. Kupgan, T. P. Liyana-Arachchi and C. M. Colina, *Polymer*, 2016, **99**, 173–184.
- 92 N. Fontanals, J. Cortés, M. Galià, R. Maria Marcé, P. A. G. Cormack, F. Borrull and D. C. Sherrington, *J. Polym. Sci. Part Polym. Chem.*, 2005, **43**, 1718–1728.
- 93 R. B. Merrifield, *J. Am. Chem. Soc.*, 1963, **85**, 2149–2154.
- 94 S. E. Van der Plas, E. Van Hoeck, F. Lynen, P. Sandra and A. Madder, *Eur. J. Org. Chem.*, 2009, **11**, 1796–1805.
- 95 S.-Y. Han and Y.-A. Kim, *Tetrahedron*, 2004, **60**, 2447–2467.
- 96 L. Sinigoi, P. Bravin, C. Ebert, N. D’Amelio, L. Vaccari, L. Ciccarelli, S. Cantone, A. Basso and L. Gardossi, *J. Comb. Chem.*, 2009, **11**, 835–845.
- 97 A. Basso, P. Braiuca, L. De Martin, C. Ebert, L. Gardossi, P. Linda, S. Verdelli and A. Tam, *Chem. - Eur. J.*, 2004, **10**, 1007–1013.
- 98 A. Poschalko, T. Rohr, H. Gruber, A. Bianco, G. Guichard, J.-P. Briand, V. Weber and D. Falkenhagen, *J. Am. Chem. Soc.*, 2003, **125**, 13415–13426.
- 99 D. C. Sherrington, *J. Polym. Sci. Part Polym. Chem.*, 2001, **39**, 2364–2377.
- 100 M. Watson, K. C. Abbott and C. M. Yuan, *Clin. J. Am. Soc. Nephrol.*, 2010, **5**, 1723–1726.
- 101 M. Baer, U.S Pat., 2533210, 1950.
- 102 H. H. Roth, E. E. Cowherd, W. C. Bauman, R. M. Willey, Br. Pat., 960502, 1964.
- 103 H. H. Roth, H. B. Smith, U.S Pat., 2663700, 1953.
- 104 H. Xu and X. Hu, *React. Funct. Polym.*, 1999, **42**, 235–242.
- 105 <http://www.phenomenex.com/ViewDocument?id=simplified+spe+solutions+brochure> Accessed 25th October 2017
- 106 http://www.waters.com/waters/en_US/Oasis-Sample-Extraction-Products/nav.htm?cid=513209&locale=en_US Accessed 24th October 2017
- 107 M.-C. Hennion, *J. Chromatogr. A*, 1999, **856**, 3–54.

- 108 C. Valderrama, X. Gamisans, F. X. de las Heras, J. L. Cortina and A. Farrán, *React. Funct. Polym.*, 2007, **67**, 1515–1529.
- 109 M. Streat and L. A. Sweetland, *React. Funct. Polym.*, 1997, **35**, 99–109.
- 110 A. Gupta, J. Sarkar and A. Kumar, *J. Chromatogr. A*, 2013, **1278**, 16–21.
- 111 D. J. Patterson and N. A. Henein, *Emissions from Combustion Engines and Their Control*, Ann Arbor Science Publishers, Ann Arbor, Michigan, 1972.
- 112 R. G. Harvey, *Polycyclic Aromatic Hydrocarbons: Chemistry and Carcinogenicity*, Cambridge University Press, United Kingdom, First., 1991.
- 113 A. Luch, *The Carcinogenic Effects of Polycyclic Aromatic Hydrocarbons*, Imperial College Press, London, 2005.
- 114 2012.
- 115 M. J. Covitch, B. K. Humphrey and D. Ripple, in *SAE Powertrain, Fuels and Lubricants Meeting*, Tulsa, Oklahoma, 1985.
- 116 R. Kornbrekke, *SAE Tech. Pap.* 982665.
- 117 O. I. Smith, *Prog. Energy Combust. Sci.*, 1981, **7**, 275–291.
- 118 B. S. Haynes and H. G. Wagner, *Prog. Energy Combust. Sci.*, 1981, **7**, 229–273.
- 119 D. R. Tree and K. I. Svensson, *Prog. Energy Combust. Sci.*, 2007, **33**, 272–309.
- 120 B. R. Stanmore, J. F. Brilhac and P. Gilot, *Carbon*, 2001, **39**, 2247–2268.
- 121 H. Richter and J. B. Howard, *Prog. Energy Combust. Sci.*, 2000, **26**, 565–608.
- 122 I. Glassman and R. A. Yetter, *Combustion*, Academic Press, San Diego, 4th edn., 2008.
- 123 W. Bartok and A. Sarafim, *Fossil Fuel Combustion*, Willey, New York, 1991.
- 124 J. P. A. Neeft, M. Makkee and J. A. Moulijn, *Fuel Process Technol.*, 1996, **47**, 1–69.
- 125 S. George, S. Balla and M. Gautam, *Wear*, 2007, **262**, 1113–1122.
- 126 S. George, S. Balla, V. Gautam and M. Gautam, *Tribol. Int.*, 2007, **40**, 809–818.
- 127 M. M. Maricq, *J. Aerosol Sci.*, 2007, **38**, 1079–1118.
- 128 M. Fiebig, A. Wiartalla, B. Holderbaum and S. Kiesow, *J. Occup. Med. Toxicol.*, 2014, **9**, 1–18.
- 129 *Official Journal of the European Union*, 1–16.
- 130 *Official Journal of the European Union*, 2016, **L 82**, 1–98.
- 131 The Environmental Protection Agency of The United States of America, 2015.
- 132 J. O'Connor and M. Musculus, *SAE Int J Engines*.

- 133 J. B. Heywood, *Internal combustion engine fundamentals*, McGraw-Hill, New York, 1988.
- 134 A. Maiboom, X. Tauzia and J.-F. Hétet, *Energy*, 2008, **33**, 22–34.
- 135 J. M. Luján, C. Guardiola, B. Pla and A. Reig, *Energy*, 2015, **90**, 1790–1798.
- 136 A.-M. Stamatellou and A. Stamatelos, *Appl. Therm. Eng.*, 2017, **121**, 537–546.
- 137 S. Q. A. Rizvi, in *Lubricant Additives*, CRC Press, 2009, pp. 143–170.
- 138 R. M. Mortier, M. F. Fox and S. T. Orszulik, Eds., *Chemistry and Technology of Lubricants*, Springer Netherlands, Dordrecht, 2010.
- 139 S. Q. A. Rizvi, in *Fuels and Lubricants Handbook: Technology, Properties, Performance, and Testing*, ASTM International, U.S.A, 2003.
- 140 F. X. Sieloff and J. L. Musser, Detroit, Michigan, 1982.
- 141 E. Obert, *Internal Combustion Engines and Air Pollution*, Intex Educational Publishing, New York, 1968.
- 142 G. J. Cochrac and S. Q. A. Rizvi, in *Fuels and Lubricants Handbook: Technology, Properties, Performance, and Testing*, ASTM International, West Coshohocken, PA, U.S.A., 2003, pp. 787–824.
- 143 K. U. Ingold, *Chem. Rev.*, 1961, **61**, 563–589.
- 144 A. Gutierrez, S. R. Won, R. D. Lundberg, R. A. Kliet U.S Pat., 5017299, 1991.
- 145 A. Gutierrez, R. A. Kliet, S. R. Won, A. Rossi, H. W. Turner, H. C. Welborn, R. D. Lundberg U.S Pat., 5435926, 1995.
- 146 L. R. Rudnick and R. L. Shubkin, *Synthetic Lubricants and High-Performance Functional Fluids*, Marcel Dekker, New York, second edition., 1999.
- 147 F. A. Stuart, R. G. Anderson, A. Y. Drummond, U.S Pat., 3361673, 1968.
- 148 R. Rense, U.S Pat., 3215707, 1965.
- 149 J. J. Harrison, D. C. Young and C. L. Mayne, *J. Org. Chem.*, 1997, **62**, 693–699.
- 150 J. Weill, J. Garapon, B. Sillion, U.S Pat., 4433157, 1984.
- 151 N. A. Minehardt, K. E. Davis, U.S Pat., 4234435, 1980.
- 152 B. Sillion and J. Weill, *Rev. Inst. Francais Pet.*, 1985, **40**, 77–89.
- 153 S. Q. A. Rizvi, in *Lubricant Additives*, CRC Press, 2009, pp. 143–170.
- 154 J. K. Pudelski, M. A. Sivik, K. F. Wollenberg, R. Yodice, J. L. Rutter, J. G. Dietz, U.S Pat., 5885944, 1998.
- 155 J. Colp, P. A. Lewis, J. G. Dietz, U.S Pat., 6077909, 2000.

- 156 J. K. Pudelski, C. J. Colp, J. G. Dietz, C. K. Baumanis, S. L. Bartley, J. D. Burrington, U.S Pat., 6165232, 2000.
- 157 C. K. Baumanis, M. M. Maynard, A. C. Clark, M. A. Sivik, C. P. Kolwall, D. L. Westfall, U.S Pat., 5708097, 1998.
- 158 K. Eller, in *Ullmann's Encyclopedia of Industrial Chemistry*, 2005, pp. 32–40.
- 159 W. M. La Suer, G. R. Norman, U.S Pat., 3172892, 1965.
- 160 T. F. Steckel, U.S Pat., 5053152, 1991.
- 161 T. J. Karol, H. S. Magaha, U.S Pat., 4554086, 1985.
- 162 W. M. La Suer, U.S Pat, 3381022, 1968.
- 163 N. A. Minehart, R. J. Widmer, U.S Pat., 3697428, 1972.
- 164 F. P. Otto, U.S Pat., 3368972, 1968.
- 165 J. F. Pinder, J. M. Cohen, C. P. Bryant, U.S Pat., 3980569, 1976.
- 166 J. R. McAtee, U.S Pat., 6179885, 2001.
- 167 R. E. Cherpeck, U.S Pat., 5300701, 1994.
- 168 J. P. Edmund, U.S Pat., 353963, 1970.
- 169 J. C. Barnes, M. Juríček, N. L. Strutt, M. Frascioni, S. Sampath, M. A. Giesener, P. L. McGrier, C. J. Bruns, C. L. Stern, A. A. Sarjeant and J. F. Stoddart, *J. Am. Chem. Soc.*, 2013, **135**, 183–192.
- 170 J. C. Barnes, M. Juríček, N. A. Vermeulen, E. Dale and J. F. Stoddart, *J. Org. Chem.*, 2013, **78**, 11962–11969.
- 171 D. W. Brownawell, D. J. Norris, H. Shaub, U.S Pat., 4977871, 1990.
- 172 D. W. Brownawell, U.S Pat., 5225081, 1993.
- 173 S. P. Lockledge, D. W. Brownawell, U.S Pat., 7520371, 2009.
- 174 D. W. Brownawell, W. Thaler, U.S Pat., 5042617, 1991.
- 175 A. M. G. Macdonald, *Analyst*, 1961, **86**, 3–12.
- 176 K. S. W. Sing, D. H. Everett, R. A. W. Haul, L. Moscou, R. A. Pierotti and J. Rouquérol, *Pure Appl. Chem.*, 1985, **57**, 603–619.
- 177 *Determination of the specific surface area of solids by gas adsorption - BET method BS ISO 3277-2010*, British Standards Organisation, London UK, 2010.
- 178 *Pore size distribution and porosity of solid materials by mercury porosimetry and gas adsorption Part 3: Analysis of micropores by gas adsorption. BS ISO 15901-3*, British Standards Organisation, London UK, 2007.

- 179 *Pore size distribution and porosity of solid materials by mercury porosimetry and gas adsorption - Part 2: Analysis of mesopores and macropores by gas adsorption.* BS ISO 15901-2, British Standards Organisation, London UK, 2006.
- 180 S. Brunauer, P. H. Emmett and E. Teller, *J. Am. Chem. Soc.*, 1938, **60**, 309–313.
- 181 I. Langmuir, *J. Am. Chem. Soc.*, 1918, **40**, 1361–1403.
- 182 B. C. Lippens, B. G. Linsen and J. H. De Boer, *J. Catal.*, 1964, **3**, 32–37.
- 183 J. H. De Boer, B. G. Linsen and T. J. Osinga, *J. Catal.*, 1965, **4**, 643–648.
- 184 B. C. Lippens and J. H. De Boer, *J. Catal.*, 1965, **4**, 319–323.
- 185 E. P. Barrett, L. G. Joyner and P. P. Halenda, *J. Am. Chem. Soc.*, 1951, **73**, 373–380.
- 186 N. Fontanals, R. M. Marce, M. Galià and F. Borrull, *J. Polym. Sci. Part A. Polym. Chem.*, 2003, **41**, 1927–1933.